Investigation of the Association Between Tissue Transglutaminase II and PLCδ_1 in Vascular Smooth Muscle.

A. Sofi E. Fexby

A thesis submitted for the degree of
Doctor of Philosophy from the University of London

Imperial College
London

Faculty of Medicine,
Imperial College of Science, Technology & Medicine,
London, UK.

2005

ACKNOWLEDGEMENT

Firstly, I would like to express my thanks and gratitude to my two supervisors Dr Joanne Lymn and Professor Alun Hughes for their guidance and support. I am thankful for Dr Joanne Lymn and family for opening your home during my time in Nottingham. I also would like to thank all past and present members of the Department of Clinical Pharmacology. I am particularly grateful to Sumangali, Mike, Louise, Gez, Simon and Mahendra for their generous advice, discussion and time during work and for making me laugh – I shall miss you. Many thanks as well to all lovely people on the 10th floor - JP, Wafa, Frusso, Safi and Eunice.

Special thanks go to all my lovely friends: Helle, Per, Johan, Tina, Danne, Peter, Mia, Hind, Alick, Huma, Tomoko, Calle, Omar, Louise and Wendy – thanks for all the memorable time together in London. Also, many thanks to the ones geographically far but always in my heart: Karin, Sara and Esther in Stockholm, friends from my year in Bruxelles: Emma, Anna, Line, Cissi, Ulrikaka & Andrea and my "ERASMUS-friends": Antoine, Ursulina, Lucia, Daniel, Steffen, Alfredo and Srdjen – you are all very special and will always be "the sunshine through my window"!

I would like to acknowledge Karen for taking care of the cells and also Ben and Ed for all help and advice with the confocal microscope at Brompton hospital. I am also grateful for the technical help and advice from Tim during my time in Nottingham, from whom I also learnt the technique of live calcium imaging and Flexstation measurements. I would like to thank Elisabeth for showing me the chromatography set-up and Louise for teaching me the PLC assay and immunofluorescent staining.

I would like to thank all members, speakers and people involved during my time with the London Hypertension Society. Special thanks to Prof. Donald Singer, Dr. Jo Knight and representative from Menarini, UK.

I would like to acknowledge the British Heart Foundation for supporting this work and my conferences. Also I am indebted to my father and another most kind and unforgettable source for their financial aid during the time of writing up my thesis.

The lovely staff, memorable time and amazing coffee at Little Italy cannot go without mention. I also would like to thank Orvel and Clive for their support and cheering me up during my many long hours in the library.

I am extremely grateful to JP, Johan and Tina for support, help and encouragement whilst trying to find my way through the dark jungle of job hunting.

Finally I am indebted to my family, Sumangali, Mike and Helen for the endless support, guidance and time you have provided and for believing in me. Thanks to you this is in one piece. This book is for you!

TABLE OF CONTENTS

ABSTRACT

ACKNOWLEDGEMENT

TABLE OF CONTENTS

LIST OF FIGURES AND TABLES

APPENDIX A

ABBREVIATIONS

TABLE OF CONTENTS **PAGE**

CHAPTER 1 – INTRODUCTION..... 1

1.1 Introduction of vascular smooth muscle.....1

1.2 Muscle skeletal, cardiac and smooth muscle.....2

1.2.1 Skeletal muscle.....3

1.2.2 Cardiac muscle.....3

1.2.3 Vascular smooth muscle.....3

1.3 Differentiation of smooth muscle/phenotype.....4

1.3.1 Cellular differentiation.....4

1.3.2 Differentiation & phenotypic change of vascular smooth muscle cells5

1.4.1 Marker proteins for SMC phenotype.....7

1.4.2 SM α-actin..... 8

1.4.3 Calponin.....8

1.5 SMC structural machinery.....9

1.5.1Cytoskeleton..... 10

1.5.1.1Actin..... 11

1.5.1.2 Microtubules..... 12

1.5.1.3 Intermediate filaments..... 12

1.5.1.4 Regulation of cytoskeleton..... 13

1.5.3.4.1 RhoA.....13

1.5.3.2.2 PIP2.....14

1.5.2 Contractile apparatus..... 15

1.5.2.1 Calcium – a rise in calcium induces contraction..... 15

1.5.2.2 Contraction of vascular smooth muscles..... 16

1.6 Cells signalling and transduction.....19

1.6.1 G-proteins – signal transducers.....19

1.6.2 Inositol Phospholipid signalling pathway.....22

1.7 Phosphoinositied-specific phospholipase C (PLC) pathway..... 24

1.7.1 Structure and catalytic function of PLC isoform.....24

1.8 PLCδ..... 27

1.8.1 PLCδ_1 expression and cellular localisation..... 27

1.8.2 Regulation of PLCδ_1..... 28

1.8.3 Function of PLCδ_1..... 29

1.8.4 PLCδ_1 -implication in disease..... 30

1.9 Tissue transglutaminase.....31

1.9.1 TGII is a member of the transglutaminase family.....32

1.9.2 Structure of TGII..... 32

1.9.3 TGII has a unique GTP-binding pocket.....33

1.9.4 Expression of TGII..... 34

1.9.5 Cellular location of TGII..... 34

1.9.6 GTPase and TGase activity of TGII..... 35

1.9.7 Regulation of TGII.....36

1.9.8 Function of TGII.....37

1.9.8.1 TGII function with GTPase activity..... 37

1.9.8.2 TGII function with transglutaminase activity.....39

1.9.9 TGII and pathological implications..... 40

1.10 TGII and PLCδ_1..... 42

1.10.1 Summary of TGII and PLCδ_1 association..... 42

BACKGROUND AND EXPERIMENTAL LAYOUT..... 45

CHAPTER 2 - MATERIALS & METHODS..... 47

2.1 Cell Culture Techniques..... 47

2.1.1 Explant technique..... 47

2.1.2 Induction of redifferentiation by serum deprivation..... 47

2.1.3 Culture of HVTs-SM1 cells..... 48

2.2 Preparation of cell lysate..... 48

2.3 Measurement of protein concentration..... 48

2.4 Immunoprecipitation.....49

2.5 Detection of TGII secretion..... 49

2.6 SDS-Polyacrylamide Gel Electrophoresis (SDS-PAGE).....50

2.7 Western blotting..... 50

2.8 Immunoblotting..... 51

2.9 Coomassie Blue staining..... 52

2.10 SYPRO Ruby protein gel stain.....52

2.11 Confocal imaging.....53

2.12 Column chromatography..... 53

2.13 PLC activity..... 54

2.14 Transglutaminase activity..... 55

2.15 [^{35}S]GTPγS binding overlay method..... 55

2.16 Measurement of intracellular calcium levels..... 56

2.16.1 Fura-2-AM loading of HVTs-SM1 cells.....56

2.16.2 Fluo-4-AM loading of HVTs-SM1 cells.....56

2.16.3 Flexstation.....57

2.16.4 Data analysis.....58

2.17 Live calcium imaging..... 58

2.18 Statistical analysis.....59

2.19 Materials..... 59

2.19.1 Primary Antibodies.....59

2.19.2 Secondary antibodies..... 59

2.19.3 Western blotting & Immunoprecipitation.....60

2.19.4 Chromatography..... 60

2.19.5 Flex..... 60

2.19.6 Disruption of actin..... 60

2.19.7 PLC assay..... 61

2.19.8 Cell culture.....61

2.20 Equipment.....61

2.20.1 Cell culture.....61

2.20.2 Centrifuges.....61

2.20.3 Spectrophotometer..... 61

2.20.4 SDS-PAGE..... 62

2.20.5 Flexstation.....62

2.20.6 Confocal Laser Microscope..... 62

CHAPTER 3 - PROTEIN EXPRESSION.....63

3.1 Aim of study..... 63

3.2 Introduction.....63

3.3 Methodology to achieve redifferentiation.....64

3.3.1 Serum deprivation.....65

3.4 Modulation of smooth muscle phenotype.....66

3.5 Control experiments for western blotting.....69

3.5.1 Intergel differences of gel loading.....70

3.5.2 Intragel differences of gel loading.....71

3.5.3 Linear range of antibody detection.....72

3.6 Effect of serum deprivation on protein expression.....73

3.7 Temporal change in TGII expression during redifferentiation.....75

3.8 Secretion of TGII.....76

3.8.1 Detection in TGII in culture media.....76

3.9 Level of TGII in cell lysate compared to media during phenotypic change...76

DISCUSSION - PROTEIN EXPRESSION..... 79

CHAPTER 4 - PROTEIN LOCALISATION.....86

4.1 Aim of localisation studies.....86

4.2 Intracellular location..... 86

4.3CLSM – confocal laser scanning microscope..... 86

4.4.1 Preparation of coverslips with cells for fluorescent staining.....88

4.4.2 Methanol fixation.....88

4.4.3 Permeabilisation.....89

4.4.4 Staining.....89

4.5 Control pictures for immuno flurorescent staining of HVSMCs.....89

4.6 The effect of serum deprivation on HVSMCs..... 92

4.7 Trouble shooting with PLCδ_1 antibody..... 94

4.8 Effect of serum deprivation on protein localisation and organisation of TGII and PLCδ_1 in HVSMCs.....96

4.9 Co-localisation of PLCδ_1 and TGII?.....99

4.10 Is there an association of PLCδ_1 and/or TGII with actin cytoskeleton?.....102

4.12 Modulation of actin cytoskeletal structure.....104

4.12.1 Modulation of actin cytoskeletal structure by Cytochalasin D.....104

4.12.2 Exposure of HVSMCs to Cytochalasin D and Colchicine..... 105

4.13. Effect of Cytochalasin D.....105

4.13.1 Effect of Cytochalasin D on actin cytoskeleton.....105

4.13.2 Effect of Cytochalasin D on PLCδ_1 and TGII expression.....107

4.13.3 Effect of Cytochalasin D on protein expression of SM α-actin.....108

4.13.4 Effect of Cytochalasin D on protein expression of PLCδ_1 and TGII 108

4.14 Modulation of actin cytoskeletal structure by Cholchicine..... 110

DISCUSSION - PROTEIN LOCALISATION.....111

CHAPTER 5 - IMMUNOPRECIPITATION.....116

5.1 Aim of Immunoprecipitation studies..... 116

5.2 The Precipitation Reaction.....116

5.3 Background of Antibody.....116

5.4 Immunoprecipitation of PLCδ_1 respectively TGII..... 117

5.4.2 Efficiency of pull down in immunoprecipitation.....119

DISCUSSION IMMUNOPRECIPITATION 121

CHAPTER 6 - GTPase OR TGase ACTIVITY?.....124

6.1 Aim of study..... 124

6.2 Introduction.....124

6.3 Measurement of Transglutaminase activity.....124

6.4 Tissue transglutamianse activity in lysates from HVSMC.....126

6.5 Modulation of transglutaminase assay.....128

6.6 Effect of differentiation state on TGase activity.....133

6.7 Effect of TGase inhibition on PLCδ_1 and TGII expression..... 134

6.8 Presence of GTPase activity by [^{35}S]GTPγS overlay assay..... 135

DISCUSSION - GTPase OR TGase ACTIVITY?.....137

CHAPTER 7 - PARTIAL PURIFICATION OF PLC..... 139

7.1 Introduction to Partial purification of PLCδ_1 in rat aorta..... 139

7.2 Overview of Ion exchange chromatography..... 139

7.3 Partial purification of PLCδ_1..... 141

7.3.1 Partial purification of PLCδ_1 in rat aorta..... 141

7.3.2 PLC activity in 12 pooled rat aortas..... 143

CHAPTER 7 - DISCUSSION.....146

CHAPTER 8 - CALCIUM MEASURMENTS..... 148

8.1 Aim of study..... 148

8.2 Calcium..... 148

8.3 Measurements of intracellular calcium by Flex station.....149

8.4 Cells..... 150

8.4.1 HVTs-SM1 cells..... 150

8.4.2 PLC isoform profile and TGII expression in HVTs-SM1 cells.....151

8.5 Measurements of intracellular calcium using Flexstation..... 153

8.6 Measurements of intracellular calcium using fluorescent dye.....154

8.6.1 Calcium dyes.....154

8.6.2 Cell loading.....156

8.6.3 Data analysis.....157

8.6.4 Fluo-4-AM versus Fura-2AM..... 159

8.7 Background fluorescence.....161

8.8 Compartmentalisation of dye.....162

8.9 Establishing loading condition for HVTs-SM1 cells.....165

8.9.1 Loading in buffer versus loading in serum containing medium.....165

8.9.2 Improvements of loading with addition of Pluronic acid.....167

8.9.3 Improvements of loading with addition of Probenecid 168

8.9.4 Improvements of loading with Albumin.....169

8.9.5 Change in intracellular calcium in response to PE (10μM).....169

8.10 Trouble shooting with detachment of HVTs-SM1 cells.....171

8.10.1 Detachment of cells.....172

8.10.2 Improvement of attachment by lysine coating of wells.....173

8.10.3 Batch problem.....174

8.11 Measurements of changes in $[Ca^{2+}]i$ following addition of agonists..... 175

8.11.1 Phenylepherine.....175

8.11.2 Dose-response to Phenylepherine, PE (10^{-10}-10^{-5}M)..... 176

8.12.1 PDGF-BB.....180

8.12.2 Dose-response to PDGF-BB (1-50ng/ml)..... 183

8.13.1 Histamine.....183

8.13.2 Dose-response to Histamine (10^{-10}-10^{-5}M)..... 186

8.14.1 Fibronectin.....186

8.14.2 Dose-response to Fibronectin (0.05-5mg/ml).....189

8.15. Summary of response to agonists..... 190

8.16.1 Response to PE and PDGF-BB in presence of Genistein (50μM).....191

DISCUSSION - CALCIUM MEASURMENTS.....193

FINAL SUMMARY & FUTURE WORK.....197

REFERENCES.....202

LIST OF FIGURES AND TABLES

CHAPTER 1 **PAGE**

Figure 1.1 Blood vessels are composed of three layers.....1

Figure 1.2. Illustration of cellular structures.....10

Figure 1.3. Illustration of smooth muscle contraction.....17

Figure 1.4 Illustration of GTP-binding protein.....20

Figure 1.5. Rise in intracellular calcium by store release and calcium entry.....23

Figure 1.6 Structure of PLCδ_1.....26

Figure 1.7. Structure of TGII.....33

Figure 1.8. Illustration of Tissue transglutaminase (TGII) coupling of receptor to Phospholipase Cδ_1 (PLCδ_1).....43

CHAPTER 2

Figure 2.1 Set-up for running a SDS gel and on the left western blotting transfer set-up.....50

Figure 2.2 Principles of enhanced chemical luminescence (ECL).....52

CHAPTER 3

Figure 3.1 Temporal effects of serum deprivation.....66

Figure 3.2 Change in protein expression of the two markers for redifferentiation, SM α-actin and calponin in redifferentiated (GA) HVSMC.....68

Figure 3.3 Morphological change of HVSMCs following redifferentiation.....69

Figure 3.4 Intergel differences of Westernblotting.....70

Figure 3.5 Intragel differences for Western blotting.....71

Figure 3.6 Limit of detection of TGII antibody.....72

Figure 3.7 Change in protein expression of PLCδ1, TGII and RhoA in randomly cycling (RC) versus redifferentiated (GA) HVSMC.....74

Figure 3.8 Temporal expression of TGII over seven days of serum deprivation. 75

Figure 3.9 Detection of TGII secreted in media.....77

Figure 3.10 TGII in cell lysates versus secreted in the media in randomly cycling (RC) compared to redifferentiated (GA) HVSMCs.....78

CHAPTER 4

Figure 4.1 Controls for immunofluroescent staining.....91

Figure 4.2 Effect of redifferentiation on the subcellular localisation of SM α-actin and calponin.....93

Figure 4.3 Immunofluorescence staining using 3 different antibodies against $PLC\delta_1$.....95

Figure 4.4 Effect of redifferentiation on the subcellular localisation of $PLC\delta_1$ and TGII.....97

Figure 4.5 Subcellular localisation and structural organisation of TGII in randomly cycling and serum deprived HVSMC.....98

Figure 4.6 Double staining of TGII and $PLC\delta_1$ in HVSMCs.....99

Figure 4.7. Dual staining of TGII and $PLC\delta_1$ in HVSMCs evaluated by LSM510 software.....100

Figure 4.8. Dual staining of SM α-actin and $PLC\delta_1$ in HVSMCs.....101

Figure 4.9 Effect of Cytochalasin D on the actin cytoskeleton.....106

Figure 4.10 Effect of Cytochalasin D on $PLC\delta_1$ and TGII expression.....107

Figure 4.11 The effect of Cytochalasin D on SM α-actin, PLCδ$_1$ and TGII expression.....109

Figure 4.12 Effect of Colchicine on actin cytoskeleton on PLCδ$_1$ and TGII expression.....110

CHAPTER 5

Figure 5.1 Immunoprecipitation of TGII respectively PLCδ$_1$ in randomly cycling (RC) versus serum deprived (GA) HVSM cells.....118

Figure 5.2 Diagram of TGII present in immunoprecipitates of PLCδ$_1$ in randomly cycling versus growth arrested HVSMCs.....119

Figure 5.2 Efficiency of the actual pulldown of PLCδ$_1$ respectively TGII immunoprecipitates.....120

CHAPTER 6

Figure 6.1 Efficiency of the three wash steps in the Transglutaminase (TGase) activity assay.....125

Figure 6.2 Effect of variation of incubation time in TGase assay.....126

Figure 6.3 TGase activity measurements in HVSMC cell lysate.....127

Figure 6.4 TGase activity of pure liver transglutaminase dissolved in sample buffer respectively lysis buffer.....129

Figure 6.5 Standard curves for TGase activity measurements capturing sample in filter paper.....131

Figure 6.6. Control measurements of TGase activity assay.....132

Figure 6.7 Complete inhibition of transglutaminase activity by MDC.....133

Figure 6.8 TGase activities in RC versus GA HVSM cells.....134

Figure 6.9 Effect on PLCδ_1 and TGII protein expression upon inhibition of TGase activity.....135

CHAPTER 7

Figure 7.1. Basis of anion exchange chromatography.....140

Figure 7.2 Elution profile of 12 rat aorta pooled (n=3) through Q-sepharose....142

Figure 7.3 Representation of activity peaks assaying for PLC activity.....144

CHAPTER 8

Figure 8.1 Picture of Flexstation and software window (SoftMaxPro 4.7.1).....149

Figure 8.2. Comparison of cell morphology of transformed HVTs-SM1cells...151

Figure 8.3. Protein profile in HVTs-SM1 cells.....152

Figure 8.4. Different seeding densities.....154

Figure 8.5. Schematic diagram of the processes involved in loading cells using acetoxymethyl (AM) ester derivatives of fluorescent indicators.....156

Figure 8.14. Quantification of the fluorescence signal. Intra cellular calcium measurements using Flexstation and Fluo-4-AM loading.....158

Figure 8.6 Comparison of loading efficiency using Fura-2-AM versus Fluo-4-AM.....160

Figure 8.7 Background fluorescence of cells.....161

Figure 8.8. Calcium live imaging of HVTs-SM1 cells.....163

Figure 8.9. Showing calcium live imaging of HVTs-SM1 cells.....164

Figure 8.10 Fluo-4-AM loading in buffer versus medium.....166

Figure 8.11. The beneficial role of presence of Pluronic acid (2.5mM) for improved intracellular calcium measurements using Fluo-4-AM.....167

Figure 8.12. The beneficial role of presence of Probenecid for improved intra-cellular calcium measurements using Fluo-4-AM.....168

Figure 8.13. The effect of BSA and Albumin on Fluo-4-AM loading in HVSMCs (37°C).....169

Figure 8.14 Measurements of $[Ca^{2+}]_i$ of HVTs-SM1 cells.....170

Figure 8.15 Detachment of cells.....171

Figure 8.16 Disruption of cells due to increase in washes.....173

Figure 8.17. Difference in growth and detachment in between batches of HVTs-SM1 cells.....174

Figure 8.18. PE-induced increase in intracellular calcium.....178-179

Figure 8.19 PDGF-BB induced increase in intracellular calcium.....181-182

Figure 8.20 Histamine induced increase in intracellular calcium measured by Flex station using Fluo-4-AM.....184-185

Figure 8.21 Fibronectin induced increase in intracellular calcium measured by Flex station using Fluo-4-AM.....187-188

Table 8.1. Summary of Mean response to agonists.....190

Figure 8.22 Mean peak fluorescent of HVT-SM1 cells kept at 37°C versus 39°C.....190

Figure 8.23 Effect of Genistein on responses to PE and PDFG-BB.....192

1. Transport media

2. Standard culture medium DMEM (15 % FCS)
DMEM medium
15% (vol/vol) Fetal Calf Serum (FCS)
25mM HEPES
100U/ml Penicillin
100μg/ml Streptomycin
100μg/ml Kanamycin

3. Trypsin EDTA (TE)
0.25% Trypsin solution
1mM Ethylenediaminetetraacetic acid (EDTA)
Phosphate buffered saline (PBS)

4. Serum-free NCTC 109 medium (SF-NCTC)
NCTC 109 medium (cat.no. 21340-039)
25mM HEPES
4mM l-alanyl-l-glutamine (Glutamax I)
100 U/ml Penicillin
100 U/ml Kanamycin
2.5mg/ml Sterile bovine serum albumin (BSA)

5. Culture medium for HMVs-SM1 cells (10% FCS DMEM)
DMEM medium
10% Fetal Calf Serum (FCS) (vol/vol)
25mM HEPES
100U/ml Penicillin 100U/ml
100μg/ml Streptomycin
100μg/ml Kanamycin
200µg/ml G-418 200µg/ml

6. Standard Lysis Buffer
50mM Tris, (pH=7.4)
150mM NaCl
1mM NP-40
0.1mM Sodium deoxycholate
100mM Ethylene glycol-bis(β-Aminoethylether)-N-N-N'-N'-Tetraacetic acid (EGTA)
1mM Phenylmethylsulfonyl fluoride (PMSF)
1mM Sodium orthovanadate (Na_3VO_4)
1mM (Sodium fluoride (NaF)
1μl/ml Aprotinin
1μl/ml Pepstatin A
1μl/ml Leupeptin

7. BCA protein assay working reagent
25 parts reagent A
8.0% w/v $Na_2CO_3.H_2O$
1.6% w/v NaOH
0.16% w/v Na_2 tartrate

24 parts reagent B
4.0% w/v 4,4'-dicarboxy-2, 2'-biquinoline (BCA-Na_2)

1 part reagent C
4% w/v $CuSO_4.5H_2O$

8. 2X Laemmli sample buffer
4% Sodium dodecyl sulphate (SDS)
20% 2-mercaptoethanol
20% Glycerol
0.004% Bromphenol blue
0.125 M Tris-HCl, pH 6.8

9. 5X Laemmli sample buffer

10% Sodium dodecyl sulphate (SDS)
25% 2-mercaptoethanol
50% Glycerol
0.01% Bromphenol blue
0.3 M Tris-HCl, pH 6.8

10. Stacking gel
4% w/v acrylamide
1M Tris-HCl, pH6.5
0.1% w/v sodium dodecyl sulphate
0.1% w/v ammonium persulphate (APS)
0.5% v/v N,N,N',N'-tetramethyl-ethylenediamine (TEMED)

11. Resolving gel
10% w/v acrylamide
1.5M Tris-HCl, pH8.8
0.1% w/v Sodium dodecyl sulphate (SDS)
0.1% w/v ammonium persulphate (APS)
0.5% v/v N,N,N',N'-tetramethyl-ethylenediamine (TEMED)

12. Gel Running Buffer
25mM Tris
192mM Glycine
3.5mM Sodium dodecyl sulphate (SDS)

13. Transfer Buffer
25mM Tris

192mM Glycine
20% v/v Methanol

14. 1 X TTBS
20mM Tris-HCl pH 7.5
500mM NaCl
0.1% v/v Polyoxyethylene-sorbitan monolaurate (Tween 20)

15. Homogenisation buffer
20mM Tris-HCl, pH 7.4
50mM NaCl
250mM Sucrose
1mM Dithiohreitol (DTT)
1mM Ethylenediaminetetraacetic acid (EDTA)
5mM MgCl
176µg/ml Phenylmethylsulfonyl fluoride (PMSF)
1µg/ml Leupeptin A
1μl/ml Aprotinin
0.7μl/ml Pepstatin

16. Column chromatography running buffer
10mM Tris-base, pH 7.5
50mM NaCl
1mM Dithiohreitol (DTT)
1mM Ethylenediaminetetraacetic acid (EDTA)
5% Glycerol
176µg/ml Phenylmethylsulfonyl fluoride (PMSF)
1µg/ml Leupeptin A
1µg/ml Aprotinin
0.7µg/ml Pepstatin

17. PLC buffer
20mM Tris-base, (pH 7.0)
100mM NaCl
2mM Ethylene glycol-bis(β-Aminoethylether)-N-N-N'-N'-Tetraacetic acid, EGTA
2.4mM $MgCl_2$
8mM $CaCl_2$
0.05% Bovine serum albumin (BSA, fatty acid free)

18. Reaction mixture Transglutaminase assay
50 mM Tris-HCl (pH=7.4)
5 mM DTT
75 nM [^{3}H]putrescine
4 mg/ml *N*,*N*-dimethylated casein

19. Washing buffer for [^{3}H]GTPγS overlay assay
50mM Tris HCl, (pH 7.5)
12μM $MgCl_2$
0.3% Tween 20

20. Binding buffer for [^{3}H]GTPγS overlay assay
50mM Tris HCl , (pH 7.5)
12μM $MgCl_2$
1mM DTT
0.3% Tween x 20
51.5TBq/mmol GTP[γ^{35}]S (75kBq/ml , NEN, UK)
10μM ATP

21. Ca^{2+}- buffer for Fura-2-AM loading
36mM NaCl, (pH=7.4)
2.5mM Glucose
0.25mM $MgSO_4$ x $7H_2O$
0.21mM HEPES
1mM $CaCl_2$ x $2H_2O$

22. Ca^{2+}- buffer for Fluo-4-AM loading
2mM Sodium Pyrovate
0.14M NaCl, (pH=7.45)
10mM D-Glucose
5mM KCl
10mM $MgSO_4$ x $7H_2O$
8.5mM HEPES
1.3mM $CaCl_2$ x $2H_2O$

ABBREVATIONS

AM – acetoxymethyl (Fluo-4-AM)

ATRA - all trans-retinoic acid

BCA- Bicinchoninic Acid

BSA – Bovine Serum Albumine

CDS – Cell dissociation solution

CDS- Cell dissociation solution

DAPI - 4'-6-Diamidino-2-phenylindole

ddH_2O – Double Distilled water

DMEM - Dulbecco's modified Eagle's medium

DMSO – Dimethyl sulfoxide

ECL - Enhanced chemical luminescence

EDTA - Ethylenediaminetetraacetic acid.

EGTA - Ethylene glycol-bis(β-Aminoethylether)-N-N-N'-N'-Tetraacetic acid

F- Filament actin

FCS - Foetal calf serum

FITC- Fluorescin isothiocyanate

G- Globular actin

GA – Growth arrested

GTP – Guanine nucleotide triphosphate

GTPase – Guanine nucleotide triphosphate binding activity

HBSS – Hank's Balanced Salt Solution

HCl-Hydrogen Chloride

HEPES- N-(2-Hydroxyethyl)piperazine-N'-(2-ethanesulfonic acid) hemisodium salt

His – Histamine

HVSMC – Human Vascular Smooth muscle cells

HVTs-SM1 - an immortalised HVSM cell line

MDC –Monodansylcadaverine

NaOH - Sodium Hydroxide

NCTC – NCTC 109 media (Sigma, N1140)

PBS – Phosphored buffered soloution

PBSX- PBS-0.1% Triton X

PDGF-BB

PE – Posphatidylethanolamine

PE- Phenylepherine

PI - Phosphatidylinositol

PI – Phosphoiniositols

PLC – Phospholipase C

PMSF - Phenylmethylsulphonylfluoride

RA – Retinoic acid

RC – Randomly cycling

SDS-PAGE – Sodium Dodecyl Sulfate-Polyacrylamide Gel Electrophoresis

SMC – Smooth Muscle Cell

SR – Sarcoplasmic Reticulum

TCA - trichloroacetic acid

TCA – Trichloroacetic acid

TG2 – Tissue transglutaminase

TGase – Transglutaminase activity

TPBS – Triton X (0.05%) in PBS

Ts – Temperature sensitive

TTBS – Transfer buffer with Tween

VSMC – Vascular Smooth Muscle Cell

CHAPTER 1 INTRODUCTION

1.1 Introduction of vascular smooth muscle

Vascular smooth muscle is a muscle that contracts without a conscious control and is found in walls of blood vessels. These cells, named "smooth" because they lack striations caused by the sarcomers in skeletal and cardiac muscle cells, interact by multiple coordination mechanisms to produce relatively long or tonic contractions associated with the function of the blood vessel. Arteries consist of three layers: endothelial, smooth muscle and adventitial layers (Figure 1.1).

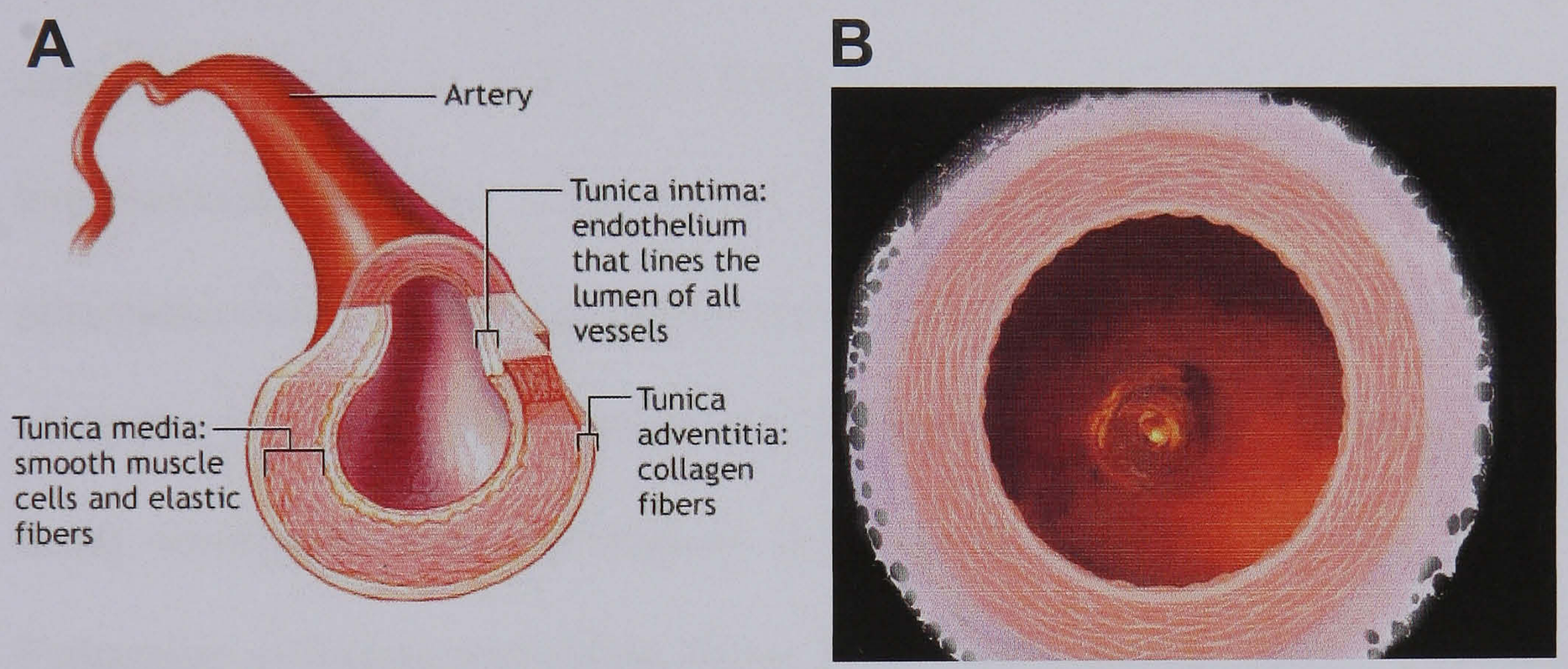


Figure 1.1 ***A****. Blood vessels are composed of three layers: the tunica intima, tunica media, and tunica adventitia. The tunica intima consists of a layer of endothelial cells lining the lumen of the vessel. The tunica media is the middle layer of the walls of arteries and veins. It is composed of smooth muscle and elastic fibers. This layer is thicker in arteries than in veins. The tunica adventitia is primarily composed of loose connective tissue made up of fibroblasts. (www.nlm.nih.gov/ency/fullsize/19194.jpg).* ***B****. A cross-section of the coronary artery. Showing how most of its wall is filled with smooth muscle cells that can contract and relax. These small changes in the vessel lumen can greatly influence blood pressure and blood flow (http://nobelprize.org/medicine, 1998).*

With its main function being contraction smooth muscles maintain the vessel tone. But upon injury or disruption of the artery wall a change in phenotype of mature SMC occurs, causing the cells to switch from their normal function of contraction and maintenance of vessel wall tone to one of repair of the wound by synthesis of matrix and/or proliferation. Once the wound is healed, cells are thought to return to their previous phenotype and function.

Smooth muscle proliferation has been recognized as central to the pathology of atherosclerosis (Faxon, D.P., *et al.* 2004; Ross, R., *et al.* 1993) and contribution to hypertension (Integan, H.D., *et al.* 2001; Pauto, M., *et el.* 2004). Both atherosclerosis and hypertension are risk factors in the development and progress of cardiovascular disease. Coronary heart disease is one of the leading cause of death worldwide with the highest numbers of death in the US, India, the Federation of Russia and China. Since 1900 Cardiovascular disease has been the number one killer in the United States every year but 1918 (Heart disease and stroke statistics, 2005 update by American Heart Association). Similarly, heart and circulatory disease is UK's biggest killer. Cardiovascular disease in the UK accounts for around 238,000 deaths a year, which is 39% of all deaths, and a shocking 2.7 million people are estimated to be living with coronary heart disease (BHF Statistics Fact sheet, 2004).

1.2 Muscle skeletal, cardiac and smooth muscle

There are three types of specialised contractile myocytes: skeletal muscle, cardiac muscle and smooth muscle. All three types of muscles contain actin and myosin

and contract by a sliding filament mechanism, thus they differ in their activation mechanism, arrangement of contractile filaments and energy supplies.

1.2.1 Skeletal muscle

Skeletal muscles are designed for rapid, forceful contractions. Speed is achieved by linking many sarcomeres in series, whilst the number of sarcomeres contracting in parallel determines force. The nervous system controls the timing, force and speed of skeletal muscle contraction over a wide range.

1.2.2 Cardiac muscle

Cardiac muscles maintain the circulation of blood and the heart is specialized for repetitive fatigue-free contractions that spread through the heart in a highly reproducible fashion. Neurotransmitters, predominantly acetylcholine and noradrenaline modulate the force and frequency of heartbeats over a narrow range. The intrinsic rhythmic beating of the heart is driven by action potentials from specialized pacemaking cells that spread from one muscle cell to the next by gap-junctions.

1.2.3 Vascular smooth muscle

Smooth muscles contract slowly compared with skeletal muscle but maintain tension very efficiently. The activity of smooth muscles is controlled by a variety of involuntary mechanisms such as nerves, hormones and intrinsic signals. One of the challenges in studying mechanisms of smooth muscle cells (SMCs) development and differentiation is the fact that unlike cardiac and skeletal muscles, which are derived from specific populations of mesodermal precursors,

SMCs are derived from multiple cell types. For example, SMCs of the ascending aorta and branchial arches are derived from neural crest (ectodermal) cells. SMCs of the coronary vessels arise from epithelial-to-mesenchymal transition of cells in the proepicardial organ. Most of the remaining SMCs, including visceral SMCs, are thought to derive from condensation of local mesenchyme under the influence of local environmental signals (Solway, J., *et al.* 1998; Hungerford, J.E. and C.D. Little, 1999). The diverse origins of SMCs likelycontribute to their heterogeneity in structure, function and SMC marker gene expression. Moreover, the signals and molecular pathways leading to SMC differentiation may prove to be somewhat different depending on the cell type of origin.

1.3 Differentiation of smooth muscle/phenotype

1.3.1 Cellular differentiation

Cellular differentiation is simply the process by which multipotential cells in the developing organism acquire those cell-specific characteristics that distinguish them from other cell types. Although the process of cellular differentiation is complex, it can be subdivided into the following three major regulatory components: selective activation of the subset of genes required for the cell's differentiated function or functions; coordinative control of expression of cell-selective genes at precise times and quantity; and continuous regulation of gene expression through effects of local environmental signals on the genetic program that determines cell lineage, including control of chromatin structure or epigenetic programming that can influence the ability of transcription factors to access regulatory regions of genes. In addition, it is important to recognise that an understanding of the differentiation of any cell type not only involves elucidating

the autonomous mechanisms that control gene expression patterns and functional properties of one individual cell but also must encompass how the cell interacts with other cells, environmental factors such as the matrix and the complex processes that control overall tissue and organ morphogenesis.

1.3.2 Differentiation & phenotypic change of vascular smooth muscle cells

During the early stages of vasculogenesis VSMCs are highly migratory and undergo very rapid cell proliferation. Recent live videos of vascular development and vascular remodelling in zebra fish indicate that there is a remarkable amount of movement of VSMCs. In addition Isogai and co-workers also discovered the presence of VSMC progenitor cells as part of the complex morphogenic events in the formation of the cardiovascular system (Isogai, S., *et al.* 2001). During vascular development, VSMCs also exhibit very high rates of synthesis of extracellular matrix components including collagen, elastin, proteoglycans, cadherins, and integrins that comprise a major portion of the blood vessel mass. At this stage of development VSMCs form abundant gap junctions with endothelial cells, and the process of investment of endothelial tubes with VSMCs or pericytes is critical for vascular maturation and vessel remodelling (Hungerford, J.E. and C.D. Little, 1999). In contrast, VSMCs in adult blood vessels show an exceedingly low rate of proliferation, are largely non migratory, show a very low rate of synthesis of extracellular matrix components, and cells are almost completely committed to carrying out contractile functions (Thyberg, J., *et al.* 1983; Chamley-Campbell, J., *et al.* 1981). However, even in adult organisms VSMCs are not terminally differentiated and are capable of major changes in its phenotype in response to changes in its local environment (Owens,

G.K., *et al.* 1995; Schwartz, S.M., *et al.*, 1990). Disturbance of the normal integrity of the tissue, such as during vascular disease, leads to a modulation of contractile VSMC, which are capable of undergoing transient modification of their phenotype to a highly "synthetic" phenotype, which exhibit altered morphology, cell function and biochemical characteristics (Absher, M., *et al.* 1989; Wissler, R.W., *et al.* 1967). These synthetic VSMCs have an enhanced capacity to replicate and migrate and play a critical role in repair of the vascular injury (Manabe, I., *et al.* 2003). Upon resolution of the injury, the local environmental cues within the vessel return to normal. Taken together, the model that has emerged is that SMCs within adult mammals are highly plastic cells that are capable of rather profound alterations in their phenotype in response to changes in the local environment. This ability of VSMCs to modulate their phenotype is critical in the vascular response to injury.

Interestingly, culture of vascular VSMC results in a similar phenotypic modulation with cells undergoing morphological changes, proliferating at greatly enhanced rate and losing of their contractile ability (Thyberg, J., *et al.* 1983; Chamley-Campbell, J., *et al.* 1981). This suggests that cultured VSMCs may represent a good model of diseased vascular tissue, indeed this concept was first hypothesized in 1967 by Wissler who showed that, enzymatically dispersed cells from arterial media placed in culture gradually assumed features of less differentiated cells with characteristics of SMCs in vascular lesions (Wissler, R.W., *et al.* 1967). Jarmolyck *et al.* and Fritz *et al.* were the first who used the term “dedifferentiation” when describing outgrowth of SMCs from pig aorta

explants in culture. They described how this modified SMCs to fibroblast-like cells turning into rapidly proliferating cells (Fritz, K.E., *et al.* 1970).

1.4.1 Marker proteins for SMC phenotype

Culture of vascular SMC results in loss of contractile ability whilst cells proliferate at greatly enhanced rates (Chamley-Campbell, J. *et al.* 1981). Modulation of culture conditions such as serum deprivation (Li, S., *et al.* 1999) or retinoic acid treatment (Axel, D.I., *et al.* 2001) can result in more redifferentiated state of the cells. However, it is not currently possible to re-establish a fully differentiated contractile phenotype in cultured VSMCs that can fully reproduce the complex *in vivo* pattern. Consequently, several markers for differentiation must be used to characterise VSMC phenotype (Kumar, M.S. and G.K., Owens, 2003). Mature fully differentiated SMC expresses a repertoire of appropriate receptors, ion channels, signal transduction molecules, calcium regulatory proteins, and contractile proteins necessary for the unique contractile properties of the SMC (Owens, G.K., *et al.* 1995). Differentiated VSMCs are characterized by high expression levels of contractile proteins, such as SM α-actin (Fatigati, V and R.A., Murphy, 1984) and SM myosin heavy chain, (MHC) (Rovner, A.S., *et al.* 1986) as well as a number of proteins that are part of the cytoskeleton or involved in the regulation of contraction such as calponin, caldesmon or desmin (Miano, J.M., *et al.* 2002; Gabbiani, G., *et al.* 1981). Synthetic or dedifferentiated cultured VSMCs exhibit an altered expression of contractile and cytoskeletal proteins as well as membrane channels and receptors (Owens, G.K., *et al.* 1995; Gollasch, M., 1998) and instead exhibit markedly increased expression of the non-muscle isoforms of these proteins. These non-muscle isoforms are not specifically

expressed in SMCs (Hedin, U., *et al.*1990) and expression of these SM and non-SM isoforms also changes during the remodelling process and following injury (Owens, G.K., *et al.* 1995).

In this study smooth muscle α-actin (SM α-actin), which is an important contractile protein, largely specific to SMCs (Gabbiani, G., *et al.* 1981) and calponin, another marker protein that is associated with the contractile apparatus and found to be highly specific to SMC (Gimona, M., *et al.* 1990) were used as an index of a more differentiated phenotype.

1.4.2 SM α-actin

SM α-actin is the most abundant protein expressed in SM cells and is the most extensively studied protein in regard to VSM cells (Gabbiani, G., *et al.* 1981). The important role of SM α-actin for vascular contractility was demonstrated in SM α-actin null mice which had compromised vascular contractility, lowered blood pressure and reduced blood flow in aortic segments (Schildmeyer, L.A. *et al.* 2000). SM α-actin is routinely used to classify cells as VSMCs but its specificity is less than perfect since SM α-actin may be found in fibroblasts (Desmouliere, A., *et al.*, 1992). This is one of the reasons why the use of several markers is recommended to gauge differentiation state in SMC.

1.4.3 Calponin

Calponin is a thin filament binding protein found in SMC and is believed to be involved in the contractile process. Calponin binds to F-actin, producing an inhibitory effect on actin-activated Mg^{2+}-ATPase activity of myosin, without

having an effect on the phosphorylation of the myosin light chain (Abe, M., *et al.* 1990, Kolakowski, J., *et al.* 1995). Confocal imaging has demonstrated that calponin is located in the thin filaments present throughout the cell and that during contraction both calponin and myosin light chain kinase are phosphorylated (Carmichael, J.D., *et al.* 1994). Calponin inhibits the myosin-actin interaction by binding to actin (segment 145-182), (Abouzaglou, J., *et al.* 2004) in a Ca^{2+}-independent manner (Winder, S.J. and M.P., Walsh, 1993), changing the conformation of actin (Noda, S., *et al.* 1992). Recent studies have shown that calponin also binds to microtubules (Fattoum, A., *et al.* 2003). The physiological importance of calponin remains unclear, since a calponin knockout mouse model, showed no change in the sensitivity of the contractile apparatus to changes in intracellular Ca^{2+} but actin expression was reduced (25%-50%) (Matthew, J.D., *et al.* 2000).

1.5 SMC structural machinery

The SMC structural machinery consists of the cytoskeletal apparatus (1.5.1) and the contractile apparatus, with SM α-actin and myosin as major constituents (1.5.2). The connection between the cytoskeleton and the contractile apparatus occurs at cytoplasmic dense bodies, α– actinin rich structures, which are distributed throughout the cytoplasm. The linkage between the cytoskeleton and the contractile machinery was demonstrated by Flavahan and co-workers who following remodelling of the cytoskeleton measured alterations in arteriolar contraction (Flavahan, N.A., *et al.* 2004). The cytoskeleton is thought to couple the contractile machinery to the cell membrane and hence to other cells and the

extra cellular matrix (ECM) but is not believed to otherwise be involved in contraction.

1.5.1 Cytoskeleton

The flexibility and complexity of eukaryotes depends entirely on filaments, collectively called the cytoskeleton. The cytoskeleton is a protein framework that enables an eukaryotic cell to maintain or change its shape and its degree of attachment to the substratum in response to extracellular signals. The fibers of the cytoskeleton can provide rigidity, in other cases the entire structure may disassemble and remodel within minutes (Ahmadian, M.R., *et al*. 2002).

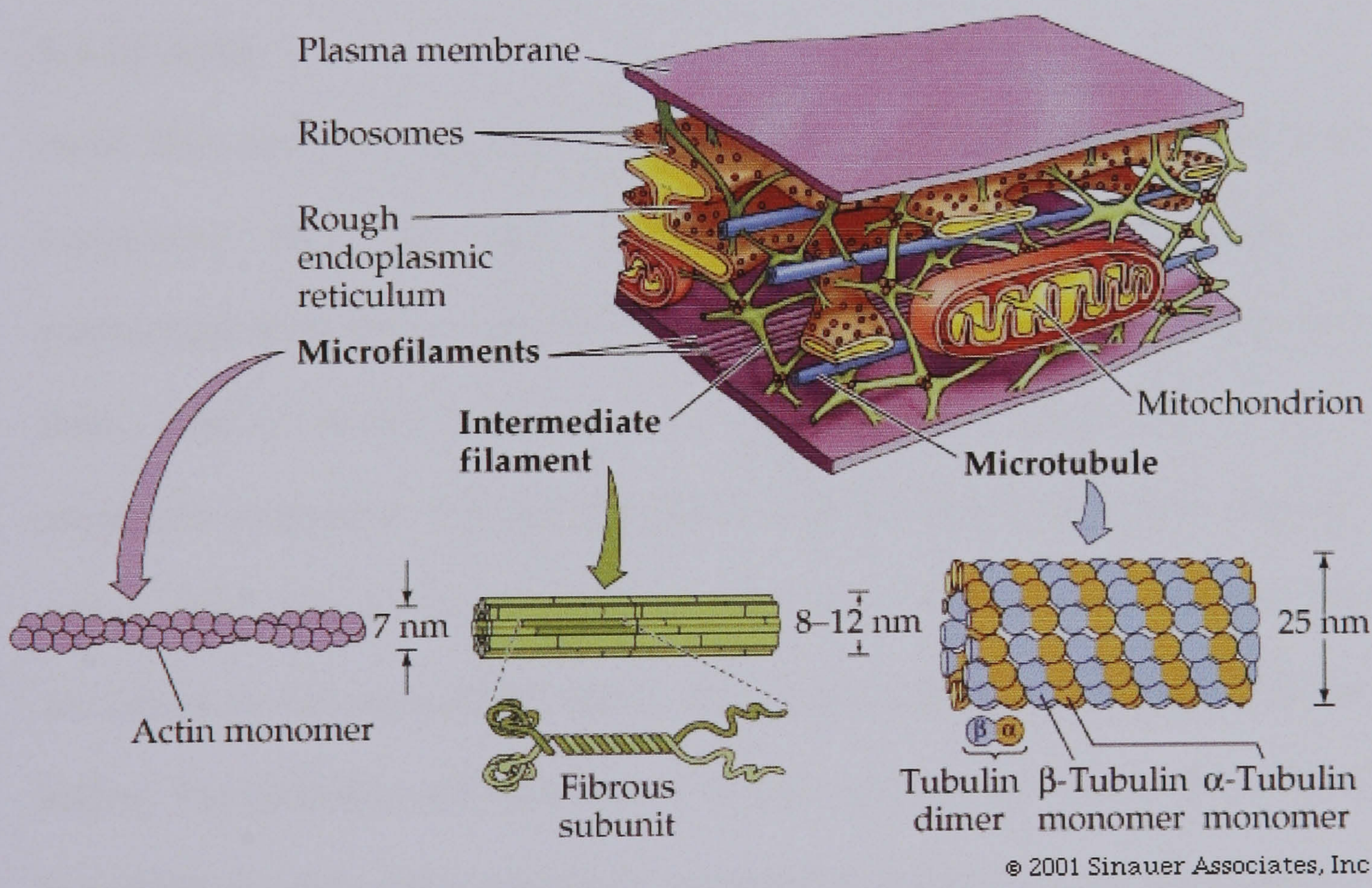


Figure 1.2. Illustration of cellular structures. The three major cytoskeletal proteins Actin, intermediate filaments and microtubules. Figure taken from (www.uic.edu).

The three major cytoskeletal elements are actin, microtubules and the intermediate filaments (Small, J.V., *et al.* 1999). Though, it is only actin and intermediate filaments that become associated with cell-cell and cell-matrix junctions. In addition to the three major types of protein filaments the actin cytoskeleton also contains many different accessory proteins, such as filamin, spectrin, α-actinin, and profiling, that either link the filaments to one another or to other cell components such as PM or influences the rate and extent of actin polymerisation (McGough, A., *et al.* 1998). For example, the connection between cytoskeleton and the contractile machinery occurs at cytoplasmic dense bodies and α-actinin rich structures which are distributed throughout the cytoplasma.

1.5.1.1 Actin

Actin filaments (also called microfilaments) are the most abundant cytoskeletal component. They form rope like threads of two intertwined strands of polymerised actin with a diameter of about 7nm (see figure 1.2). In its monomeric form, actin is usually referred to as Globular-actin (G-actin). When these monomers polymerise they associate head-to-tail yielding Filamentous actin (F-actin). Actin stress fibers are bundles of actin filaments that traverse the cell and are linked to the extracellular matrix (ECM) through focal adhesions or dense bodies. The assembly and disassembly of the actin filaments (F-actin) is needed to provide the cells with a contractile apparatus or prepare them for migration and proliferation and polymerisation of this framework is particularly critical for differentiated vascular function (Janmey, P.A., *et al.* 1998; Worth, N.F., *et al.* 2001). In cultured cells F-actin is generally organised into a number of discrete structures: Filopodia, a finger-like protrusion, contain a tight bundle of long actin

filaments in the direction of the protrusion; Lamellipodia, thin protrusive actin sheets, dominates the edges of many motile cells; Membrane ruffles, observed at the leading edge of the cell, result from lamellipodia that lift up off the substrate and fold backward (Small, J.V., *et al.* 1981).

1.5.1.2 Microtubules

Microtubules are strong, rigid fibres frequently packed in bundles with a diameter of about 22nm. Microtubules are composed of a protein called tubulin and dimers of α- and β-tubulin constitutes the building blocks in the composition of 13 filaments (profilaments) that encircles the hollow core (see figure 1.2). Microtubules radiate from a point in centre of the cell, near the nucleus and only occasionally extend to the edge of the cell. Besides serving as a kind for internal skeleton in the cytoplasm microfilaments also form the mitotic spindle during mitosis. During mitosis, the structure of the nucleus breaks down and is replaced by a cage-like spindle (largely composed of microtubules) that pulls the chromosomes apart after duplication. This suggests its role is in moving and redistribution of components within the cell (Nogales, E., *et al.* 2000; Desai, A. and T.J. Mitchison., 1997).

1.5.1.3 Intermediate filaments

Intermediate filaments, as its name implies, are intermediate in diameter (10nm) between actin filaments and microtubules. Assembled monomers form a rope-like structure made up by several monomers intertwining together (see figure 1.2). Most intermediate filaments are long, and form a meshwork that lines the inside of the nuclear envelope and extends outward from the nucleus to the periphery of

the cell (Chang, L. *et al.* 2004). These filaments are most prevalent in static cells, such as skin and heart muscles cells, which have to resist externally applied forces, indicative of its role in strengthening the cell, in particular against pulling and shear stresses.

1.5.1.4 Regulation of cytoskeleton

1.5.3.4.1 RhoA

RhoA is an important regulator of cytoskeleton and actin polymerisation and links between the level of RhoA activity and G- and F-actin ratios have been demonstrated (Hall, A. *et al.* 1999; Sotiropoulos, A., *et al.* 1999). The GTPase Rho has been shown to be required for many actin-dependent cellular processes, such as platelet aggregation, lymphocyte and fibroblast adhesion, cell motility, contraction, and cytokinesis (Narumiya, S., *et al.* 1997). Direct evidence for the involvement of Rho in stress fiber formation was obtained from microinjection of constitutively active Rho into quiescent fibroblasts that resulted in the induction of stress fibers and the appearance of focal adhesions (Ridley, A.J. and A. Hall, 1992). Focal adhesions are the regions where stress fibers are anchored to the plasma membrane and where the cell adheres most tightly to the substratum. The cytoplasmic components of focal adhesions include cytoskeletal proteins such as α-actinin, vinculin, talin, scaffolding proteins such as paxillin and signalling molecules such as the focal adhesion kinase, FAK (Burridge, K. and M. Chrzanowska, 1996). Blocking RhoA or RhoA kinase p160 interferes with the organisation of actin into stress fibers and coronary SMC differentiation during embryonic development as well as vascular remodelling during atherogenesis (Lu, J., *et al.* 2001; Morishige, K., *et al.* 2001). RhoA has been shown to promote

focal adhesion and stress fibre formation, whilst rac and cdc42 induce lamellopida and filopodia formation respectively (Hall, A. and C.D., Nobes, 2000; Machesky, L.M. and A. Hall, 1997). These phenomena are important in wound healing, bone remodelling, phagocytosis, embryonic cell migration and neurogenesis. Rho A also acts on the contractile apparatus by inhibiting myosin phosphatase via Rho-kinase, this leads to Ca^{2+} sensitization (Uehata, M., *et al.* 1997).

1.5.3.2.2 PIP_2

Phosphoinositides, such as PIP_2 are involved in the regulation of actin cytoskeletal assembly (Meiri, K.F., *et al.* 2004). It has been shown that PIP_2 synthesis is regulated by Rho A. Chong *et al.* demonstrated that GTPγS, a non-hydrolysable analogue of GTP that activate G-proteins (1.6.1), stimulated PIP 5-kinase activity in cell lysates and that this was blocked by botulinum C3 exoenzyme, a specific inhibitor of Rho A. GTP-bound recombinant Rho A stimulated PIP 5-kinase activity, whereas GDP-Rho A was much less potent and GTP-bound Rac was ineffective. In addition, microinjected botulinum C3 exoenzyme diminished calcium mobilization in response to PDGF or thrombin, whereas this decrease was reversed following microinjection of activated Rho A (Chong, L.D., *et al.* 1994). PIP_2 also interacts with a number of actin binding proteins such as profilin (Sohn, R.H., *et al.* 1995) and gelsolin (Janmey, P.A. and T.P. Stossel, 1989). Banno and colleagues examined the interaction between gelsolin, PLC isoforms and PIP_2 hydrolysis in human platelets. These authors also demonstrated that free gelsolin, but not in complex with actin, inhibited PIP_2 hydolysis to varying extents. (Banno, Y., *et al.* 1992).

1.5.2 Contractile apparatus

Contraction in smooth muscle is a product of the interaction between actin and myosin coupled with ATP hydrolysis. The degree of this interaction is determined by the net level of phosphorylation of the 20-kDa myosin light chain, which, in turn, is dependent on the relative activities of myosin light chain kinase (MLCK) and myosin light chain phosphatase (MLCP). MLCK is activated by Ca^{2+}-bound calmodulin (Figure 1.3).

1.5.2.1 Calcium – a rise in calcium induces contraction

A rise in cytoplasmic intracellular calcium is the major signal for contraction in smooth muscle, cardiac as well as skeletal muscle. But the mechanism by which Ca^{2+} activates crossbridge formation differs markedly between cardiac, skeletal and smooth muscle (Lipp, P. and E. Niggli, 1996). The calcium ion (Ca^{2+}) is an almost universal intracellular messenger, controlling a diverse range of cellular processes, such as gene transcription, muscle contraction and cell proliferation (Berridge, M.J., *et al.* 2003; Clapham, D.E., *et al.* 1995). However, although these different cellular activities require Ca^{2+}, Ca^{2+} does not necessarily activate the same signalling pathways. Instead, cells employ different components selected from the "Ca^{2+} signalling tool kit", as befits their physiology.

1.5.2.2 Contraction of vascular smooth muscles

When SMCs are at rest the intracellular Ca^{2+} concentration is ~10-100nmol (Bukoski, R.D., *et al.* 1989; Jensen, P.E., *et al.* 1992). However, when SMC are stimulated by various means (e.g. depolarization, mechanical deformation or hormones) cytosolic Ca^{2+} concentration increases to levels of 10-100μmol Ca^{2+} or more (Bolton, T.B., *et al.* 2002).

Contractile force begins to develop shortly after a rise in intracellular calcium. The delay (>200msec) is attributable to time required for three biochemical reactions to occur (figure 1.3): the first step in the pathway for smooth muscle contraction is for calcium in the muscle cell to combine with calmodulin. The calcium/calmodulin complex activates myosin light chain kinase (MLCK) that following activation catalyses the phosphorylation of serine on myosin light chain. Phosporylated myosin leads to myosin-actin crossbridging, which results in contraction (Somlyo, A.V. and A.P. Somlyo, 1993). Myosin of SM, in common with myosin with non-muscle cells, is able to interact with actin only when phosphorylated. Concurrently myosin light chain phosphatase (MLCP) removes the phosphate from the myosin, opposing muscle cell contraction. When MLC is dephosphorylated the myosin cannot interact with actin and the muscle relaxes. Smooth muscle relies on actin and myosin and the cross-bridge cycling mechanism to cause cell shortening in the same way as skeletal and cardiac muscle.

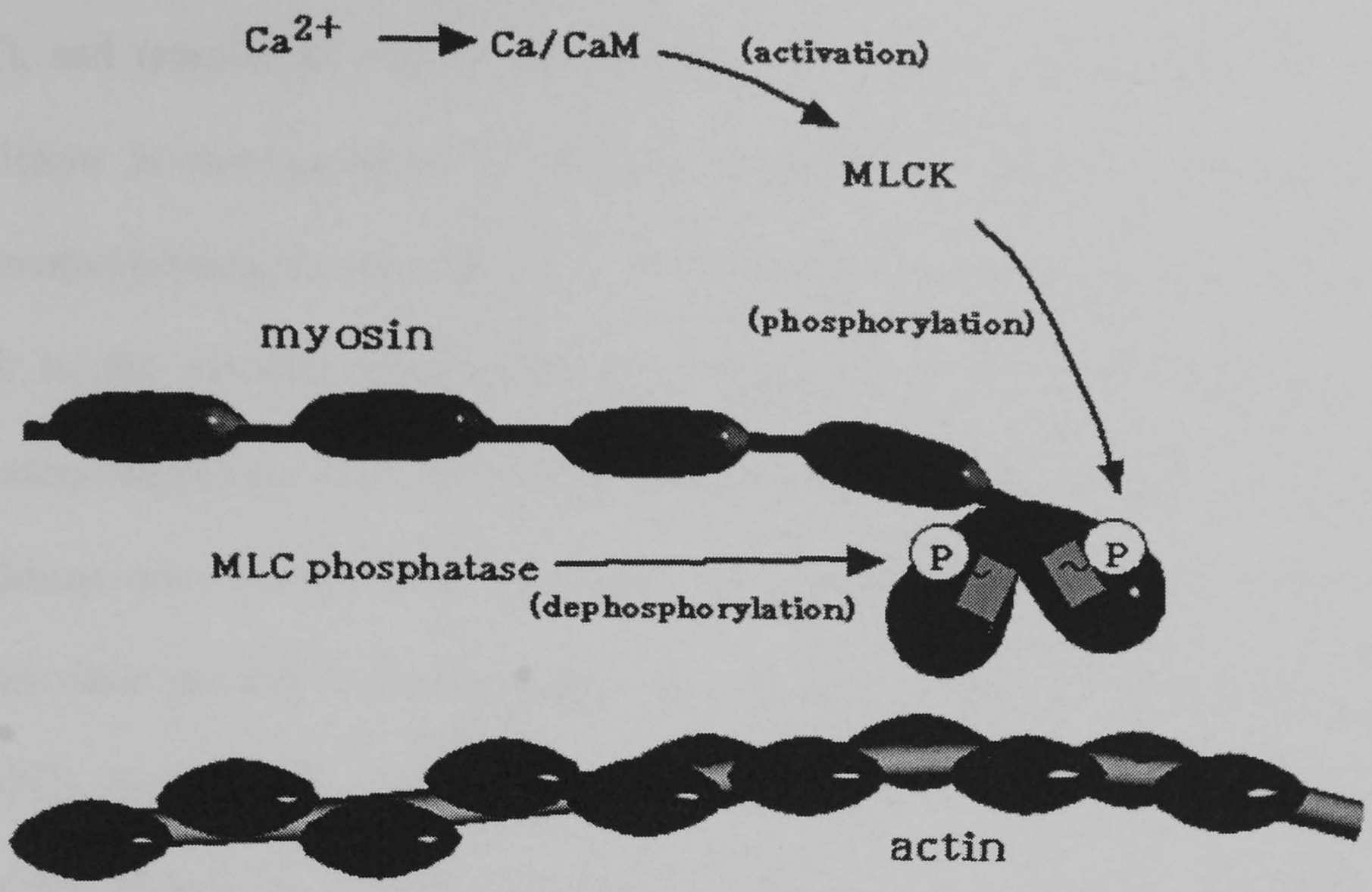


Figure 1.3. Illustration of smooth muscle contraction. The illustration shows the mechanism by which an increase in intracellular calcium, $[Ca^{2+}]_i$ stimulates VSM contraction. The free calcium binds to a special calcium binding protein called calmodulin. Calcium-calmodulin activates myosin light chain kinase (MLCK), an enzyme that is capable of phosphorylating myosin light chains (MLC) in the presence of ATP. Myosin light chains are 20-kD regulatory subunits found on the myosin heads. MLC phosphorylation leads to cross-bridge formation between the myosin heads and the actin filaments, and hence, smooth muscle contraction.

Vascular smooth muscle contractility can be regulated at different levels: through the mechanism for controlling $[Ca^{2+}]i$; by the mechanism for transduction of the Ca^{2+} signal to activate the contractile apparatus and/or by altering the sensitivity of the contractile machinery to $[Ca^{2+}]i$. The concentration of intracellular calcium depends upon the balance between the calcium that enters the cells, the calcium

that is released by intracellular storage sites (largely the Sarcoplasmic reticulum, SR), and removal of calcium either back into storage sites or out of the cell. Calcium is re-sequestered to the SR by an ATP-dependent calcium pump (sarco(endo)plasmic reticulum Ca^{2+}-ATPase, SERCA) and is removed from the cell to the external environment by either a ATP-dependent calcium pump (plasma membrane Ca^{2+}-ATPase (PMCA) or by the sodium-calcium exchanger. Calcium entry occurs partly through voltage-gated Ca^{2+} channels (VOC) that open when the cell is depolarised and partly through receptor-operated channels (ROC) (Bolton, J.P., *et al.* 1979; Del Valle-Rodriguez, A., *et al.* 1994). The opening probability of voltage-dependent channels can be influenced by second messengers produced in response to receptor occupation (Bezanilla, F., *et al.* 2000). Release of calcium from internal stores can occur as a result of Ca^{2+}-induced Ca^{2+} release (CICR), due to ryanodine receptors (RyR) or through inositol-1,4,5- trisphosphate-induced Ca^{2+} release (IICR) mediated by IP_3-receptors (Burdyga, T., and S. Wray, 2002; Lee, Y.H., *et al.* 1996). Many vasoconstrictors stimulate the activity of Phospholipase C (PLC), which hydrolyses PIP_2 to give IP_3 and DAG. Subsequently, IP_3 binds to IP_3 - receptors on the SR, (the main storage site of releasable $[Ca^{2+}]_i$) resulting in the release of stored $[Ca^{2+}]$i in the cytoplasm. The precise role of RyR in VSMC is less well understood but this mechanism also seems to contribute to agonist-induced release of Ca^{2+} from the SR.

Increased phosphorylation of smooth and non-muscle myosin can be effected not only by an increase in $[Ca^{2+}]_i$, which activate MLCK, but also by inhibition of MLCP (Somlyo, A P. and B. Himpens, 1989). The inhibitory signal for calcium

sensitization is communicated by RhoA to a Rho-kinase that phosphorylates the myosin regulatory subunit (Fujihara, H., *et al.* 1997; Taggard, M.J., *et al.* 1999) and similarly the 17-kDa Protein Kinase C (PKC) activated phosphatase inhibitor CPI-17 causes MLCP inhibition and thereby inhibits the catalytic activity of MLCP, resulting in increased myosin phosphorylation and subsequently contraction (Eto, M., *et al.* 2004).

1.6 Cells signalling and transduction

There are several signal transduction mechanisms that modulate intracellular calcium concentration and therefore the state of vascular tone. Two different mechanisms will be described here: G-protein-coupled pathway (1.6.1) and phosphatidylinositol pathway (1.6.2).

1.6.1 G-proteins – signal transducers

GTP binding proteins, often referred to as G-proteins, are transducers of information acting as a signal mediator between the receptor site and effectors. They function as molecular switches and transiently convey information by being turned on and then quickly turned off again (see figure 1.4). This efficient function has resulted in their involvement in the regulation of many aspects of cell growth, differentiation, gene expression, and cell movement. As a group, they form a universal mechanism that allows a cell to adapt to its surroundings

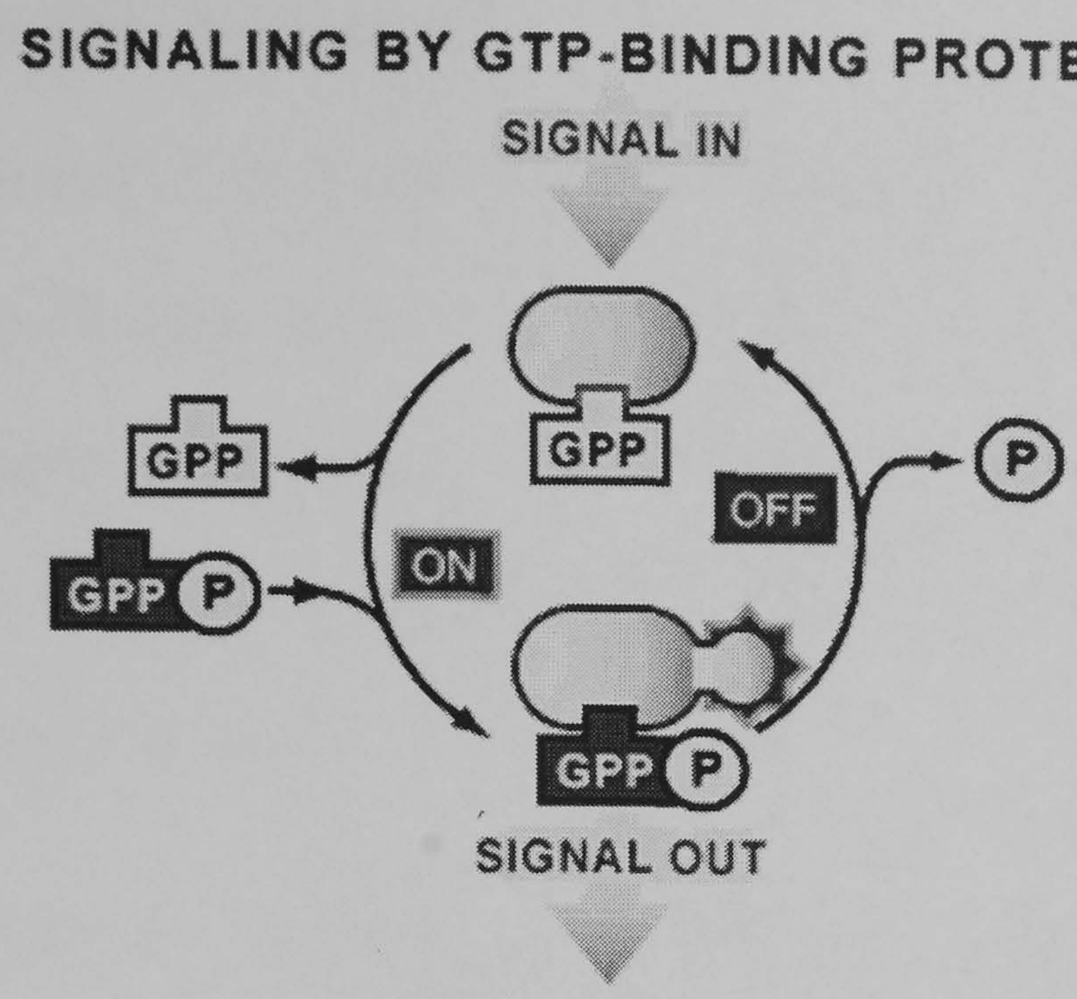


Figure 1.4 Illustration of GTP-binding protein. G-proteins function as molecular switches, controlled by a GTPase cycle, shuttling between an active GTP-Mg2+-bound "on"-state and an inactive GDP-Mg2+ bound "off" state (www.bioteach.ubc.ca/CellBiology/GProteins).

The wide range of G-proteins is divided into the following three groups: Heterotrimeric; Monomeric and Unconventional G-proteins. Heterotrimeric G-proteins are composed of three subunits α, β and γ and are found to associate with receptors in cells. These receptors (called G-protein-linked receptors) are the largest group of surface receptors known in mammals. They respond with a wide range of extracellular signals (including hormones and neurotransmitters) and span the membrane of the cell. The α-subunit is the "messenger" between receptor site and effecter. In the inactive state, the α- subunit binds to GDP and the three subunits are attached together. Conformational change of receptor, following ligand binding, result in exchange of GDP to GTP of α-subunit leading

to its activation resulting in decreased affinity to the β- and γ- subunits resulting in their dissociation. The separated α- and/or β- and γ- subunits can then interact with their effector. After α-subunit has activated the effecter it returns to the resting state by cleaving the GTP, binding again to GDP and reuniting the β and γ subunit. Examples of members of this family are: Gs – activating adenylate cyclase; Gi – inhibiting adenylate cyclase; Gq – activating PLCβ and G_{12} – activating Phospholipase D.

Small G-proteins are monomers with molecular weight of 20-40 kDa. Like heterotrimeric G proteins, their activity depends on the binding of GTP and its subsequent hydrolysis. Normally, in the absence of stimulation, they are bound to GDP and inactive. Upon the reception of a signal, they exchange GDP for GTP and become active. They differ in their mode of activation from heterotrimeric G-proteins by not being directly associated with the receptor. Instead, small GTPases are several steps away from the receptor (often termed an enzyme-linked receptor) that ultimately cause their activation. In between are a variety of adaptor proteins that are activated by the enzyme-linked receptors. Once in the active state, the GTPase will initiate a cascade in which a series of proteins will phosphorylate each other to transmit the signal. More than 100 small G proteins have been identified. They are classified into five families: Ras, Rho, Rab, Ran and Arf (Hall, A., *et al*. 1990).

Unconventional G-proteins differ from both heterotrimeric and small G-proteins, an example is Tissue transglutaminase (TGII), which stimulates $PLC\delta_1$ and possesses an unconventional GTP binding pocket. The main focus on this thesis is the study of this unconventional G-protein and its association with $PLC\delta_1$.

1.6.2 Inositol Phospholipid signalling pathway

A role for inositol phopholipids in signal transduction was first recognised by Mabel and Lowell Hokin (1953), who discovered an increased turnover of radioactive phosphate into phosphatidylinositol (PI), a minor phospholipid, upon stimulation of muscarinic acetylcholine receptors in pancreas (Hokin, M.R., *et al* 1953). It was later shown that this incorporation results from the breakdown and subsequent re-synthesis of inositol phospholipids. The inositol phospholipids found to be the most important in signal transduction are two phosphorylated derivatives of PI, PI-phosphate (PIP) and PI (4,5-) biphosphate (PIP_2). These two phospholipids are thought to be located mainly in the inner half of the plasma membrane lipid bilayer. The chain of events leading to PIP breakdown begins with activation of Phosphoinositides-specific phospholipase C (PLC), which hydrolyses PIP_2 to generate two second messengers: 1,2 - diacyl glycerol (DAG) and Inositol 1,3,5-triphosphate (IP_3). Inositol triphosphate (IP_3) is a small water-soluble molecule that leaves the plasma membrane and rapidly diffuses through the cytosol. Upon binding to and opening IP_3-gated calcium release channels in the SR membrane calcium is released and consequently leading to a rise of calcium in the cytosol. The other cleavage product DAG remains embedded in the membrane, where it has two potential signalling roles. First, it can be further cleaved to release arachidonic acid, which can either act as a messenger in its own right or be used in the synthesis of other small lipid messengers called eicosanoids. The second and more important function of DAG is to activate a crucial serine /threonin protein kinase called Protein kinsase C (PKC).

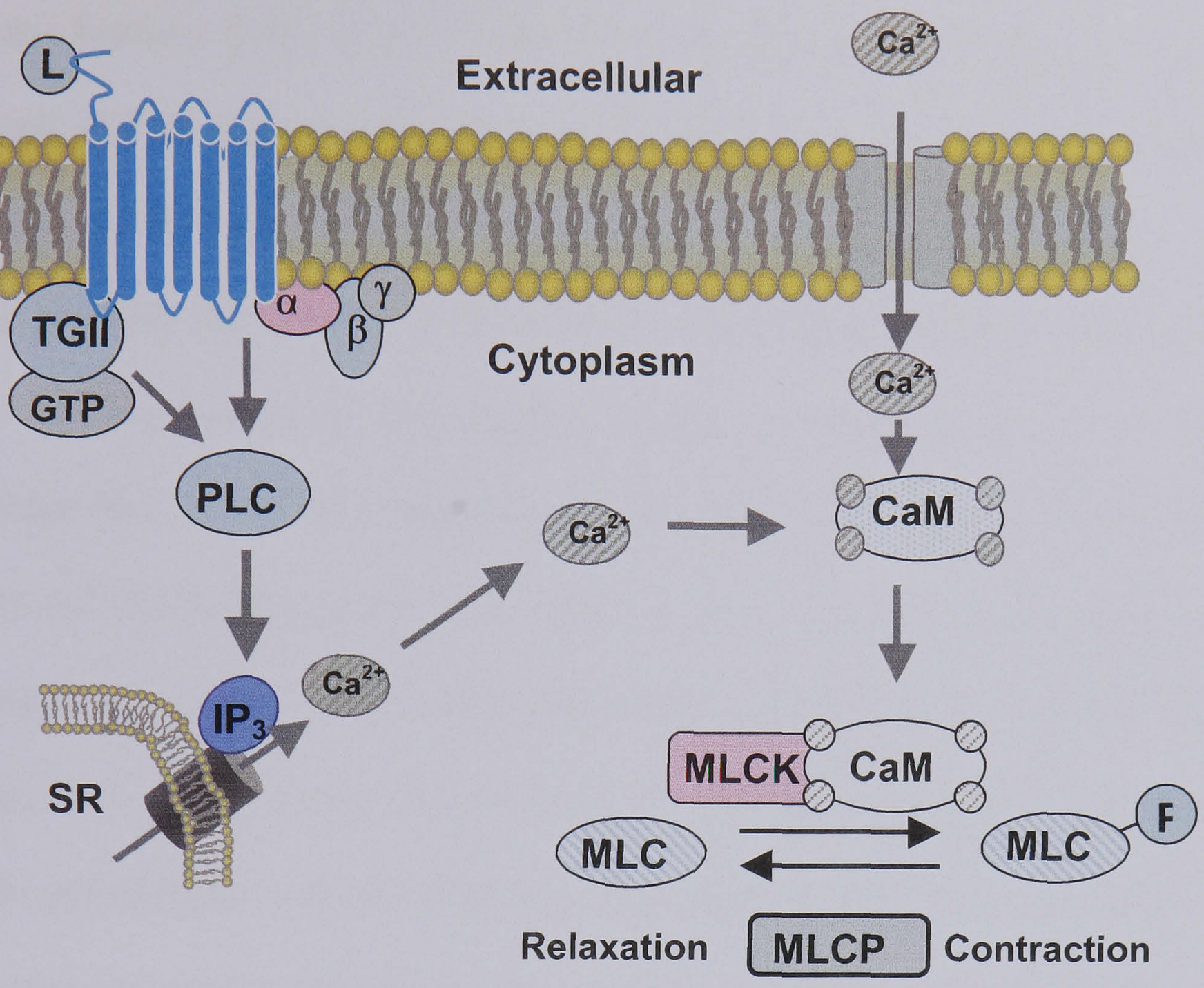


Figure 1.5. Rise in intracellular calcium by store release and calcium entry. Agonist activated receptor stimulate the activity of Phospholipase C (PLC), resulting in hydrolysis of Phosphoinositide (4,5-) biphosphate (PIP_2) generating Inositol 1,3,5-triphosphate (IP_3) and 1,2 - diacyl glycerol (DAG) (not included in picture). Binding of and opening of IP_3-channels in the sarcoplasmic reticulum (SR) membrane result in a rise in cytosolic calcium. An increase in calcium by calcium entry and store release trigger an event of signals, involving calcium binding to Calmodulin (CaM), which activate myosin light chain kinase (MLCK) that phosphorylate myosin light chain (MLC), which enabling its binding to actin, with the final result being contraction.

1.7 Phosphoinositied-specific phospholipase C (PLC) pathway

The first report of PLC activity was made by Sloane-Stanley in brain suspension (Sloane-Stanley, G.H., *et al.* 1953). Early observations by Hokin (1953) and Michell (1975) demonstrated the role of PLC as a key enzyme in agonist-stimulated PI metabolism and calcium signalling (Hokin, M.R. and Hokin, L.E., 1953; Michell, R.H., *et al.* 1975). Further work revealed the direct link between PLC and the release of intracellular calcium stores (Streb, H., *et al.* 1983; Berridge, M.J., *et al* 1987). Rhee *et al.* isolated and sequenced mammalian PLCβ, PLCγ and PLCδ (Rhee, S.G., *et al.* 1991). PLCβ is shown to be regulated by G-protein (Taylor, S.J., *et al.* 1991) whilst PLCγ is regulated by tyrosine kinases (Vega, Q.C., *et al.* 1992). The twelve PLC isoforms identified to date are all single polypeptides and are divided in four families based on their amino acid sequence and size [β (4),γ (2),δ (4),ε (1), η(1)] (Cockroft, S. and G.M. Thomas, 1992; Rhee, S.G. and Y.S. Bae, 1997; Kelley G.G., *et al.* 2001, Stewart, A.J., *et al.* 2005). All PLC isoforms recognise phosphatidylinositol (PI), phosphatidylinositol 4-monophosphate (PIP) and PIP_2 and carry out the Ca^{2+}-dependent hydrolysis of these lipids, though apart from variation in amino acid sequence and size they also differ significantly in their mode of activation. (Rhee, S.G., *et al.* 2001).

1.7.1 Structure and catalytic function of PLC isoform

Structural analysis of the PLC family revealed that it is a multidomain and calcium binding protein. The presence of a pleckstrin homology (PH) domain indicates membrane attachment and is consistent with its role as a signalling protein. Insights into the structure of the PLC family members has been gained

from work of the 2.4 Å crystal structure of mammalian PLCδ_1 (Essen, L.O., *et al.* 1996) and the three dimensional structures of the isolated domains and groups of domains (Ferguson, K.M., *et al.* 1995; Kohda, D., *et al.* 1993; Pascal, S.M., *et al.* 1994; Grobler, J.A., *et al.* 1996). The sequences of the eukaryotic PLC contain a string of modular domains organised around a catalytic α/β-barrel formed from the characteristic X- and Y-box regions found in all PLC enzymes (Essen, L.O., *et al.* 1996). The PH domain, found in the amino-terminal, is a conserved lipid binding module (Yin, H.L. and M.L. Janmay, 2003) found mainly in proteins implicated in cellular signalling and cytoskeletal functions (Tuzi, S., *et al.* 2003). The PH-domain binds to charged headgroups of specific phosphorylated IP-lipids, produced in the plasma membrane, and in response to an extracellular signal they thereby enable the protein to dock onto the membrane and interact with other recruited signalling proteins. Four EF structure motifs within the EF-hand domain are distributed in two lobes, showing similar arrangement as described for calmodulin (Essen, L.O., *et al.* 1996). A single C2 domain immediately follows the Y-box region with an eight-stranded β-sandwich architecture and a calcium-binding region formed by flexible loops that coordinate binding of multiple calcium ions.

PLCδ_1, unlike PLCβ isoforms, does not have a long carboxyl tail and does not bind heterotrimeric G-proteins. Similarly PLCδ_1 is not tyrosine phosphorylated by activated growth factor receptors like PLCγ isoforms which contain the additional SH2 and SH3 domains. The Src homology 2 (SH2) domain binds to phosphorylated tyrosines in a particular peptide sequence on activated receptors or intracellular signal proteins whilst Src homology 3 (SH3) domains binds to a short proline rich amino acid sequence.

Structure of PLCδ_1

A



B

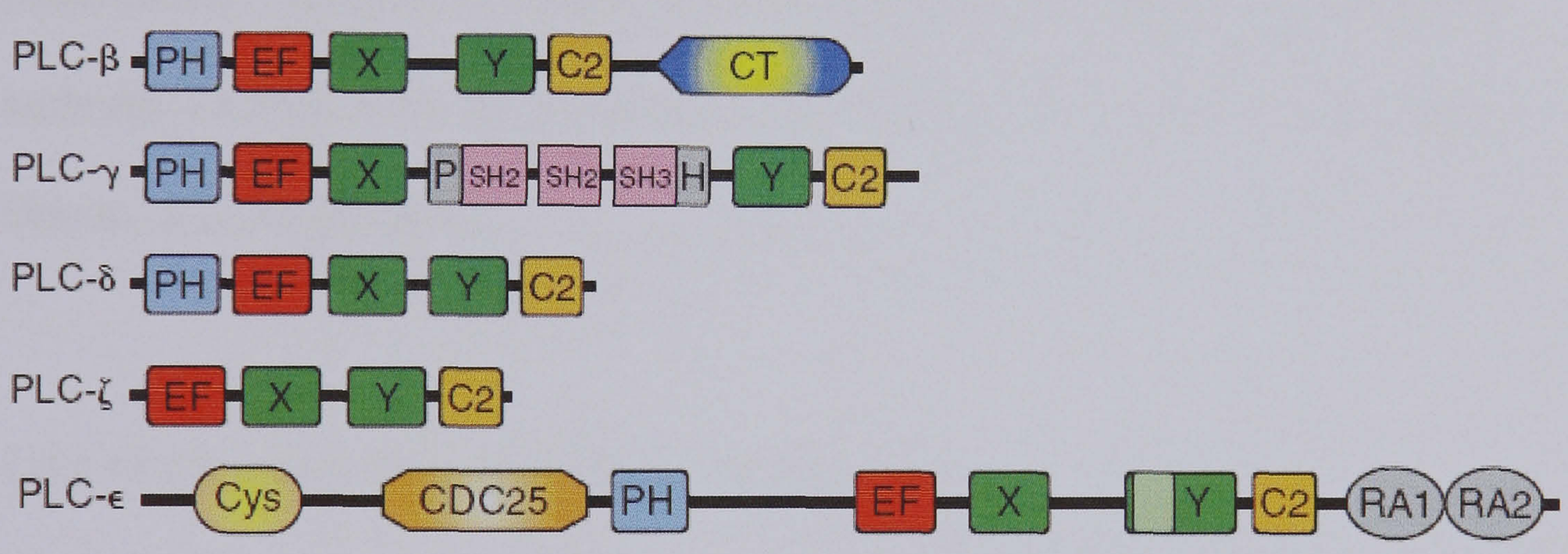


*Figure 1.6. Structure of PLCδ_1. (**A**). Crystal structure of PLCδ_1 (Essen, L.O., et al. 1996) thus lacking the PH domain which is presented separately (Ferguson, K.M., et al. 1995) and (**B**) a linear illustration of the multidomains found in PLC isoforms. PLCβ, δ and γ family members consists of four common domains: pleckstrin homology (PH) domain, the EF-hand domain, the catalytic domain (made up of X and Y regions) and the C2 domain (Ca^{2+}/lipid-binding domain). In addition PLCβ possesses a long carboxy tail; PLCγ a SH2-SH2-SH3 insert and PLCε contains a Cys, (cysteine-rich region), CDC25 (guanine nucleotide exchange domain conserved among guanine nucleotide) and RA1 and RA2 (Ras-associating domains) (Wing, M.R. et al. 2003).*

The diversity in primary structure together with different regional and cellular expression of the isoforms suggests that each isoform has a defined function and specific physiological role.

1.8 PLCδ

The δ-type of PLC, consists of four isoforms δ_1–δ_4 (Irino, Y., *et al.* 2004; Pawelczyk, T., *et al.* 1999) and PLCδ_1 is believed to be the most primitive PLC (Irvine, R., *et al.* 1996). Its existence in both lower and higher eukaryotes (yeast, slime model, filamentous fungi, plants and mammals) suggests that the other isoforms evolved from the archetypal PLCδ (Flick, J.S. and J. Thower, 1993; Drayer, A.L., *et al.* 1994).

1.8.1 PLCδ_1 expression and cellular localisation

PLCδ_1 has been found to be the predominant isoform of the PLC family in isolated blood vessel and primary cultured rabbit aortic VSMCs (Homma, Y., *et al.* 1993, Kato, H., *et al.* 1992, LaBelle, E.F. and E. Polyak, 1996). PLCδ_1 has been detected in various animal tissues and expression levels vary. PLCδ_1 is mainly a cytoplasmic protein (LaBelle, E.F., *et al.* 2002) and following activation PLCδ_1 associates with the cell periphery and areas of cell-cell contact (Paterson, H.F., *et al.* 1995). This subcellular localisation to the plasma membrane is eliminated following injection of PLCδ_1 mutants lacking the PH domain of part of its PIP_2 binding site. Expressing a chimera of green fluorescent protein (GFP) linked to the PLCδ_1-PH- domain cultured cell lines, have revealed that most of

the fusion protein localises to the plasma membrane (Stauffer, T.P., *et al.* 1998). The PH-PLCδ_1-domain binds PIP_2, which anchors the enzyme to the plasma membrane (PM) and enhances its catalytic activity (Garcia, P., *et al.* 1995; Yagisawa, H., *et al.* 1998). A recent in vitro study revealed the important role of the C2 domain for membrane targeting of PLCδ_1 (Ananthacayan, B., *et al.* 2002).

1.8.2 Regulation of PLCδ_1

There are two different stages of PLCδ_1 activation: binding to the membrane surface and interaction with the substrate PIP_2. Therefore, its activity depends on factors modulating the association of the enzyme with the lipid membrane and factors influencing the interaction of PLCδ_1 with the substrate. Despite being the earliest isoform of PLC in evolutionary terms (Irvine, R.F., *et al.* 1996) our knowledge of the mechanism of regulation of this enzyme remains unclear.

However, the role of GTP-binding proteins in regulating the activity of PLCδ_1 is now becoming clearer. Among other modes of regulation compelling evidence points to an atypical GTP-binding protein, Tissue transglutaminase (TGII) playing an important role in regulating PLCδ_1 activity in a number of tissues (Feng, J.F., *et al.* 1996; Hwang, K.C., *et al.* 1995; Murthy, S.N., *et al.* 1999). Homma & Emori isolated a novel rhoGAP protein, which had PLCδ_1 stimulatory activity (Homma, Y. and Y. Emori, 1995). Similarly, data from this laboratory have suggested a role for the monomeric G-protein RhoA in modulating PLCδ_1 activity. Partially purified PLCδ_1 from bovine aorta co-immunoprecipitates with a number of GTP-binding proteins including the monomeric GTP-binding protein RhoA while exoenzyme C3, which inhibits RhoA, has been shown to enhance the

activity of PLCδ_1 suggesting that RhoA acts as an inhibitory modulator of PLCδ_1 activity (Hodson, E., *et al.* 1998). Interestingly, the addition of GTPγS following exoenzyme C3 treatment resulted in a further increase in PLCδ_1 activity suggesting a dual regulation by GTP-binding proteins (Hodson, E., *et al.* 1999). Recently Guy *et al.* demonstrated that PLCβ_2 inhibited PLCδ_1 activity *in vitro* and in living cells (Guy, Y., *et al.* 2004) and hypertonicity in neurons has also been shown to influence PLCδ_1 activity (Caprini, M., *et al.* 2003).

1.8.3 Function of PLCδ_1

While the mechanism of PLCδ_1 regulation remained obscure so did the possible functions of this isoform. It is now recognised however that PLCδ_1 can act as an effector for receptor signalling with TGII coupling α_{1B}- and α_{1D} -AR in heart and liver cells (Baek, K.J., *et al.* 2001; Nakaoka, H., *et al.* 1994; Feng, J.F., *et al.* 1999), oxytocin receptors in human myometrium (Baek, K.J., *et al.* 1996) and thromboxane receptors (Vezza, R., *et al.* 1999). Unlike the PLCβ and PLCγ family members PLCδ_1 is not active at basal Ca^{2+} levels (~0.1μM) but is fully activated at calcium concentrations of 1-10μM (Pentyala, S.N. and M.J. Rebecchi, 2000; Pawelczyk, T. and A. Matechi, 1998). This makes PLCδ_1 the most calcium-sensitive of the PLC family members (~50-100 fold higher than PLCβ and PLCγ) PLCδ_1 has been suggested to play a role in calcium sensitisation, where it may amplify rather than initiate calcium-mobilizing signals (Allen, V., *et al.*, 1997). Measurements of the $InsP_3$ and Ca^{2+} levels in intact cells also support the idea that PLCδ_1 amplifies the PLCβ generated signal (Kim, Y.H., *et al.* 1999). Immunofluorescence studies of its binding partner p122RhoGAP

(p122) showed that this protein was present in focal adhesions and membrane ruffles, suggesting a role in regulation of the actin-cytoskeleton, (Kawai, K., *et al.* 2004). p122RhoGAP is also found in caveolin-enriched membranes (Yamaga, M., *et al.* 2004). Expression patterns of PLCδ_1 in skin with demonstration of an eight times greater proliferative activity of epidermal keratinocytes from PLCδ_1-deficient mice imply that PLCδ_1 may play an important role in regulating growth and differentiation (Nakamura, K., *et al.* 2003). Results from the same *in vivo* study also revealed that both heterozygous knockout mice of PLCδ_1 and homozygous knockout mice (PLCδ_1-deficient mice) appeared phenotypically normal and fertile and disruption of PLCδ_1 did not cause embryonic lethality.

1.8.4 PLCδ_1 -implication in disease

It has been suggested that PLCδ_1 is involved in Alzheimer's disease. Shimohama and co-workers have demonstrated that PLCδ_1 accumulates aberrantly in the brains of patients with Alzheimer's disease. In further study, using gel filtration chromatography they revealed that PLCγ_1 activity was significantly decreased and the PLCδ_1 activity was significantly increased in Alzheimer's disease brains compared with controls (Shimohama, S., *et al.* 1998). In vivo studies of PLCδ_1, using spontaneously hypertensive rats (SHR) Yagisawa *et al.* observed an augmented PLC activity in the SHR. Following hybridisation studies of an aortic cDNA library of SHR, cloning of PLCδ_1 cDNA and digestion studies they found an amino acid substitution, situated in the putative catalytic X domain of PLCδ_1. This substitution may be the major cause of the augmented PLC activity, possibly leading to hypertension-related phenonemoma such as abnormal calcium

homeostasis and increased intracellular calcium ion concentrations (Yagisawa, H., *et al.* 1991; Kato, H., *et al.* 1992). PLCδ_1 may contribute to the alterations in calcium homeostasis in myocardial ischemia. Hwang *et al.* demonstrated that in normal rat heart tissue PLCδ_1 was the most abundant isoform compared to PLCβ_1 and PLCγ_1. However, in ischemic heart and hypoxic neonatal cardiomyocytes, PLCδ_1, but not PLCβ_1 or PLCγ_1, was selectively degraded. Interestingly, by overexpressing PLCδ_1 in these hypoxic neonatal cardiomyocytes they demonstrated that the intracellular Ca^{2+} overload, induced by the ischemic conditions, was dramatically rescued (Hwang, K.C., *et al.* 2004). PLCδ_1 is also suggested to be implicated in remodelling (Pandey, S.C., *et al.* 1996). Findings by Panday and co-workers showed an increased PLCδ_1 expression with chronic ethanol exposure (4 days) of primary cultures of astorcytes, whilst no significant alteration of PLCβ, PLCγ, or α-subunit Gq/11 occurred.

1.9 Tissue transglutaminase

Heinrich Waelsch and colleagues identified the first transglutaminase more than 40 years ago as a liver enzyme incorporating amines into proteins (Mycek, M.J., *et al.* 1959). Tissue transglutamianse was discovered in 1989 (Nara, K., *et al.* 1989) and not until a few years later following microsequencing of a novel G-protein (TGII/Gh) did Nakaoka and co-workers demonstrate a high degree of similarity to human tissue transglutaminase II (TGII), and thus for the first time provided evidence that TGII not only possessed transglutaminase activity but also GTP-binding activity (Nakaoka, H., *et al.* 1994).

1.9.1 TGII is a member of the transglutaminase family

TGII is a member of a large family of at least nine transglutaminases, including plasma factor XIIIa, epidermal TG1, epidermal TG3, prostatie TG4, keratinocyte TG1, Tgase X, transglutaminases VI and VII (Greenberg, C.S., et al 1991; Aeschlimann, D., *et al.* 1998; Grenard, P., *et al.* 2001). These enzymes catalyze the formation of covalent -glutamyl-lysine bonds between proteins or polyamines and protein substrates. Such modifications play a role in different biological processes such as blood coagulation, epidermal differentiation or extracellular matrix organisation (Aeschlimann, D. and V. Thomazy, 2000; Esposito, C. and L. Caputo, 2005).

1.9.2 Structure of TGII

Recently Liu *et al.* reported the structure of TGII in complex with GDP (Liu, S., *et al.* 2002). The x-ray crystallographic model has six independent TG molecules, and they are organised as three dimers. The overall structure of TGII dimmer is shown in Figure 1.7A. Similar to other transglutaminases, each monomer of TGII consists of four domains: an amino-terminal β-sandwich (with a fibronectin and integrin binding site) and a catalytic core with an active site cysteine (Cys-277) that is important for transglutamination, followed by two carboxyl-terminal β-barrels of which the second contains the PLCδ_1 binding sequence (Liu, S., *et al.* 2002).

An earlier structural study performed by Iismaa *et al.* revealed that the N-terminal domain of TGII is required for its transglutaminase activity, whereas its core domain is essential for the hydrolysis of GTP and ATP (Iismaa, S.E., *et al.* 1997).

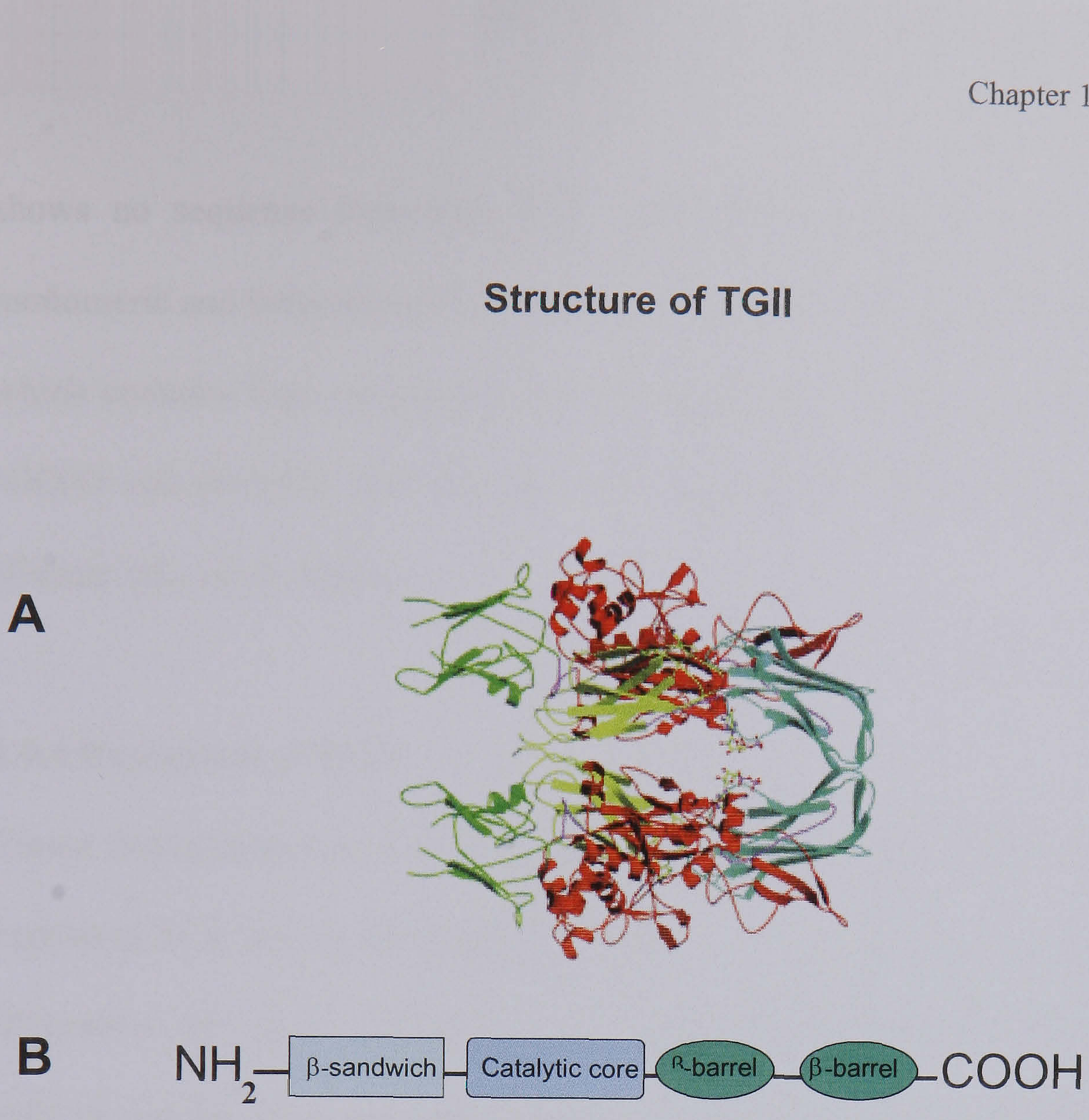


*Figure 1.7. Structure of TGII. (**A**).3-Dimensional structure GDP-bound TGII dimer (Liu, S., et al. 2002) and (**B**) an illustration of the multidomains that forms TGII.*

1.9.3 TGII has a unique GTP-binding pocket

TGII has a unique GTP-binding site, which has not been found in any other protein. The three nucleotide binding pockets are located between the catalytic core and the first β-barrel and formed by residues coming from both domains (Liu, S., *et al*. 2002). In the GDP- bound form access to the transamidation active site of TGII is blocked by two loops and the active site cysteine (Cys-277) is hydrogen-bonded to a tyrosine residue. The structure of the calcium bound TGII is unresolved. Iismaa *et al*. located GTP binding to a region involving amino acids 139-185 of the core domain (Iismaa, S.E., *et al*.1997). However, TGII

shows no sequence homology with other GTP-binding proteins such as the monomeric and heterotrimeric G-proteins, elongation factors, or dynamin, each of which contains four consensus GTP-binding motifs: GXXXXGK(S/T), DXXG, NXXD and (C/S)AX that fold into a structurally conserved GTP binding site (Iismaa, SE., *et al.* 2000).

1.9.4 Expression of TGII

Tissue transglutaminase (TGII) is ubiquitously expressed. TGII is constitutively expressed both during development (Nagy, L., *et al.* 1997) and in adult tissues (Piacentini, M., *et al.* 1995) and is abundant in smooth muscle and endothelial cells in arteries, veins and capillaries. TGII is also present in other organ-specific cells such as mesengial, renomedullary interstitial and colonic pericryptal fibroblast cells (Thomazy, V., and L. Fesus, 1989; Gendek-Kubiack, H. and E.G. Gendek, 2004). A high level of TGII expression is also found in macrophages (Murtaugh, M.P., *et al.* 1983) and chondrocytes (Aeschlimann, D., *et al.* 1993). In some cell types TGII expression is increased in response to retinoic acid (Ou, H., *et al.* 2000), IL-6 (Suto, N., *et al.* 1993), interferon-β (Nair, S., *et al.* 1994), TNF-α (Kweon, S.M., *et al.* 2004) and ionizing radiation (Gross, S.R., *et al.* 2003).

1.9.5 Cellular location of TGII

TGII is found in membrane, cytosolic and nuclear, with a higher level of GTP binding (GTPase) activity measured in membrane fraction whilst transglutaminase (TGase) activity is higher in cytoplasm (Park, H. *et al.* 2001). In nucleus it may associate with the pore complex (Fesus, L. and M. Piacentini, 2002). This variety in subcellular localisation of TGII may reflect its many

distinct biochemical functions (Milakovic, T., *et al.* 2004; Park, H., *et al.* 2001). Interestingly, TGII is also found extracellularly at the cell surface in association with the extracellular matrix (ECM) and have been reported to colocalize with β_1-integrin (Gaudry, C.A., *et al.* 1999). Interaction of a cell with its ECM can mediate a number of biochemical events important to cellular function. The ECM not only binds the cells together but also influences their survival, development, shape, polarity and behaviour (Bon-Gharios, G., *et al.* 2004).

1.9.6 GTPase and TGase activity of TGII

The two enzyme activities of TGII are mutually exclusive, and independently regulated. Receptor signalling activity requires GTP binding and upon binding of GTP the TGase activity is down regulated. On the other hand, the GTPase activity is down-regulated by calcium binding (Folk, J.E., *et al.* 1967). Several studies suggest that a conformational change is involved in the switch between the two different enzyme functions (Festoff, B.W., *et al.* 2002; Monsonego, A. *et al.* 1998). Although reciprocally regulated, TGase and GTPase activities are separable and can function independently. Following incorporation of a point mutation in GTP binding by site directed mutation of cDNA (position 480-452, S171E), expression of mutant TGII in COS-1 cells, resulted in an altered signal transduction whilst no effect on TGase activity was detected (Iismaa, S.E., *et al.* 2000). Similarly alteration of TGase activity by deletion of Cys-277 in the active site had no effect on the GTPase activity (Lee, K.N., *et al.* 1993).

In most in vitro studies the physiological level of GTP is higher than GDP and therefore conditions promote inhibition of TGase activity of TGII. It is therefore assumed that in physiological situations, TGase activity is turned off and TGII mainly acts as a G-protein. Studies have demonstrated that an increase in TGII following retinoic acid treatment or overexpression of TGII is not accompanied by an increase of its TGase activity. Therefore, to trigger TGase activity in cells requires both a decrease in the level of GTP and increase in intracellular calcium (Smethurs, P.A. and M. Griffin, 1996). In pathological situations these two events occur during cell senescence, degeneration or apoptosis. In physiological states, TGase activity of TGII is likely to be limited to the cell surface where guanine nucleotides are largely absent and [Ca^{2+}] concentrations are at the millimolar range (Mhaouty-Kodja, S., *et al.* 2004).

1.9.7 Regulation of TGII

TGII is regulated at both the transcriptional level and by post-translational mechanisms (Bailey, C.D., and G.V., Johnson, 2004). Retinoids act as direct regulators of tissue transglutaminase gene transcription in HeLa cells (Nagy, L., *et al.* 1996) and in macrophages (Chiocca, E.A., *et al.* 1988). Studies by Shan and Davies suggest that alterations in DNA methylation may be one of the mechanisms regulating TGII (Shan, L., and P.J. A. Davies, 1997). The expression of TGII is regulated by a variety of molecules including retinoids, interleukin-6, and transforming growth factor-β1 (TGF-β1) (Ritter, S.J., *et al.* 1997). Regulation of the TGII activity is accomplished through the binding of different cofactors. Apart from calcium (Folk, J.E., *et al.*1967) and guanine nucleotides (Lai, T.S., *et al.* 1993) other factors such as; nitric oxide (NO) (Lai, T.S., *et al.* 2001; Park,

K.C., *et al.* 2004), sphingosyl-lipophosphocholine (Lai, T.S., *et al.* 1997), PI3-Kinase (Antonyak, M.A., *et al.* 2002) and retinoids (Chiocca, E.A., *et al.* 1988) have been shown to regulate tissue transglutaminase. Recently, Chae *et al.*, showed a relation of pH and the dual enzymatic functions of TGII. Their in vitro study revealed a difference in optimal pH for GTPase activity (pH=7) and TGase activity (pH=9). In addition their study demonstrated evidence for the involvement of pH in TGII-mediated α_1-adrenoceptor signalling (Chae, K.J., *et al.* 2005).

1.9.8 Function of TGII

TGII is involved in a variety of cellular processes, including signal transduction (Nakaoka, H., *et al.* 1994), apoptosis and tissue stabilisation (Nicholas, B, *et al.* 2003; Nanda, N., *et al.* 2001), cell adhesion, spreading and migration (Gentile, V., *et al.* 1992; Fesus, L., *et al.* 2002), wound healing and bone ossification (Upchurch, H.F., *et al.* 1991).

1.9.8.1 TGII function with GTPase activity

TGII was until recently the only known transglutaminase family member with the ability to bind and hydrolyse GTP. However, recent studies have demonstrated that TGase5 and TGase 3 like TGII are dual-function enzymes with both a calcium-dependent transamidation activity as well as GTP binding and calcium-dependent GTP hydrolysis (Candi, E. *et al.* 2004; Ahvazi, B., *et al.* 2004). TGII acts as a G-protein that signals to PLCδ_1 when coupled to α_{1B}- and α_{1D}-adreno receptors in heart and liver (Feng, J.F., *et al.* 1998; Baek, K.J., *et al.* 2001), thromboxane (Vezza, R., *et al.* 1999) and oxytocin in myometrium (Baek, K.J. *et*

al. 1996). Activation of the receptor induces exchange of GDP for GTP and results in dissociation of GTP-TGII (α-) from the TGII (β-) subunit, (TGIIβ has recently been identified as calreticulin) (Feng, J.F., *et al.* 1999). GTP-bound TGII interacts with downstream effector PLCδ$_1$ (Park, E.S., *et al.* 1998 and Feng, J.F., *et al.* 1996), thereby resulting in phosphoinositide hydrolysis and release of Ca^{2+} from the SR. Deactivation of this signalling pathway is triggered by GTP hydrolysis and reassociation of TGII$_\alpha$ with a free TGII$_\beta$ subunit. Activation of transglutaminase activity of TGII is not required for coupling of α_1-adrenergic receptors to PLCδ$_1$ (Iismaa, S.E., *et al.* 2000). There appears to be an inverse relation between activation of PLCδ$_1$ by GTP-charged TGII and its intrinsic transamidation activity, which is suppressed by GTP and α_1-adrenergic stimulation (Baek, K.J., *et al.* 2001). GTP-bound TGII also regulates large conductance calcium activated potassium channels (Ca^{2+}-activated K^+- channels) in smooth muscle (Lee, M.Y., *et al.* 1997; Guo, Y., *et al.* 2004). Lee et al. measured by inside-out patch clamp of SMC a 2.5 fold increase in channel activity following addition of GTPγS and this was reversed when GDPγS was applied (Lee, M.Y., *et al.* 1997). Deactivation of this signalling pathway is triggered by GTP hydrolysis and reassociation of TGII$_\alpha$ with a free TGII$_\beta$ subunit. The GTPase activity of TGII has also been shown to be involved in regulation of cell cycle progression (Mian, S., *et al.* 1995) and protection of proteolysis of GTP bound TGII serves a dual function by inactivating transglutaminase activity and as well stabilising ATP/GTP hydrolysis. Cell surface TGII has been implicated in cell adhesion and migration in association with integrin- β_1 and β_3 subunits by a mechanism that is independent of TGII activity (Akimov, S.S., *et al.* 2000; Kang, S.K., *et al.* 2004). Kang *et al.* demonstrated how TGII modulates cell migratory

activity through the interaction of GTP (GTPγS)-TGII with integrins via the GFFKR motif located in the cytoplasmic tail of integrin subunits (Kang, S.K., *et al.* 2004). Akimov *et al.* showed how TGII promotes fibronectin assembly mediated by $\alpha_5\beta_1$ integrin and how this is also independent of transglutaminase activity (Akimiov, S.S., *et al.* 2001).

1.9.8.2 TGII function with transglutaminase activity

Transglutaminase activity has been shown to be involved in cell adhesion and cross-linking of interacting ECM (Verderio, E., *et al.* 1998). The crosslinking activity of TGII plays an essential role in generating tension in the matrix, as suggested by the fact that TGII-deficient cells and cells overexpressing inactive TGII display reduced ability to contract when exposed to a collagen lattice (Stephens, P., *et al.* 2004). One particular cell type, which is rich in TGase, is the human umbilical endothelial cell and it has been suggested that TGase is important in basement membrane stabilisation (Martinez, J., *et al.* 1994) and in fibrin stabilisation (Greenberg, C.S., *et al.* 1987) by this cell type. TGII has also been proposed to play a role in apoptosis, where it is thought to stabilize the integrity of the apoptotic cells, preventing the release of harmful intracellular components into the extracellular space and consequently prevent inflammation and scar formation (Johnson, T.S., *et al.* 2003). To clarify the implication of TGII in apoptosis De Laurenzi and Melino generated mice lacking TGase by homologous recombination techniques. They showed that the disruption of TGase did not produce a major phenotype and that apoptosis still occurred normally in the absence of TGase (De Laurenzi, V. and G. Melino, 2001). Their explanation was that either TGase was not involved in apoptosis or not crucial for apoptosis,

but it could be part of a regulatory or side pathway elicited only by specific inducers or only in specific tissues. Consistent with this latter proposal other studies in $TGII^{-1/-1}$ mouse found a deficiency of the clearance of apoptotic cells (Szondy, Z., *et al.* 2003). Recent studies demonstrate that cell damage or inflammation causes TGII secretion, which leads to formation of autoantibodies against TGII (Korponay-Szabo, I.R., *et al.* 2004; Mohan, K., *et al.* 2003) and that the TGII antibody inhibits transendothelial migration of $CD8^{+}$ T cell (Mohan, K., *et al.* 2003). Singh *et al.* have demonstrated, by overexpression studies that an increased transglutaminase activity results in an augmented transamidation of RhoA and consequently an increase in RhoA function as an active G-protein and increases binding to ROCK-2. This was confirmed by treatment of Monodansylcadaverine (MDC), an inhibitor of TGase activity, which blocked retinoic acid-stimulated interaction between RhoA and ROCK-2 (Singh, U.S., *et al.* 2001).

1.9.9 TGII and pathological implications

TGII is implicated in several pathological conditions, including fibrosis (Grenard, P., *et al.* 1999), atherosclerosis (Haroon, Z.A. *et al.*, 2001), AIDS (Amendola, A., *et al.* 2002), Alzheimer's (Citron, B.A., *et al.* 2001), Parkinson's (Andringa, G., *et al.* 2004) and Huntingdon's disease (Mastroberardino, P.G. *et al.* 2002). TGII is also implicated in cancer metastasis where its expression is found to be up-regulated in drug-resistant and metastatic breast cancer cells, and its role as a prognostic marker for the development of these phenotypes has been suggested (Mehta, K., *et al.* 2004). Transglutaminase activity is increased in the mucosa of patients with coeliac disease (D'Argenio, G., *et al.* 1989) and TGII is used as a

marker for the screening of this disease (Collin, P., *et al.* 2005; Lenhardt, A., *et al.* 2004).

It has been observed that TGII expression is increased in human failing heart (ischemic and dilated cardiomyopathy) and hypertrophic heart (Zhang, Z., *et al.* 2003). Zhang and co-workers demonstrated that TGII overexpression results in cardiac hypertrophy and apoptosis due to enhanced thromboxane A_2 receptor signalling that leads to extracellular signal-regulated kinase ERK1/2 activation. Similarly, TGII-coupled thromboxane receptors have also been associated with hypertrophy of neonatal rat cardiomyocytes (Lee, K.H., *et al.* 2003) and COX-2 dependent cardiac failure (Zhang, Z., *et al.* 2003). Hwang *et al.* showed that there is a down-regulation of TGII in the setting of cardiac dysfunction (Hwang, K.C., *et al.* 1996). However in a recent study of 8-10 weeks mice with inactivated TGII ($TGm2^{-/-}$) mice were found to be viable, phenotypically normal and with no detectable change in either blood pressure or left ventricular function (Nanda, N., *et al.* 2001).

TGII is thought to play a major function in tissue repair, suggested by reports of abnormal wound healing response and reduced machrophage activity in TGII knockout mice (Mearns, B., *et al.* 2002; Szondy, Z., *et al.* 2003). TGII is found to accumulate in cells undergoing terminal differentiation and in sites of tissue injury and inflammation and although TGII null mice developed normally defects in wound healing was revealed in adults (Echtermeyer, F., *et al.* 2001). TGII is rapidly upregulated during healing of skin wounds with the highest levels of TGII found in the early phase of the wound healing response (Haroon, Z.A. *et al.* 1999). Mearns and co-workers demonstrated a delayed skin wound healing in

$TG2^{-/-}$ mice. In addition fibroblast lacking TGII showed to migrate slower than mock transfected cells and these cells also failed to repopulate the wound (Mearns, B., *et al.* 2002).

1.10 TGII and PLCδ_1

1.10.1 Summary of TGII and PLCδ_1 association

Das *et al.* purified a 69kDa PLC complex with Gαh by incubating bovine liver membranes with α_1-agonist and GTP. In reconstitution studies they also showed how the three components effectively couple to each other (Das, T., *et al.* 1993). Similar results were confirmed by Nakaoka *et al.* who also identified Gαh as tissue transglutaminase, TGII (Nakaoka, H., *et al.* 1994). Using a 20 amino acid peptide from Gαh, containing the PLC binding region Hwang *et al.* showed for the first time how PLCδ_1 is structurally similar to 69kDa PLC and that PLCδ_1 is stimulated by TGII. Hwang *et al.* showed that TGII co-immunoprecipitated with PLCδ_1, but only in presence of GTP, and also how an increase in GTP concentration and consequent stimulation of GTP binding activity increased PLCδ_1 activity in a calcium dependent manner (Hwang, K.C., *et al.* 1995). Although studies have shown that calcium inhibits GTPase activity, the calcium chelator, EGTA also inhibits the coupling of TGII and PLCδ_1 suggesting that the presence of a certain level of calcium is needed for the interaction (Das, T., *et al.* 1993). Interestingly, stimulation of PLCδ_1 by GTP-bound TGII increases the sensitivity of PLCδ_1 to calcium leading to its stimulation by 0.1-5μM [Ca^{2+}], while PLCδ_1 enzyme activity showed less calcium sensitivity in presence of GDP or buffer alone (Baek, K.J, *et al.* 1993, 2001).

Further evidence for physiological interactions between TGII and PLCδ_1 is provided by the findings that TGII, or a small peptide corresponding to the TGII sequence 654-673, binds to and activates intact PLCδ_1 in cell lysates (Feng, J.F., *et al.* 1996). This same sequence, which is located near the carboxy terminus of TGII, is also required for coupling α_{1B} -adrenergic receptors to PLCδ_1 (Hwang, KC., 1995). Feng *et al.* found that there are multiple interactions between TGII and α_{1B}-AR and that binding occurs at three different sites. (Feng, J.F., *et al.*1999). An eight amino acid sequence (Leu^{665}-Lys^{672}) near the C-terminal on TGII was critical for recognition and binding of PLCδ_1 (Feng, J.F., *et al.* 1995). Beak *et al.* further characterised the PLCδ_1 -TGII complex and demonstrated that PLCδ_1 not only acts as guanine exchange factor (GEF) for TGII, promoting exchange of GDP to GTP but also stabilises the GTP-bound form of TGII and inhibits transglutaminase activity (Baek, K.J., *et al.* 2001).

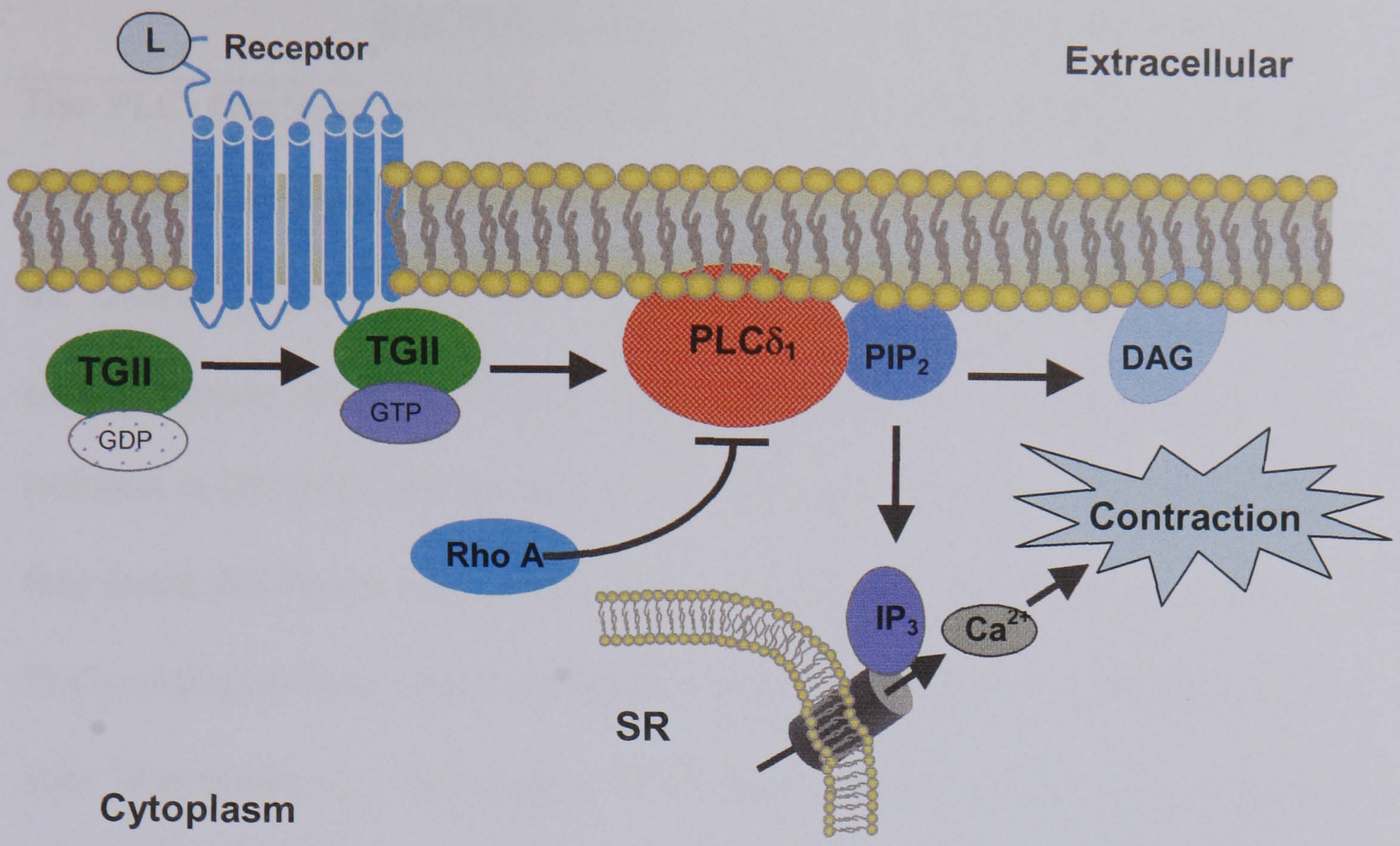


Figure 1.8. Illustration of Tissue transglutaminase (TGII) coupling of receptor to Phospholipase Cδ_1 (PLCδ_1). Briefly, once activated PLC hydrolyses PIP_2 to DAG (Diacylglycerol) and IP_3 (Inositol triphosphate), leading to rise in intracellular calcium and smooth muscle contraction.

Although TGII is implicated in coupling α_{1B}- and α_{1D} -AR to PLCδ_1 cotransfection of α_{q11} found to be more effective in coupling α_{1B}-adrenergic receptors to PLCδ_1 than is cotransfection of TGII in coupling to PLCδ_1 (Chen, S., *et al*. 1996 and Zhang, J., *et al*. 1999). The function of this association is unclear and more work is needed to clarify the relationships among the GTP-bound state of TGII, their transamidating potential, and the activated state of PLCδ_1.

BACKROUND AND EXPERIMENTAL STUDY

The PLC family of enzymes consists of a variety of isoforms, which are differentially expressed, in vascular smooth muscles (VSM). Previous results in the laboratory showed that PLCγ_1 and PLCδ_1 were present in human vascular smooth muscle cells (HVSMCs) whilst unable to detect any of the other PLC isoforms in HVSMCs nor in fresh or cultured human saphenous vein. In addition they found that PLCδ_1 expression was linked to a more differentiated state whilst PLCγ_1 expression decreased as HVSMCs were pushed into a more differentiated state (Harrington, L., Ph.D thesis). With these indications of PLCδ_1 being the predominant isoform in differentiated contractile VSM the continued work in this study was with a focus on the PLCδ_1 isoforms.

The regulation of PLCδ_1 still remains unclear. PLCδ_1 unlike PLCβ isoforms does not bind heterotrimeric G-proteins. Similarly PLCδ_1 is not tyrosine phosphorylated like PLCγ isoforms. Previous results in the laboratory have demonstrated, by partial purification of PLC isoforms in bovine aorta, that PLCδ_1 activity may be dual regulated by GTP-binding proteins with the monomeric G-protein RhoA, acting as an inhibitory modulator of PLCδ_1 activity. The role of GTP-binding proteins in regulating the activity of PLCδ_1 is now becoming clearer. Literature data has shown that the bifunctional enzyme tissue transglutaminase II (TGII), which also acts as a GTPase, modulates PLCδ_1 activity in some tissue.

The overall aim of this study was to investigate the possible role of TGII in regulating PLCδ_1 activity in VSM and provide clearer evidence regarding the role of this regulation in determining VSM differentiation status.

As a model to study phenotypic change randomly cycling (RC) cells were compared to seven days of serum deprived cells (referred to as growth arrested, GA). Both SM α-actin and calponin were used as protein markers, confirming that induction of redifferentiation was achieved. In order to investigate the possible association of PLCδ$_1$ and TGII with VSM phenotypic status Western blotting was used to study the change in protein expression and level of secreted TGII and immunofluorescent staining was performed to study cellular localisation in serum deprived cells compared to randomly cycling cells. In addition, the level of transglutaminase activity versus GTP-binding activity was examined in the two conditions by a transglutaminase activity.

The possible association between PLCδ$_1$ and TGII in HVSMC was studied by co-localisation staining and immunoprecipitation. And finally, three different studies were performed in hope to gain a more functional understanding of this association: PLCδ$_1$ was partially purified from rat aorta, the possible association of PLCδ$_1$ and/or TGII with the cytoskeleton was examined by disruption of the cytoskeleton by chemical treatment, which was monitored by immunofluorescent staining. In the last study the change in intracellular calcium was measured as an indication of receptor coupling by PLCδ$_1$ and TGII upon agonist activation of receptor using Flexstation and the fluorescent dye Fluo-4.

CHAPTER 2 MATERIALS & METHODS

2.1 Cell Culture Techniques

2.1.1 Explant technique

HVSMCs were obtained from saphenous vein using the method previously described (Chan, P., *et al,* 1993). Use of tissues was approved by the local Ethic committee at St Mary's Hospital (London, UK). Tissue samples were obtained from patients undergoing cardiac artery bypass surgery and stored in transport media (Appendix A: 1) prior to use. After collection the vein was cleaned of the external fat and adventitia. The cleaned vessel was cut open lengthways and endothelial cells were removed by rubbing gently with forceps and the vein segment was cut into 2-3 mm^2 pieces. These were placed into 80 cm^2 tissue culture flasks and maintained in 7mls Dulbecco's modified Eagle's medium (DMEM) supplemented with 25 mM HEPES, 15% (v/v) foetal calf serum (FCS) mixed 50/50 with medium removed from explants. The medium was changed to 15% FCS DMEM (Appendix A: 2) after the first cells began to migrate from the explant. Cells were maintained at 37°C in a humidified atmosphere of 5% CO_2 in air and all cell culture procedures were performed in a laminar flow cabinet.

2.1.2 Induction of redifferentiation by serum deprivation

Confluent flasks of HVSMC, at passages 2-4, were trypsinised by addition of trypsin-EDTA (Appendix A: 3) and cells were counted using a Z1 Coulter counter. Cells were either seeded onto sterile coverslips placed into each well of a 24-well plate ($2x10^4$ cells per well – for confocal microscopy) or $10cm^3$ tissue culture flasks, in 15% FCS DMEM and allowed to attach overnight. Following this the medium was removed and cells washed twice with PBS and replaced with either serum free NCTC media (Appendix A: 4, Cat. No.21340-034) for seven

days in order to induce redifferentiation or in the case for controls 15% FCS DMEM.

2.1.3 Culture of HVTs-SM1 cells

HVTs-SM1 is an immortalised HVSM cell line transfected with a nonreplicative retroviral vector containing a temperature-sensitive (ts) mutant of SV40 LT antigen (Hsieh, J.K., *et al*, 2000). Cells were maintained in 10% FCS DMEM (Appendix A:5) under G-418 (200µg/ml, Sigma G1279) selection at 36°C, 37°C or 39°C in a humidified atmosphere of 5% CO_2.

2.2 Preparation of cell lysate

Prior to lysing the cells the culture medium was removed and cells were washed twice with ice-cold PBS. Cells were then lysed by scraping into 1ml of ice-cold standard lysis buffer (Appendix A: 6). Lysates were vortexed and allowed to rest on ice for 10 mins following centrifugation in a refrigerated microfuge at 4°C (10 minutes, 14,000 rpm/10 000g). The resulting supernatant was retained and frozen at -20°C prior to analysis.

2.3 Measurement of protein concentration

Protein concentration of cell lysates was determined using the Bicinchoninic Acid (BCA) method (Smith, P.K., *et al*, 1985). A standard curve was obtained over a concentration range of 0–1000μg/ml of bovine serum albumin (BSA) in standard lysis buffer. Cell lysates of sample to be measured were prepared 1:1 in standard lysis buffer prior to the assay. All samples were prepared in duplicate to a total volume of 100µl. A working reagent of reaction buffer A, B and C (25:24:1,

Appendix A: 7) was made up and 2ml added to both BSA standards and cell lysates, which were vortexed and incubated for about 30 minutes at room temperature followed by spectrophotometric readings at 562nm.

2.4 Immunoprecipitation

Proteins were immunoprecipitated from 200µg of total cell lysate by the method routinely used in the laboratory (Hodson, E., *et al*, 1999). 200µg cell lysate was incubated with 50μl albumin agarose at 4°C on a rotator for one hour, prior to centrifugation for 10 minutes to remove any non-specific agarose binding. Primary antibody (1µg/100µg cell protein) was added to the supernatant and left to incubate for at least 3 hours (to overnight) at 4°C on a rotator. The antigen-antibody complexes were then captured by the addition of 50μl of Protein A-agarose for at least two hours at 4°C. The immunoprecipitate was collected by centrifugation at 4°C for 10 minutes and washed three times with 800μl standard lysis buffer. In order to dissociate immunocomplexes from the protein A agarose beads, the pellet was resuspended in 50µl 2x Laemmli sample buffer (Appendix A: 8) and heated to 95°C for 5 minutes followed by centrifugation at 4°C for 10 minutes. Supernatant was retained for analysis using Western Blotting (described below).

2.5 Detection of TGII secretion

To detect TGII secretion into the growth medium, confluent VSMC (passage 2-4) were grown in serum-free culture medium for seven days. A 200µl fraction of media was then collected and centrifuged to remove any floating cells. 40µl of 5xSDS Laemmli sample buffer (Appendix A: 9) was added and the mixture was

boiled for 5 min at 95°C and left on ice for 10 min. Samples were analysed following SDS-PAGE and Western blotting for specific proteins.

2.6 SDS-Polyacrylamide Gel Electrophoresis (SDS-PAGE)

Proteins were separated on 10% gels by sodium dodecyl sulfate-polyacrylamide gel (SDS-PAGE), electrophoresis, using a Bio-Rad 1.5mm mini-gel system with a 4% SDS-PAGE stacking gel (Appendix A: 10) and separated on a 10% SDS-PAGE resolving gel (Appendix A: 11). Protein samples were loaded with MultiMarker Rainbow marker, Novagen Perfect protein (15-150 kDa) and controls into individual wells of the gel and the gel tank was filled with fresh running buffer (Appendix A: 12). Gels were run at constant voltage for 2 hours or until the dye front had run off the bottom of the gel.

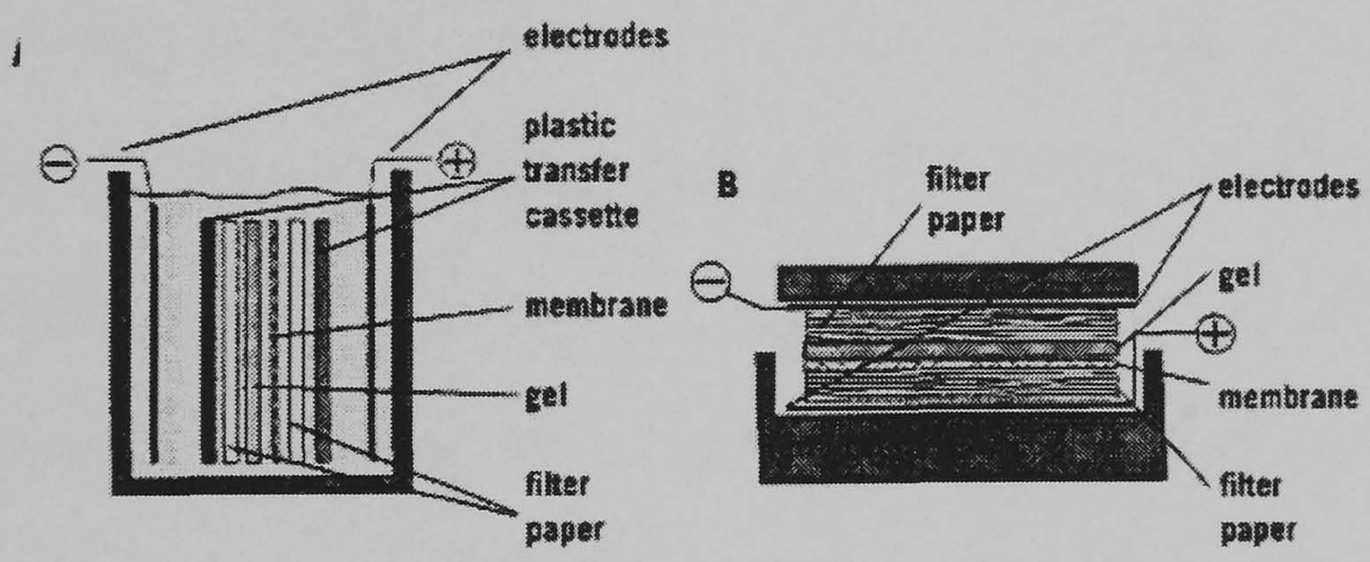


Figure 2.1 Set-up for running a SDS gel and on the right western blotting transfer set-up. Picture taken from Amersham Biosciences.

2.7 Western blotting

Western blotting is a process by which physically separated proteins are transferred from a matrix to the surface of an immobilized membrane prior to immunodetection. The separated proteins were transferred onto a nitrocellulose membrane, Hybond-P, (Millipore) using wet transfer system in a Trans-Blot Electrophoresis Transfer Tank. Prior to transfer the nitrocellular membrane and

SDS-polyacrylamide gel were equilibrated in transfer buffer (Appendix A: 13) to remove salts and detergents. Transfer of proteins to the membrane is accomplished by using electrotransfer where proteins are transferred toward the anode because of the anionic SDS and the slightly alkaline pH of the transfer buffer. Also the addition of 20% (v/v) methanol in the transfer buffer counteracts swelling of the gel and increases the binding of the proteins to nitrocellulose. Efficiency of the protein transfer to the membrane was determined by staining with Ponceau S. This reversible stain can be completely removed from the protein bands by continued washing prior to immunoblotting.

2.8 Immunoblotting

To reduce non-specific IgG binding, nitrocellulose blots were blocked in 3% (w/v) bovine serum albumin (BSA) in 1 x TTBS (Appendix A: 14) at room temperature for one hour on a shaker. Prior to the addition of primary antibody (usually 1:1000), in 3% (w/v) BSA – TTBS blots were left to incubated on a shaker for 1hr at room temperature. Following this the nitrocellulose was washed, (4 x 5 minutes and 1 x 20 minutes in 1x TTBS) prior to addition of the appropriate horse radish peroxides (HRP) linked -secondary antibody (usually 1:2000) for 1hr on a shaker. Following incubation with the secondary antibody the nitrocellulose blot was washed thoroughly in TTBS (3x 5min, 2x 20min) to remove non-specific binding. Protein bands were visualised by enhanced chemiluminescence reagent (ECL) which bind to HRP on the secondary antibody (Figure 2.2). The blots were wrapped in cling film and were exposed to Hyperfilm ECL until the protein bound IgG was detected as dark bands. The band

intensity was quantified with a Bio-Rad model GS-690 Imaging Densitometer and analyzed using Molecular Analyst software, version 1.4.

Principles of enhanced chemical luminescence

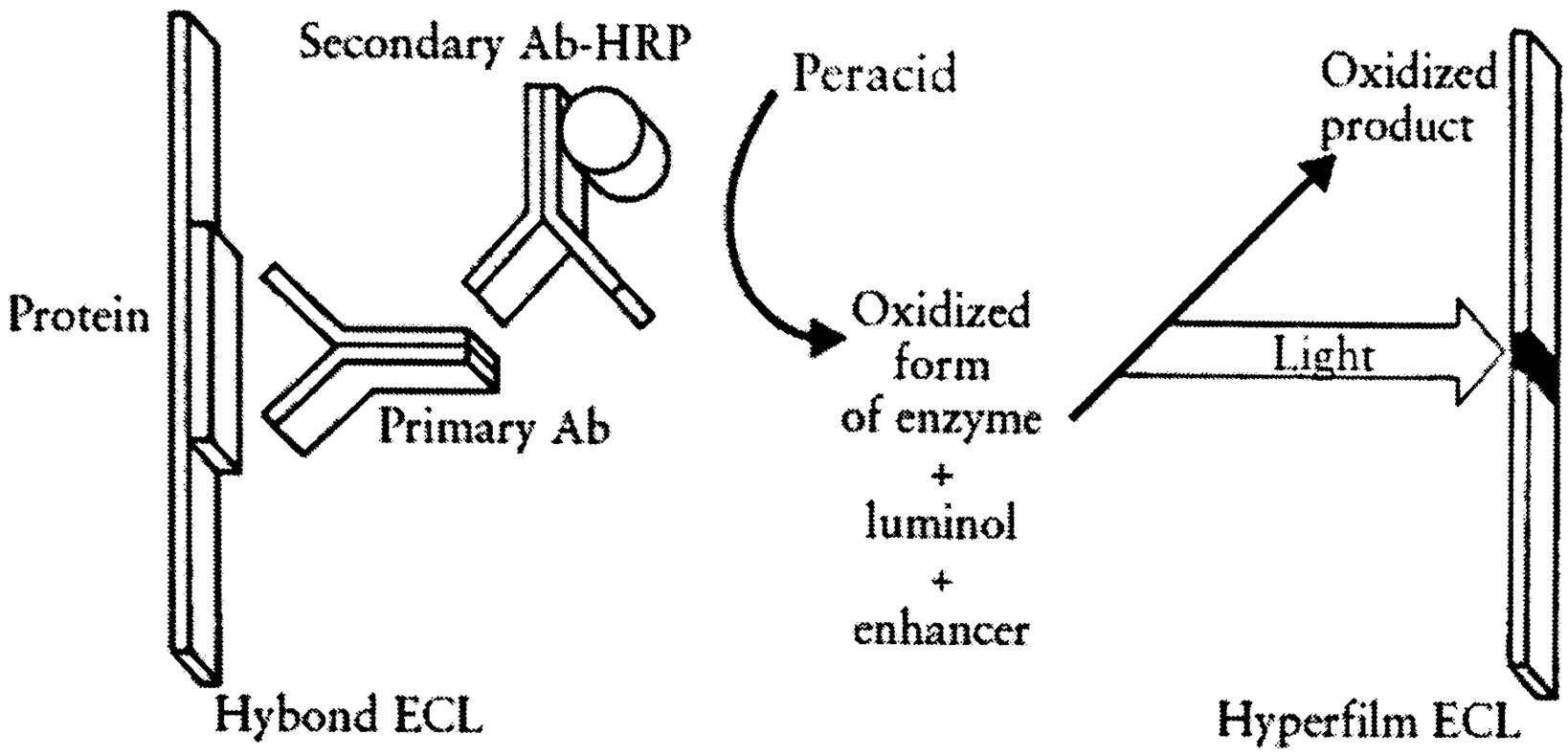


Figure 2.2 Principles of enhanced chemical luminescence (ECL). ECL was used in combination with Western blotting to detect protein of interest. Primary antibody was detected by a Horse-Radish peroxidase (HRP)-labelled secondary antibody following addition of ECL and exposure to film. Picture taken from AmershamBioscience

2.9 Coomassie Blue staining

To detect the total amount of protein, gels were stained with 0.1% (w/v) coomassie brilliant blue in 40% (v/v) methanol and 10% acetic acid (glacial) for 30 min at room temperature. Non-specific background stain was removed with 40% (v/v) methanol and 10% (v/v) acetic acid. Stained gels were dried on whatman paper.

2.10 SYPRO Ruby protein gel stain

SYPRO Ruby protein gel stain is a ready-to-use luminescent stain for detection of proteins separated by polyacrylamide gel electrophoresis. Gels were fixed at room temperature of 15 min in 50% (v/v) methanol and 10% (v/v) acetic acid. This was followed by overnight incubation in undiluted stain at room temperature. Gels were washed twice in 10% (v/v) methanol and 7% (v/v) acetic acid for 30min to reduce background fluorescence and increase sensitivity. Before imaging gels were rinsed in double distilled water (ddH_2O) to prevent possible corrosive damage to the imager. Proteins stained with SYPRO Ruby protein gel stain were visualized by transillumination.

2.11 Confocal imaging.

HVSMC, seeded onto sterile coverslips in each well of a 24 well plate, were washed twice with cold PBS and fresh media (either serum free, or DMEM with 15% FCS) was added for a period of seven days. Following this period cells were washed twice with cold PBS and fixed in methanol for 20 min. Coverslips were then blocked for 30min in 1ml 5% (w/v) BSA in PBS-0.1% (w/v) Triton X (PBSX) prior to incubation with primary antibody (1:50) for two hours at room temperature and followed by one hour washing with three changes of PBSX. Secondary antibody (1:100, in 5% (w/v) BSA in PBSX) was left for two hours at room temperature and kept away from light. In case of double staining the two primary antibodies were added sequentially while the secondary antibodies were added together. Coverslips were then washed for a further hour with two changes of buffer. DAPI (1:1000 (v/v)) was added to the third wash and left for 5 min prior to one last wash in buffer. Coverslips were carefully mounted with a drop of

mounting media and slides were sealed with nail varnish to avoid drying out. Immunoflourescence was examined by confocal microscopy using a Leica TCS NT SP. The presence of co-localisation was determined using the Zeiss LSM 510 software.

2.12 Column chromatography

This was performed using the method previously described (Hodson, E., *et al*, 1999). Briefly, aortas freshly removed from male Wistar rats (~200g) were cleared of fat and incubated at 37°C in 2 mg collagenase for 15 min and kept on ice for 10 min to ease removal of adventitia (Gonzalez, M.C., *et al,* 2001). The medial smooth muscle was then homogenised in ice-cold homogenisation buffer (Appendix A: 15) by 4x30 second bursts using an Ultra-Turrax TP 18/10 homogeniser. Cell debris and nuclei was sedimented by centrifugation for 10min at 2000rpm/200g, 4°C and the supernatant was equilibrated overnight at 4°C in column chromatography running buffer (Appendix A: 16). The equilibrated sample was then applied to a low pressure ion-exchange chromatography column (200ml, 2.6cm x 40cm) containing Q-sepharose resin, a small volume was retained for protein measurements. To remove unbound substances the column was washed with 600 ml of running buffer at a flow rate of 30ml/h. A linear NaCl gradient (50mM-550 mM) was then applied to enable separation of PLC isoforms according to their difference in affinity for the anion exchanger. Eluates were collected in 5ml fractions using a Pharmacia Frac-100 fraction collector. Every third fraction of eluate was tested for the presence of both protein (section 2.3) and PI-PLC activity (section 2.13).

2.13 PLC activity

PLC activity was measured in a 30µl aliquot of protein in a final volume of 100µl containing PLC buffer (Appendix A: 17) as previously described by us (Hodson, E., *et al*, 1998). The reaction was initiated by adding 10 µl substrate (unilamellar vesicles containing 350µM PI, 360µM PE (Phosphatidylethanolamine) and 0.015µCi [^{3}H]-PI, prepared by a 5min sonication in 0.1% sodium deoxycholate and 50mM Tris-base after which the mixture was incubating at 37°C for 10 minutes. The reaction was stopped by adding 0.5mls ice-cold chloroform:methanol:HCl (1:1:0.6 v/v) followed by 150 µl ice cold 1M HCl containing 5mM EGTA. The mixture was left on ice for 10 minutes to enable phase separation, prior to centrifugation at 7,000 rpm for 2 minutes. An aliquot (200µl) of the upper aqueous phase (containing the water soluble hydrolysis products) was counted for radioactivity, measuring the [^{3}H] counts, in a Liquid Scintillation Analyser Assays were performed in triplicate.

2.14 Transglutaminase activity

The kinetics of TGase activity were assayed by measuring the incorporation of putrescine into *N,N*-dimethylated casein. Confluent monolayers of cells were detached from flasks adding 1 ml of cell dissociation solution (CDS, Sigma). After 2 min incubation cells were detached by pipetting and an aliquot of 200µl were saved for cell count and measurements of protein concentration. The remaining sample was centrifuged at 2000rpm for 10min to collect cells which was further dissolved in sample buffer (Appendix A,) following disruption of cell membrane by freeze (-70) thaw. The mixture of cell lysate and reaction buffer (Appendix A: 18) was incubated for one hour at 37°C prior to being placed on

ice. Cold trichloroacetic acid (TCA) was added to a final concentration of 10% (v/v) for 15 minutes. Samples were centrifuged (14000rpm, five minutes, room temperature). The pellet was washed three times with 1 ml of 5% (v/v) TCA, once with acetone:ethanol (v/v) and finally just with acetone. Samples were air dried and resuspended in 0.2 ml of 0.1 M NaOH. Radioactivity was measured in 3 ml of scintillation liquid and counted for radioactivity, measuring the [^{3}H] counts, in a Liquid Scintillation Analyser. Assays were performed in triplicate.

2.15 [^{35}S]GTPγS binding overlay method.

To evaluate the GTPase activity of TGII, nitrocellulose blots which had previously been probed for the presence of total TGII protein expression, by Western blotting, were exposed to [^{35}S]GTPγS. This technique was performed using the method of Drøbak *et al.* with minor modifications (Drøbak, B.K., *et al.*1995). Nitrocellulose blots of TGII and PLCδ_1 were rinsed briefly in washing buffer (Appendix A: 19). Blots were then further incubated in binding buffer (Appendix A: 20) containing 1mCi/ml [^{35}S] GTPγS and ATP (10μM) for 90 minutes at room temperature. Blots were washed three times in washing buffer and allowed to air dry before being exposed to a phosphoimager.

2.16 Measurement of intracellular calcium levels

2.16.1 Fura-2-AM loading of HVTs-SM1 cells

HVTs-SM1 cells were seeded the day before experiment in a clear, flat-bottom, black-wall 96-well tissue culture plates (10^5cells/well). Following removal of medium HVTs-SM1 cells were gently washed three times with Ca^{2+}-buffer (Appendix A, 21). 100μl of Fura-2-AM (Molecular Probes), dissolved in DMSO

as a stock solution (1mM), was mixed with Ca^{2+}-buffer to give a final concentration of Fura-2AM (2μM). The loaded plate was wrapped in foil and left to incubate for 1h at 37°C or 39°C. Excess dye was removed by three washes in Ca^{2+}-buffer after which cells were left for 15min (37°C or 39°C, plate wrapped in foil) to allow complete desterification of the dye. Prior to reading 100μl of fresh Ca^{2+}-buffer was added to each well.

2.16.2 Fluo-4-AM loading of HVTs-SM1 cells

HVTs-SM1 cells were seeded the day before experiment in clear, flat-bottom, black-wall 96-well tissue culture plates (10^5cells/well). 50μg aliquots of Fluo-4-AM (acetoxymethyl) were prepared to a 1mM solution in DMSO (22.8μl) with 10% pluronic acid. Fluo-4 was then added to 20ml of Ca^{2+}-buffer (Appendix A, 22) supplemented with 10% FCS and 2.5mM probenecid to give a loading buffer containing Fluo-4AM (2μM). This loading buffer was then added to the cells at 100μl per well and left to incubate wrapped in foil for 1h at 37°C. Once the cells were loaded, excess dye was removed and cells washed twice with HBSS (Appendix A, containing 0.1mM Ca^{2+} and 1mM Mg^{2+}) with 2.5mM probenecid and allowed to rest for 30 minutes in foil at 37°C before stimulation. The 96-well plate with loaded cells was then placed in the Flexstation and changes in intracellular level of calcium following addition of 20μl agonist was measured at excitation wave length, λ=485 and emission at λ=520, using a cut off at λ=515.

2.16.3 Flexstation.

Flexstation II 96/384 (Molecular Devices) is a benchtop scanning fluorometer that can perform 96 well microplate screening and with its 8 integrated channel

pipettor allows precise compound transfer at microliter amounts. To observe changes in $[Ca^{2+}]_i$ levels, cells are loaded with a calcium-sensitive fluorescent dye. In our study we used Fluo-4-AM, which is a cell permeant dye that does not bind to calcium until the aetoxymethyl (AM) ester is removed by cytoplasmic esterases. Flexstation allows the measurement of adherent cells and can thereby monitor what happens in the cell under normal physiological and morphological conditions.

2.16.4 Data analysis.

Fluo-4 is not a ratiometric indicator dye (compared to the frequently used Fura-2. Ca^{2+} calibrations were performed upon completion of experiments, by the addition of 10 μM ionomycin (Sigma, No.I-0634) to permeabilized the cells to Ca^{2+} and saturate Fluo-4 with Ca^{2+} resulting in maximum fluorescence (F_{max}). Subsequent to this the Ca^{2+} chelator Ethylene glycol-bis(β-Aminoethylether)-N-N-N'-N'-Tetraacetic acid, EGTA (10mM) was added to the cells to a certain minimal fluorescence, (F_{min}) Ca^{2+}. The single wavelength calibration equation $[Ca^{2+}]$=Kd [(F x Fmin)y(Fmax2 F), Kd = 345 nM] was used based on the equation of Grynkiewicz *et al.* (Grynkiewicz, G., *et al*, 1985).

2.17 Live calcium imaging

Live cell calcium imaging was performed to verify that the cells were properly loaded with Fluo-4 and to determine whether compartmentalisation of the dye occurs. This technique also allows each step of the assay procedures to be monitored for possible changes in both morphology and intracellular level of calcium. Live calcium imaging was visualised using a confocal microscope (Zeiss

LSM 510uv META combi confocal) with a 40x objective. HVTs-SM1 cells were cultured on specific petri dishes containing coverslip chamber slides (22mm and 32mm round coverslips, 35mm MatTek dishes, P35G-1.5-14-C), the day prior to the experiment. Solutions added during the course of the experiment were kept at 37°C or 39°C. Images were analysed with Zeiss LSM 5 imaging software.

2.18 Statistical analysis

In terms of protein expression and TGII activity data from randomly cycling, control, cells was defined as 100% and all experimental data was expressed in relation to this. Statistical differences between means were calculated using a paired Student t-test. A p-value of less than 0.05 was considered to be statistically significant.

2.19 Materials

2.19.1 Primary Antibodies:

PLCδ_1 antibodies (sc-7521 & sc-7520) were obtained from Santa Cruz Biotechnology Inc (California, USA), (05-343) Upstate Biotechnology (Claydon, Buckingham, UK) and (610356) BD Bioscience Pharmingen (Oxford, UK). Transglutaminase II Ab-1 (MS-224 - P1) and Transglutaminase II, Ab-3 (MS300) were obtained from Lab Vision (Newmarket Suffolk, UK). SM α-actin was obtained from DAKO (Ely, Cambridgeshire, UK). Calponin was obtained from Santa Cruz Biotechnology (California, USA).

2.19.2 Secondary antibodies

HRP conjugated swine anti-rabbit, rabbit anti-mouse, rabbit anti-goat and FITC conjugated rabbit anti-mouse were all obtained from DAKO (Ely, Cambridgeshire, UK). Rhodamine conjugated rabbit anti-goat was obtained from Santa Cruz Biotechnology (California, USA).

2.19.3 Western blotting & Immunoprecipitation

Hybond C nitrocellulose membranes were obtained from Amersham Life Sciences (Buckinghamshire, UK). Protein A agarose was obtained from Calbiochem (Cambridge, UK). Protogel 30% (w/v) acrylamide stock solution was obtained from National Diagnostics (Hull, UK). Perfect protein markers and rainbow markers were obtained from Novagen (Madison,WI, USA). ECL reagent was obtained from Amersham (Little Chalfont, UK). All other reagents were obtained from Sigma-Aldrich (Poole, Dorset, UK).

2.19.4 Chromatography

Q-sepharose resin was obtained from Sigma (Poole, Dorset, UK). All other chemicals were obtained from BDH (Poole Dorset, UK).

2.19.5 Flex

Phenylephrine (PG126), histamine (H7250) and fibronectin (F4759) were all obtained from Sigma.(Poole, Dorset, UK). PDGF-BB (IB1031) was obtained from Insight Biotechnology (Wembley, Middlesex, UK).

2.19.6 Disruption of actin

Cytochalasin D and colchicine were both obtained from Sigma (Poole, Dorset, UK).

2.19.7 PLC assay

Nitrogen (Oxygen free) was obtained from BOC Ltd (S Yorkshire, UK). [^{3}H] PI was obtained from Perkin Elmer (Herts, UK).

2.19.8 Cell culture

5% Carbondioxide/95% Oxygen was obtained from BOC Ltd (S Yorkshire, UK). NCTC 109 media (Sigma, N1140), DMEM (Dulbecco' Modified Eagle medium) and all other cell culture reagents were obtained from Life Technology, Gibco BRL (Paisley, Scotland).

2.20 Equipment

2.20.1 Cell culture

All sterile procedures were performed in a Biomat Class II Microbiology cabinet.

All cell and tissue cultures were maintained in a Napco water-jacket CO_2 incubator. Cells were counted on a Beckman Coulter Counter Z1.

2.20.2 Centrifuges

The following centrifuges were used throughout this work: Refrigerated Eppendorf Centrifuge 5402 and a bench top Eppendorf Centrifuge 5415C.

2.20.3 Spectrophotometer

All determinations of the optical absobance of solutions were performed using a Shimadzu UV-1201 UV-VIS spectrophotometer and program pack for measuring of protein at 562nm.

2.20.4 SDS-PAGE

All equipment used for SDS-PAGE was obtained from Bio-Rad Laboratories Ltd (Hemel Hempstead, Herts, UK).

2.20.5 Flexstation

FlexStation II was obtained from Molecular Devices (Winnersh, Wokingham, UK).

2.20.6 Confocal Laser Microscope

The confocal microscope used in these studies was a Leica TCP-SP scanning confocal microscope.

CHAPTER 3 PROTEIN EXPRESSION

3.1 Aim of study

The aim of this study was to investigate the effect of phenotypic change on PLCδ_1 and TGII protein expression in HVSMCs.

3.2 Introduction

The primary function of VSMCs in the adult vascular wall is contraction. These differentiated cells have a low rate of protein synthesis and proliferation (Lindqvist, A., *et al*, 2001; Owens, G.K., *et al.* 1998). Disturbance of the normal integrity of the tissue, such as during vascular disease, leads to a modulation of VSMC towards a 'synthetic' phenotype, which exhibits an altered morphology, cellular function and biochemical characteristics (Absher, M., *et al*, 1989; Wissler, R.W., *et al.* 1967). These synthetic VSMC lose their ability to contract and have enhanced capacity to replicate and migrate. As a result these synthetic, or dedifferentiated, VSMCs exhibit an altered expression of contractile and cytoskeletal proteins as well as membrane channels and receptors (Owens, G.K., *et al.* 1995). Culture of VSMC results in a similar phenotypic modulation with the cells undergoing morphological changes, proliferating at greatly enhanced rates and losing their contractile ability (Chamley-Campbell, J., *et al*, 1979). This suggests that cultured VSMCs may represent a good model of diseased vascular tissue. Indeed this concept was first hypothesized back in 1967 by Wissler, who showed that, enzymatically dispersed cells from arterial media placed in culture gradually assumed features of less differentiated cells with characteristics of SMCs in vascular lesions (Wissler, R.W., *et al.*1967)

It is not currently possible to re-establish a fully differentiated contractile phenotype in cultured VSMCs. Modulation of culture conditions, however, can result in the cells expressing certain features of differentiated cells. In this study an enhanced expression of SM α-actin and calponin (Shanahan, C.M., et al. 1993; Weissberg, P.L., *et al.* 1995) were used as a measure of redifferentiation.

3.3 Methodology to achieve redifferentiation.

Several different methods can be applied to induce redifferentiation of VSMCs including culturing cells on matrigel (Li, X., *et al.* 1994; Gerecht-Nir, S., *et al.* 2003) and addition of chemical agents such as retinoic acid (Axel, D.I., *et al.* 2001) or lovastatin (Wang, C.Y., *et al.* 2003; Gray-Bablin, J. *et al.* 1997). Lovastatin treatment results in G_1 arrest of cells in association with induction of the cyclin-dependent kinase inhibitors (CDKIs) such as p27 (Gray-Bablin, J., *et al.* 1997) but has been shown to promote apoptosis in some cells (Wang, C.Y., *et al.* 2003). Similarly retinoic acid (RA) treatment exerts antiproliferative effects which rely on regulation of many biological processes including proliferation, differentiation and apoptosis (Nagy, L., *et al.* 1998). Kosaka *et al.* showed how treatment of rat aortic smooth muscle cells with all-trans retinoic acid ATRA (ATRA) markedly elevated the mRNA and protein levels of SM α-actin. ATRA strongly suppressed the Retinoblasoma protein (pRb) kinase activities of the cyclin-dependent kinases (Cdks), thus the expressions of Cip/Kip family Cdk inhibitors were not influenced, suggesting that ATRA targets multiple genes essential for entry into the cell cycle and for the subsequent progression to G_1 - phase (Kosaka, C., *et al.* 2001).

Prolonged serum deprivation has also been shown to promote redifferentiation in VSMCs (Li, S., *et al.*1999). A clone (HITB5) from human internal thoracic artery expressing SM α-actin, smooth myosin heavy chains, heavy caldesmon and calponin also showed transient calcium response to histamine and angiotensin II. On serum withdrawal, these cells adopted an elongated and spindle-shaped morphology, slow migration and cell proliferation with almost no [^{3}H]thymidine incorporation. In this state, agonist-induced elevation of cytoplasmic calcium was even more pronounced. Upon readdition of 10% serum cells returned to a noncontractile, proliferative phenotype.

While we have previously used all of these methods to induce a measure of redifferentiation of HVSMCs in our laboratory (Figure 3.1, performed by Harrington, L.) we chose to utilise prolonged serum deprivation to redifferentiate our HVSMCs in this study. This technique is easy to use, consistent and exclusive of differences in incubation time or concentration. Lack of toxicity is another great advantage.

3.3.1 Serum deprivation

When proliferating cells in culture are deprived from serum, they stop dividing but continue to pass through the cell cycle until they reach the G_1- phase. On reaching this part of the cycle, they come to a halt in a specialised, non-growing state, the G_0 ("G zero") resting state. The resting state is a sort of a cell-cycle sleep where the cell-cycle control system is disabled from proliferating. The effect of serum deprivation is to depress protein synthesis and cell growth.

3.4 Modulation of smooth muscle phenotype

Data from this laboratory has previously shown that, [^{3}H]-thymidine incorporation decreases rapidly and significantly over the first 24 hours post serum-deprivation and further decreases significantly between day one and day three.

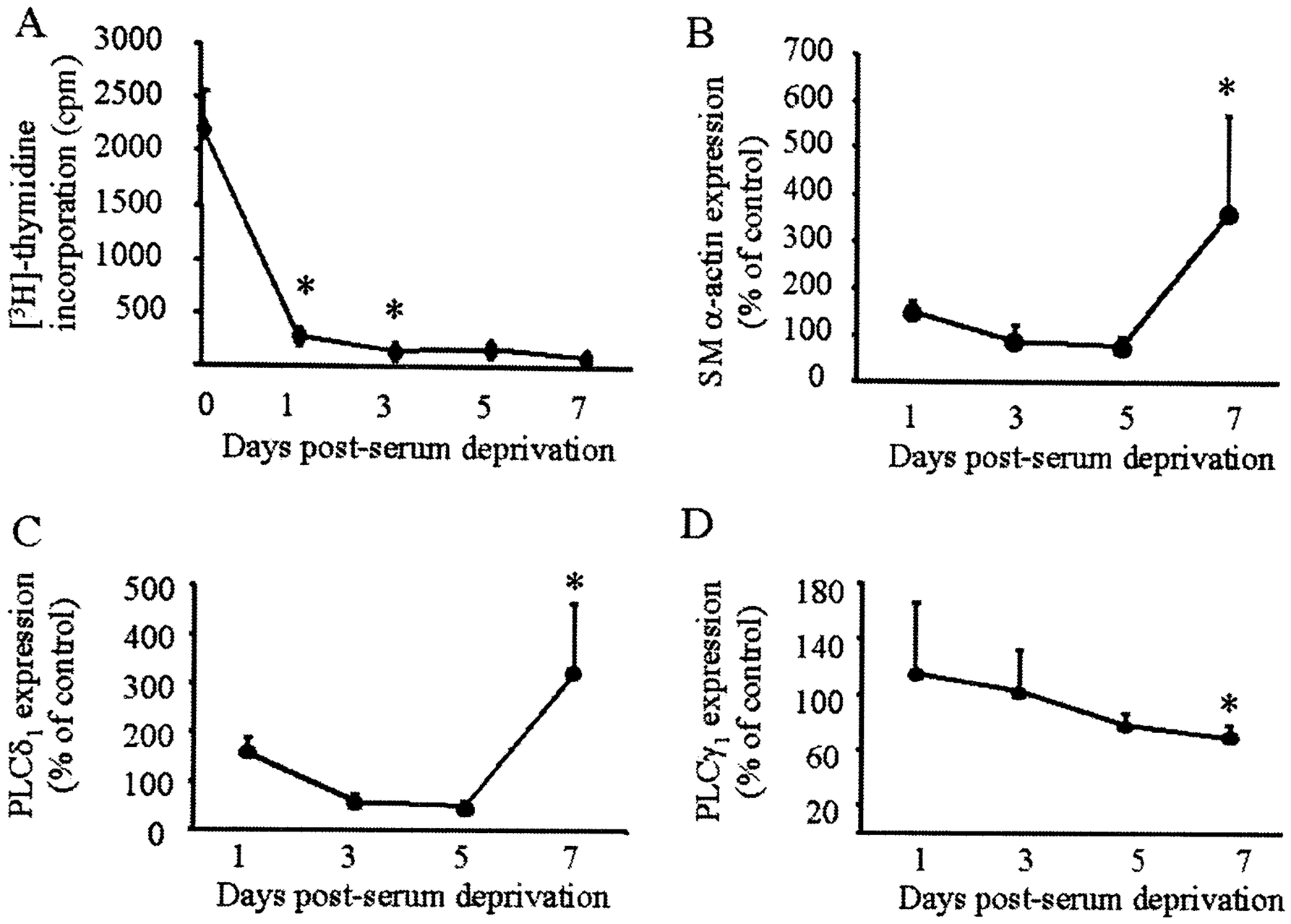


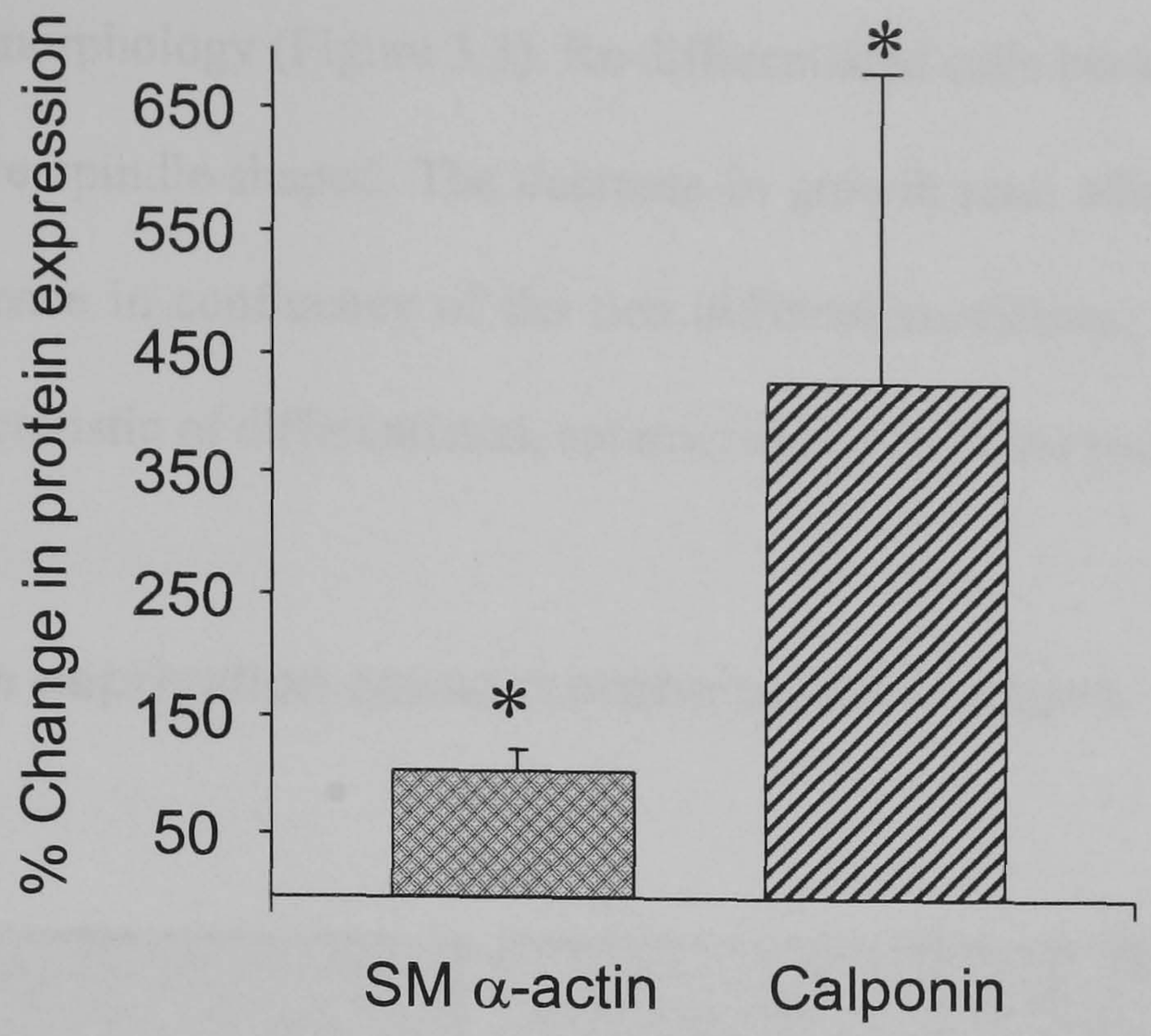
Figure 3.1. Temporal effects of serum deprivation. ***A.*** *Graph shows [^{3}H]-thymidine incorporation in randomly cycling cells and following serum deprivation for 1, 3, 5 and 7 days (n=4).* ***B.*** *Graph represents the effect of serum deprivation on expression of SM α-actin (n=8).* ***C.*** *Graph represents the effect of serum deprivation on expression of PLCδ$_1$ (n=8).* ***D.*** *Graph represents the effect of serum deprivation on expression of PLCγ$_1$ (n=8). Expression of SM α-actin, PLCδ$_1$ and PLCγ$_1$ in randomly cycling cells were taken to be 100% and all other data is expressed with respect to this. Data represents mean ± SEM of n separate cell strains, * represents $p \leq 0.05$.*

As seen in figure 3.1 no additional changes in [^{3}H]-thymidine incorporation were seen after three days, suggesting that maximal growth arrest has occurred by this time (Figure 3.1A, performed by Gallagher, K.).

More importantly these data also demonstrated that an increase in SM α-actin expression does not occur in these cells until 7-days post-serum deprivation, suggesting that this is a post growth arrest phenomenon which may be indicative of redifferentiation (Figure 3.1B, performed by Harrington, L.). Consequently in this study we used 7 days serum deprivation to induce a more differentiated phenotype in VSMCs.

In order to verify that cells were redifferentiated the expression level of both SM α-actin and calponin were used as markers. Only HVSM cell lines showing a significant increase in these two marker proteins were included in our study (Figure 3.2).

A



B

	Average ± SEM
SM α-actin	103 ± 19
Calponin	430 ± 258

C

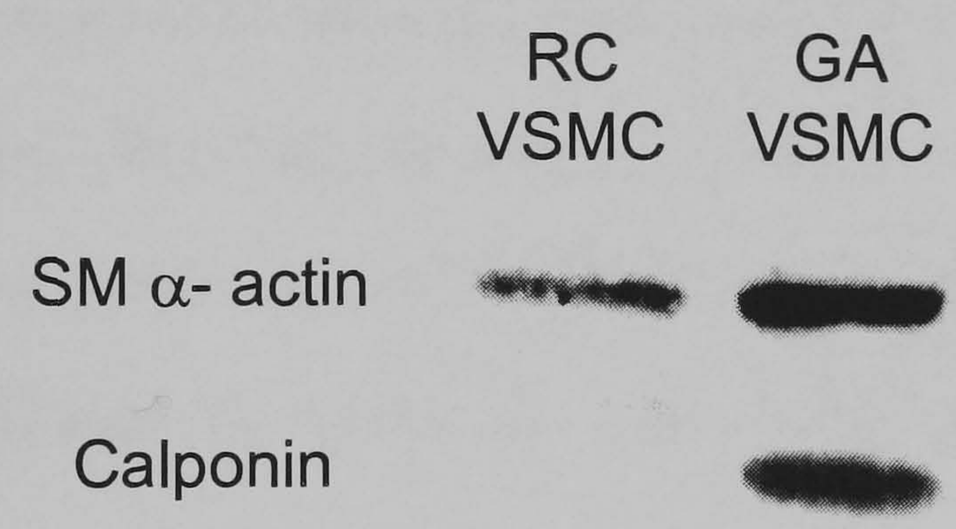


*Figure 3.2 Change in protein expression of the two markers for redifferentiation, SM α-actin (n=9) and calponin (n=4) in redifferentiated (GA) HVSMC. Graph (**A**) and table (**B**) shows the % change in protein expression as a mean ± SEM above that seen in randomly cycling (RC) cells. $P < 0.05$(*). **C**. Representative bands from western blots.*

Following 7 days of serum withdrawal serum deprived HVSMCs also exhibited a notable change in morphology (Figure 3.3). Re-differentiated cells became highly elongated and more spindle-shaped. The decrease in growth rate, which can be seen by the difference in confluency of the two different conditions, is another fundamental characteristic of differentiated, contractile SMCs in the vessel wall.

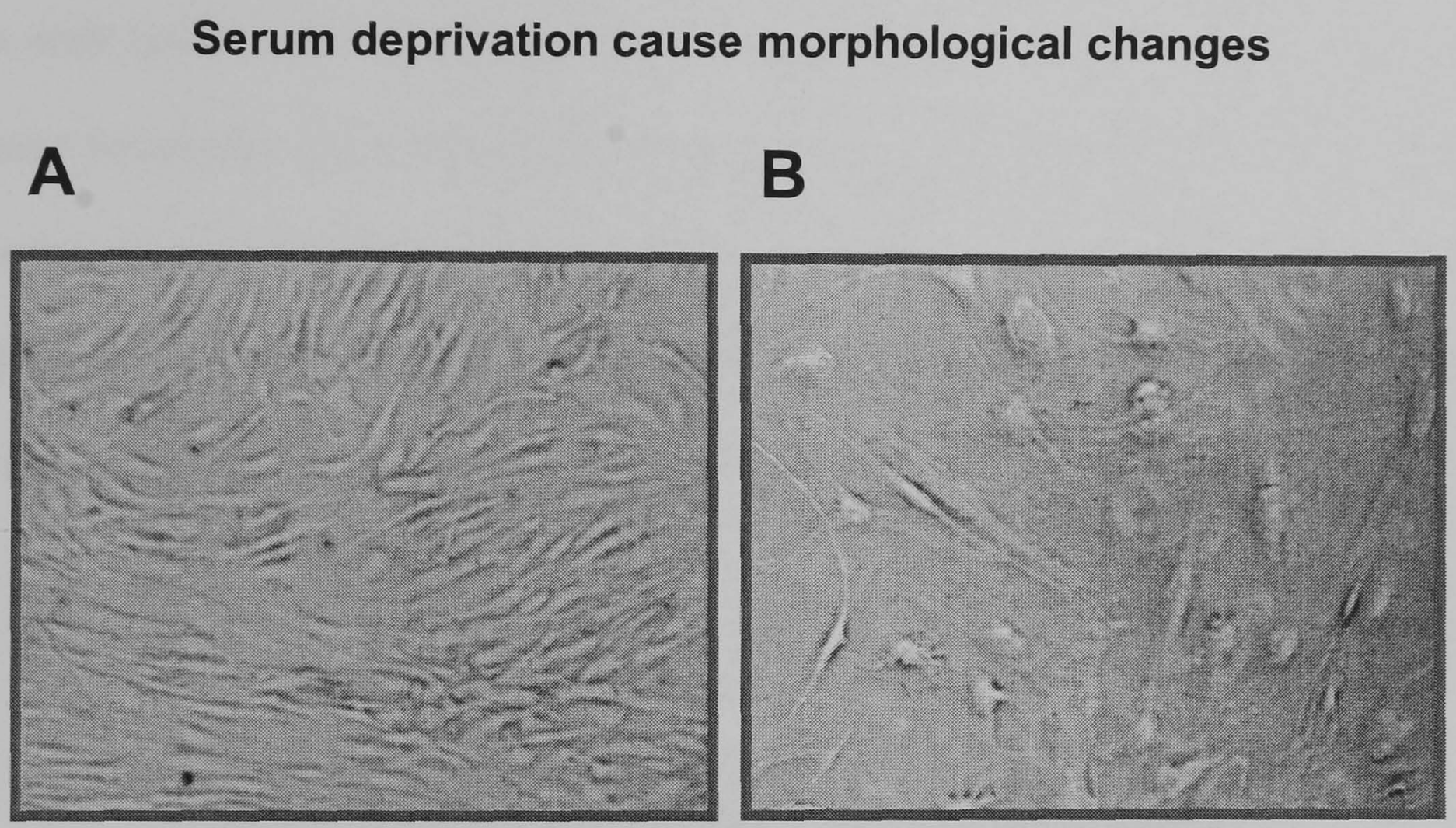


*Figure 3.3 Morphological changes of HVSMCs following redifferentiation. Phase contrast microscopic pictures (Magnification x40) of randomly cycling (**A**) compared to seven days of serum starved HVSMCs (**B**). Cells that are redifferentiated are highly broaden and spread and take a more spindle-shape appearance.*

3.5 Control experiments for western blotting

The change in protein expression between randomly cycling and serum-deprived cells was to be studied using Western blotting techniques. Consequently we investigated the reproducibility of this technique using a number of different methods.

3.5.1 Intergel differences of gel loading

We first examined the potential difference in loading that may occur between gels. Four different HVSM cell lysates (20μg) were loaded on the same gel and this was repeated three times. All gels were transferred to blots as described in methods (section 2.7), stained with SYPRO® Ruby protein gel stain (section 2.10) and visualised with a transilluminator. Several protein bands were detected in each lysate with the same pattern of bands appearing on all of the blots. To assist comparisons the largest and strongest of the protein bands on the blots were examined and compared. Visual analysis of the blots suggests that there was no difference in the level of protein expression of any of the lysates and that the same pattern of expression was seen in all three gels.

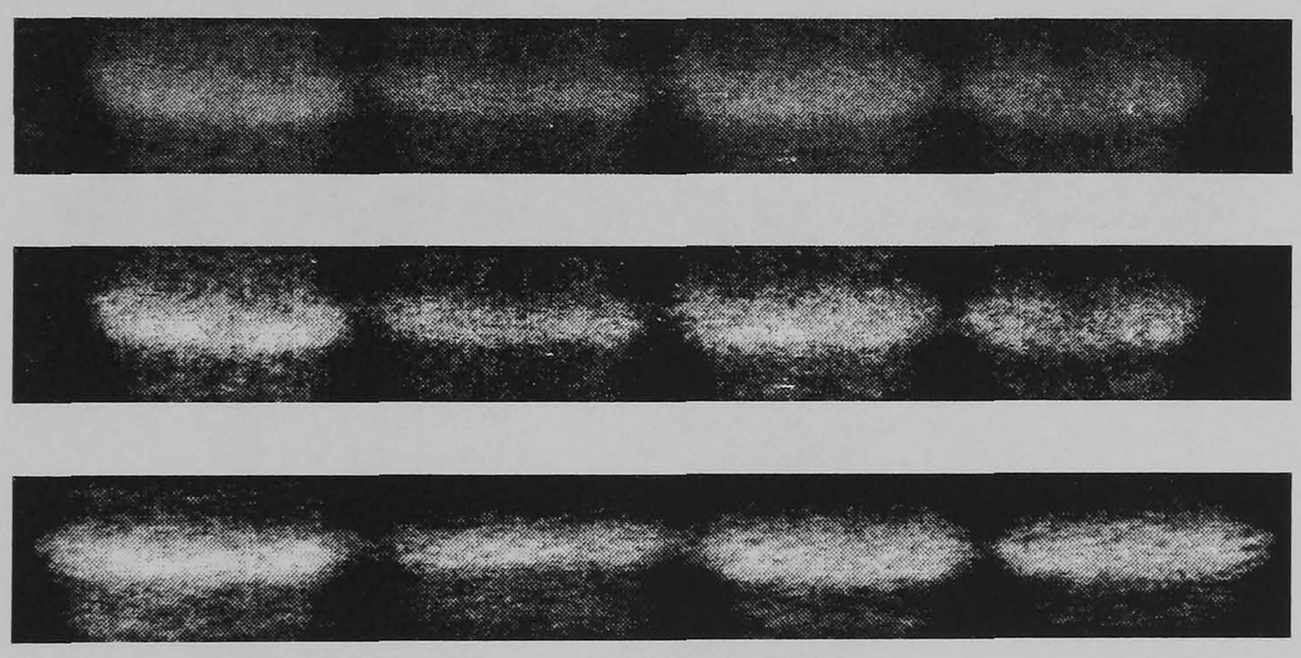


Figure 3.4 Intergel differences of Western blotting. Representative blots monitoring the reproducibility of detecting cell lysates of HVSMCs between gels. Four different cell lysates were loaded to three separate gels, which were further stained with SYPRO® Ruby protein gel stain and visualised with a transilluminator, (n=3).

3.5.2 Intragel differences of gel loading

In terms of the reproducibility of gel electrophoresis techniques we also investigated the possible variance in different wells of the same gel. This is important as bands may appear larger by eye when in actuality there is just a slightly wider gap width of wells, which can occur when casting gels. To this end 10μg of the same cell lysate from randomly cycling HVSMCs was loaded into different wells on the same gel. This gel was transferred to nitrocellulose as described in methods and stained with SYPRO® Ruby protein gel stain. As seen in figure 3.5 the left band appears slightly wider but following further densitometric analysis it can be seen that there is no significant difference between the wells (1.546±0.009). This suggests that the methodology of lysate preparation and protein separation by SDS-PAGE does indeed give reproducible results and is therefore suitable for use in this study.

*Figure 3.5 Intragel differences for Western blotting. **A**. Control experiment monitoring the reproducibility of detecting cell lysates of HVSMCs between wells on the same gel. Gels were stained with SYPRO® gel stain and visualised with a transilluminator, (n=4). **B**. Diagram showing densitometric units detected by densitometry analysis in between wells (1-4) of the same gel.*

3.5.3 Linear range of antibody detection

A further area where inconsistencies can occur is at the level of application of antibodies to the nitrocellulose membrane. Sensitivity of protein antibody binding was investigated by loading different concentrations of protein from a HVSMC lysate and probing with TGII antibody followed by densitometry measurements (figure 3.6). Linearity of PLCδ_1 has previously been conducted in our group (L. Harrington's thesis, p112).

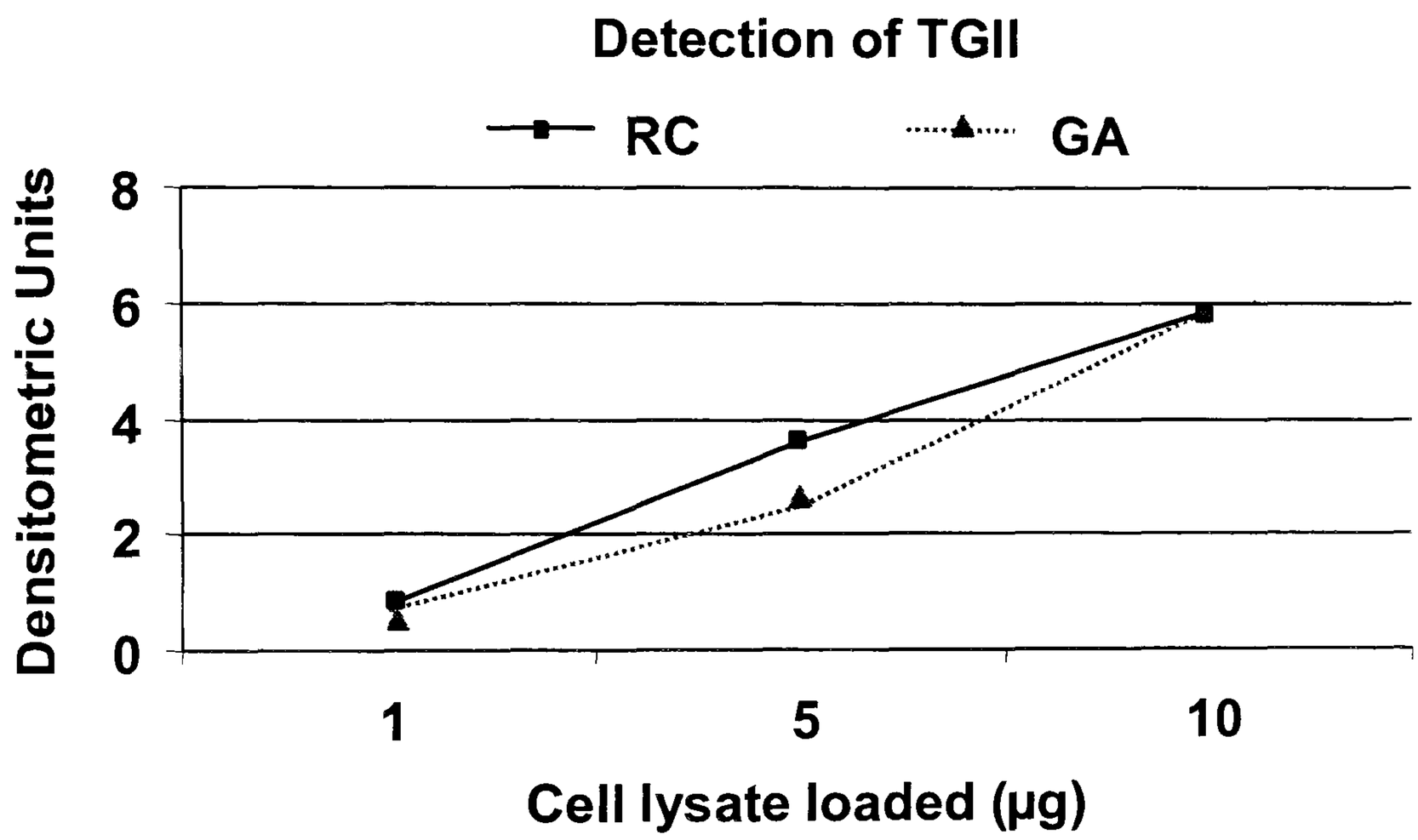


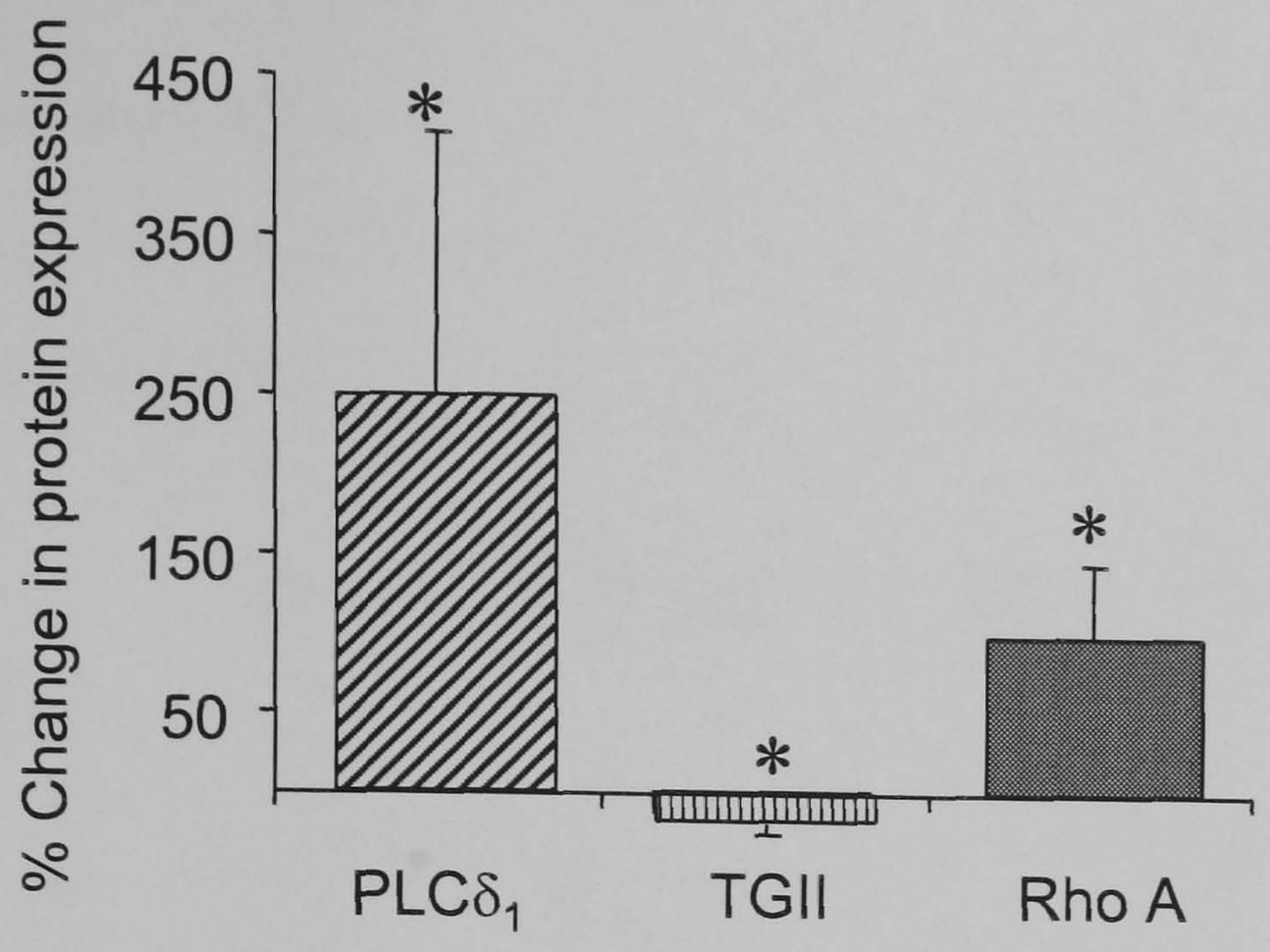
Figure 3.6 Limit of detection of TGII antibody. Different concentration (1µg, 5µg and 10µg) of lysates from randomly cycling compared to serum deprived HVSMC lysates (done at one occasion in triplicate) was loaded on SDS-PAGE gel following western blotting, probing for antibody against TGII. Results show a linear relation between amount of cell lysate loaded and detection of TGII.

This data clearly indicate that there is a linear relation between amount of cell protein loaded on the gel and TGII detection by western blotting. Also, as clearly demonstrated in figure 3.6, TGII is present in HVSMCs and can be effectively detected in this range of protein concentration.

3.6 Effect of serum deprivation on protein expression.

Following the success of control experiments to determine the suitability of the proposed techniques the effect of 'redifferentiation' by serum deprivation was investigated on PLCδ_1 and its potential regulatory proteins TGII and RhoA. As previously shown (figure 3.2) HVSMCs demonstrate a significant increase in both SM α-actin and calponin expression following serum deprivation for 7 days suggesting that redifferentiation had occurred. This significant increase of marker proteins was coupled with a significant increase in both PLCδ_1 and RhoA protein expression whilst TGII expression was significantly decreased. A preparation of brain from WKY (Wistar Kyoto) was used as a positive control (Rhee 1991) in addition to a commercially available positive control for TGII (Labvision, Cat. # MS-300 - PCL). Thus one should bear in mind that no negative control or house-keeping gene was probed for in this study. This would have been a great control to exclude the potential of experimental factors causing a difference to the two conditions compared. The use of a negative control or probing for a housekeeping gene is definitely something to include for future studies.

A



B

	PLCδ1	TGII	RhoA
Average (%)	247	-17	100
SEM (%)	167	7	46

C

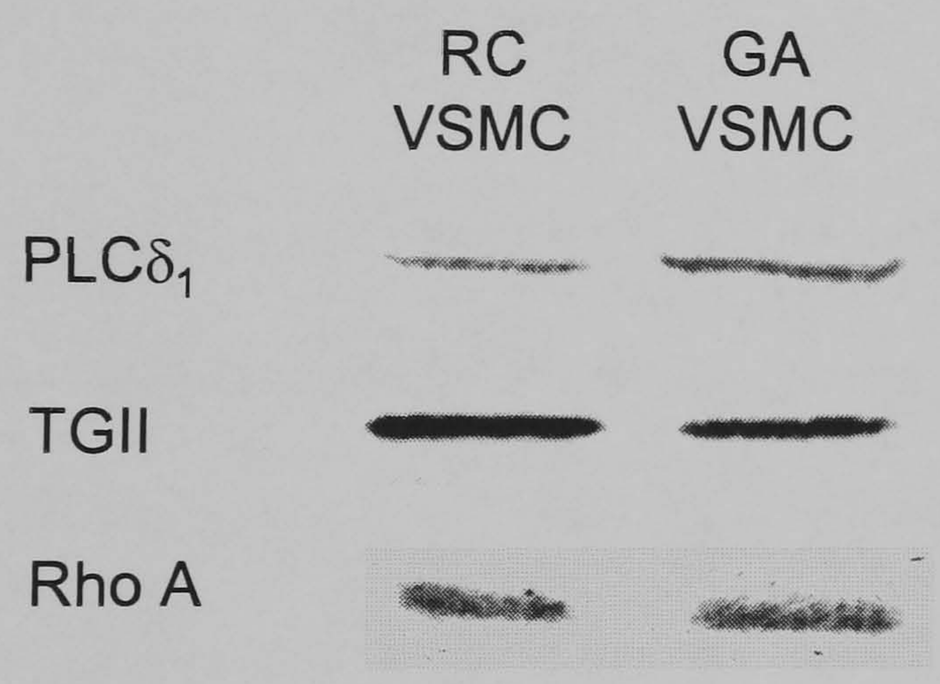


*Figure 3.7 Change in protein expression of PLCδ1, TGII and RhoA in randomly cycling (RC) versus redifferentiated (GA) HVSMC. Graph (**A**) and table (**B**) shows the % change in protein expression of PLCδ1(9), TGII (9) and RhoA (4) as a mean ± SEM. $p < 0.05$(*). **C**. Shows a representative blot.*

3.7 Temporal change in TGII expression during redifferentiation

In order to further elucidate the changes in protein expression that occur during redifferentiation of HVSMCs the temporal change in TGII expression was measured over the seven days of serum deprivation.

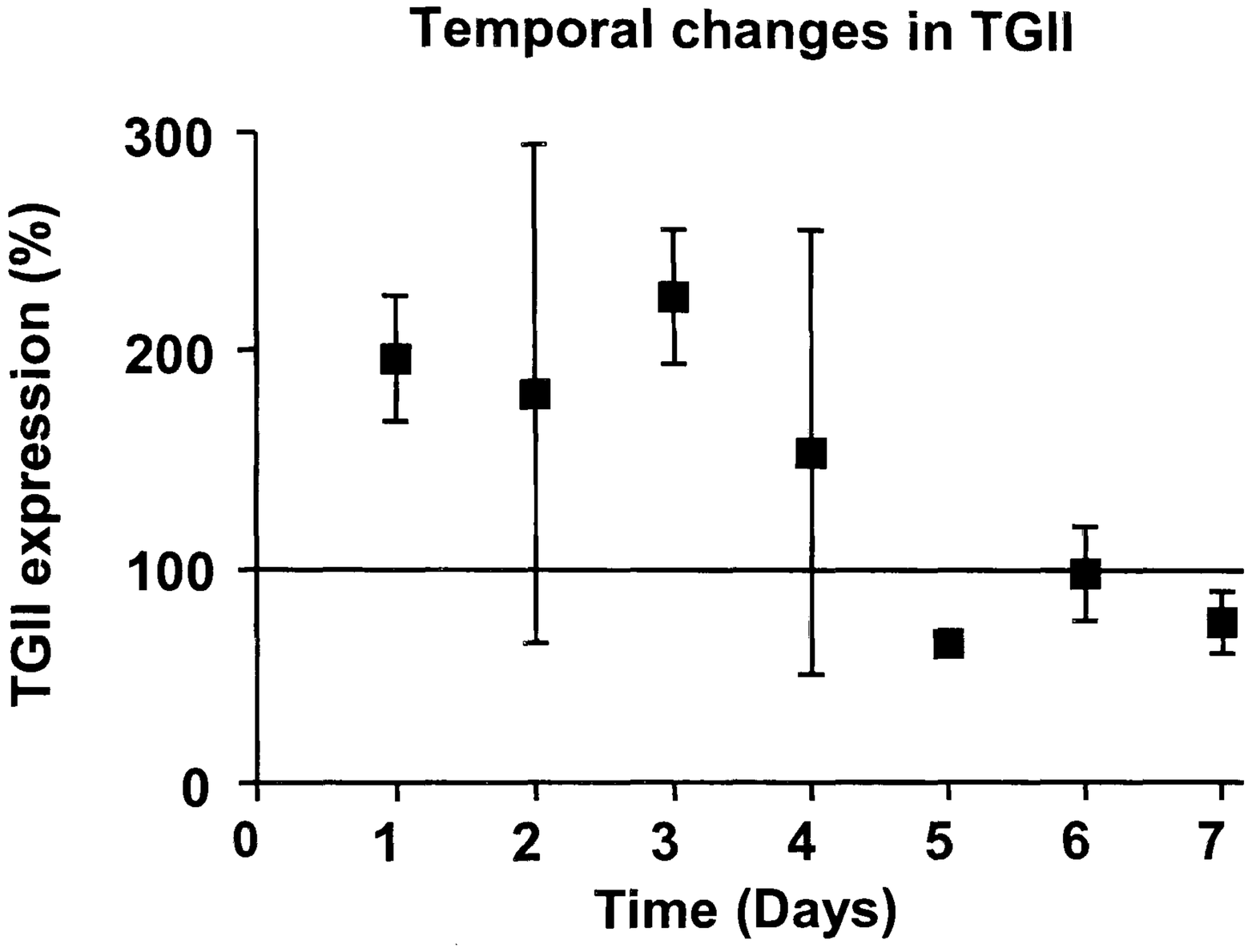


Figure 3.8 Temporal expression of TGII over seven days of serum deprivation. TGII protein expression is shown in per cent over seven days of serum deprivation of HVSMCs in comparison to randomly cycling cells, which are expressed as 100%. Thus, large error bars at day two and three make it difficult to define at what stage changes occur. Though, it does appear that TGII expression drops following five days of serum deprivation and suggest an increase in TGII expression over the first four days. (n=2).

The large error bars seen at day two and four in figure 3.8 make it difficult to accurately determine at what point the change in TGII expression occurs. Although TGII expression appears to increase compared to randomly cycling

cells over the initial four days in culture and at around day five post-serum deprivation expression drop below the level of randomly cycling cells. The expression of TGII is decreased at day seven (-26±15) which correlates well with the data previously demonstrated in figure 3.7 (-17±7).

3.8 Secretion of TGII

Although TGII is essentially a cytosolic enzyme there is increased evidence suggesting that the enzyme is externalised (Balklava, Z., *et al.* 2002; Jones, R.A., *et al.* 1997). The decrease in TGII protein level we detected in cell lysates may be explained by secretion of TGII into the cell culture media following its change in enzymatic activity.

3.8.1 Detection in TGII in culture media

In order to study this further successful and accurate detection of TGII in the culture medium first needed to be established. Therefore, confluent HVSMCs (passage 2-4) were grown in serum-free DMEM culture medium for seven days. The culture medium was then collected and centrifuged to remove any floating cells. Initially a protocol by Balklava and co-workers (Balklava, Z., *et al.* 2000) was followed. Briefly, proteins from the culture medium were precipitated by addition of trichloroacetic acid to a final concentration of 10% (w/v), followed by centrifugation. The protein pellet was washed once with 10% (w/v) trichloroacetic acid followed by ethanol/acetone (1:1) and acetone, dried, and resuspended in 5xLaemmli buffer (Appendix A: 9). Unfortunately, however, we experienced a number of problems with this methodology. It was difficult both to dissolve the pellet and to measure the protein content, even following pH adjustment.

Consequently we decided to measure the level of TGII secreted directly in the culture media. Briefly, floating cells were removed from the culture media by centrifugation, prior to the addition of 5xSDS Laemmli sample buffer. The mixture was then boiled at 95°C for 5 min and left on ice for 10 min. This method proved effective and to further verify this detection method of the level of secreted TGII different amounts of media were loaded and analysed by Western blotting. As seen by the stronger bands in figure 3.9 an increase in amount of loaded sample of culture media yielded an increase in presence of secreted level of TGII.

Detection of TGII secreted in media

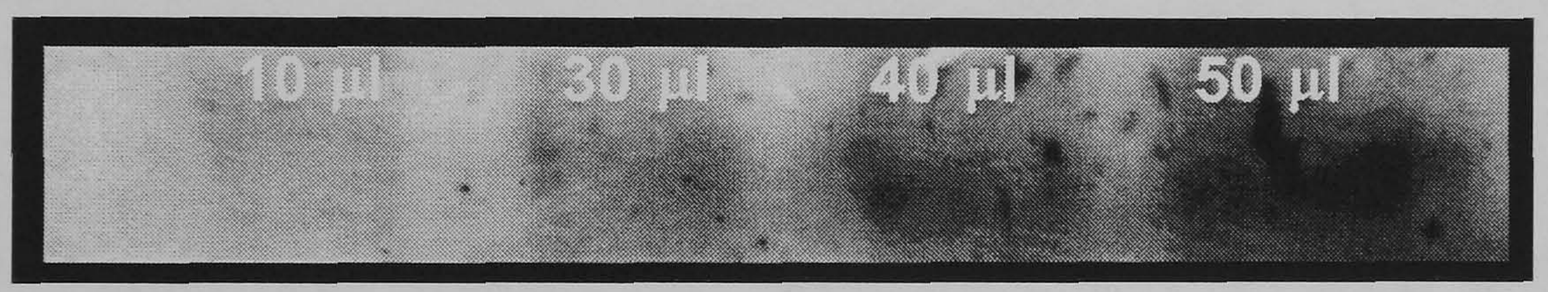


Figure 3.9 Detection of TGII secreted in media. The efficiency of the technique was verified by loading different volumes of prepared media; 10, 30, 40 respectively 50µl of serum free DMEM from HVSMCs was removed after 7 days. An increase in the level of TGII was detected with increased loading of medium. (n=1)

3.9 Level of TGII in cell lysate compared to media during phenotypic change

Having established a method for detecting secreted TGII in the culture media potential differences in the level of secreted TGII in the two phenotypic states were investigated, by Western blotting. As seen in figure 3.10 a decrease in the level of secreted TGII occurred with a change to the more redifferentiated state of

HVSMCs (n=2). Ideally a ratio of TGII in cell lysate and medium in the two phenotypic states should be compared in order to get an indication if redifferentiation of HVSMCs not only affects the protein expression of TGII but as well have an impact on secretion of the enzyme. Unfortunately due to the high degree of saturation of TGII in cell lysates compared with very weak bands indicating the level of TGII secreted in the medium made this impossible to evaluate.

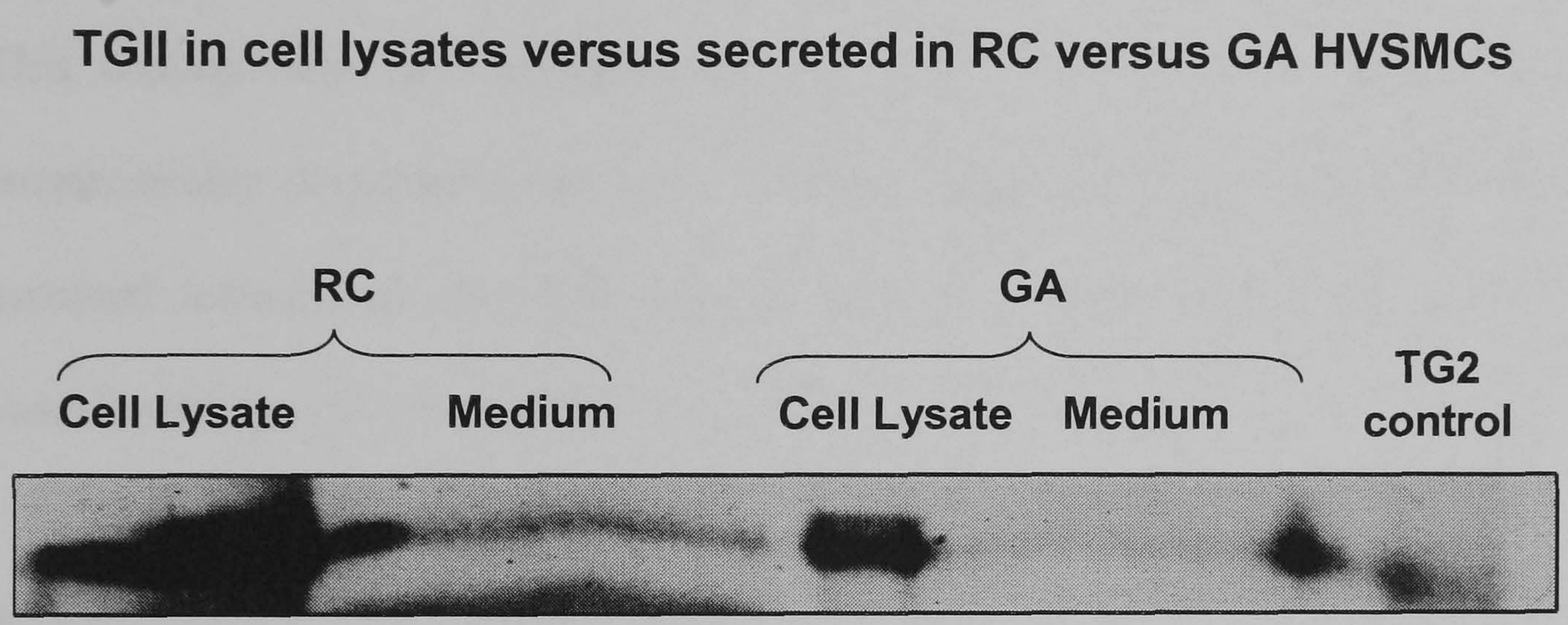


Figure 3.10 TGII in cell lysates versus secreted in the media in randomly cycling (RC) compared to redifferentiated (GA) HVSMCs. Bands appeared on western blot as expected, indicated by positive control for western blot (Labvision, MS-300 – PCL) , (n=2).

Bearing in mind that TGII is a bifunctional enzyme the actual level of protein or change in protein expression may not be as relevant as the nature of the enzyme activity, transglutaminase or GTP binding activity, and rather the actual intracellular location of TGII determining its function (Gaudry, C.A., *et al.* 1999)

DISCUSSION PROTEIN EXPRESSION

A change in the phenotype of mature SMC appears to be a normal response of the artery wall to injury or disruption causing cells to switch from their normal function of contraction and maintenance of vessel wall tone to one of repair of the wound by synthesis of matrix and/or proliferation. Once the wound has healed, cells are presumed to return to their previous phenotype and function.

Culturing of VSMCs may represent a good model of diseased vascular tissue. This concept was first hypothesized in 1967 by Wissler who showed that, enzymatically dispersed cells from arterial media placed in culture gradually assumed features of less differentiated cells with characteristics of SMCs in vascular lesions (Wissler, R.W., *et al.*1967).

Redifferentiation of our HVSMCs was achieved by prolonged serum deprivation, which resulted in a change in morphology with the cells becoming less rounded and taking on a more typical VSMC spindle shape. Apart from the characteristic morphological changes associated with a more differentiated state of the cells a significant increase in the two marker proteins SM α-actin and calponin were used as a measure of redifferentiation, confirming that we indeed were comparing two different phenotypic states of HVSM cells. Previous studies from this laboratory have shown that at higher passage numbers cells become terminally dedifferentiated and once cells reached this stage even prolonged serum deprivation does not result in any increase in marker protein expression. In our study, passage number was minimised by using cells at passages two to four only to enhance our ability to study redifferentiation.

Using this model, imitating a physiological condition of contractile (redifferentiated cells, referred to as growth arrested, GA in the study) SMCs to the so called "synthetic state" (referred to as randomly cycling, RC cells in the study), representing SMCs in a condition of an injury, enable us to compare the effect of phenotypic change on protein expression of PLCδ_1 and TGII.

TGII protein expression

TGII was detected in our HVSMCs. Similarly Thomazy and co-workers found a high level of TGII expression in smooth muscle as well as an abundant level in endothelial cells in arteries, veins and capillaries and other organ-specific cells such as mesengial, renomedullary interstitial and colonic pericryptal fibroblast cells (Thomazy, V., and L. Fesus, 1989; Gendek-Kubiack, H. and E.G. Gendek, 2004). A high level of TGII expression is also found in macrophages (Murtaugh, M.P., *et al.* 1983) and chondrocytes (Aeschlimann, D., *et al.* 1993).

In association with redifferentiation of HVSMCs we found a significant decrease of TGII (-17%±7%, n=9). The time course of TGII expression following serum deprivation showed a small rise followed by a decrease in TGII levels by day five. A decease in TGII protein expression was still measured at day seven of serum deprivation (-26±15, n=2). Although, the presence of large error bars at day two and three make it difficult to draw definite conclusions. It does however appear that TGII expression drops below that seen in randomly cycling cells following five days of serum deprivation and no further changes seem to occur between day five, six or seven.

Interestingly, previous temporal studies in HVSMCs showed that no further change in thymidine incorporation occurred after day five (Figure 3.1). This may indicate that the modulation of TGII expression is related to growth arrest of cells rather than redifferentiation. Another reason for this change in protein expression may relate to the switch in the dual enzymatic function of TGII.

In contrast to our data most studies investigating TGII and its association with cell cycle progression, differentiation or apoptosis have used RA treatment, rather than serum deprivation and have demonstrated mixed results in terms of TGII expression. Retinoic acid did not induce any change in TGII expression in HeLa cells (Singh, U.S., *et al.* 2001) but increased TGII protein expression in rat aortic SMC (Ou, H., *et al.* 2000), human epithelial cells (Pasqali, D., *et al.*1999), human promonocytic leukemia cells (U937) (Olivero, S., *et al.* 1997) and mouse fibroblast cells (NIH3T3) (Antonyak, M.A., *et al.* 2001). Interestingly, Antonyak *et al.* found that retinoic acid treatment of mouse fibroblast cells (NIH3T3) resulted in the activation of PI 3-kinase, which is required for the induction of TGII expression and GTP binding ability (Antonyak, M.A., *et al.* 2003). These different findings in TGII expression following modulation of culture condition resulting in change of phenotype may be due to species differences or tissue studied. Also, differences in method used to induce growth arrest or redifferentiation may result in the cells studied attaining a certain degree of variance in the spectrum between growth arrested and degree of redifferentiation. One important factor to bear in mind when comparing results with the different treatments is that as retinoids directly regulates TGII gene transcription (Nagy, L.,

et al. 1996; Chiocca, E.A., *et al.* 1988) RA treatment would affect TGII expression independent of growth arrest on redifferentiation.

While Ou *et al.* demonstrated a retinoic acid -induced increase in TGII expression this was not coupled with an increase in calponin expression while SM α-actin expression was not measured (Ou, H., *et al.* 2000). Consequently this may not represent a true redifferentiation of these vascular cells. Previous data from this laboratory has indicated that redifferentiation of HVSMCs, as measured by an increase in SM α-actin expression, requires 72hours treatment with RA (Harrington, L.S., PhD thesis, 2003). Bearing in mind the results of the temporal changes of TGII expression following serum deprivation shown here, it is possible that redifferentiation with RA may follow a similar pattern with TGII expression actually being increased initially following RA treatment. Our data would then fit quite well with the increased TGII expression seen at 24 and 48hours RA treatment seen in other studies. In terms of the effects of culture on TGII expression Schnabel *et al.* found an upregulation of TGII protein level following transdifferentiation of myofibroblasts in culture which was coupled with an upregulation in SM α-actin expression (Schnabel, C., *et al.* 2004). Perhaps more importantly Vincan and co-workers demonstrated a reduction in TGII expression with transdifferentiation, suggesting a possible association between TGII and the contractile phenotype. (Vincan, E., *et al.*1996).

A role for TGII in differentiation has also been suggested by Tucholski *et al.* who showed in human neruroblastoma cells (SH-SY5Y) that overexpression of antisense, which results in suppression of endogenous TGII, resulted in cells that

were unresponsive to retinoic acid and that continued to proliferate without extension of neurites (Tucholski, J. and G.V. Johnson, 2003). Piacentini *et al.* found that during retinoic acid treatment SH-SY5Y cells underwent apoptosis and the apoptotic cells in particular expressed a high level of TGII. He also demonstrated that TGII protein level was very low in cells expressing neuronal ("N-type") phenotype compared to so called S-type (substrate adherent) (Piacentini, M., *et al.* 1992).

Secretion of TGII

Although TGII is essentially a cytosolic enzyme there is literature evidence suggesting that the enzyme is externalised (Balklava, Z., *et al.* 2002; Jones, R.A., *et al.* 1997). Once externalised from the cell, TGII has been shown to bind and cross-link a number of extracellular proteins, in particular fibronectin (Achyuthan, K.E., *et al.* 1995). Jones *et al.* showed that a decrease in expression of TGII, by silencing, in ECV 304 endothelial like cells leads to a reduced ability of these cells to spread and adhere (Jones, R.A., *et al.* 1997).

We investigated the level of secreted TGII, by analysing medium removed from cells. Our results suggest that TGII is secreted to a larger extent in randomly cycling cells as compared to growth arrested cells. This could suggest that reduced secretion of TGII occurs in association with inhibition of proliferation or growth arrest as we previously shown that seven days of serum deprivation is a post growth arrest phenomena, indicated by a significant increase in SM α-actin. However, this higher level of TGII secretion measured in RC could be due just to a higher amount of cells and the actual amount of TGII secreted per cell could be

the same. Thus, our results do correlate with work performed by Balklava *et al.* who demonstrated that in fibroblasts expression of TGII lacking transglutaminase activity result in no deposit of the enzyme into the ECM or secretion into the cell culture medium (Balklava, Z., *et al*. 2002).

Similarly to the protein expression study we measured a higher level of TGII expression in RC versus GA cells. As the bands on the blots indicating level of secreted TGII were very weak whilst over saturated bands were found when investigating the level of TGII in lysates it was difficult to base a ratio of the level of TGII in lysates to medium in the two phenotypic states.

Temporal changes of secreted TGII were also studied. Unfortunately no bands were detected (n=3). A possible explanation to this phenomenon is the break down of proteins. As the level of secreted TGII is investigated by examining level of TGII directly in medium removed from cells no protease inhibitors are added compared to in lysates where protease inhibitors are present in the lysis buffer.

Expression of PLCδ_1

A significant increase in PLCδ_1 was detected in HVSMCs pushed to a more differentiated state by serum deprivation. This correlates well with previous studies in the laboratory that showed a significant increase in PLCδ_1 expression coupled with a concomitant decrease in PLCγ_1 expression in HVSMCs following serum deprivation, lovastatin or retinoic acid treatment (Harrington, L.S., PhD-thesis, 2003). The same study showed that the increase in PLCδ_1 expression did not occur until day seven, when levels of SM α-actin increased (Figure 3.1). In

contrast to the temporal study of TGII expression, this suggests that the increase in PLCδ_1 is a feature of redifferentiation rather than growth arrest and reflects a possible functional role of PLCδ_1 in redifferentiation and/or a more contractile phenotype of the HVSMCs studied.

With evidence suggesting a linkage of TGII and PCLδ_1 combined with the detected reciprocal regulation of PLCδ_1 and TGII expression may indicate that the complex formation is under strict regulation. Also, the increase in PLCδ_1 expression, concomitant with a reduced level of TGII expression, may be a way to limit the possibility for their association to occur only during a specific condition.

CHAPTER 4 PROTEIN LOCALISATION

4.1 Aim of localisation studies

To investigate the effect of phenotypic change, to a more redifferentiatied state, on the intracellular localisation of both PLCδ_1 and TGII individually as well as their subcellular localisation in relation to each other. Also, the possible involvement and/or association of PLCδ_1 and/or TGII with the actin cytoskeleton and its organisation were investigated.

4.2 Intracellular location

Subcellular compartmentalisation of signalling molecules is not only an important component of defining how a signal pathway is activated but can also aid in the investigation of that pathway under certain physiological conditions, as in our case the effect of phenotypic change and cytoskeletal changes.

Analysis of intracellular protein localisation has traditionally been examined using immunofluroescence of permeabilized cell preparations fixed to glass slides. However, in our study we used a confocal laser scanning microscope (CLSM) which is an improved design of light microscope, used for imaging fixed or living tissues that are usually labelled with one or more fluorescent probes.

4.3. CLSM – confocal laser scanning microscope.

The basic concept of confocal microscopy was originally developed by Marvin Minsky in the mid-1950s. Following Minsky's work and the contributions of several investigators the first commercial instruments appeared in 1987. During the 1990s, advances in optics and electronics afforded more stable and powerful lasers, high-efficiency scanning mirror units and detectors with reduced noise characteristics. In addition, fluorochromes, which were more carefully matched to laser excitation lines, were beginning to be synthesized and this was coupled with the rapidly advancing computer processing speeds and technology that was emerging in the late 1990s.

Biological laser scanning confocal microscopy relies heavily on fluorescence as an imaging mode, primarily due to the high degree of sensitivity afforded by the technique coupled with the ability to specifically target structural components and dynamic processes in chemically fixed as well as living cells and tissues.

One of the advantages of the confocal laser scanning microscopy (CLSM) for imaging fluorescently labelled specimens is its ability to produce images, called optical sections that are free from contaminating fluorescence from structures out of the focal plane of interest. This gives improved contrast and resolution of the images when compared with those collected with a conventional epifluorescence microscope. Also, a real image is not formed in the CLSM instead the output of the photo multiplicatior transducer (PMT) is translated into an image of the region of interest using a digital imaging system. The images can be processed, measured, displayed and recorded using digital methods.

Unfortunately our HVSM cells are too flat to take several different sections throughout the cell. Instead an average section of four scans of the cell examined was used.

4.4.1 Preparation of coverslips with cells for fluorescent staining

To enable studying the proteins of interest HVSMCs, plated on cover slips, are fixed to stabilise all structures within the cell without altering them, preventing loss of soluble proteins and yet allowing complete access of antibodies to their epitope (Hopwood, D., *et al.* 1969). Fixation methods generally fall into two classes: organic solvents and cross-linking reagents. Organic solvents such as alcohols and acetone remove lipids and dehydrate the cells, while precipitating the proteins on the cellular architecture. Compared to methanol fixation, chemical cross-linkers as Formaldehyde (Blanchette–Mackie, E.J., *et al.* 1995) or Gluteraldehyde (Campbell, G.R. and J.H. Chamley, 1975) instead works by forming a meshwork of cross-links between the cellular proteins, normally through free amino groups. As the proteins (PLCδ_1 and TGII) of interest may be implicated in the regulation of the cytoskeleton we chose to use methanol fixation as it is keeps the cytoskeletal structure intact (DiDonato, D., *et al.* 2003).

4.4.2 Methanol fixation

Fixation of our coverslips was performed with cold methanol (Osborn, M., and K. Weber, 1977) which works by precipitating the cellular proteins onto the coverslip.

4.4.3 Permeabilisation

To enable access of our antibodies to the intracellular structures and our protein of interests our cells needed to be permeabilised. Triton X-100 (0.05%, Sigma), a widely used non-ionic surfactant is a detergent which permeabilises the cell membrane, was added to the washing solution (TPBS).

4.4.4 Staining

Fixed and permeabilised cells were incubated with 1ml of 5% BSA (in TPBS) to block any non-specific antibody labelling prior to antibody staining. Primary antibody was then added at a concentration of 1:50 for two hours diluted in 5% BSA in TTBS. The antibody was used in a sandwich step whereby the unlabelled primary antibody is recognised by a fluorescently labelled secondary antibody. The secondary antibody recognises the primary antibody chains rather than a specific epitope, which has two advantages; the same secondary antibody can be used against any primary antibody raised in that species and signal amplification occurs through multiple secondary antibodies binding to each primary antibody. In the case where double labelling with antibodies was performed similar procedure was performed. Thus two primary antibodies were added sequentially and following washes the two secondary antibodies were added together.

4.5 Control pictures for immuno flurorescent staining of HVSMCs

Control experiments to verify staining specificity are of major importance when using immunofluorescence. Ideally all staining would result from the protein of interest only with no additional staining from other sources. Unfortunately the cell

itself often has a certain degree of autoflurorescence. Determination of background fluorescence was defined by staining our HVSMCs with just blocking solution, 5% BSA in TTBS. As seen in figure 4.1 (A) there was very little background fluorescence, with just a small amount of staining around the nucleus of the cell. To reveal the extent of non-specific binding of secondary antibodies, cells were stained with just secondary antibody. Anti-goat-Rhodamine linked secondary antibody (figure 4.1: C) showed a higher level of non-specific binding compared to anti-mouse-FITC linked secondary antibody (figure 4.1: B) where very little non-specific binding seemed to occur. The level of non-specific binding provides useful information about the level of staining which is unrelated to the antigen of interest. As for dual stained slides a control was examined for the possible cross-reaction of the two antibodies by simultaneous addition of the anti-goat-Rhodamine linked and the anti-mouse-FITC linked secondary antibody (figure 4.1:D). A slight level of background fluorescence is present which was taken into consideration when analysis of double staining was performed. When the primary antibodies have been raised in very different species they can be used at the same time in the primary antibody incubation. Care must then be taken in the secondary antibody step that the two secondary antibodies were raised in the same species. For example both were raised in donkey against rabbit and mouse immunoglobulins. This will ensure that the secondary antibodies do not cross react with each other. It is possible to buy secondary antibodies that have been pre-absorbed to ensure that there is no cross reactivity with a whole range of other species.

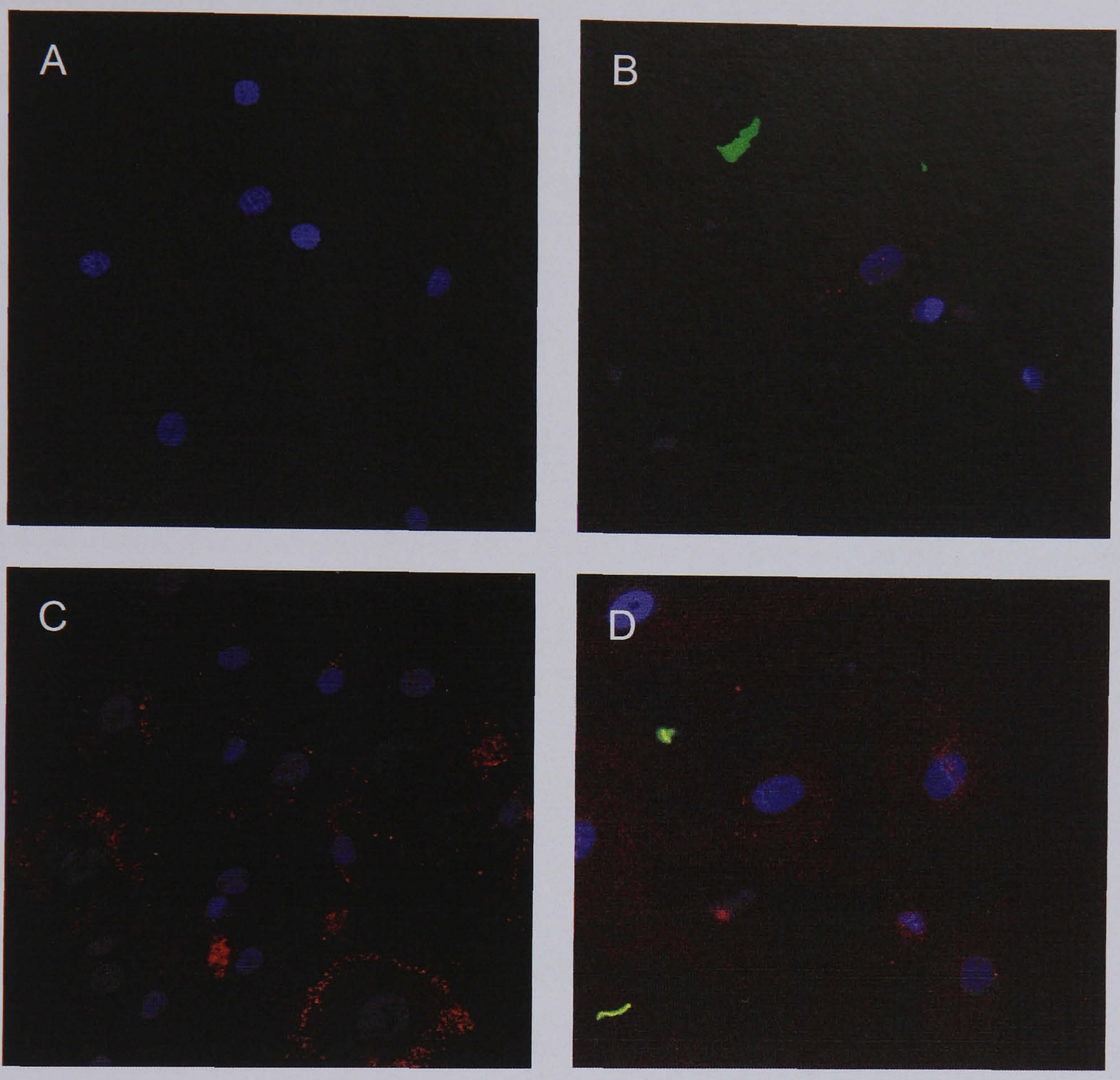


Figure 4.1 Controls for immunofluorescent staining. ***A****. Cells stained with 5% BSA in TTBS to examine the level of autofluorescence of HVSMCs.* ***B*** *&* ***C*** *Information of specificity of secondary antibodies was shown by addition of just secondary antibody without presence of primary antibody,* anti-mouse-FITC linked secondary antibody *demonstrated in* ***B*** *and* Anti-goat-Rhodamine linked secondary antibody in ***C****. Little background and/or autofluorescence was seen in our cells.* ***D*** *Low level of cross reaction in double stained cells. Nucleus seen in blue by DAPI staining. Images taken with a Leica TCP-SP scanning confocal microscope, x40 lens).*

4.6 The effect of serum deprivation on HVSMCs

Redifferentiation by seven days of serum deprivation resulted in clear structural changes in both the two marker proteins SM α-actin and calponin. In randomly cycling cells SM α-actin formed Globular (G-) actin with thin branching fibers of actin throughout the cell. Following prolonged (7-day) serum deprivation SM α-actin took a more defined structure with a greater proportion of SM α-actin present as Filament (F-) actin, characterised by the thick, long fibers running in parallel lines along the length of the cell. A similar change to a more structured appearance is seen in redifferentiated cells stained with antibodies for calponin (figure 4.2), with large numbers of long fibres being seen running the length of the cell. Confocal microscopy also demonstrated a clear increase in the expression level calponin following redifferentiation and to a smaller extent an increase in SM α-actin expression. These data correlated well with Western blotting data previously observed (chapter 3.1) and suggests that redifferentiation has indeed occurred.

The effect of redifferentiation on SM α-actin and calponin expression

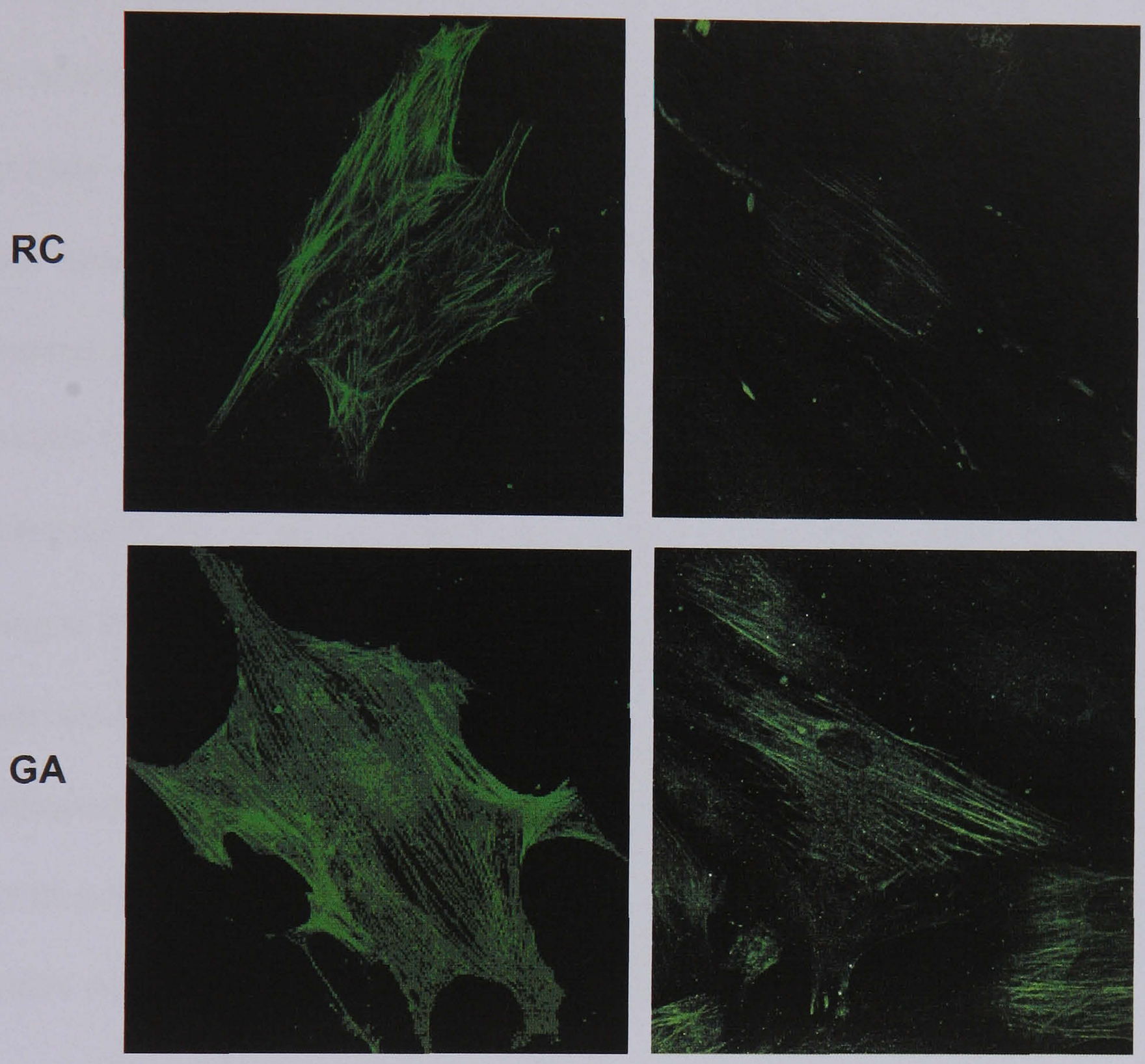


Figure 4.2 Effect of redifferentiation on the subcellular localisation of SM α-actin and calponin. Confocal microscopy images showing the subcellular localisation and structural organisation of SM α-actin and calponin in randomly cycling (RC) and serum deprived (GA) HVSMC. Pictures showing average of four scans of one section obtained from a single cell strain and are representative of four separate cell strains. Images taken with a Leica TCP-SP scanning confocal microscope, x40 lens).

4.7 Trouble shooting with PLCδ_1 antibody

In our initial experiments we used an anti-PLCδ_1 antibody from Santa Cruz Biotechnology Inc. (anti-goat, *sc-7521*, Lot #D091), which worked very well in our cells (see figure 4.3, A). Unfortunately midway through this project production of this antibody targeting the C-terminal was stopped and no further batches of this antibody were available. At this point we tried out a replacement PLCδ_1 antibody from Santa Cruz Biotechnology Inc. (anti-goat, sc-7520) with epitope for the N-terminal instead of the targeted C-terminal. Unfortunately this antibody was not suitable for immunofluorescence studies in these cells, as shown in figure 4.3.B, where no PLCδ_1 at all could be detected. Similarly no staining was detected when using a PLCδ_1 antibody from Upstate (05-343, pictures not shown). Although, these antibodies did not work for staining they were suitable for Western blotting. Following much searching we finally located a new PLCδ_1 antibody produced by BD Bioscience Pharmingen (610356) which was suitable for immunofluorescence studies within the cells (figure 4.3.C).

Trouble shooting with PLCδ_1 antibody

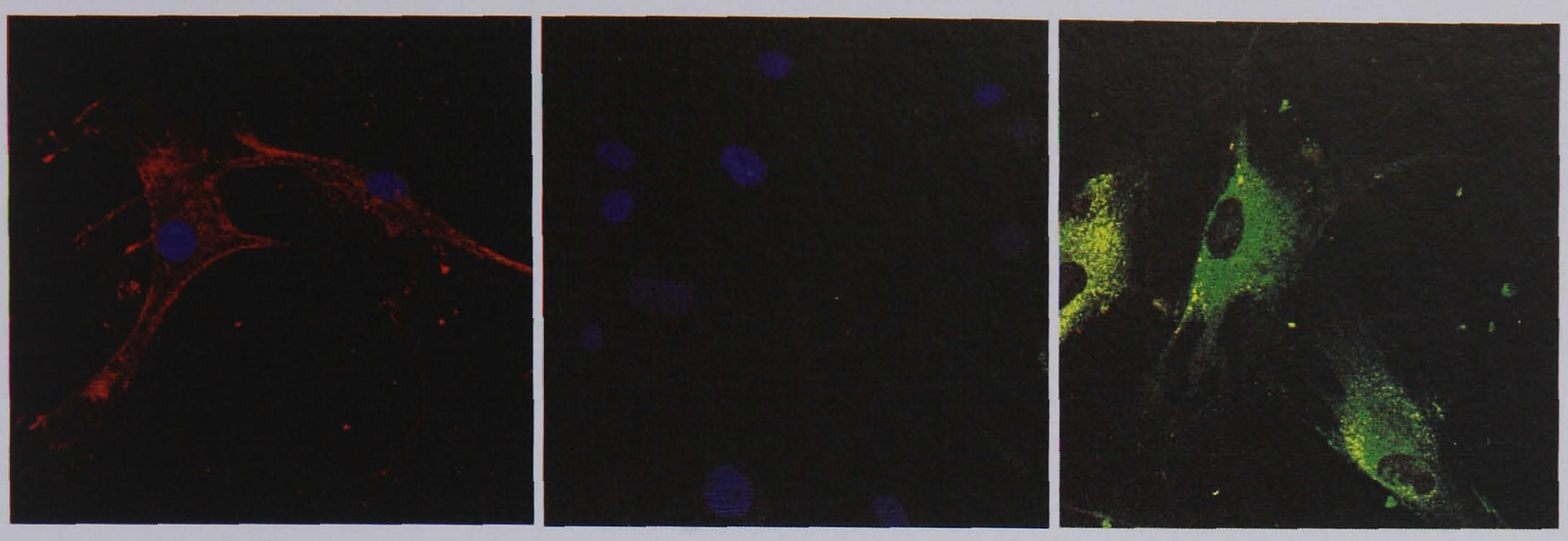


Figure 4.3 Immunofluorescence staining using 3 different antibodies against PLCδ_1. ***A.*** *Successful staining of PLCδ_1 when using a PLCδ_1 antibody from Santa Cruz Biotechnology Inc. (anti-goat, sc-7521, Lot #D091), a Rhodamine linked donkey anti-goat antibody (sc-2094, Santa Cruze biotechnology) was used to monitor PLCδ_1.* ***B****. No staining detected with replacement antibody from Santa Cruz Biotechnology Inc. (anti-goat, sc-7520).* ***C****. Finally staining of PLCδ_1 was achieved with a new antibody from BD Bioscience Pharmingen (Cat No: 610356). This monoclonal mouse antibody was detected with a secondary-FITC linked antibody. Nucleus is seen in blue by DAPI staining. Images taken with a Leica TCP-SP scanning confocal microscope, x40 lens).*

4.8 Effect of serum deprivation on protein localisation and organisation of TGII and PLCδ_1 in HVSMCs.

If the changes in protein expression of PLCδ_1 and TGII are linked to changes in cellular function it is possible that they may be associated with changes in subcellular localisation. The intracellular localisation and possible redistribution of both PLCδ_1 and TGII was studied by immunofluorescence staining in isolated HVSMCs following redifferentiation (by 7 days of serum deprivation). Again the induction of redifferentiation was confirmed by the more structural appearance of the two marker proteins SM α-actin and calponin (figure 4.2). These changes were paralleled by a clear shift in localisation of both TGII and PLCδ_1 in redifferentiated cells (figure 4.4). PLCδ_1 relocalises from a more perinuclear region to the entire cytoplasm after treatment showing a more structured localisation. PLCδ_1 expression was also clearly increased by redifferentiation of HVSMCs which correlates well with western blotting data (see figure 3.6). In randomly cycling cells TGII was ubiquitously expressed throughout the cytoplasm and appeared to relocalise to a more localised cytoplasmic subcellular localisation or the difference in staining pattern seen following redifferentiation could be due to a reduction in the cytoplasmic levels of TGII. Interestingly, in some cases TGII appeared in a different subcellular localisation in randomly cycling cells, forming what appeared to be a negative image to the SM α-actin structure and thus did not appear to directly bind to it (figure 4.5). Similar structures were seen in growth arrested cells to a lesser extent. TGII also appear to localise at areas of the edges of the cells. With redifferentiation TGII seemed to decrease as was previously seen with western blotting studies (see figure 3.5).

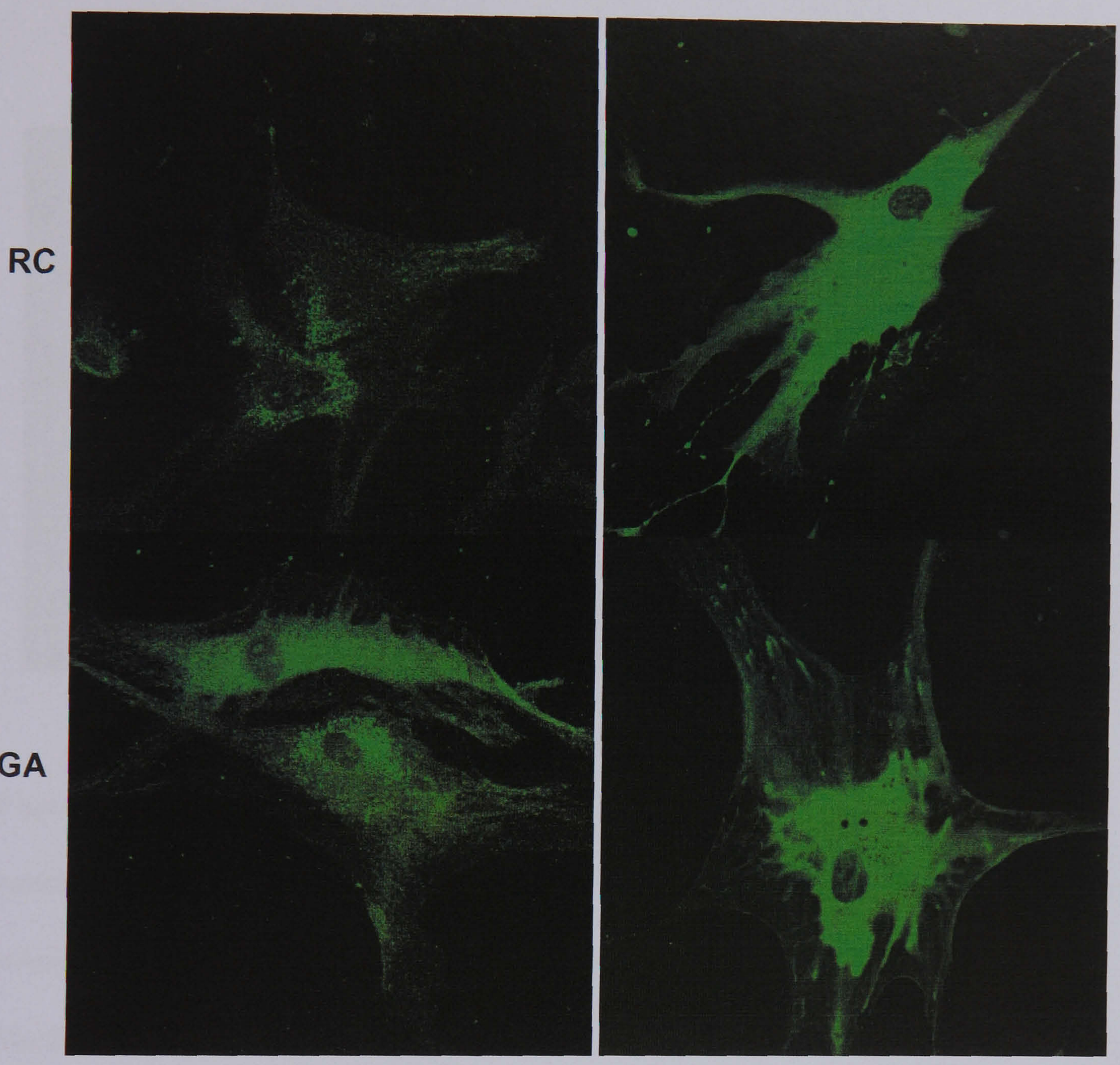


Figure 4.4 Effect of redifferentiation on the subcellular localisation of PLCδ_1 and TGII. Both proteins re-localises upon a change of phenotypic change, from randomly cycling (RC) to redifferentiated (GA, growth arrested) HVSMCs. Images, visualised with confocal microscopy are showing one section (average of four scans) of one single cell strain and are a representative of n=5 separate cell strains. Images taken with a Leica TCP-SP scanning confocal microscope, x40 lens).

Subcellular localisation of TGII in RC versus GA HVSMCs

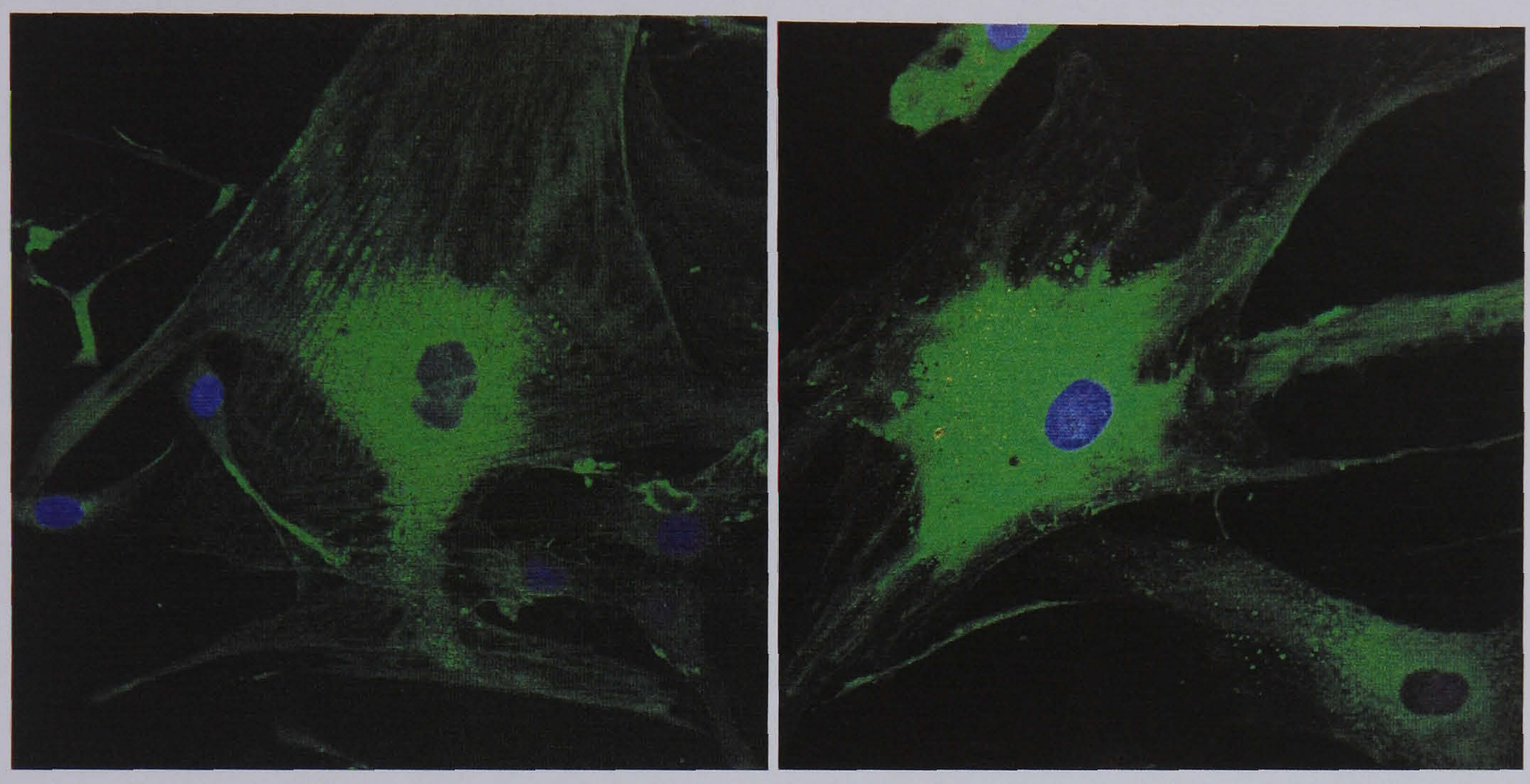


Figure 4.5 Subcellular localisation and structural organisation of TGII in randomly cycling and serum deprived HVSMC. Staining of TGII appears to form whole-like lines, looking like a negative image to the SM α- actin structure. Similar structures seen in growth arrested (GA) cell thus to a less extent compared to in randomly cycling (RC) cell. Images, visualised with confocal microscopy are showing one section (average of four scans) of one single cell strain. Nucleus is seen in blue by DAPI staining. Images taken with a Leica TCP-SP scanning confocal microscope, x40 lens).

4.9 Co-localisation of PLCδ_1 and TGII?

TGII and PLCδ_1 seem to appear in similar subcellular regions. Therefore, to examine the possibility of co-localisation of the two within the cell dual staining for these proteins were performed on both randomly cycling and serum deprived HVSMCs. Dual staining revealed co-localisation of TGII with PLCδ_1. This co-localisation can be distinguished by the yellow fluorescence as seen in figure 4.6, resulting from a mix of green (TGII) and red (PLCδ_1) wavelengths emitted from the FITC respectively Rhodamine labelled secondary antibodies. It is clear, however, that co-localisation occurs predominantly in redifferentiated cells and is markedly less apparent in randomly cycling cells. The great difference in level of protein expression of the two proteins made it difficult in some cells to visualise a yellow colour due to the higher level of TGII present in the cell, seen by the intensive green emission. Figure 4.7 represent a good example of cells that are stained for both PLCδ_1 (red) and TGII (green) thus no or just very faint red can be visualised. In these cells we evaluated the presence of co-localisation using the software Zeiss LSM 510. This software monitors the presence of co-localisation by showing the presence of green and red pixels within a specified area chosen in white. By assessment using the software figure 4.7 (lower pictures) show that co-localisation actually did occur even in these cells, as confirmed by the white dots indicating the presence of overlapping red and green pixels. Similarly to images in figure 4.7 a higher degree of co-localisation was found in redifferentiated cells.

Co-localisation of TGII and PLCδ_1 in RC versus GA HVSMCs

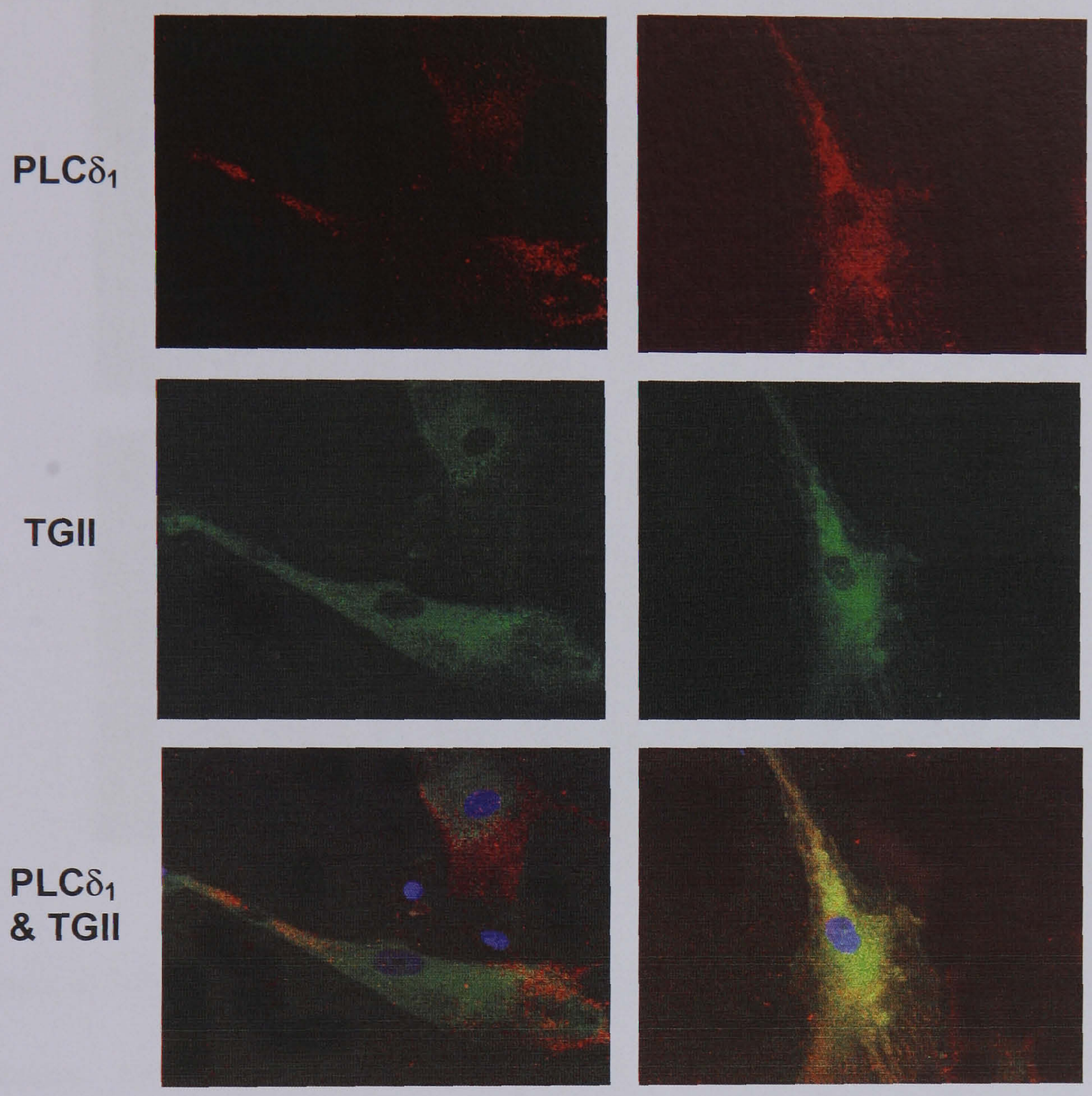


Figure 4.6 Double staining of TGII and PLCδ_1 in HVSMCs. Randomly cycling (RC) and growth arrested (GA) HVSMCs double stained with TGII and PLCδ_1 (green: TGII tagged with FITC; red: PLCδ_1 tagged with Rhodamine, nucleus is seen in blue by DAPI staining). Images, visualised with confocal microscopy are showing one section (average of four scans) of one single cell strain. Increased level of co-localisation is visualised by the more yellow colour seen by the overlapping red and green pixels (n=4). *Images taken with a Leica TCP-SP scanning confocal microscope, x40 lens).*

Co-localisation evaluated by Zeiss LSM510 software

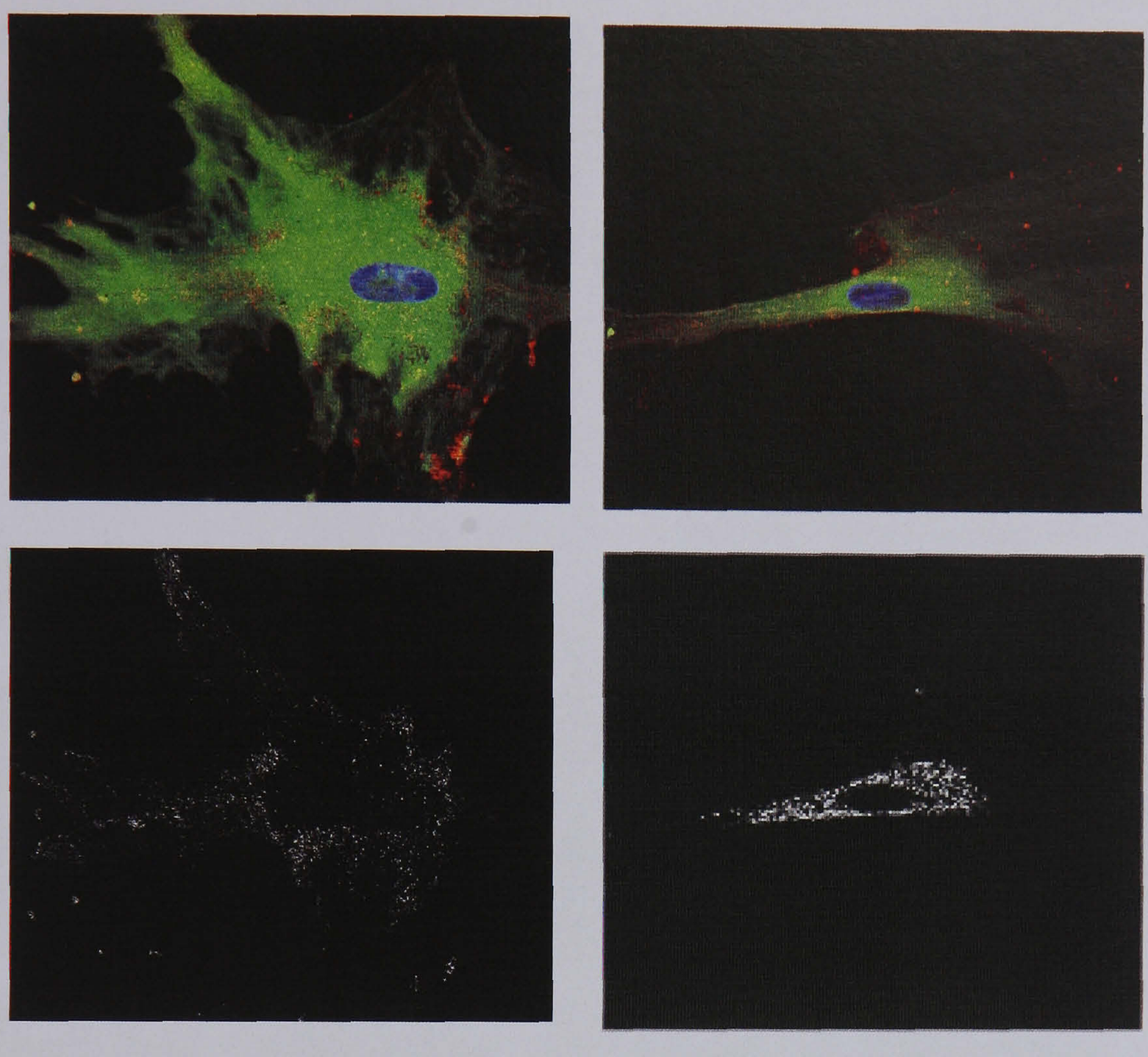


Figure 4.7 Dual staining of TGII and PLCδ_1 in HVSMCs evaluated by LSM510 software. Images are showing HVSMC double stained with TGII and PLCδ_1 (green: TGII tagged with FITC; red: PLCδ_1 tagged with Rhodamine). Co-localisation of double staining was analysed by Zeiss LSM 510 software. Areas where co-localisation occurs are indicated in white by the software. An increase in co-localisation of the two proteins occurs in redifferentiation HVSMCs, seen by the higher level of white in serum deprived cells. Images are representative from four separate cell strains. Images taken with a Leica TCP-SP scanning confocal microscope, x40 lens).

4.10 Is there an association of PLCδ_1 and/or TGII with actin cytoskeleton?

Previous work by L. Harrington (Figure 4.8) suggest that co-localisation between PLCδ_1 and SM α-actin occurrs in redifferentiated HVSMCs. This association with an increase in PLCδ_1 protein expression with redifferentiation suggests some role for this enzyme in attaining differentiated status of the cell and a possible association with the actin cytoskeleton.

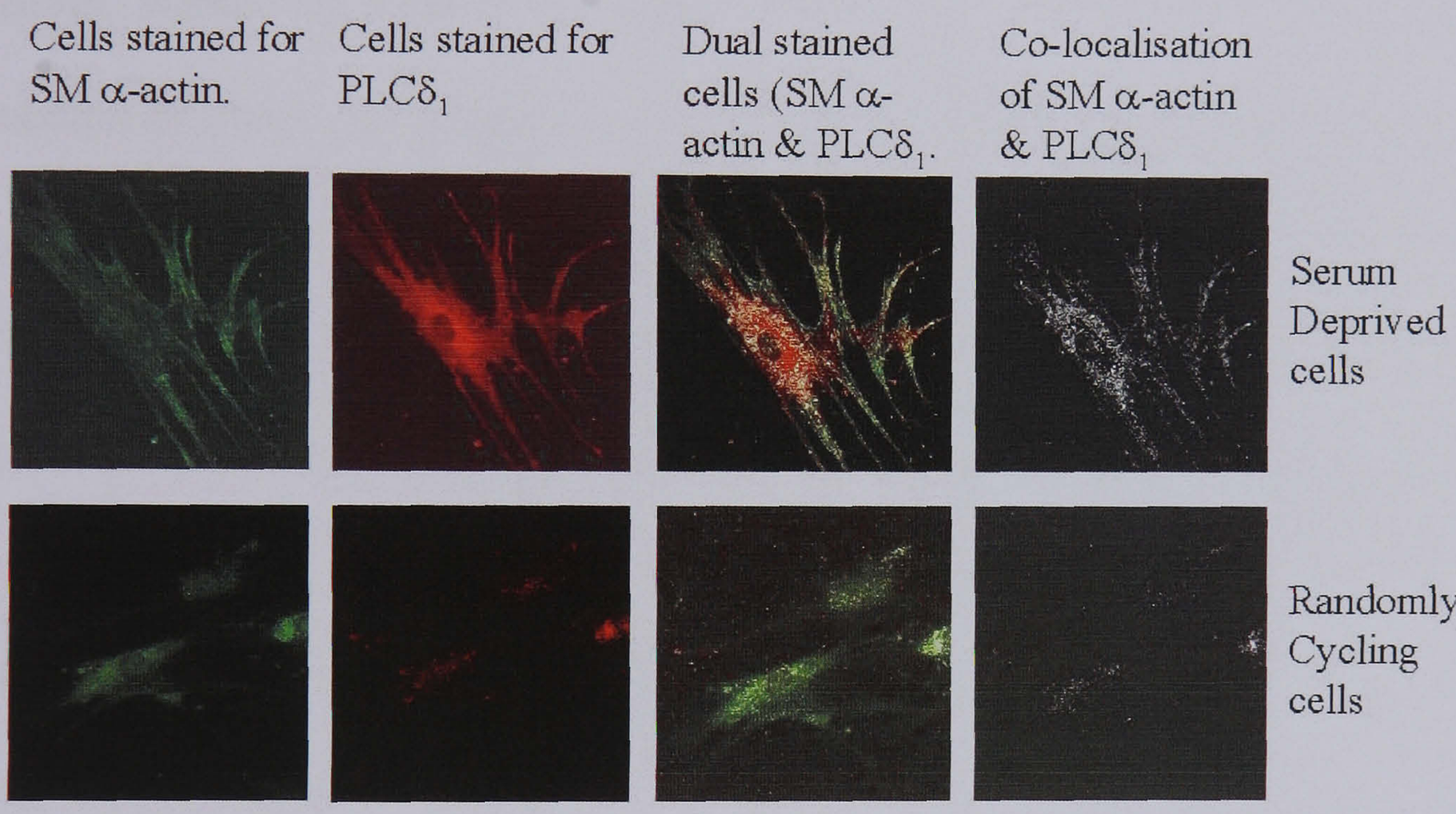


Figure 4.8. Dual staining of SM α-actin and PLCδ_1 in HVSMCs. Randomly cycling and growth arrested HVSMCs stained with SM α-actin (green: tagged with FITC) and PLCδ_1 (red: PLCδ_1 tagged with Rhodamine). Images, visualised with confocal microscopy are showing one section (average of four scans) of one single cell strain. Zeiss LSM510 software was used to analyse presence of co-localisation, which appear as white. Images are representative of 3 separate cell strains.

There is good evidence in the literature suggesting that TGII, with transglutaminase activity associates with cytoskeletal components. Mearns and co-workers revealed following phalloidin staining of fibroblasts lacking TGII how these cells were lacking reorganisation and stress fibre formation in response to wound stimulus whilst TGII overexpressing cells showed more extensive stress fibre formation than mock transfected cells and only small level of stress fibre formation was detected in TGII deficient cells (Mearns, B., *et al.* 2002). Moreover, studies by Singh *et al.* demonstrated that TGII is required for the stimulation of RhoA and consequently ERK1/2, JNK1, p38γ, MAPkinases (Singh, U.S., *et al.* 2003). RhoA, has also been shown to act as a negative modulator of PLCδ_1 activity (Hodson, E., 1998; Homma, Y. and Y. Emori, 1995) and has long been known to be involved in the regulation of actin polymerisation (Hall, A. and C.D. Noble, 2000; Kaibuchi, K., *et al.* 1999; Worth, N.F., *et al.* 2004). Recently Murthy *et al* demonstrated inactivation of PLCδ_1 by direct binding to RhoA (Kang, K., *et al.* 2004).

In order to further investigate the possible involvement and/or association of PLCδ_1 and TGII with the actin cytoskeleton and its organisation the cellular localisation of these proteins was examined following treatment with both Cytochalasin D, to disrupt the actin cytoskeleton structure, and Colchicine, which disrupts the microtubular system. Cellular localisation of the proteins was again visualised using fluorescent labelled antibodies and monitored with confocal microscopy as previously described. (Method section 2.11)

4.11 Actin cytoskeleton

The regulation of SMC phenotype appears to be intimately coupled to the organisation of the cytoskeleton (Doevendans, P.A. and G. van Eys, 2001;Worth, N.F., *et al.* 2001). The flexibility and complexity of eukaryotic cells depends entirely on intracellular filaments, collectively called the cytoskeleton (for more information see introduction, section 1.5.1). The cytoskeleton is a protein framework that enables an eukaryotic cell to maintain or change its shape and its degree of attachment to the substratum in response to extracellular or intracellular signals. The fibers of the cytoskeleton can provide rigidity, but the entire structure may disassemble and remodel within minutes. There are three cytoskeletal elements: microtubules, actin and the intermediate filaments, though it is only actin and intermediate filaments that become associated with cell-cell and cell-matrix junctions.

4.12 Modulation of actin cytoskeletal structure

4.12.1 Modulation of actin cytoskeletal structure by Cytochalasin D

Actin cytoskeleton integrity has proved to be a major requirement in many signalling events and is a powerful regulator of cell shape. Addition of cytochalasin D, a drug that disrupts the integrity of the microfilament lattice by inhibiting actin polymerization, results in inhibition of cell spreading in many cell types (Rescan, C., *et al.* 2001). Cytochalasin, meaning "cell relaxing" is so named because it causes regression of the cleavage furrow during cytochinesis and disrupts many structures containing actin filaments in cells. Cytochalasins are therefore often used for investigating the involvement participation of actin filaments in cellular processes.

4.12.2 Exposure of HVSMCs to Cytochalasin D and Colchicine

Briefly, third passage HVSMC, cultured on sterile coverslips, were serum deprived for seven days following two hours treatment with either cytochalasin D (100nM) or colchicine (2 μM). These two concentrations were chosen based on studies previously performed in our group (Abdel-Hadi, H., 2003). Cells were then fixed, washed and mounted onto glass slides. Fixed cells were stained as outlined before (see methods 2.11) and immunofluoresence staining was viewed using a Leica TCS SP confocal microscope.

4.13. Effect of Cytochalasin D

4.13.1 Effect of Cytochalasin D on actin cytoskeleton

The disruptive action of the actin cytoskeleton by cytochalasin D was seen by the structural loss seen when staining for SM α-actin.

Effect of Cytochalasin D on SM α-actin

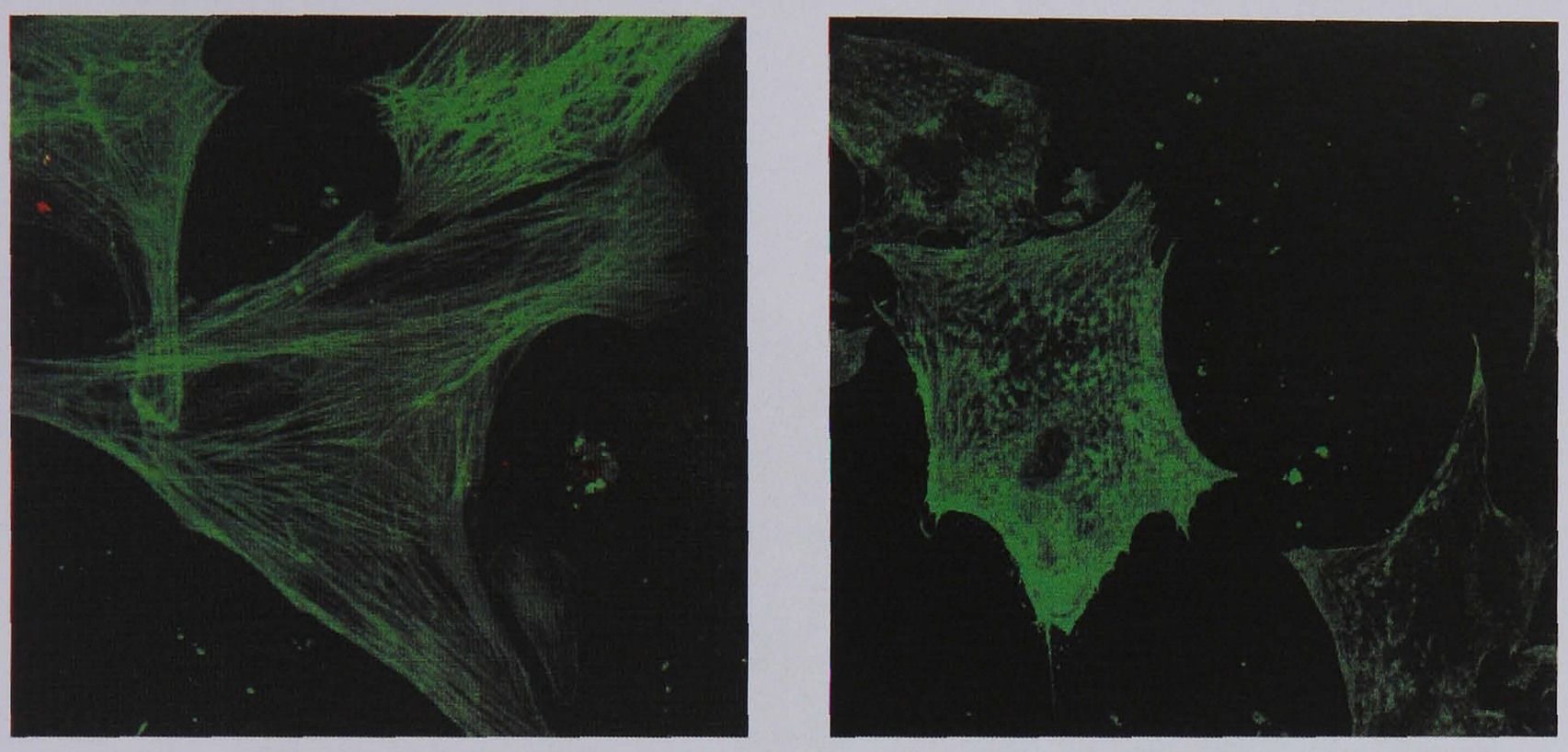


Figure 4.8 Effect of Cytochalasin D on the actin cytoskeleton. Confocal microscopy showing the subcellular localisation and structural organisation of SM α-actin in serum deprived (Growth arrested, GA) HVSMC in the presence and absence of 100 nM cytochalasin D. Pictures are the average of four scans of one single section of a cell and are representative of findings in 3-4 separate cell strains. Images taken with a Leica TCP-SP scanning confocal microscope, x40 lens).

4.13.2 Effect of Cytochalasin D on PLCδ_1 and TGII expression.

In parallel with the disruption of the actin cytoskeleton following Cytochalasin D treatment (100nM for 2h) the level of PLCδ_1 and TGII seemed to decrease and take a less structural appearance.

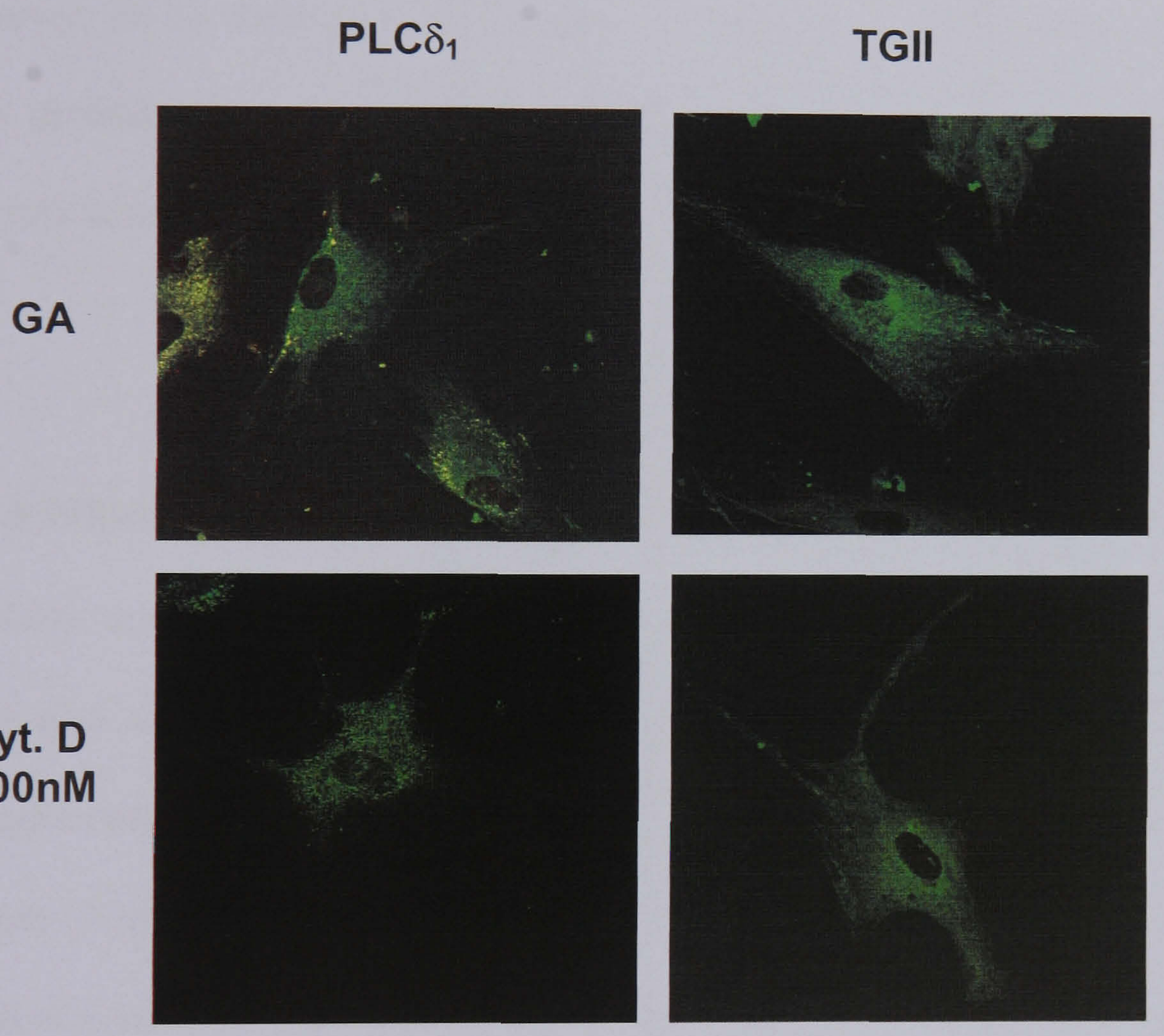


Figure 4.9 Effect of Cytochalasin D on PLCδ_1 and TGII expression. Confocal microscopy showing the subcellular localisation and structural organisation of PLCδ_1 and TGII in serum deprived (Growth arrested, GA) HVSMC in the presence and absence of 100nM Cytochalasin D. Pictures are the average of four scans of one single section of a cell and are representative of findings in 3-4 separate cell strains. Images taken with a Leica TCP-SP scanning confocal microscope, x40 lens).

4.13.3 Effect of Cytochalasin D on protein expression of SM α-actin

To further confirm the disruptive effect of Cytochalasin D on the actin cytoskeleton we examined the expression of SM α-actin in cell lysates in GA cells and those treated with Cytochalasin D. Cells were incubated for 2h with 10nM and 100nM of Cytochalasin D. Cell lysates were further examined with Western blotting for changes in SM-α-actin expression. As seen in blots in figure 4.10 exposure of 10nM of Cytochalasin D was not enough to affect levels of actin. However, 2h incubations of the higher concentration (100nM) decreased SM α-actin protein expression to 53%. This confirms the disruption of the actin structure seen in figure 4.8.

4.13.4 Effect of Cytochalasin D on protein expression of PLCδ_1 and TGII

Similarly the disruptive effect of Cytochalasin D on PLCδ_1 and TGII protein expression was examined. Along with a decrease in SM α-actin, confirming the disruptive effect of Cytochalasin D (100nM) on the actin cytoskeleton, a decrease in both TGII (-23%) and PLCδ_1 (-59%) was detected. Exposure of cells with 10nM of Cytochalasin D resulted in a slight increase in PLCδ_1 (6%) and a marked increase in TGII expression was measured (65%).

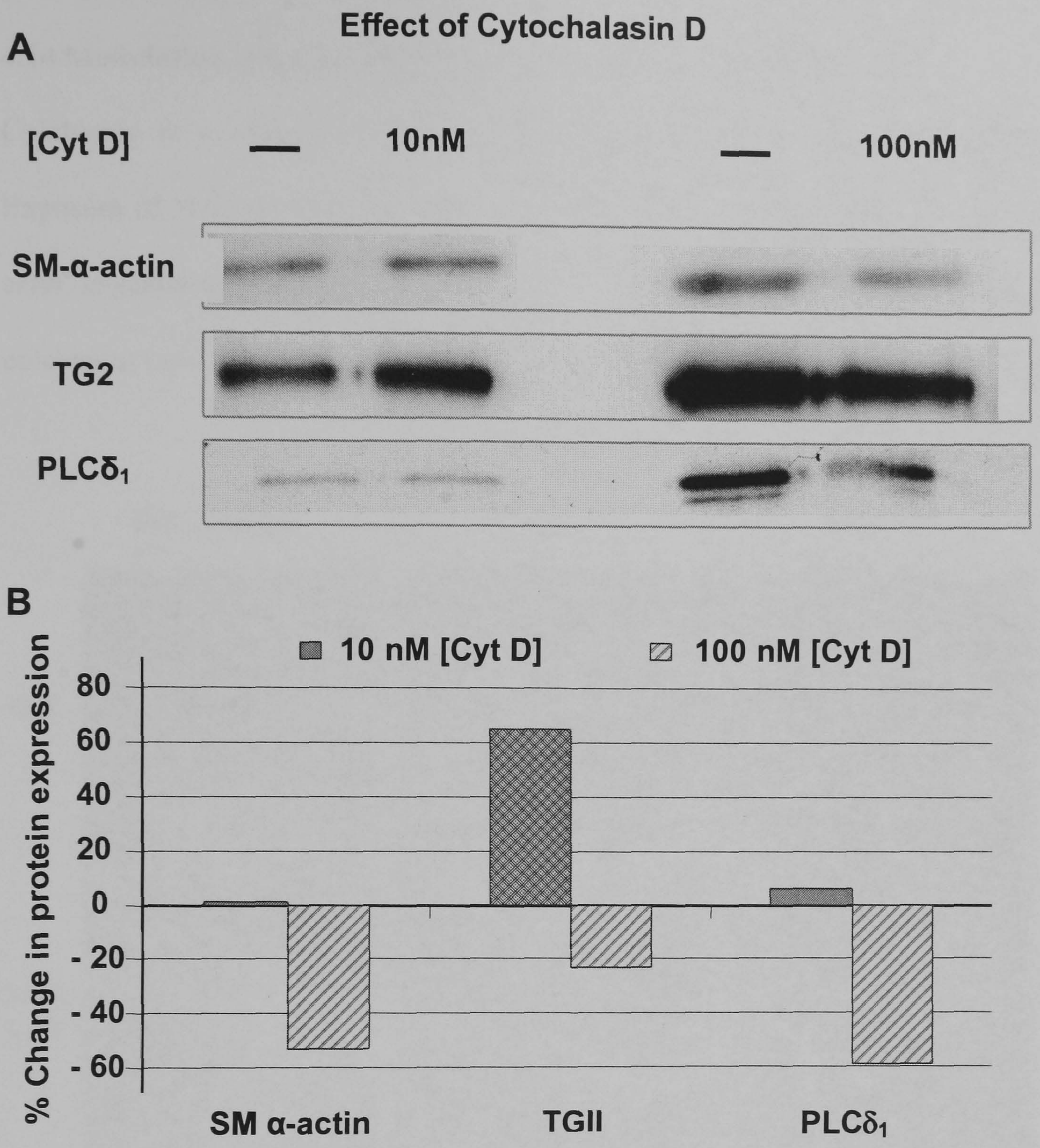


Figure 4.10 Effect of Cytochalasin D on SM α-actin, PLCδ_1 and TGII expression.

No change in SM α-actin expression was detected at 10nM but with exposure to a higher concentration of Cytochalasine D (100nM for 1h) resulted in a reduction of SM α-actin (53%) and similarly TGII protein expression (23%) and PLCδ_1 (59%) (n=1). Interestingly, TGII increased with 65% following treatment of 10nM.

4.14 Modulation of actin cytoskeletal structure by Cholchicine.

Colchicine is a microtubule disrupting agent (Nakamura, M., *et al.* 2000). Exposure of HVSMCs to Colchicine (5μM) had only a small effect on SM α-actin organisation with some disruption of the filament structure. Similarly colchicine had only a slight effect on PLCδ$_1$ and TGII localisation (Figure 4.11).

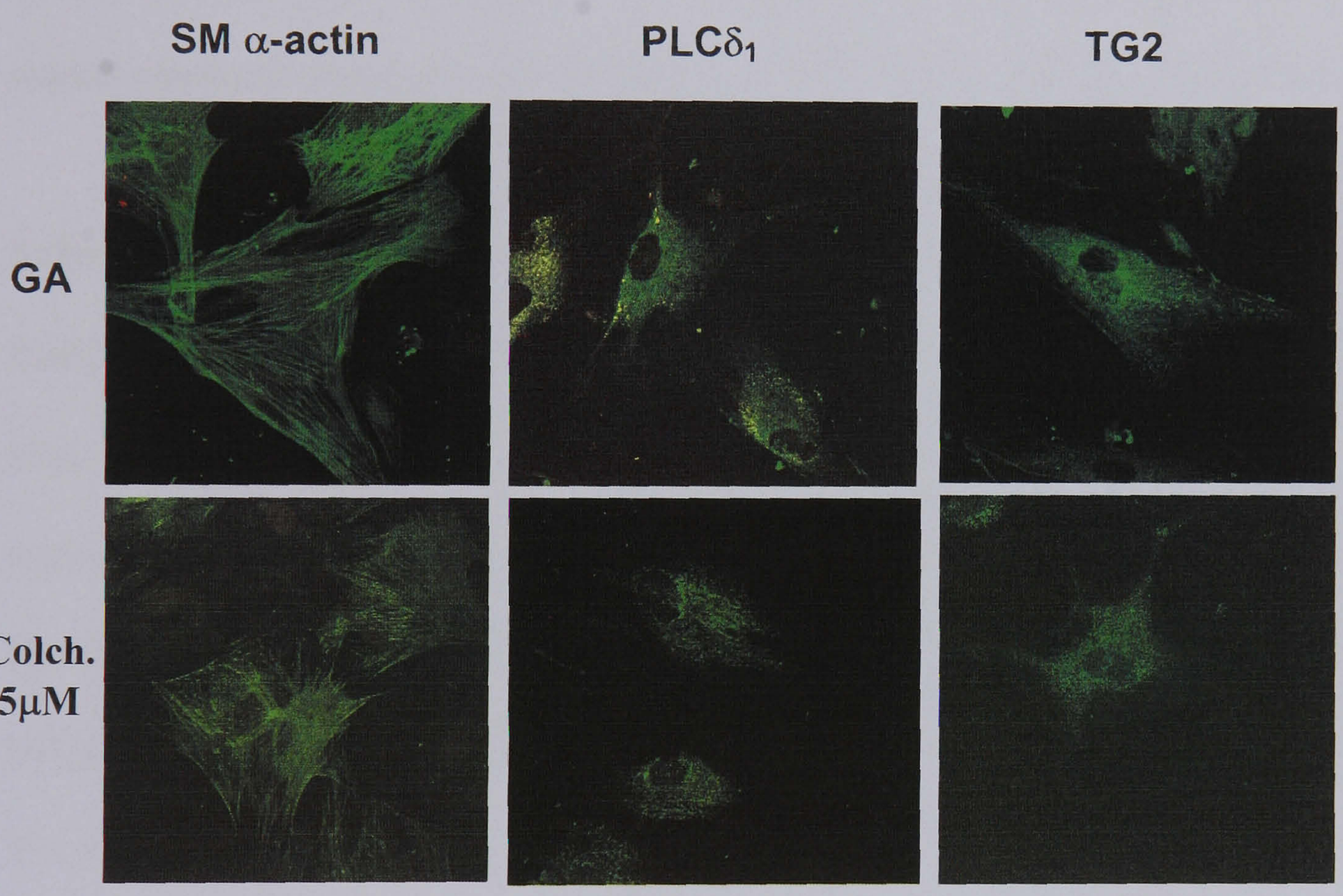


Figure 4.11 Effect of Colchicine on actin cytoskeleton on PLCδ$_1$ and TGII expression. Confocal microscopy showing the subcellular localisation and structural organisation of SM α-actin, PLCδ$_1$ and TGII in serum deprived (Growth arrested, GA) HVSMC in the presence and absence of 5μM colchicine. Pictures are one section (an average of four scans) or one cell. n= 3-4 separate cell strains.

DISCUSSION PROTEIN LOCALISATION

Modulation of synthetic phenotype by serum deprivation results in loss of contractile function and consequently changes in compartmentalisation. Immunofluorescence, which enables investigation of the cellular compartment in which a particular protein is located, showed that following redifferentiation of HVSMCs the subcellular localisation of both TGII and PLCδ_1 changed. Redifferentiation was confirmed by the more structural appearance of the two marker proteins SM α-actin and calponin.

Subcellular localisation of PLCδ_1

Redifferentitiaon of PLCδ_1 not only results in an increased level of protein but a clear shift in its subcellular localistion. PLCδ_1 relocalises from a more perinuclear region to the entire cytoplasm following serum deprivation. We did not detect any PLCδ_1 in the nucleus as expected as PLCδ_1 has a functional nuclear export signal (NES) sequence in amino acid residues 164-177 of the EF-hand domain (Yamaga, M., *et al.* 1999).

One of the initial steps for stimulation of PLCδ_1 is translocation to the plasma membrane where it binds to the lipid-water interface via the noncatalytic lipid binding PH domain, located near the N-terminus of PLCδ_1, and binds multiple phosphoinositides such as PIP_2. The PH domain anchors PLCδ_1 to the membrane by binding PIP_2 in the presence of Ca^{2+} (Grobler, J.A. and J.H. Hurley, 1998). Similarly, Paterson and co-workers demonstrated the importance of a functional PH domain for the interaction of the enzyme with both the plasma membrane and inositol 1,4,5-trisphosphate following microinjections of deletion mutants of

PLCδ_1 (Paterson, H.F., *et al.* 1995). The PH domain allows hydrolysis of substrate (enzymatic domain, C2) whilst still being bound to the interface (Lomasney, J.W., *et al.* 1996).

Subcellular localisation of TGII

In randomly cycling cells TGII is ubiquitously expressed throughout the cell whilst serum deprived HVSMCs show a more defined cytoplasmic subcellular localisation. This reduction in the cytoplasmic levels of TGII is consistent with the reduced level of TGII protein expression by Western blotting previously described (chapter 3). Literature evidence suggests that, in line with the data presented here, TGII is widely expressed throughout all human tissues and is found in the cytosol, plasma membrane (PM), nucleus and extracellular space (Fesus, L. and M. Piacentini, 2002; Greenberg, C.S., *et al.* 1987; Lesort, M., *et al.* 1998). Interestingly, TGII unlike the other transglutaminase family members has also been found in the nucleus (Lesort, M., *et al.* 1998). Other features particular to TGII compared to most of its family members are the GTP binding activity (similarly TGase5 and TGase 3 also posses GTP binding activity, Candi, E. *et al.* 2004; Ahvazi, B., *et al.* 2004) and integrin binding that is not dependent on its transglutaminase activity (Iismaa, S.E., *et al.* 2000). Identification of nuclear target proteins for TGII could provide a crucial understanding of how TGII mediates specific biological processes.

In randomly cycling cells TGII occasionally appeared to take a different subcellular localisation, forming a negative image to the SM α-actin structure rather than directly binding to it. This feature as seen in figure 4.5 is very obvious

in RC cells whilst just noticeable in GA. It is possible this pattern of staining is related to the position of the cell in the cell cycle. Structural rearrangements occur, for example in S-phase and during mitosis, the structure of the nucleus breaks down and is replaced by a cage-like spindle (largely composed of microtubules) which pulls the chromosomes apart after duplication. What we see could be an association of TGII with the microtubules, indirectly or directly. However, treatment of cells with colchicine, which disrupts microtubles, did not affect TGII staining. This could also be a reflection of the important role of TGII, with tissue transglutaminase activity, on the cytoskeletal regulator RhoA and its downstream factors (Singh U.S., *et al.* 2001). There is also accumulated evidence to suggest that TGII associates with cytoskeletal components and induces their covalent modifications (Bernassola, F., *et al.* 2002). Mearns and co-workers revealed following phalloidin staining of fibroblasts lacking TGII how these cells were lacking reorganisation and stress fibre formation in response to wound stimulus whilst TGII overexpressing cells showed more extensive stress fibre formation than mock transfected cells and only small level of stress fibre formation was detected in TGII deficient cells (Mearns, B., *et al.* 2002). Complementary immunoprecipitation studies of myosin and SM α-actin probing for the presence of TGII could further clarify this relationship.

Based on the cellular localisation of TGII our findings suggest that TGII may not bind directly to actin. In correlation with these data TGII purified from liver has been shown to be associated with myosin. Chowdhury and co-workers demonstrated co-localisation of TGII with stress fibers in human umbilical vein endothelial cells, human arterial and venous smooth muscle cells and additional

immunoprecipitation experiments revealed that TGII co-immunoprecipitated with myosin and not with actin (Chowdhury, Z.A., *et al.* 1997).

Another interesting structural appearance of TGII was its formation of large pools in lamellopodia of GA cells (see figure 4.4), which is an area of the cells with a high turnover of SM α-actin. TGII is also found at the edges of the cells, suggesting its possible association with focal adhesions which has been shown in other cell types by several studies (Chowdhury, Z.A., *et al.* 1997; Akimov, S.S., *et al.* 2000; Stephens, P., *et al.* 2004). Interestingly, a reduced level of TGII expression results in an impaired cell spreading and adhesion suggesting that TGII may play a functional role in focal adhesions (Gaudry, C.A., *et al.* 1999).

Co-localisation of TGII and PLCδ$_1$

Dual staining revealed that co-distribution of TGII with PLCδ$_1$ and co-localisation of these two proteins occurred to a greater level in redifferentiated cells. To our knowledge this is the first time co-localisation of these two proteins has been demonstrated in HVSMCs and is certainly the first data to suggest an effect of differentiation status on this association.

Disruption of cytoskeleton

The regulation of SMC phenotype appears to be intimately coupled to the organisation of the cytoskeleton (Doevendans, P.A. and G. van Eys, 2001; Worth *et al.* 2002) which is the protein framework that maintains cell shape.

The possible involvement and/or association of TGII and/or PLCδ_1 with the cytoskeleton and its rearrangement were studied following cytochalasin D and colchicine treatment. The possible effect on structural changes was visualised using fluorescent labelled antibodies for the two different proteins, monitored with confocal microscopy whilst Western blotting studies revealed the effect on protein expression. Our data suggests that in HVSMCs colchicine procuses a small effect on the actin cytoskeletal structure with similar small effects on TGII and PLCδ_1.

The results presented here show that immunofluoresent staining of HVSMCs following treatment with cytochalasin D rearranged cytoskeleton as indicated by immunofluorescent staining for SM α-actin. The effect of cytochalasin D was also examined by Western blotting which revealed a decrease in SM α-actin protein expression as well as PLCδ_1 and TGII. There is always a possibility that cytochalasin D may exert a toxic effect as cytochalasin D can inhibit protein synthesis, possibly by reducing the amount of polyribosomes. However, Fey, E., *et al.* demonstrated that this occur at higher levels (3T3 cells, 2h, 64μg/ml (1.26μM)) of cytochalasin treatment (Fey, E., *et al.* 1986).

CHAPTER 5 IMMUNOPRECIPITATION

5.1 Aim of Immunoprecipitation studies.

From our investigation of the cellular localisation of TGII and PLCδ_1 we found indications of co-localisation of the two proteins. This co-localisation was increased in serum deprived compared to randomly cycling HVSMCs. In order to confirm the specific co-localisation of PLCδ_1 with TGII in redifferentiated cells we performed a series of immunoprecipitation studies.

5.2 The Precipitation Reaction

Immunoprecipitation allows rapid and efficient purification of proteins in a native and biochemically active form. In principle, all immunoprecipitations are based on two kinds of interactions: the interaction between antigen and antibody and that between the antibody and an immunoadsorbent, we used Protein A-Agarose (Oncogene, Cat. No. IP02). Thus, in a typical reaction the antigen–antibody complex will be bound to an insoluble matrix that can be easily pelleted and thereby removed from the bulk protein. The immobilized complex can then be washed and released by boiling and subsequently analysed.

5.3 Background of Antibody

The finding that epitopes consist of short amino acid sequences has led to the idea of generating antibodies against synthetic peptides that will recognize the protein from which the sequence was derived. This possibility has greatly facilitated the identification of unknown proteins whose existence was only predicted from the cDNA sequence (Walter, G. et al. 1986).

Antibodies are generally composed of two identical heavy and light chains that are complexed via noncovalent and disulfide bonds. These four subunits form a Y-shaped molecule in which the arms are formed by the aminoterminal part of the heavy chains complexed to a light chain and the stem is formed by the carboxy-terminal parts of the heavy chains. Each of the subunits is composed of a constant region common for a class of antibodies and a variable region that is unique for a particular antibody. It is these variable regions that comprise the antigen-binding site.

5.4 Immunoprecipitation of PLCδ_1 respectively TGII

PLCδ_1 and TGII were respectively immunoprecipiated from cell lysates of randomly cycling and serum deprived HVSM cells and Western blotting identified the nature of any immunocomplexes. Figure 5.1 shows a representative blot of where immunoprecipiated TGII is probed for PLCδ_1 and respectively where PLCδ_1 is immunoprecipiated from cell lysates and probed for TGII. In randomly cycling cells PLCδ_1 is only barely detected in the TGII immunoprecipitate. On the other hand, PLCδ_1 is clearly detected in the TGII IP from serum deprived cells. Similarly to this we found that in randomly cycling cells TGII is present to a less extent in the PLCδ_1 immunoprecipitate itself. Then again, an increased level of complex formation is found in redifferentiated cells with TGII clearly detected in the PLCδ_1 IP from serum deprived cells. A 49% increase in PLCδ_1 was found in immunopreicipated TGII of serum deprived cells, which was significantly ($P=0.006$) higher level of PLCδ_1 compared to randomly cycling cells. However, no significant difference was detected in the level of TGII in immunoprecipitated PLCδ_1.

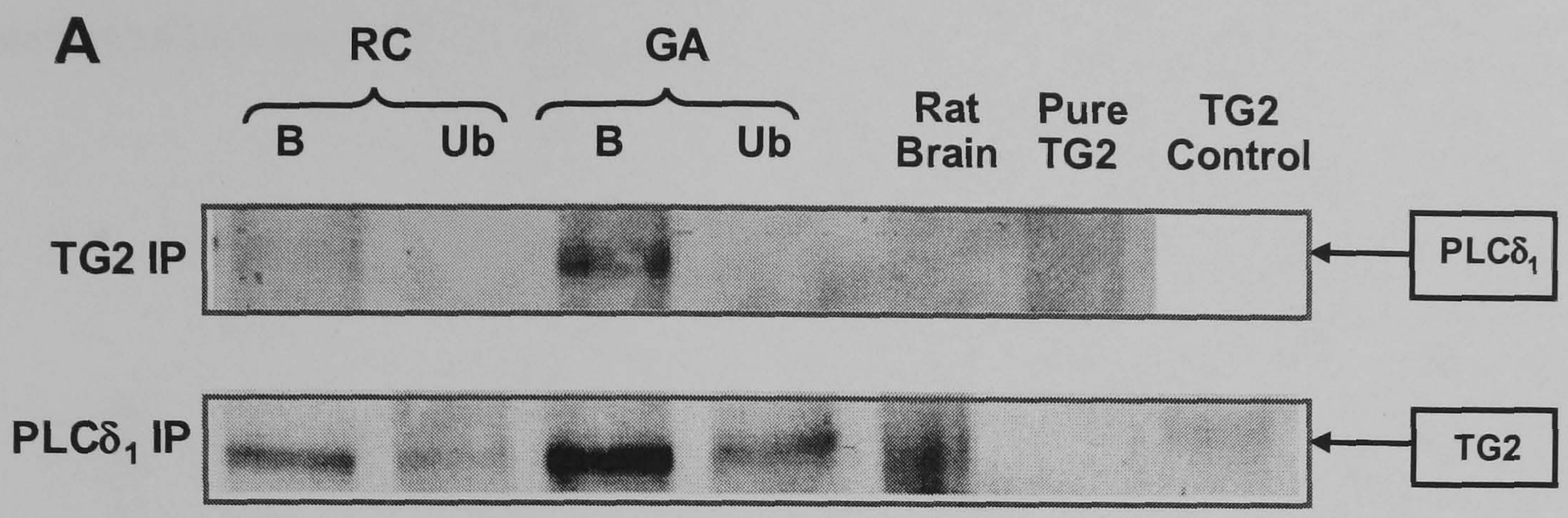


*Figure 5.1 Immunoprecipitation of TGII respectively PLCδ_1 in randomly cycling (RC) versus serum deprived (GA) HVSM cells. **A**. Blots show representative blot of TGII Immunoprecipitates (IPs) and probing for PLCδ_1 (n=4), and PLCδ_1-IPs probed for TGII, (n=3). A higher level of complex formation between TGII and PLCδ_1 is found in redifferentiated compared to randomly cycling cells. B – Bound Ub-Unbound. **B**. Diagram of % change (arbitrary units from densitometry measurements) of TGII in PLCδ_1 IP's (37%±17%, p=0.37, n=4) and PLCδ_1 in TGII IP's (49%±1%, * P=0.006, n=3).*

The level of TGII present in immunoprecipitates of PLCδ_1 was further analysed with ANOVA and no significant difference could be detected (P=0.4, n=4).

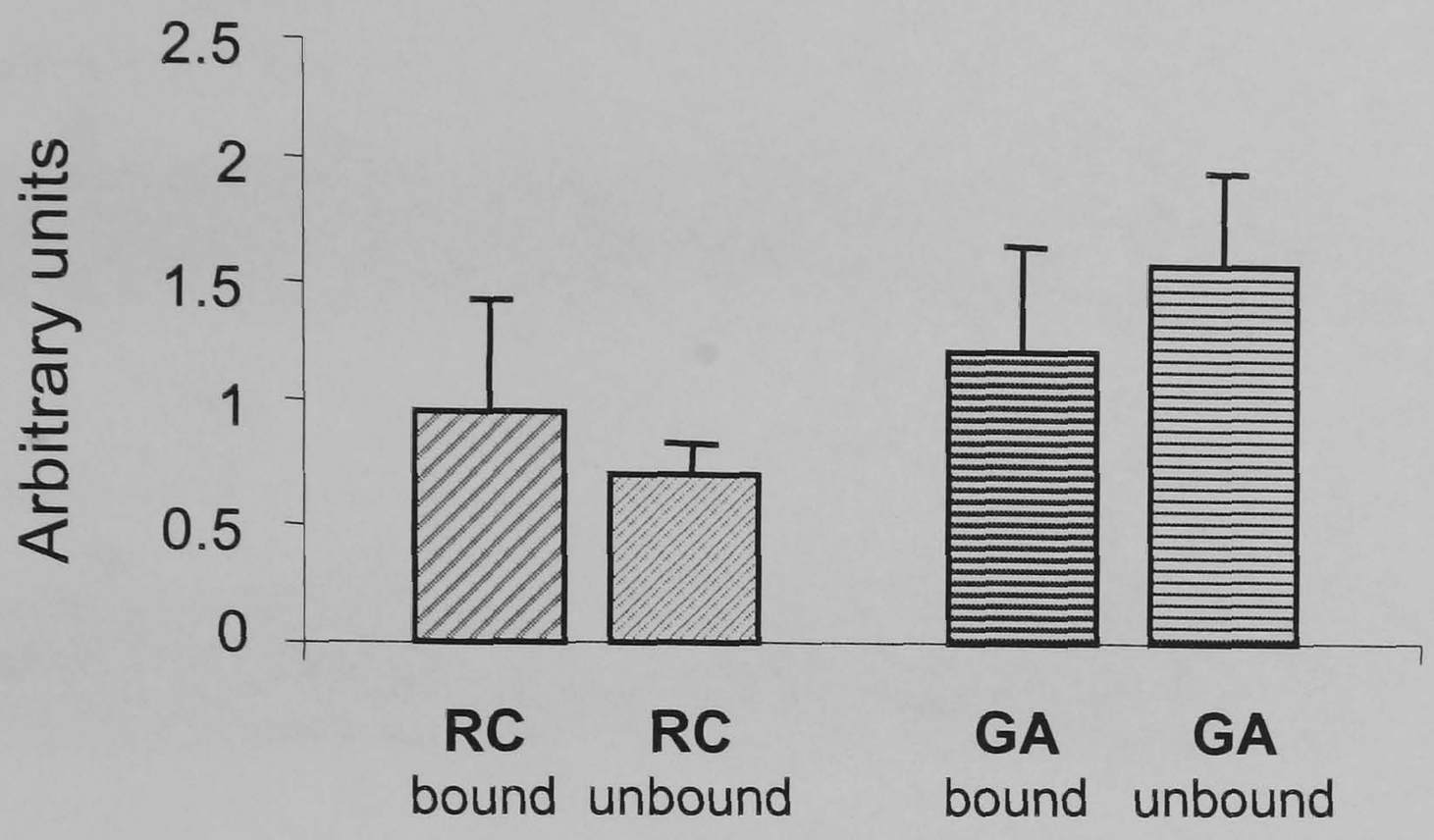


Figure 5.2 Diagram of TGII present in immunoprecipitates of PLCδ_1 in randomly cycling versus growth arrested HVSMCs. No significant difference was detected according to ANOVA (p=0.4, n=4).

5.4.2 Efficiency of pull down in immunoprecipitation

The efficiency of the actual pull down was studied by probing the blots with the same antibody used for the immunoprecipitation. When the same antibody is used for the two steps a strong band is expected. As seen in figure 5.3 clear bands appeared at the expected size of 79kDa. Thus, a slight thicker band in the bound fraction of the TGII IP in serum deprived cells (GA, growth arrested) was detected.

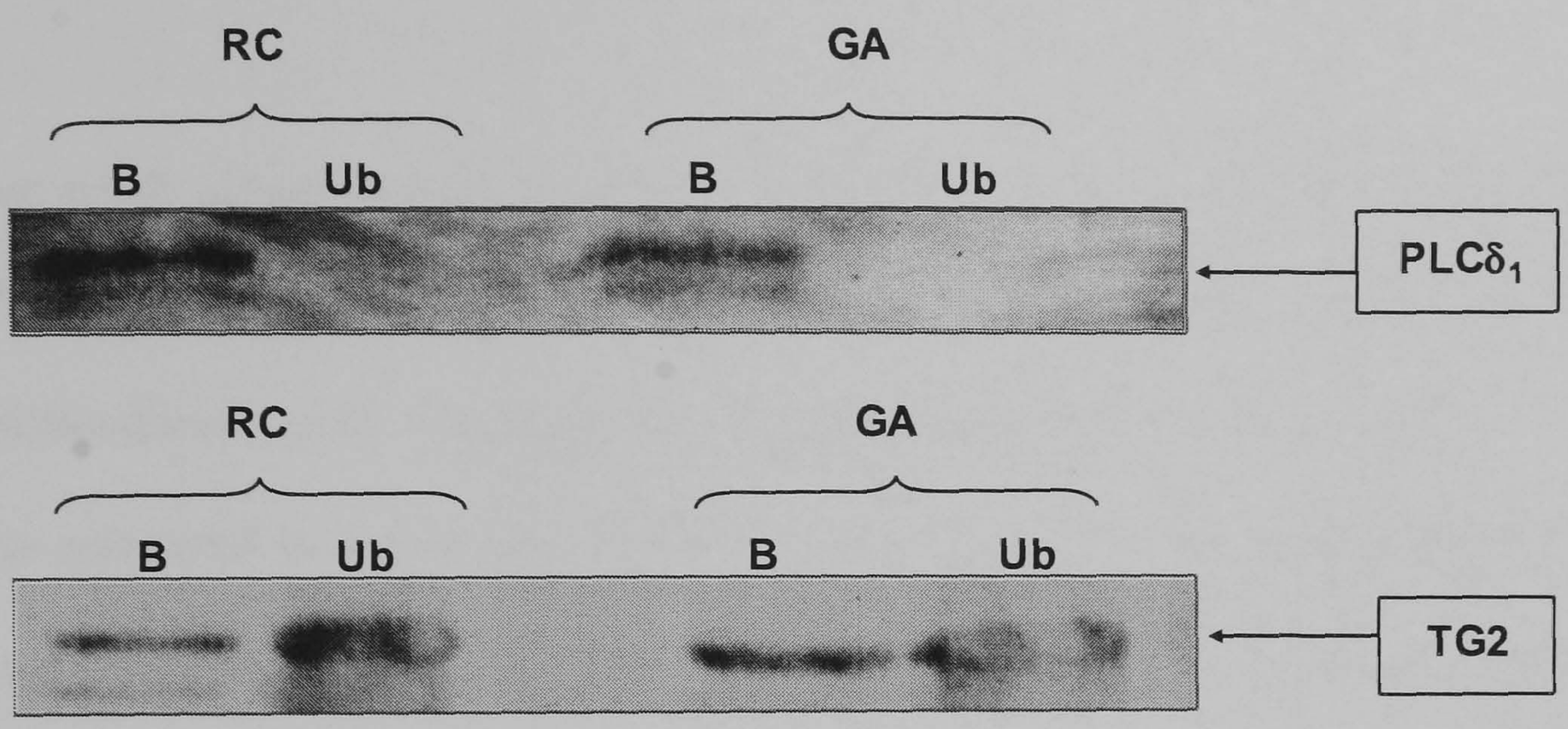


Figure 5.3 Efficiency of the actual pulldown of PLCδ1 respectively TGII immunoprecipitates. Western blot showing immunoprecipitation in randomly cycling (RC) versus serum deprived (GA) HVSMC where same antibody is used both in the pull down and as well for probing in order to looking at the efficiency of the actual pull down. (n=3). B – Bound, Ub-Unbound

DISCUSSION IMMUNOPRECIPITATION

In order to confirm the specific co-localisation of PLCδ_1 with TGII in redifferentiated cells we performed a series of immunoprecipitation studies in HVSMC lysates.

Our result suggests that a complex formation of the two proteins occur in HVSMCs. Blots clearly indicated that this association was greater in redifferentiated cells. Unexpectedly, no significant difference in the level of TGII was measured in immunoprecipitated PLCδ_1 in randomly cycling compared to serum deprived cells. Although the PLCδ_1 IP pull down was successful, and hence ruled out that as a potential problem, the bands on the Western blots detecting TGII were in most cases weak. This could be due to a low level of PLCδ_1 present in the cells or some antibody problem with overlapping of epitopes or interference of some kind. In case a new and more efficient PLCδ_1 antibody is produced this may be worth trying out. More successful was the detection of PLCδ_1 in TGII immunoprecipitated. A 49% higher level of PLCδ_1 in serum deprived cells was measured, which was significantly different to the level detected in randomly cycling cells. This data correlates well with that obtained from confocal studies and gives further weight to the concept that there is an association between PLCδ_1 and TGII in HVSMCs and likewise this association is more evident in redifferentiated cells.

This difference in complex formation detected in the two phenotypic states suggest a biological feature reinforced by the examinations of the pull down

efficiency of PLCδ1 revealing that there was no significant difference in the efficiency of the PLCδ1 immunoprecipitation in either state.. Similarly to our results Hwang *et al.* showed how TGII coimmunoprecipitates with PLCδ$_1$ and in addition they demonstrated how this coimmunoprecipitation only occurs in the presence of GTPγS bound TGII (Hwang, K.C., *et al.* 1995).

Unfortunately investigation of the efficiency of the TGII immunoprecipitation demonstrated the presence of TGII protein in the unbound fraction, indicating an incomplete pull down. The degree of efficiency of the TGII immunoprecipitation however appeared to be similar in both phenotypic states indicating that there is no influence of differentiation state on this process. It would be useful to increase the concentration of the TGII antibody used in the immunoprecipitation process to determine whether this increases the efficiency of the procedure. It is also possible that the incomplete immunoprecipitation may be explained by antibody problem, which will, of course, greatly influence the success of an experiment with respect to yield and purity of the antigen to be isolated. Generally, polyclonal antisera are more efficient than monoclonal antibodies in precipitation reactions, because polyclonal antibodies will bind to several different epitopes and eventually form a network that is rather stable and readily precipitable. When using monoclonal antibodies, it may be favourable to employ two or more antibodies recognizing different epitopes on the same antigen.

For further investigation of protein interactions it would be interesting to apply the latest technique for examination of in vivo protein–protein interactions called fluorescence resonance energy transfer (FRET), which is based on

immunofluorescence techniques using antibodies labelled with fluorescent dyes (Kenworthy, K.F., *et al.* 2001; Sata, M., *et al.* 2002).

CHAPTER 6 GTPase OR TGase ACTIVITY?

6.1 Aim of study

TGase and GTPase activity of TGII are reported to be mutually exclusive and to date it is only through its GTPase activity that TGII regulates and bind to PLCδ_1 (Feng, J.F., *et al.* 1996; Baek, K.J., *et al.* 2001). As our interest concerns this association particularly with regard to the differentiation status of the cell we examined to what extent the two different activities are present in randomly cycling and redifferentiated cells. This was assessed by applying two different methods, a transglutaminase activity assay and [^{35}S] GTPγS overlay assay. Our aim was to get a clearer picture of the two enzyme activities in the two different phenotypic states of HVSMCs.

6.2 Introduction

TGII is a bifunctional enzyme which can act either as a signal transduction molecule, with GTPase activity, coupling α_{1B}- and α_{1D}-adrenoreceptors in heart and liver (Feng et al. 1998), thromboxane (Vezza, R., *et al.* 1999) and oxytocin in myometrium (Baek, K.J., *et al.* 1996) receptors to PLCδ_1 or act as a transglutaminase (TGase), involved in several functions such as apoptosis and posttranslational modification (Greenberg, C.S., et al. 1991; Verderio, E., *et al.* 1998).

6.3 Measurement of Transglutaminase activity

Cell lysates from HVSMC were assayed for transglutaminase activity by measuring the incorporation of [^{3}H]-putrescine into N, N-dimethylated casein. We initially used a protocol by Monsonego *et al.* which, briefly, is based on the

incorporation of [^{3}H]-putrescine into N, N'-dimethylcasein followed by precipitation of proteins by the addition of TCA, several washes and measurements in a Liquid Scintillation Analyser (1900CA TRI-CARB Packard) (Monsonego, A., *et al*. 1997). Pure guinea pig liver transglutaminase (Sigma) was used to set up the assay. The pure enzyme has a short half life and to improve its stability it was equilibrated in Tris 0.1 M pH 8.3 and kept on ice. By measuring the counts of supernatant after each wash, figure 6.1 clearly demonstrate that the three different wash steps are efficiently removing unbound radioactivity.

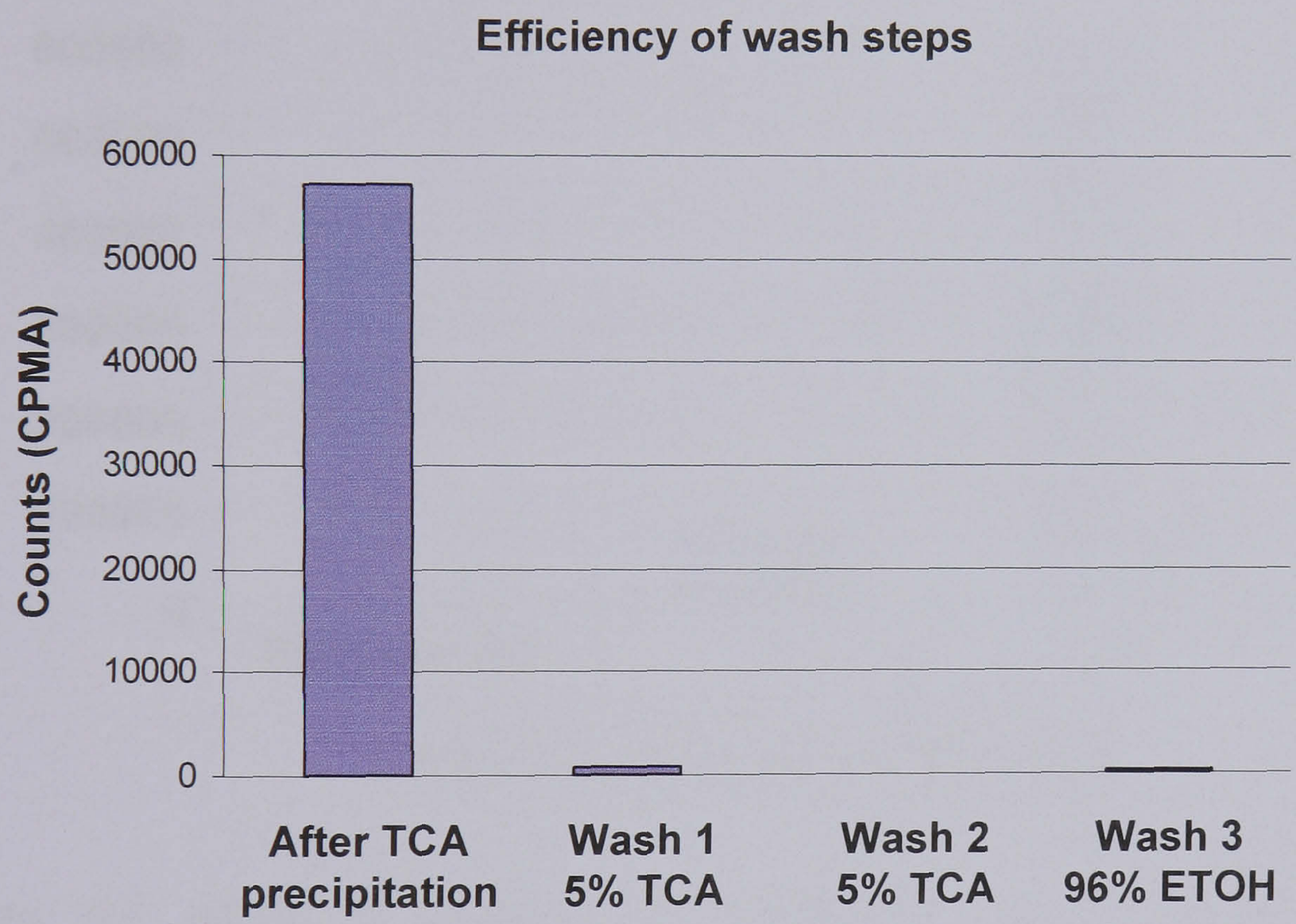


Figure 6.1 Efficiency of the three wash steps in the Transglutaminase (TGase) activity assay. The assay is based on the incorporation of [^{3}H]-putrescine into N,N'-dimethylcasein, following precipitation TCA precipitation and three different washes. Radioactive measurements of supernatant of pellet after each wash step show that unbound radioactivity is clearly removed by the three washes, indicated that absence of unbound radioactivity (n=1) .

Another parameter we investigated was incubation time as from the literature we found the use of different incubation times. As seen in figure 6.2 the shorter (15 min) incubation time is more suitable than 12 hours for measuring transglutaminase activity in our HVSMCs (Monsonego, A., *et al*. 1998). The longer incubation time resulted in lower activity measurments, which could be due to breakdown of enzyme with time.

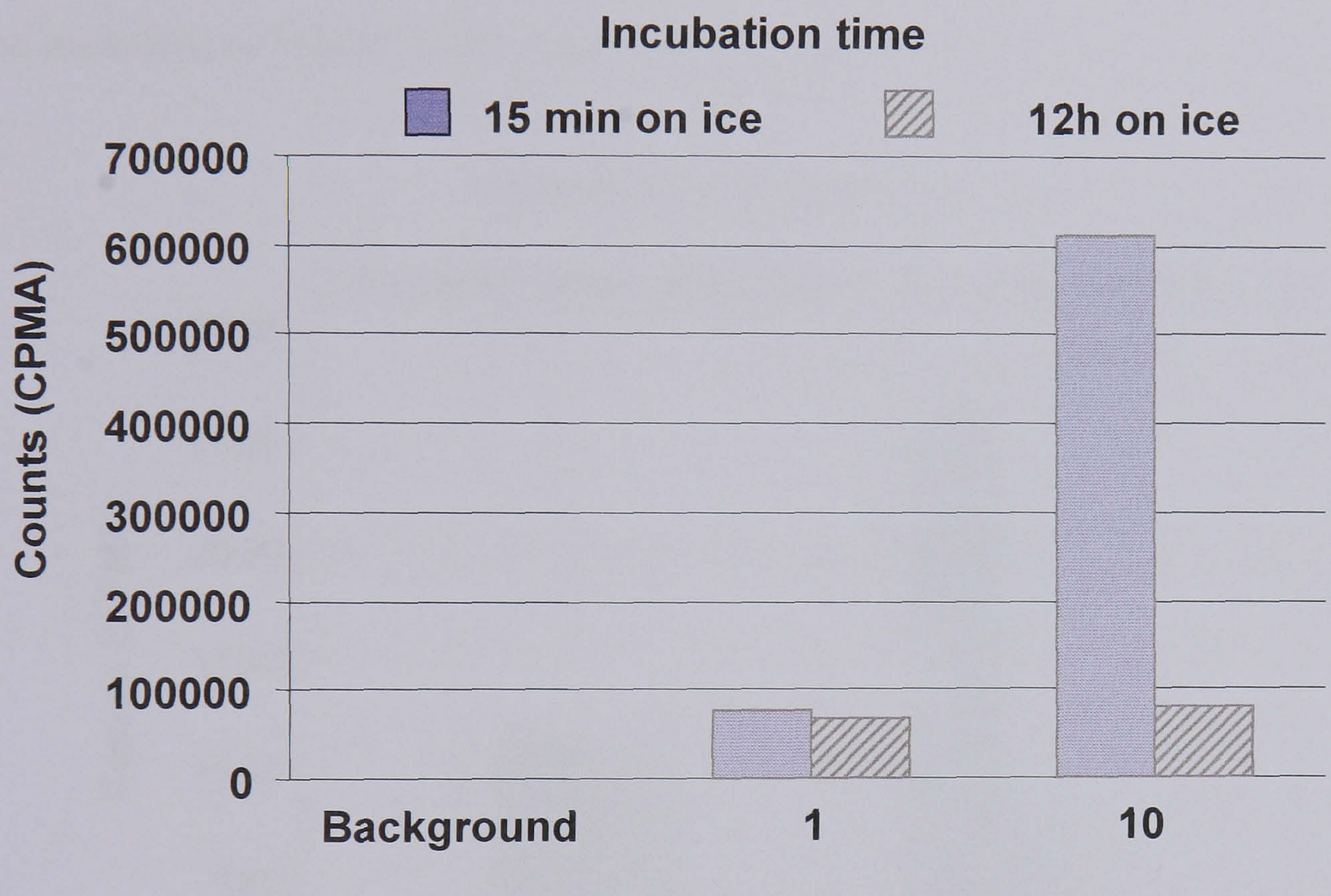


Figure 6.2 Effect of variation of incubation time in TGase assay. Transglutaminase assay based on the incorporation of [^{3}H]-putrescine into N,N'-dimethylcasein. Incubation for 15min rather than 12h is more advantageous for transglutaminase activity measurements in our HVSMCs (n=1).

6.4 Tissue transglutamianse activity in lysates from HVSMC

With optimised conditions we were ready to investigate the activity in our HVSMCs. The first measurements of transglutaminase activity in lysates from randomly cycling HVSM cells gave no significant difference in TGase activity

compared to just sample buffer (1105±77, p=0.34). However, pooling two confluent flasks of randomly cycling HVSMCs cells ($2x10^5$cells/ml, 50µg) enabled us to detect a significantly difference in TGase activity compared to sample buffer alone (2604±193, * p=0.01). The measured activity was abolished by heat inactivate (by boiling) the active cell lysate, pooled from two flasks (723±40, **p=0.0021). No significance (p=0.10) in tranglutaminase activity could be measured in boiled lysate of just one flask of HVSMCs.

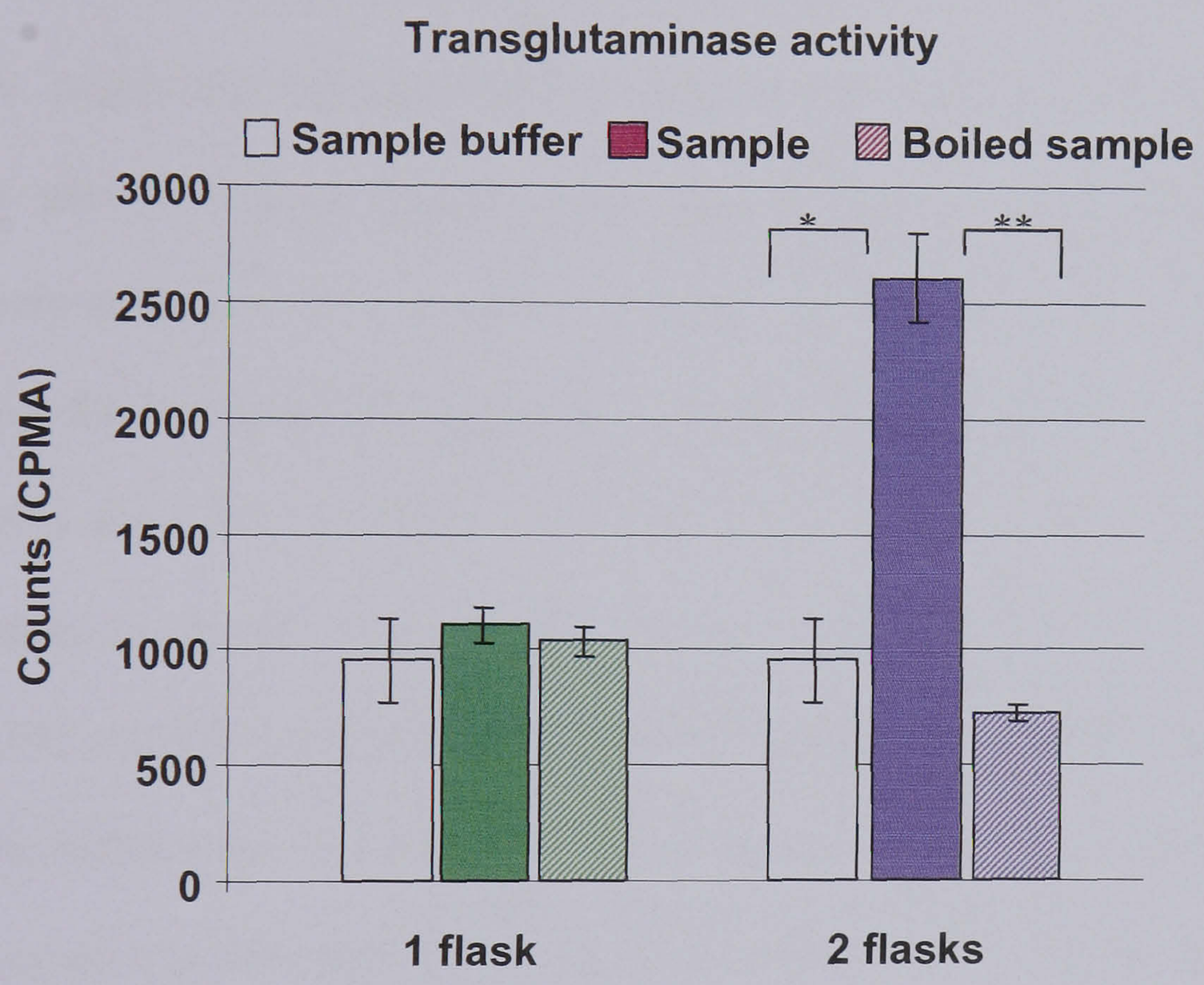


*Figure 6.3 TGase activity measurements in HVSMC cell lysate. Cell lysate examined from just one flask of HVSMCs did not yield a significant difference in TGase activity compared to sample buffer alone (p=0.32). Whilst when pooling two flasks of HVSMCs a significant difference (*p=0.01) in TGase activity was measured. Heat inactivated lysate from two pooled flasks was significantly different to active lysate (**p=0.0021) confirming that the activity measured was not due to higher level of protein present as heat inactive lysate from one flask only showed no significantly difference in (p=0.10) TGase activity.*

6.5 Modulation of transglutaminase assay

We noted that it was difficult dissolving the protein pellet fully. We therefore assessed the possibility of using lysis buffer instead, which is routinely used for lysing cells in our laboratory (Appendix A:6). An improperly dissolved pellet could account for the variance in the assay. As seen in figure 6.4, when assaying the same HVSMC lysate at two different concentrations (50μg and 81μg) a significantly higher transglutaminase activity was measured when the protein pellet was dissolved in lysis buffer compared to when it was dissolved in sample buffer, suggesting that lysis buffer may be a better solvent. Although lysis buffer alone gave a slightly higher background activity this was not significantly different to the activity measured in sample buffer alone and hence is unlikely to account for the higher cell lysate activity measured. An increase in TGase activity of 109% and 129% ($p=0.002$) was measured in cell lysate prepared in lysis buffer compared to control, whilst an increase in TGase activity of only 78% and 87% ($p=0.04$) could be measured in cell lysates prepared in sample buffer compared to sample buffer alone. Another notable advantage with the use of lysis buffer was a less variance in between triplicate, as noted by the smaller error bars.

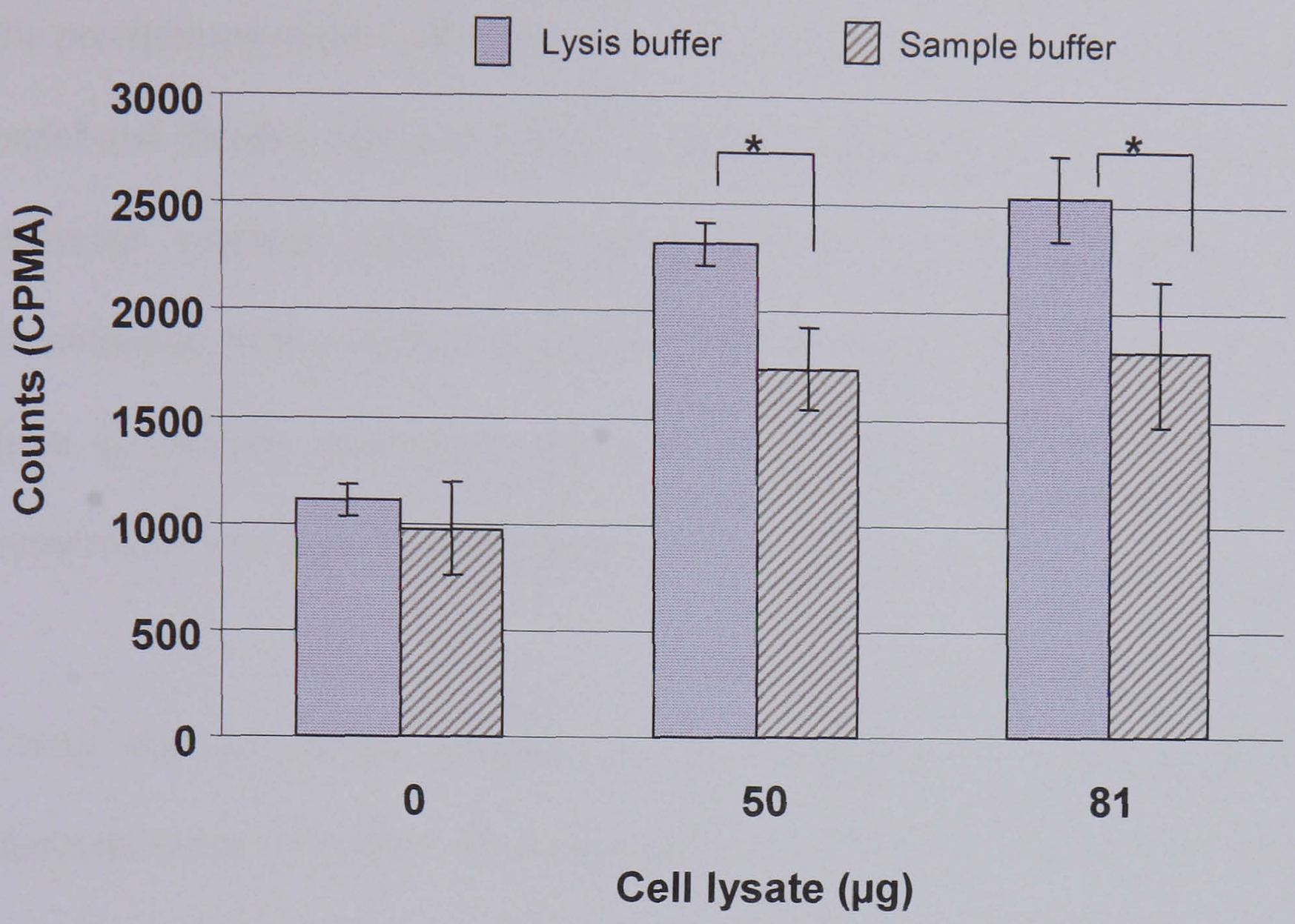


Figure 6.4 TGase activity of pure liver transglutaminase dissolved in sample buffer respectively lysis buffer. TGase activity measurements of 50µg respectively 80µg of total protein from lysates of HVSMCs prepared in sample buffer respectively lysis buffer. Measurements of TGase activity was performed by [^{3}H]-putrescine incorporation. A higher level of transglutaminase was measured with lysis buffer, (* $p<0.05$).

Unfortunately however this methodology remained time consuming particularly with respect to dissolving the pellet. Consequently, in order to get around this problem we applied a new technique, based on the method of Iismaa *et al*. where the precipitated pellet was filtered through pre-soaked (50% TCA) Whatman filter paper and thereby captured within the filter paper (Iismaa, S.E., *et al*. 2000). The different washing steps were performed by washing the filter paper in combination with a suction set up. By using this assay we avoided the critical and time consuming procedures involved with the washes including removal of supernatant and dissolving the pellet.

Using this improved methodology we measured the activity of different concentrations of pure liver transglutaminase to determine whether this TGase assay could be used to accurately determine the activity of unknown samples. Figure 6.9A demonstrates that assay sensitivity was lost at concentrations higher than 500μM of pure liver transglutainase. However over the concentration range 0-500μM this TGase activity assay produced a linear standard curve (R^2=0.959).

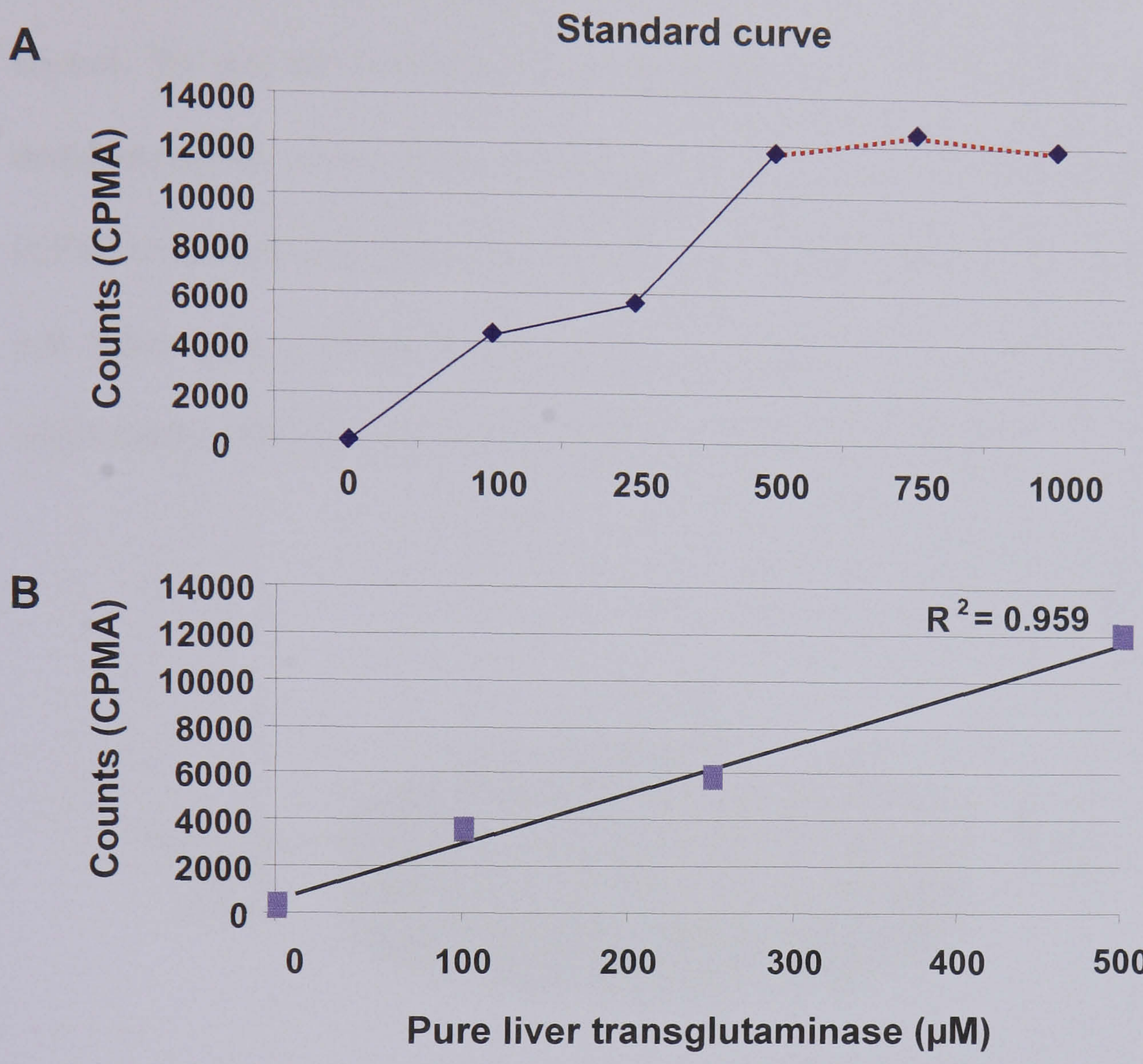


Figure 6.5 Standard curves for TGase activity measurements capturing sample in filter paper. Different concentrations of pure liver transglutaminase was assayed. ***A.*** *A plateau is reached at concentrations higher than 500 µM.* ***B*** *The transglutaminase assay shows a linear dose response curve in the range of 0-500µM of pure transglutaminase with transglutaminase activity. (R^2=0.959). Experiment performed once in triplicates.*

Another often performed control for activity assays is so called spiking a sample. This involves the addition of a known concentration of pure enzyme to an unknown sample. This addition to, or spiking, of a sample, works as an internal control. To test the accuracy of our methodology we used 0.3µg pure liver transglutaminase with a TGase activity of $7.2 \times 10^4 \pm 3.5 \times 10^3$ counts per minute (CPM) to spike a, cell lysate (TGase activity of $1.1 \times 10^3 \pm 1 \times 10^2$ CPM). The spiked cell lysate gave a TGase activity of $7.8 \times 10^4 \pm 1.1 \times 10^3$ CPM which is not significantly different to the additive effect of lysate and substrate.

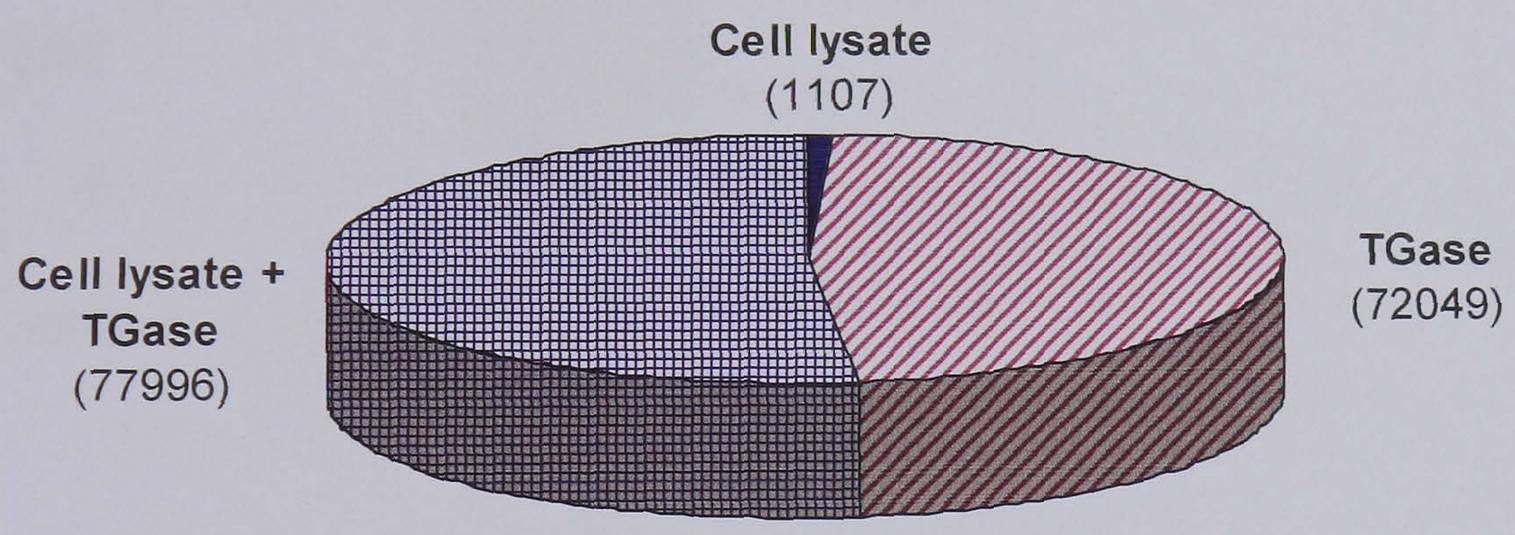


Figure 6.6. Control measurements of TGase activity assay. Spiking cell lysate of HVSMCs with known amount of pure liver transglutaminase (0.3µg) was not significantly different to activity measurements of lysate and same amount of pure transglutaminase added together. Measurements were performed in triplicate.

As a last control we treated HVSMCs with Monodansylcadaverine (MDC), which is a membrane permeable compound with specific and competitive inhibitory activity of transglutamianse activity (Singh, U.S., *et al*. 2001). Two-hour incubation with MDC (200μM) completely inhibited transglutaminase activity in our HVSMCs.

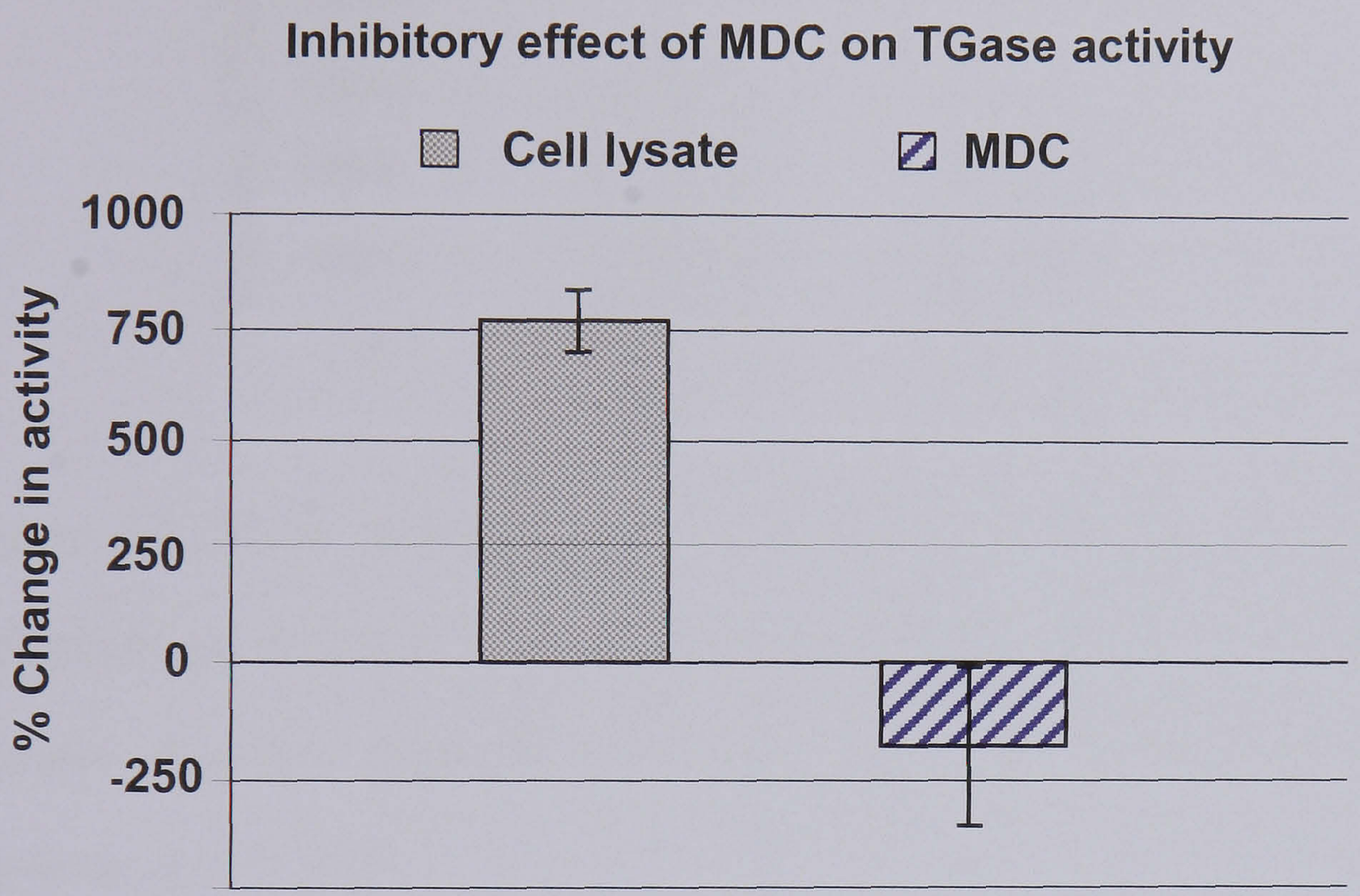


Figure 6.7 Complete inhibition of transglutaminase activity by MDC. 2h treatment of 200μM of Monodansylcadaverine (MDC, inhibitor of TGase activity) completely inhibited TGase activity. Measurements were performed in triplicate, n=1

6.6 Effect of differentiation state on TGase activity

Once assured that our activity assay was efficiently measuring transglutaminase activity we were able to utilise this methodology to measure and compare the TGase activity in lysates from randomly cycling versus redifferentiated HVSMCs (figure 6.8). The results of this experiment indicate a decrease in transglutaminase

activity occurs following redifferentiation. Measurements were performed in triplicate at one occasion only and as noted by the great error bar there was no significant difference in the transglutaminase activity.

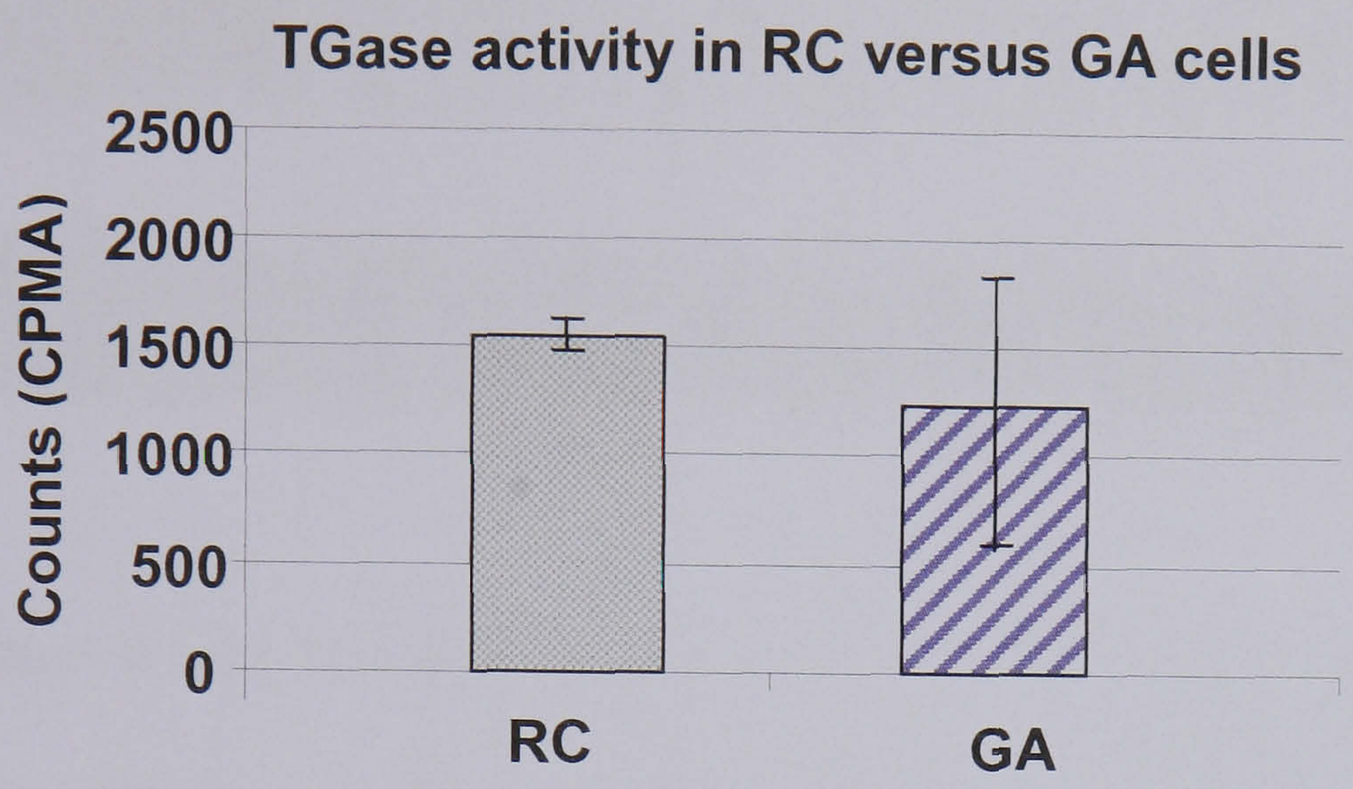


Figure 6.8 TGase activities in RC versus GA HVSM cells. No significant difference was measured between lysates of randomly cycling cells compared to lyasates of serum derprived cells (GA). Measurements were performed in triplicate, n=1(p>0.5).

6.7 Effect of TGase inhibition on PLCδ_1 and TGII expression

Only TGII with its GTPase activity has been associated with PLCδ_1. Therefore we wanted to look at the effect of TGase inhibition, using MDC and look at the consequence this had on PLCδ_1 and TGII protein expression. As shown in figure 6.9 an increased inhibition of TGase activity, with MDC, resulted in a decrease in expression of PLCδ_1 in a concentration dependent manner. Treatment with lower concentration of MDC had no effect on TGII expression, however with higher activities the level of TGII was increased following inhibition of transglutaminse activity. Strangely enough, incubation with the highest concentration of MDC (200μM) resulted in a weak band indicating that a decrease in TGII occurred.

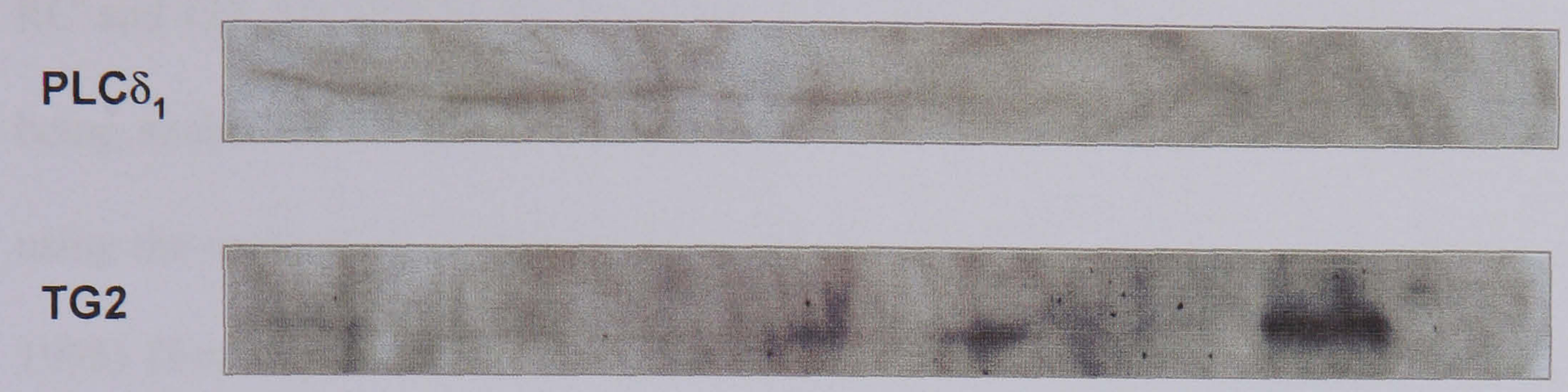


Figure 6.9 Effect on PLCδ_1 and TGII protein expression upon inhibition of TGase activity. Blots showing the change in protein expression of PLCδ_1 respectively TGII upon treatment for 2h with different concentrations of MDC (0, 25, 50, 100, 150 and 200μM). PLCδ_1 expression showed to decrease with greater inhibition of TGase activity.

To further evaluate the contribution of transglutaminase activity versus GTPase activity of TGII in the two phenotypic states, blots probed for the presence of total TGII protein expression, in randomly cycling compared to serum deprived cell lysates, by Western blotting, was exposed to [^{35}S]GTPγS to enable to distinguish the two activities.

6.8 Presence of GTPase activity by [^{35}S]GTPγS overlay assay

The nucleotide exchange process can be monitored by measuring the binding of [^{35}S]GTPγS. This is an analogue of GTP that is resistant to the GTPase activity of the G-protein α-subunit that functions to provide a kinetic restraint on the duration of the signal. GTPγS, a non hydrolysable analogue of GTP can bind and

stimulate G-proteins in the absence of receptor. [^{35}S]GTPγS overlay assay was performed on blots with samples of RC and GA lysates of HVSMCs.

Briefly, nitrocellulose filter containing immobilised denatured proteins (lysates of RC and GA HVSMCs) were pre-washed three times in binding buffer prior to being soaked in [^{35}S]GTPγS solution (1mCi/ml). This technique was performed using the method of Drøbak *et al.* with minor modifications (Drobak, B.K., *et al.* 1995) (For more details see method section 2.15). After washing of the filter bands were developed using Hypercassette (Amersham Pharmacia biotech, UK). An intensifying screen (Biomax, Kodak) was used to improve radioactive uptake with highly sensitive film (Biomax Film, Kodak, and Cat 8294985). The film was developed after one day, one week and two weeks. To enhance detection ability the incubation time was increased from 1h up to overnight. With still no success concentration of labelled nucleotide was increased ten times from 1mCi/ml to 10mCi/ml. Thus several modifications no bands could be seen.

DISCUSSION GTPase OR TGase ACTIVITY?

TGII is a bifunctional enzyme, acting either with GTPase or with transglutaminase (TGase) activity. The two activities are reported to be mutually exclusive (Monsonego A., *et al.* 1998). To date evidence suggests it is only through its GTPase activity that TGII regulates and bind to PLCδ_1 (Feng, J.K., 1996, Beak, 2001). TGII has been associated with differentiation by several studies. However there are divergent reports in the literature on the character of activity involved in this function (Antyoak, M., *et al.* 2001; Chioccia, E.A., *et al.* 1989, Tucholski, J., *et al.* 2001). In hope of getting a clearer picture whether one of the two activities is favoured in the two different phenotype states, of HVSMCs, we assessed randomly cycling and redifferentiated cells by applying a transglutaminase activity assay and [^{35}S] GTPγS overlay assay.

Efficiency of our method for measurement of transglutaminase activity was confirmed by complete inhibition of transglutaminase activity with MDC treatment (200μM) of HVSMCs and absence of tranglutaminase activity following heat inactivation of cell lysates. Unfortunately level of TGase activity was performed at one occasion only and although results indicated a lower level of TGase activity with differentiation there was no significant difference between randomly cycling and serum deprived cells. This would indicate that a change in VSMC phenotypic is not associated with a switch in TGII activity. Growth arrest may be of more relevance for the change in TGII activities and would correlate well with the observations of reduced protein expression of TGII by Western blotting described previously. But more samples need to be examined before further conclusions can be drawn.

The relationship between GTP binding activity and transglutaminase activities of TGII still remains unclear. In vitro studies of TGII with deficient transglutaminase activity following mutation of its active site (Cys-277) showed that TGase-inactive TGII have no effect on the ability of TGII to functionally couple the α_1-adrenoreceptors to PLCδ_1 (Chen, S., *et al.* 1996). Although transglutaminase activity is not required for coupling of α_1-adrenergic receptors to PLCδ_1 there appears to be an inverse relation between activation of PLCδ_1 by GTP-bound TGII and its intrinsic transamidation activity, which is suppressed by GTP and α_1-adrenergic stimulation (Nakaoka, H., *et al.* 1994).

Why PLCδ_1 expression decreased with inhibition of transglutaminase activity is unclear. It could be as suggested by Murthy *et al.* who indicated that GTP controls PLCδ_1 activity by releasing this protein from an inhibitory association with TGII (Murthy, S.N.P., *et al.* 1999). Further measurements of PLCδ_1 in the supernatant or performance of pulse chase experiments could confirm the possibility that PLCδ_1 is broken down or secreted. It is also possible that MDC treatment causes an effect upstream of PLCδ_1 expression.

Inhibition of transglutaminase activity does not necessarily result in an increase in GTPase activity. However, an increase rather than a reduction in PLCδ_1 expression was expected with the combined evidence showing the essential presence of TGII, with TGase activity, for the expression of RhoA and its downstream factors with the role of RhoA as negatively regulating PLCδ_1.

CHAPTER 7 PARTIAL PURIFICATION OF PLC

7.1 Introduction to Partial purification of PLCδ_1 in rat aorta

The aim of this study was to characterise the complex of PLCδ_1 and TGII by using a partially purification of PLCδ_1 isolated from rat aorta smooth muscle, using a combination of ion exchange and affinity chromatography. Having purified PLCδ_1 the aim was to study the effect of a variety of chemical modulators, including C3 and CNF1 (which modulate Rho activity), monodansylcadaverine (MDC) and cystamine, (inhibitors of transglutaminase activity) and GTPγS (activation of G-protein activity) on the position and/or size of the respective enzyme activities

7.2 Overview of Ion exchange chromatography

Ion exchange chromatography is a common feature of protein purification. The method for separating complex mixtures is based on their differing tendencies to bind to a specific ligand coupled to a chromatographic matrix. The target molecule is eluted from the stationary medium by reversing the interaction. This can be performed by either specifically using a competitive ligand, or non-specifically, by changing the pH, polarity or as in our case by changing the ionic strength by applying a NaCl gradient (50-550mM).

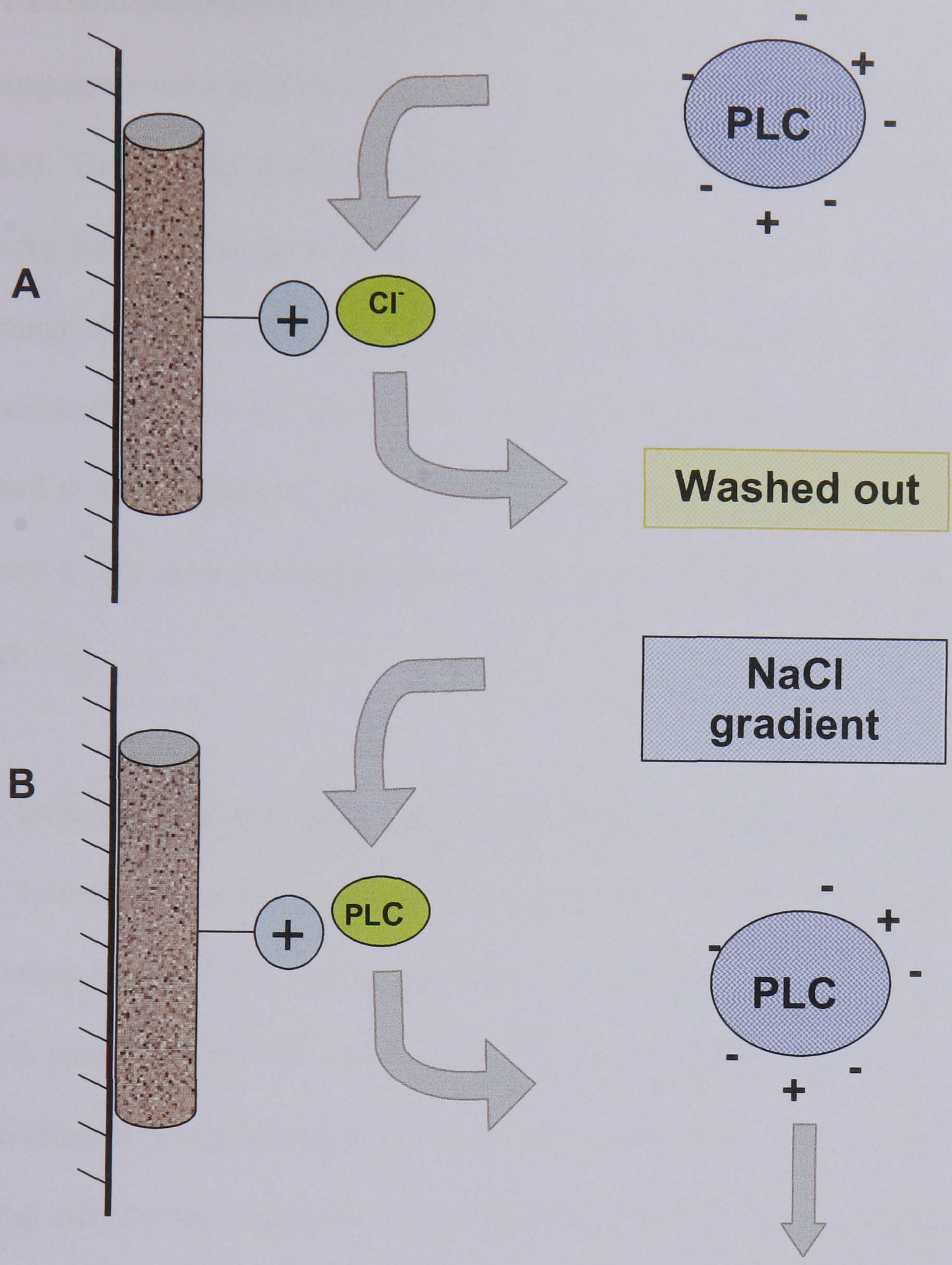


*Figure 7.1. Basis of anion exchange chromatography. The positively-charged ion exchange group immobilised on the stationery phase is charged with Cl^-. (**A**) PLC with a net negative charge exchanges with Cl^- and is held on the ion exchange group by electrostatic attractions. Following addition of a NaCl gradient (50-500mM) PLC is eluted by exchange with Cl^- ions (**B**).*

7.3 Partial purification of PLCδ_1

7.3.1 Partial purification of PLCδ_1 in rat aorta

Homogenates were prepared from the thoracic aortas of two rats (Wistar rats, 6-8 weeks). The sample was homogenised then dialysed and pre-equilibrated with running buffer (Appendix A:16) prior to being applied to a low pressure ion exchange chromatography column containing Q-sepharose resin. The column was pre-washed with running buffer and a linear NaCl gradient (50-500mM) was then applied to enable separation of the PLC isoforms according to their difference in affinity to the anion exchanger (for further details see method section 2.12 and figure 7.1).

This technique has previously been used for partial purification of the different PLC isoforms from bovine aorta. The same protocol was used in these studies collecting every 5th fraction eluted which was further examined for the presence of both protein and PI-PLC activity (Hodson, E., *et al*, 1998 & 1999). To increase the likelihood of identifying peaks of PI-PLC activity from such a relatively small starting sample we measured the activity of every third fraction instead of every fifth fraction eluted from the column. Unfortunately we were unable to detect any PI-PLC activity using this methodology and hence increased the starting sample from two to twelve pooled rat aortas.

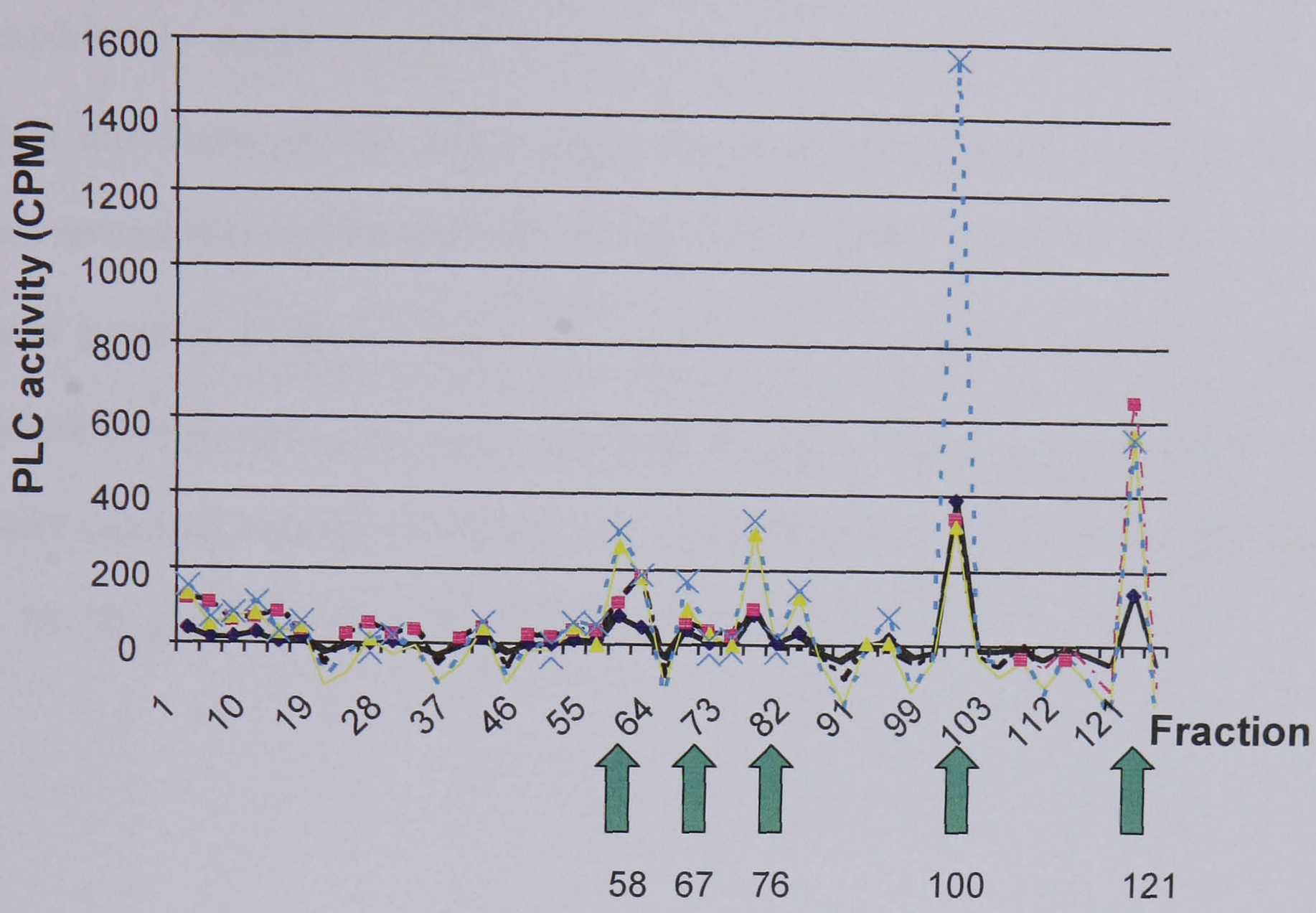


Figure 7.2 Elution profile of 12 rat aorta pooled (n=3) through Q-sepharose. PLC activity peaks shown are from three separate activity measurements of fractions from collected column elute as seen in yellow filled circles, pink filled squares and turquoise crosses. An average of the three runs are shown in black. Following collection of every third fraction eluted the presence of PI-PLC activity, using [^{3}H]PI as a substrate was examined. Only very small peaks were achieved and there was also a certain inconsistency with only the last peak (fraction 121) reoccurring in all three sets of experiments.

7.3.2 PLC activity in 12 pooled rat aortas.

With this increased number of aortas loaded onto the column enabled us to measure PI-PLC activity. As seen in figure 7.2 activities measured were still small and peaks were inconsistent. In addition to the small peaks data from a few experiments suggested a loss in activity over time, as seen in figure 7.3A. The data, after linear adjustment for loss of activity with time, is shown in figure 7.3B but no consistent peaks could be distinguished. Despite the use of 12 rats levels of total proteins measured were still ten fold less than those in previous studies where bovine aorta was used. Although the protein levels were low four peaks were detected over the following fractions; protein peak 1 - 64-67; protein peak 2 – 70- 76; protein peak 3 - 85 and protein peak 4 -109.

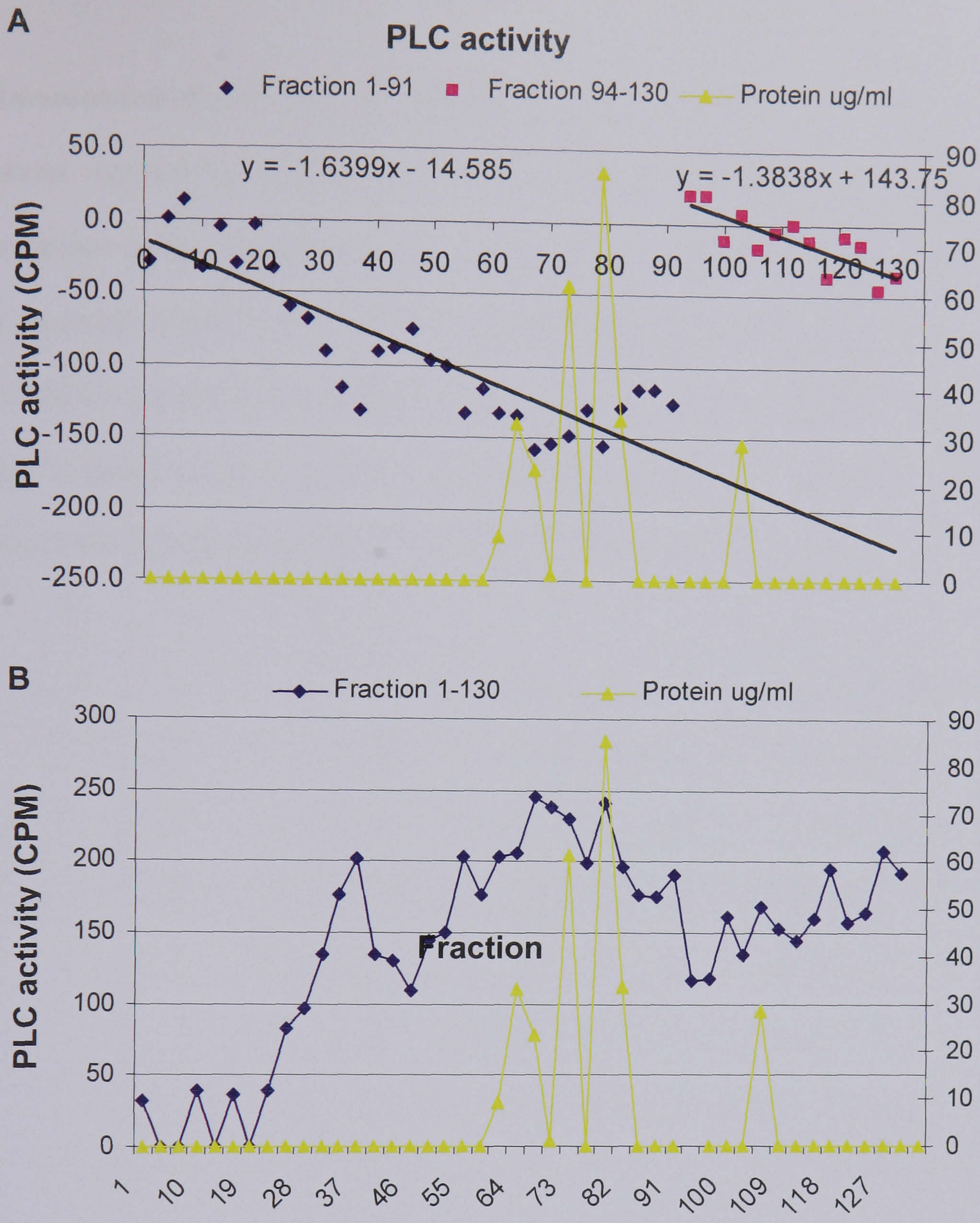


*Figure 7.3 Representation of activity peaks assaying for PLC activity. Every third fraction was measured following loading of sample of 12 pooled rat aortas on an ion exchange chromatography column. Raw data from activity measurements show a slight decrease in activity of isotope, which seem to occur over time (**A**). The loss in activity was corrected for (**B**) however the activities in the different fractions were in most cases equal or even lower than the assay mix without sample itself. Unfortunately pooling 12 rat aortas was not enough contractile tissue.*

7.4 Immunodetection of partially purified PLC preparations

Fractions representing the detected individual protein peaks were pooled and concentrated using ultra filtration prior to SDS-PAGE. Similarly fractions which may represent putative PLC peaks were also pooled and concentrated prior to SDS-PAGE. Lysate of rat brain was used as control. Unfortunately we were unable to detect any PLC isoforms in these pooled, concentrated samples using western blotting techniques (blots not included).

CHAPTER 7 DISCUSSION

Bovine aorta has previously been used in our group for partial purification of the different PLC isoforms. Four peaks of PLC activity were consistently detected and western blotting revealed that two of the peaks contained PLCδ whilst the other two consisted of a PLCγ and an unidentified PLC (Hodson, E., *et al*. 1999). We used the same protocol for the partial purification of PLC isoforms but instead rat aorta smooth muscle was examined since use of bovine aorta was no longer acceptable due to the risk of variant CJD. Although the sample loaded onto the column was scaled up to twelve pooled rat aortas and the PLC assay was performed on every third fraction collected, instead of every fifth fraction, only very small peaks in PLC activity could be detected. Analysis was also complicated by loss of activity with time. The activity loss, as indicated by figure 7.3, seems to occur after 5min (around sample 10). This is an inevitable consequence of having a large number of samples performed in triplicate. It is arguable what factors are of the greatest importance to avoid when comparing a set of samples as one want to ensure that measurements are performed under exactly the same conditions. Several possible external factors may influence the activity measurements such as difference in incubation time, loss of activity due to "waiting time" for starting/ending incubation or during detection when assaying a large set of samples. Other factors are changes in pH or temperature as well as the access of substrate and /or labelled substrate (which often used in methods for monitoring the level of activity). Our assay was carefully composed and performed in such a way as to avoid all these factors as samples were kept on ice when not assayed and incubation time with labelled substrate was strictly timed. However, due to cost labelled substrate was prepared at the same time and

then kept on ice prior to addition. This is one of the factors that may have lead to the loss in activity noted as there is a difference in 34min from first to the last addition of substrate. We rather felt the importance of assaying as many samples as possible under the same condition and correct for this loss in activity. Thus, as this loss in activity was just occurring at certain times another source behind this phenomenon could be the difference of batches used of [^{3}H] labelled PI. Unavoidably, there was a certain variance of age of the labelled substrate within measurements and care was taken to only use isotope without significant loss in activity. According to technical information from Perkin Elmer the loss in activity is approximately 2% for 3 months from date of purification, if stored according to manufacturers (-20°C and in its original solvent and concentration).

Measurements of total protein concentration revealed that we had a ten times lower level of total proteins compared to when bovine aorta was studied, which may explain the low and inconsistent levels of PLC activity measured. The small peaks of PLC activity detected in the fractions of elute containing an increase in total protein were all examined for the presence of PLCβ_1, PLCγ_1, PLCδ_1 using western blotting. However, none of the isoforms could be detected. It was concluded that 12 rat aortas was still not enough tissue as source for PLC purification and it seems impractical to use rat arterial tissue for this purpose.

Because of the low level of PLC activity measured and as neither of the PLC isoforms could be detected further experiments were not performed.

CHAPTER 8 CALCIUM MEASURMENTS

8.1 Aim of study

In attempt to get an understanding of the functional aspect of the association of TGII-PLCδ_1 we examined the receptor coupling of TGII-PLCδ_1 in vascular smooth muscle cells, resulting in an increased level of intracellular calcium, $[Ca^{2+}]_i$. Moreover, we wanted to compare this signal pathway in randomly cycling to redifferentiated cells. As a measure for signal transduction changes in intracellular calcium were measured by a combination of Flexstation, which allows fluorescent measurements and a dye that fluoresce upon binding to calcium.

8.2 Calcium

The contractility of smooth muscles is primarily regulated by the free calcium concentration in the cytosol, $[Ca^{2+}]_i$. Upon stimulation by various means such as depolarization, mechanical deformation or hormones the cytosolic Ca^{2+} concentration rises from 10-100nmol (Bukoski, R.D., *et al.* 1989; Jensen, P.E., *et al.* 1992) to levels of 10-100µmol Ca^{2+} or more (Bolton, T.B., *et al.* 2002). This increase in $[Ca^{2+}]_i$ induces binding of calcium to calmodulin (CaM) producing conformational change which allows the binding or myosin light chain kinase (MLCK) to give an activated Ca^{2+}-CaM-MLCK-complex. MLCK then catalyses the phosphorylation of serine on myosin light chain, increasing the rate of interaction between actin and myosin, resulting in contraction (Somlyo, A.V. and A.P. Somlyo, 1993).

Different pathways couple receptor activation to vasoconstriction. The initial stimulus may operate through changes in surface membrane potential (electromechanical coupling) or mediate changes in force independence of changes in membrane voltage (pharmacomechanical coupling). The effectiveness of this coupling may be regulated by the degree of elevation in $[Ca^{2+}]_i$.

8.3 Measurements of intracellular calcium by Flex station

Calcium fluorescent measurements in live cells were performed on a Molecular Devices FlexStation® II. The FlexStation is capable of performing up to three separate transfers of different compounds from a 96 microplate to the 96 well assay plate. This system is also capable of taking measurements at different temperatures. Moreover, the Flexstation system allows calcium measurements to be made in adherent cells thereby allowing us to monitor the signal pathway taking place in the cells at their proper physiological and morphological condition.

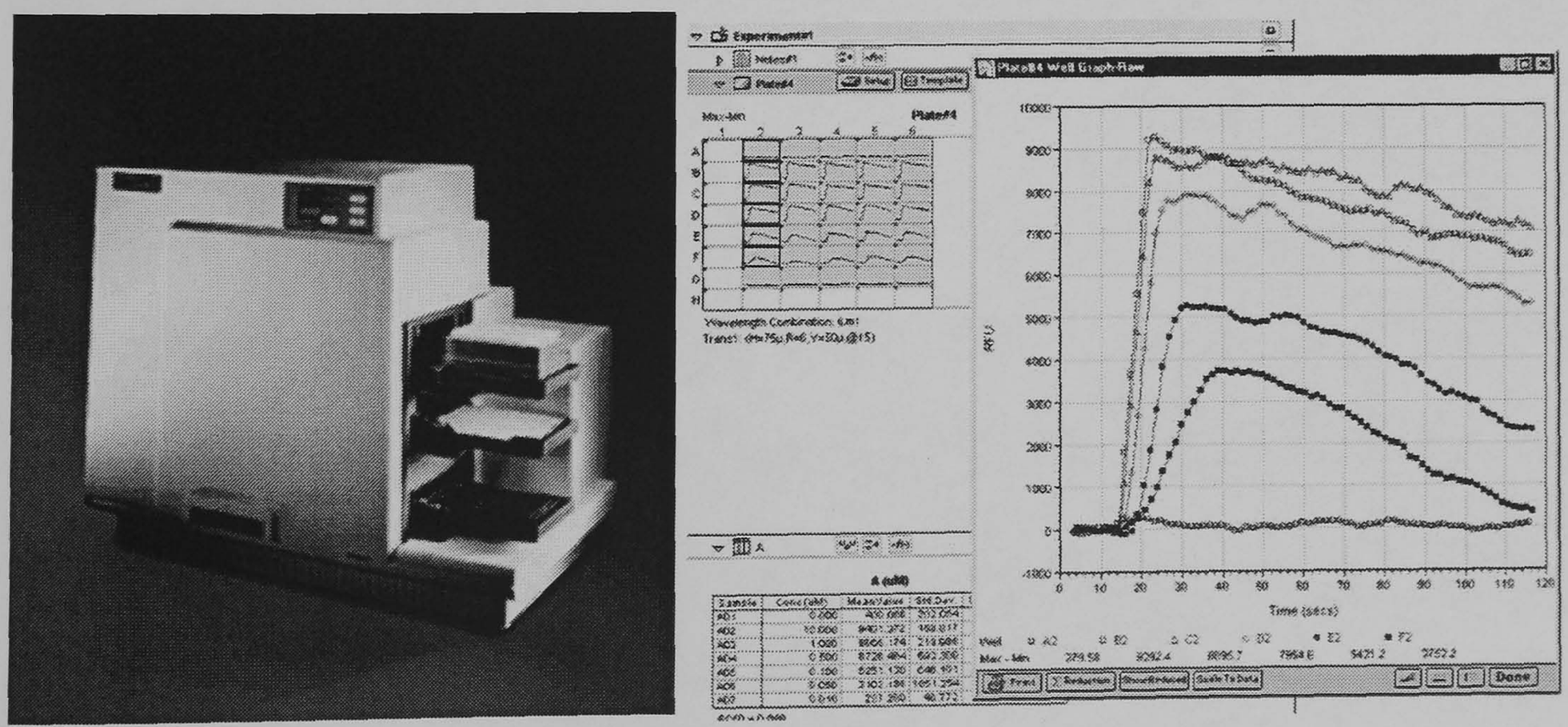


Figure 8.1 Picture of Flexstation and software window (SoftMaxPro 4.7.1). Picture is taken from Molecular device (http://www.moleculardevices.com).

8.4 Cells

8.4.1 HVTs-SM1 cells

For this data to be comparable with previous studies in this thesis measurement of intracellular calcium levels was performed in HVSMCs. In order to facilitate comparisons between the two different phenotypic states we utilised the HVTs-SM1 cell line (see section 2:1:3). This is an immortalised HVSM cell line transfected with a nonreplicative retroviral vector containing a temperature-sensitive (ts) mutant of SV40 LT antigen (Hsieh, J.-K., *et al*. 2000). While normal HVSMCs stop dividing after 12 passages these HVTs-SM-1 cells can be in continuous in culture at the permissive temperature for more than 200 passages. The beauty of this cell line is that it goes through a phenotypic change following change in culture temperature. The more proliferative, synthetic phenotype persists at 36°C whilst switching the temperature to 39°C pushes the cells towards the more differentiated state. The practicality of having incubators set at both 36°C and 39°C as well as maintaining cells at the standard 37°C however meant that we had to modify the protocol slightly. Consequently our studies were instead performed at 37°C and 39°C. Before our measurements of intracellular calcium we started off with some basic examinations of the cell line kept at the two different temperatures. Morphological comparison using phase contrast microscopy showed that cells cultured at 39°C have a similar morphology to the HVSMCs from which they derive (figure 8.2). Transformed cells grew 6 times more rapidly (doubling time of 49±9h) compared to normal doubling time 132±36h) of HVSMCs (Hsieh, J.-K., *et al*. 2000).

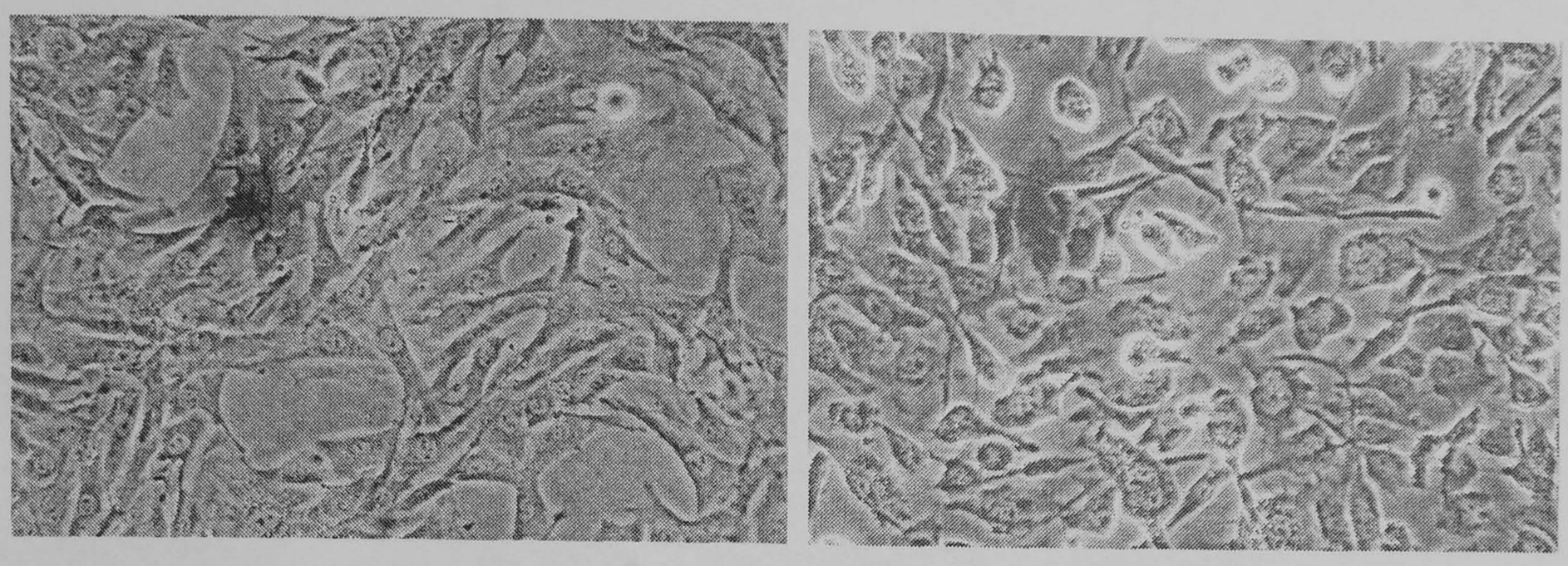


Figure 8.2. Comparison of cell morphology of transformed HVTs-SM1cells. Phase contrast microscopy of transformed HVTs-SM1 cells kept at 37℃ and 39℃. Magnification x 40.

8.4.2 PLC isoform profile and TGII expression in HVTs-SM1 cells

The profile of PLC isoform expression and presence of SM α-actin and TGII in HVTs-SM1 cells was investigated using western blotting technique to attain a clearer understanding of which PLC isoform(s) are present in the HVTs-SM1 cell line and may be potential candidate(s) for contributing to receptor coupling following agonist stimulation.

In terms of PLC isoforms present in HVTs-SM1 cells PLCβ_1, PLCβ_2, and PLCβ_4 were not detected in cells cultures at either 37°C or 39°C. PLCβ_3 however was undoubtedly detected in cells cultured at 37°C but could not be detected in cells cultured at 39°C. PLCδ_1 was clearly detected at cells cultured at both temperatures. Moreover PLCδ_1 expression appeared to be upregulated in cells at 39°C, which represent the more differentiated phenotype. TGII was present in cells cultured at both 37°C and 39°C. Likewise SM α-actin was detected at both temperatures but to a less degree in HVTs-SM1 cells kept at 39°C.

Protein profile of PLC isoenzymes in HVTs-SM1 cells

A

	PLCβ$_1$	PLCβ$_2$	PLCβ$_3$	PLCβ$_4$	PLCδ$_1$	TGII	SM α-actin
37°C	-	-	√	-	√	√	√
39°C	-	-	-	-	√	√	√

B

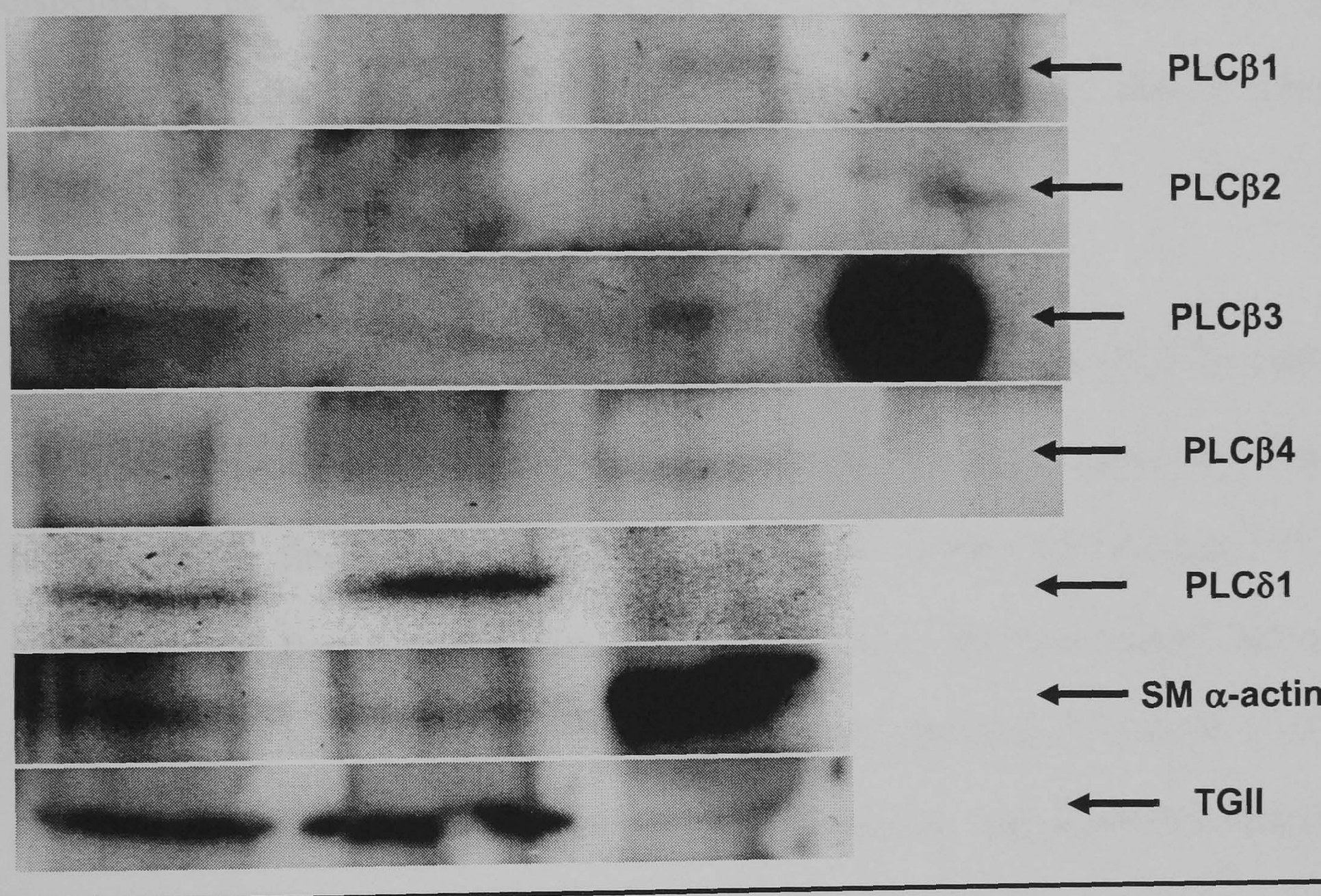


Figure 8.3. Protein profile in HVTs-SM1 cells. ***A****. Illustrative overview of the effect of temperature switch on the expression of PLCβ$_1$, PLCβ$_2$, PLCβ$_3$, PLCβ$_4$, PLCδ$_1$, SM α-actin and TGII.* ***B.*** *Representative blot showing the presence or absence of specific PLC isoforms in lysates (50 μg total protein) of HVTs-SM1 at 37℃ respectively 39℃ (n=3). Lysate of rat brain and A43-cells were used as controls. Blot was probed with primary antibody at 1:1000 for 2 hour followed by secondary antibody (rabbit anti-mouse-HRP - PLCβ$_1$, PLCδ$_1$, swine anti-rabbit-HRP - PLCβ$_2$, PLCβ$_3$, PLCβ$_4$) at 1:1000 for 2 hour and visualised using enhanced chemiluminesence.*

8.5 Measurements of intracellular calcium using Flexstation

HVTs-SM1 cells were seeded onto 96-well-plates and allowed to attach overnight at the appropriate temperature prior to loading. Following loading cells were washed and the plate was moved to the chamber of the Flexstation. The 96-well drug plate was placed into its holder where it is accessible to 8 automated pipette dispensers. The dispenser uses disposable tips and allows the addition of drug directly above the imaging system without having to move the sample plate (figure 8.1).

The Flexstation take 6 random measurements of an area in the centre of the well and it is therefore critical to have a uniform monolayer of cells covering 90-100% of the well. To find the optimal seeding density HVTs-SM1 cells kept at 37°C were seeded at four different densities and allowed to attach overnight before being examined microscopically. The two higher cell densities (7.5 and 10 x 10^5 cells/well) formed layers of cells due to over confluency and areas of detached cells. Consequently the lower density of 2.5 x 10^5 cells/well was used all through the study for HVTs-SM1 at 37°C whilst HVTs-SM1 cells kept at 39°C, were instead seeded at 5 x 10^5 cells/well as they proliferate to a lower extent.

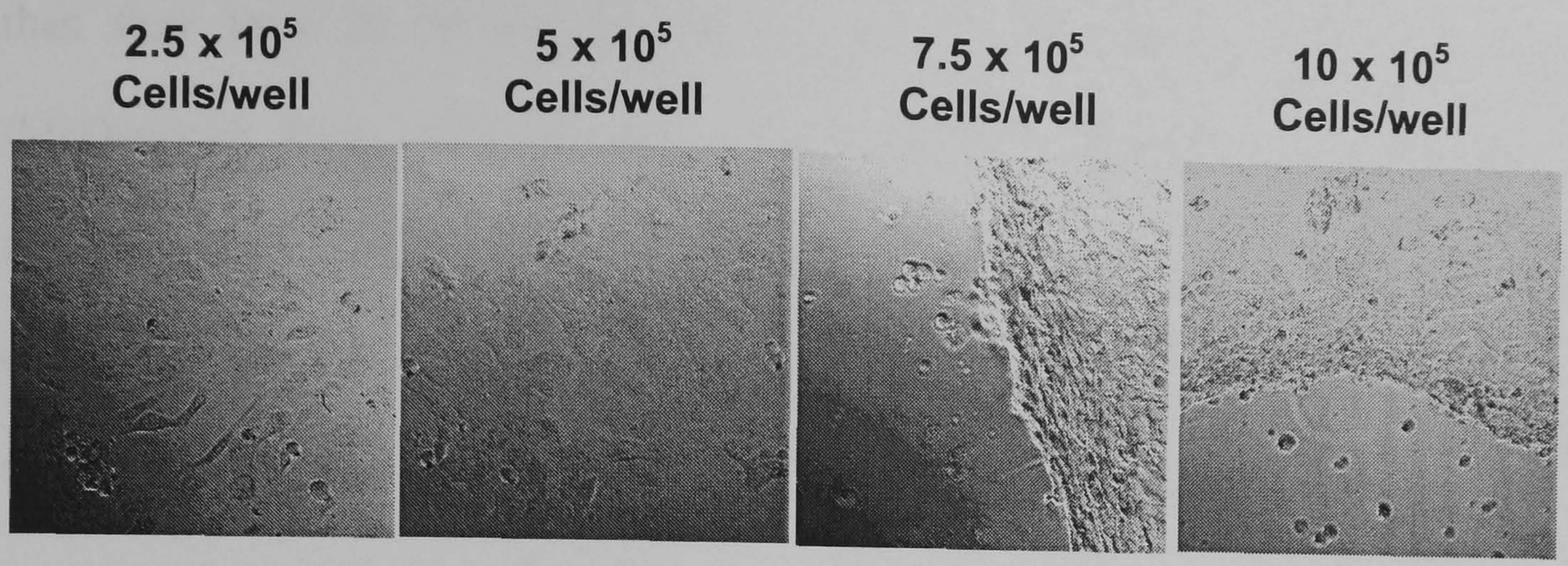


Figure 8.4. Different seeding densities. Optimising formation of a monolayer covering 90-100% of the well of 96-well plate. Phase contrast microscope pictures of HVTs-SM1 cells (kept at 37℃) in wells from 96 wells plate, seeded with different seeding densities. The two higher densities show areas of cell disruptions, in the shape of cell free round circles, occurring already after the first wash. This is probably due to suction applied upon removal of old buffer or the slight pressure from pipette upon addition of fresh buffer. A seeding density in the range of the two lower seem suitable.

8.6 Measurements of intracellular calcium using fluorescent dye

8.6.1 Calcium dyes

Detection and quantification of intracellular calcium is in most cases measured with the use of sensing probes or dyes. These dyes undergo large fluorescence enhancement or spectral shift upon calcium binding. Calcium ion probes are the most widely used intracellular indicators. Calcium indicator dyes can be categorized into two groups; the first are the indicator dyes or nonratiometric dyes such as calcium green-1 and -2 and Fluo-4, which only fluoresce in the presence of calcium, while the second group known as ratiometric dyes, such as Fura-2,

have different excitation and/or emission wavelengths in the presence of calcium than they have in its absence. Fura-2 changes from 338 nm to 366 nm (McDonough, P.M. and D.C. Button, 1989). When the sample is viewed with a fluorescent microscope, the colour or intensity of the fluorescence coming off the cell corresponds to the amount of free calcium in the cell. A measure of the ratio of the two wavelengths obtained before and after binding indicates the concentration of calcium and its location in the cell.

There are advantages and disadvantages to each of the two groups of calcium indicators. The ratiometric dyes are excited by UV-light, which can result in high background fluorescence from the microplate or cause cellular photo-damage due to its higher energy. Ratiometric determinations also require rapid filter switching by the microplate reader, particularly when intracellular calcium levels are changing rapidly. Optimally both wavelengths are being measured simultaneously, but this is not always possible. Photo-bleaching of the compound itself may present a problem if only one filter set is used, but is corrected for if ratiometric determinations are being made. Additionally, ratiometric analysis can also correct for dye leakage. Direct measurement dyes have been developed for excitation in the visible wavelength range resulting in less phototoxicity. In general, direct measurement indicators have a greater fluorescence response to calcium than the ratiometric dyes. This may allow for the use of lower intracellular concentrations of indicator dye reducing any cytotoxic effects of the dye.

8.6.2 Cell loading

To introduce the dye into our cells we used acetoxymethyl (AM) ester loading. This is a non-invasive technique that uses dyes in which the carboxylate groups have been converted with acetoxymethyl esters resulting in a nonpolar compound that is permeable to cell membranes. Once inside the cell, these compounds are hydrolyzed by intracellular esterases (illustrated in figure 8.5), resulting in an activated and now polar indicator that is no longer capable of freely diffusing through the cell membrane, essentially trapping the compound inside the cell.

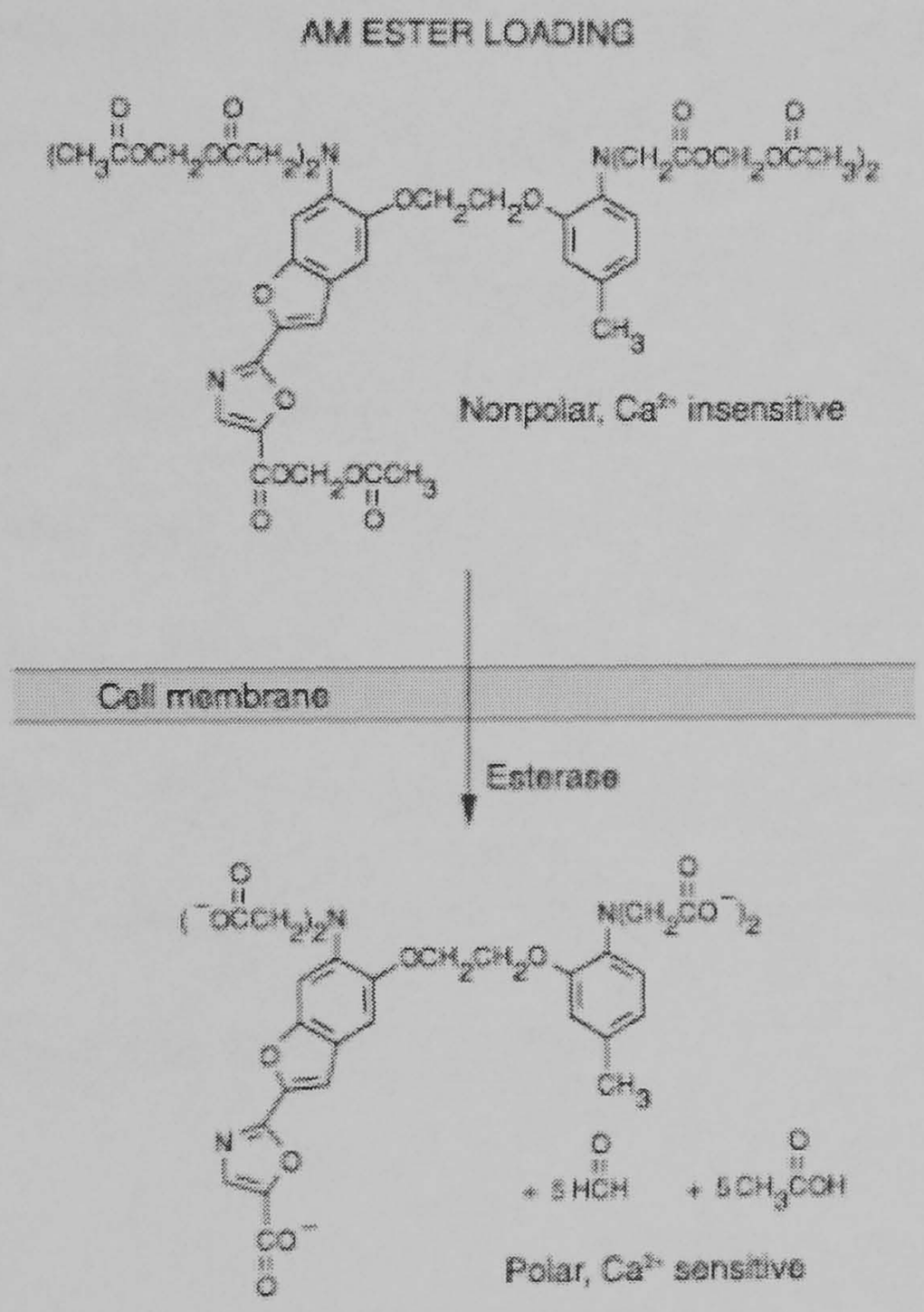


Figure 8.5. Schematic diagram of the processes involved in loading cells using acetoxymethyl (AM) ester derivatives of fluorescent indicators. Fura-2-AM is used as an example. Picture taken from (http://www.probes.com)

8.6.3 Data analysis.

Fluo-4 AM is a non ratiometric indicator; thus, changes in $[Ca^{2+}]i$ levels cannot be expressed as changes in absolute calcium concentrations. To quantify the fluorescence signal, we introduced Ionomycin (10μM), a Ca^{2+}-ionophore and EGTA (10mM) a Ca^{2+} chelator at the end of the experiment. Ionomycin is a mobile ion carrier that transports divalent cations such as Ca^{2+} and Mg^{2+}. It normally acts as an ion-exchange shuttle, carrying two H^+ out of the cell for every divalent cations it carries in. The addition of inonomycin induces a massive Ca^{2+}-influx across the plasma membrane into the cytoplasm resulting in a collapse of the transmembrane gradient and should swamp endogenous Ca^{2+} buffers and elevate intracellular concentration of $[Ca^{2+}]$ to roughly the same level as $[Ca^{2+}]$ extracellularly and thereby giving Maximum fluorescence, Fmax. Minimal fluorescence (Fmin) was achieved upon addition of the calcium chelator EGTA. The compound EGTA is a calcium-chelating agent that sequesters calcium ions and effectively lowers the calcium ion concentration. The level of intracellular calcium was estimated using the equation: $[Ca^{2+}]i = Kd \times (F - F_{min})/(F_{max} - F)$ (Grynkiewicz, G., et al. 1985). K_d is the dissociation constant of Ca^{2+}-Fluo-4-AM complex (345nM).

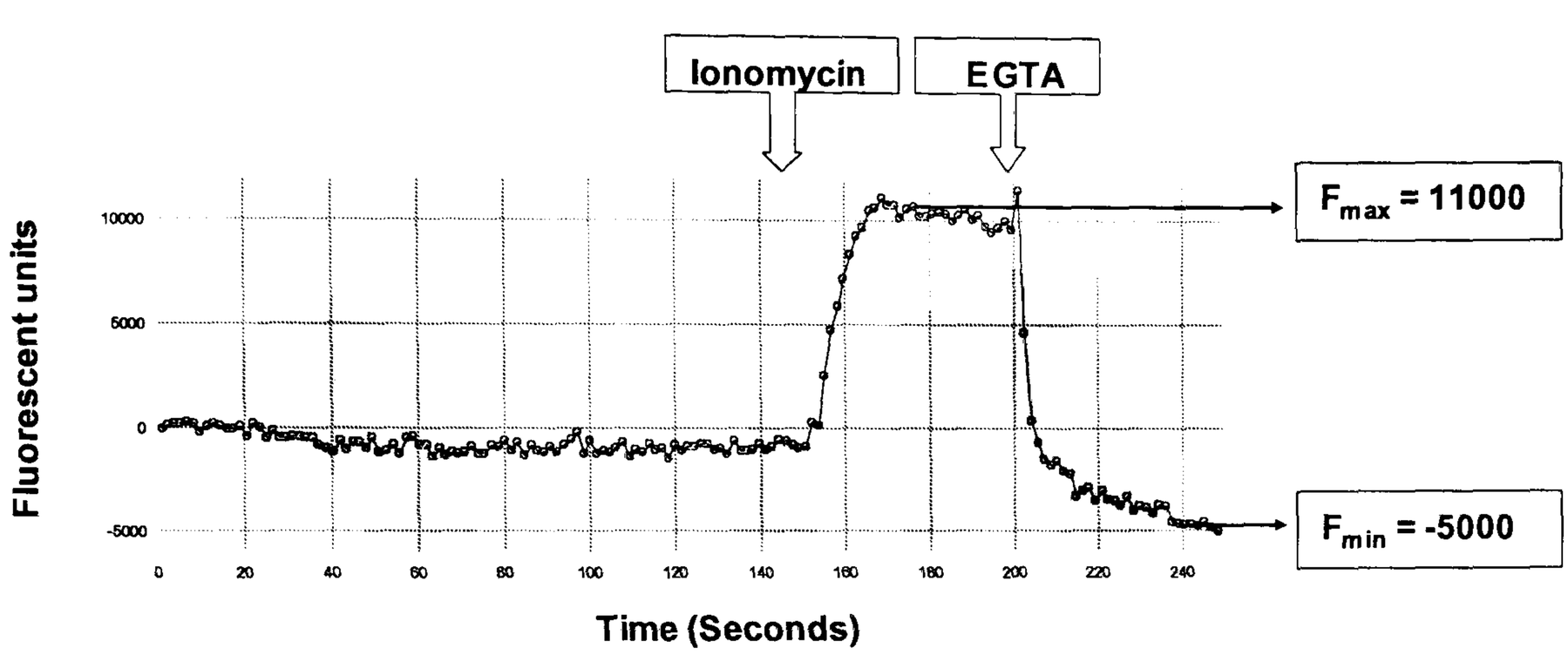


Figure 8.14. Quantification of the fluorescence signal. Intra cellular calcium measurements using Flexstation and Fluo-4-AM loading. HVTs-SM1 cells at 37°C were studied upon addition of Ionomycin (10μM) after 150sec following addition of EGTA (10mM) at t=200sec. $[Ca^{2+}]_i$=156nM.

8.6.4 Fluo-4-AM versus Fura-2AM

As mentioned earlier there are advantages and disadvantages with the different calcium dyes. To examine which dye was the most suitable for measuring changes in $[Ca^{2+}]i$ in our HVTs-SM1 cells, loading with the calcium-sensitive fluorescent dyes Fura-2-AM and Fluo-4-AM were compared. The actual loading procedure, including buffers for loading and washing as well as loading times, is different for the two different dyes (See method section 2.16.1 and 2.16.2 for further details). Changes in the level of intracellular calcium were compared using the two dyes following addition of Phenylepherine, PE (10μM). To quantify the fluorescence signal, we introduced Ionomycin (10μM) and EGTA (10mM) at the end of the experiment and the level of intracellular calcium was estimated using the equation: $[Ca^{2+}]i = Kd \times (F - F_{min})/(F_{max} - F)$. As seen in figure 8.6 a higher level of intracellular calcium was measured fdlowing addition of PE (10μM) when using Fluo-4-AM (484nM) compared to Fura-2-AM (168nM). Although Fura-2 have that advantages that come with being a ratiometric dye and its protocol involve shorter incubation times as well as fewer wash steps it resulted in much smaller fluorescence changes than those seen with Fluo4. The more sensitive nature of fluorescence measurements seen with Fluo4 coupled with the fact that it also allowed us to perform live imaging measurements of calcium using the confocal microscope made this the dye of choice for these experiments.

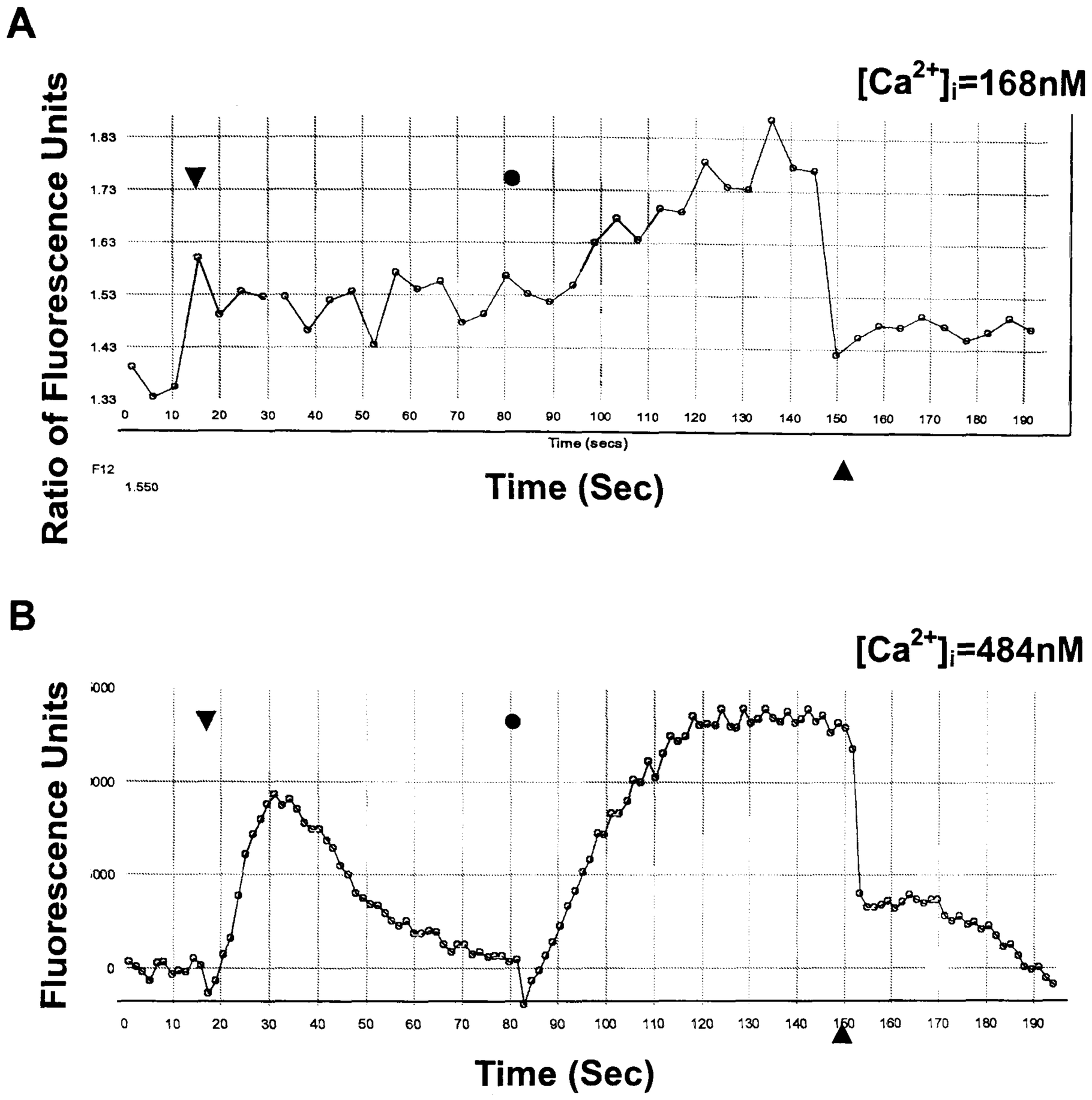


*Figure 8.6 Comparison of loading efficiency using Fura-2-AM versus Fluo-4-AM. Time course from Flexstation showing fluorescence intensity following addition of PE (▼ 10^{-5}M), Ionomycin (●10μM) and EGTA (▲10mM) to HVTS-SM1 cells (kept at 37℃) loaded with **A**. Fura-2-AM respectively **B.** Fluo-4AM. [Ca2+]i was calculated by $[Ca^{2+}]_i = K_d \times ((F-F_{min})/(F_{max}-F))$ (Grynkiewicz, 1985).*

A. [Ca2+]i = 224 x (1.596 – 1.415)/(1.858 – 1.596)= **168nM**

B. [Ca2+]i = 324 x (9177 – -929)/(15943 – 9177)=324=**484nM**

8.7 Background fluorescence

Incomplete AM ester hydrolysis of dyes can in certain cases be a problem, where residual unhydrolyzed AM esters may be present extracellularly due to incomplete removal due to insufficient washing. However, as the AM ester of Fluo-4 is nonfluorescent this should not be a problem in our case. Different cell types fluoresce to different degrees and we therefore looked at the level of fluorescence in an unloaded compared with a Fluo-4-AM loaded cells. Measurements were performed upon addition of Ionomycin (10μM) and EGTA (10mM). As seen in figure 8.7 no background fluorescence seem to exist in our cells HVTs-SM1 cells.

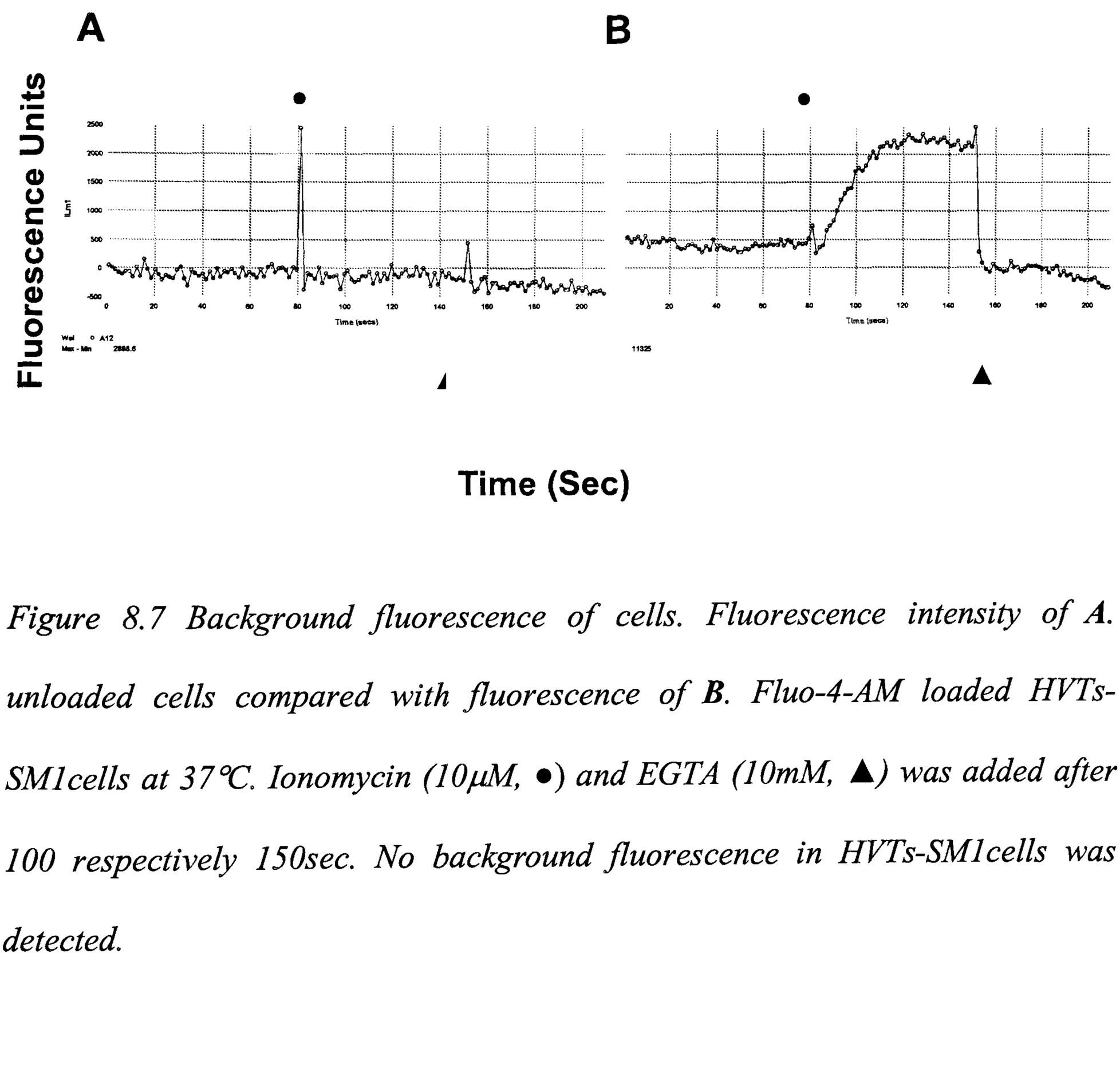


Figure 8.7 Background fluorescence of cells. Fluorescence intensity of ***A****. unloaded cells compared with fluorescence of* ***B****. Fluo-4-AM loaded HVTs-SM1cells at 37℃. Ionomycin (10μM, ●) and EGTA (10mM, ▲) was added after 100 respectively 150sec. No background fluorescence in HVTs-SM1cells was detected.*

8.8 Compartmentalisation of dye

It is assumed that the calcium indicator dye distributes evenly throughout the cell cytosol and is equally responsive to intracellular calcium concentrations. However, AM esters and their hydrolysis products are capable of accumulating in any membrane-enclosed structure within the cell. In some instances, these molecules, particularly the polyanionic-hydrolyzed moieties, can be partitioned by active transport systems. Cells with low levels of intracellular esterase activity may not completely activate the indicator dye. Cellular esterase activity may vary greatly from one cell type to another. The extent of compartmentalization can be assessed by image analysis. To assess the success of loading we performed live calcium imaging using confocal microscopy combined with phase contrast microscopy to correlate location and spread of dye in the cells (method 2.17). Briefly, cells were seeded in petri dishes (35mm MatTek dishes, P35G-1.5-14-C), 22mm and 32mm round coverslips, Labtek coverslip chamber slides) and in parallel the same 96-well- plates used for flexstation to ensure examination was performed at same conditions and allowed to attach over night prior to experimental analysis. The advantage with using the petridishes is that it enables the use of a lens at higher magnification. As seen in figure 8.8 (A) cells are successfully loaded with Fluo-4-AM and base level was measured over 15min without any changes confirming the absence of dye leakage. Three cells were chosen at random and their calcium concentrations were measured following the addition of PE (10μM). The three cells showed similar transient response and level of fluorescence units measured.

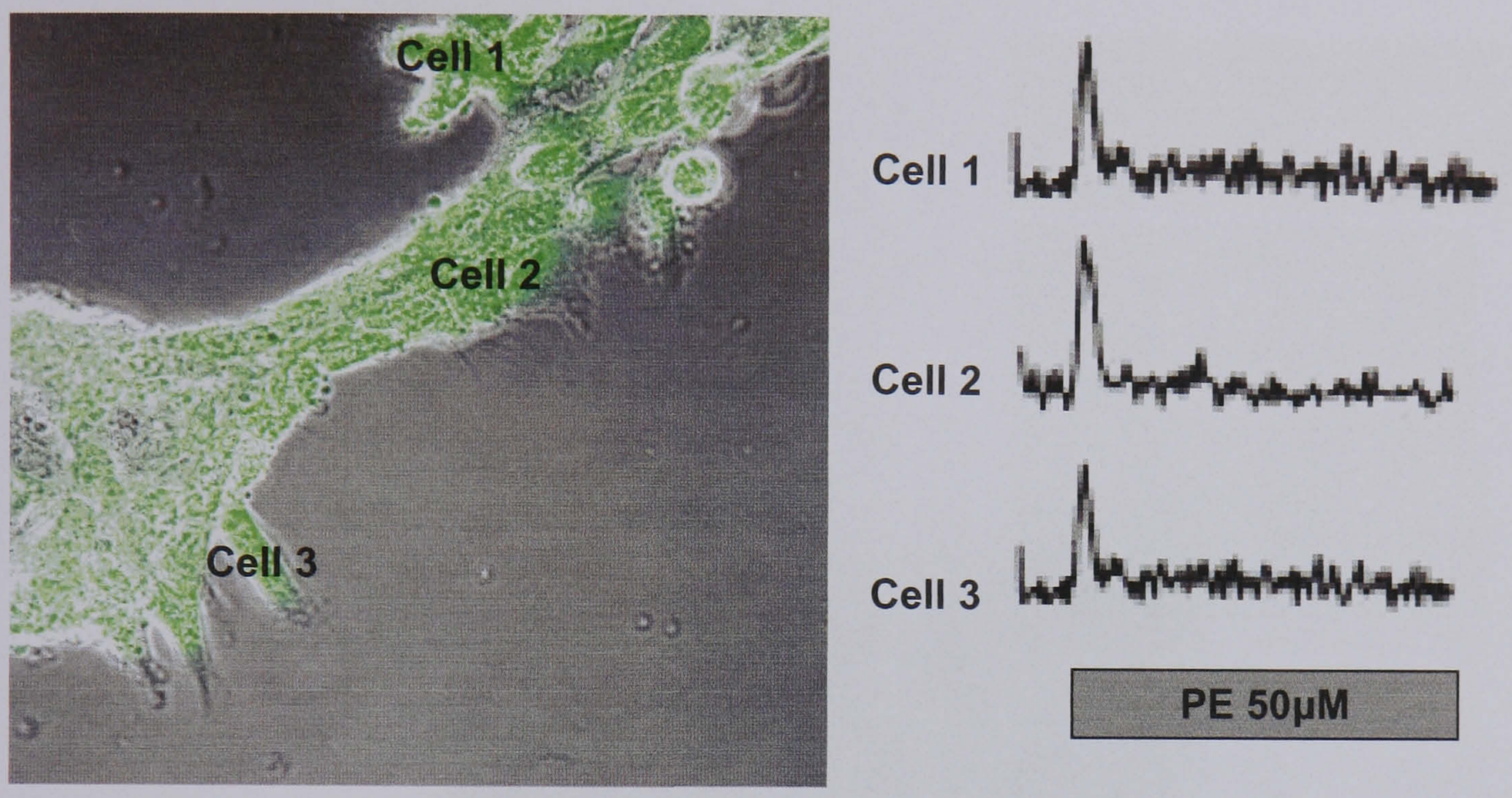


Figure 8.8. Calcium live imaging of HVTs-SM1 cells. ***A****. Nicely Fluo-4-loaded HVTs-SM1 cells.* ***B****. Illustration of three randomly chosen HVTs-SM1 cells (at 37℃) showing similar transient increase and peak fluorescence upon stimulated by the exposure to PE (10µM). Dye loading was monitored by live calcium imaging (Zeiss Axiovert 100M, x40 lens, software Carl Zeiss LSM 5). The image clearly verify that HVTs-SM1 cells are loaded with Fluo-4-AM and in addition the dye is not compartmentalised. The nicely loading of Fluo-4-AM may be due to gap junctions, which are junctions between cells that allow different molecules and ions to pass freely between cells.*

It must be noted that complete hydrolysis of the dye results in the formation of cytotoxic compound by-products, such as a formaldehyde and acetic acid and long incubations with dye should therefore be avoided. To study this effect cells were loaded with Fluo-4-AM and monitored over time using calcium live imaging. Figure 8.9 show how compartmentalisation of the dye occurred after one hour, as demonstrated by the more granular appearance of the dye. Measurements never exceeded 15min so as a consequence we ensured that the possibility of compartmentalistion of Fluo-4-AM did not have to be taken into account.

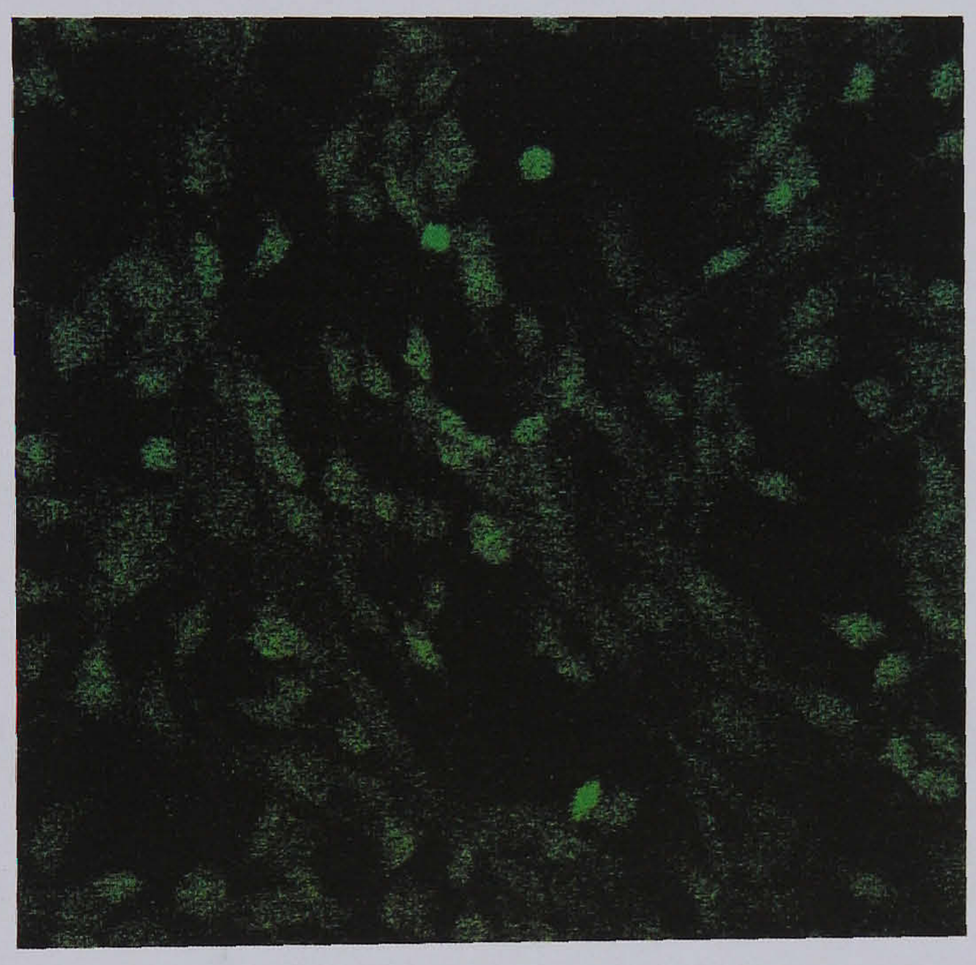


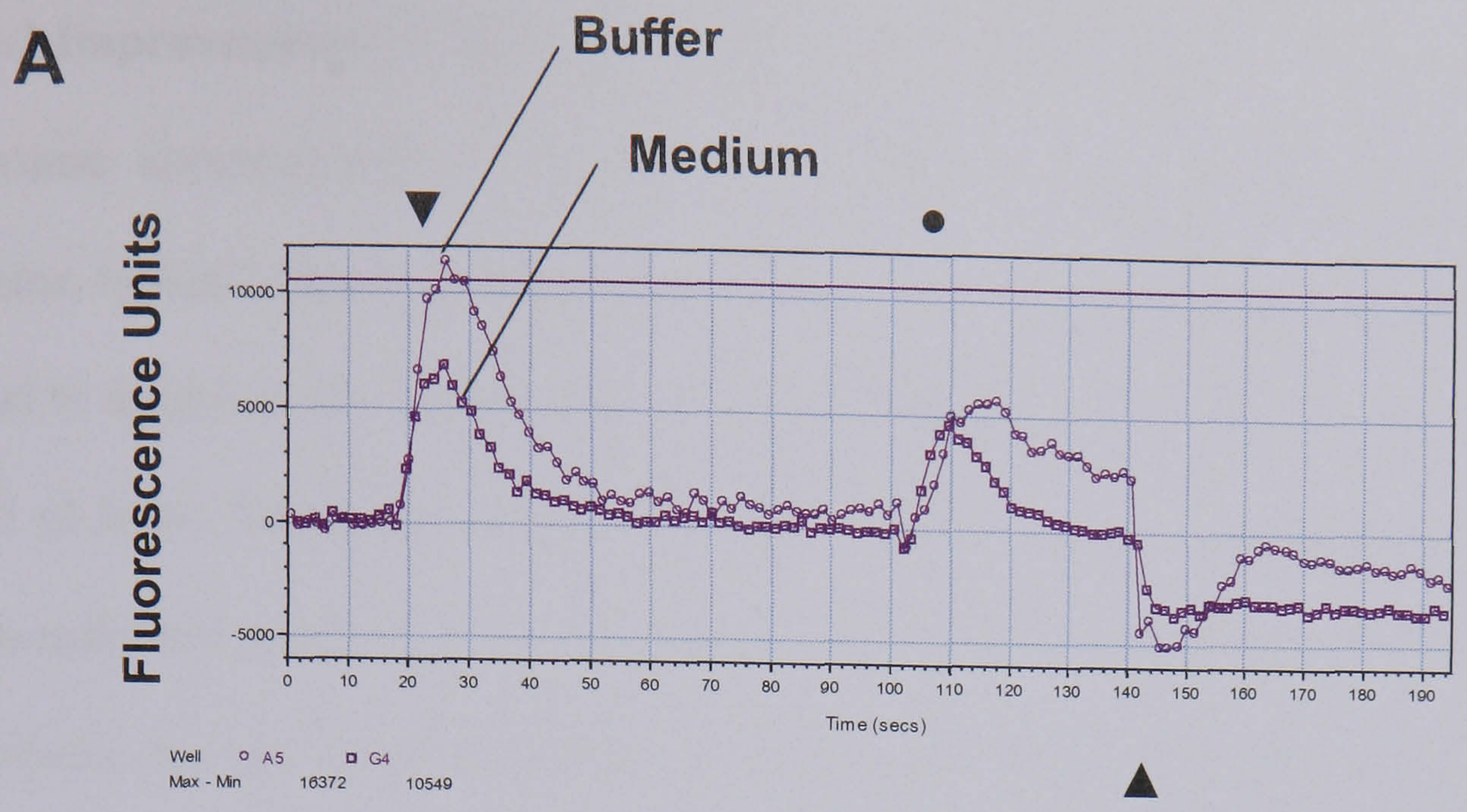
Figure 8.9. Showing calcium live imaging of HVTs-SM1 cells. One hour following start of measurement the dye is compartmentalised seen by the more granular appearance. Dye loading was studied using live calcium imaging (Zeiss Axiovert 100M, x40 lens, software Carl Zeiss LSM 5).

8.9 Establishing loading condition for HVTs-SM1 cells

At this stage we knew by live calcium imaging that dye loading was successful and no compartmentalisation of our dye occurred. Also, Fluo-4AM was a more successful choice of dye in our cells compared to Fura-2-AM. There are a few factors that may improve dye loading, which differ greatly for each cell type. We therefore examined the effect of loading our cells with Fluo-4-AM in medium versus buffer and as well the effect of loading in presence of Pluronic acid, Probenecid and the effect of addition of 1% Albumin.

8.9.1 Loading in buffer versus loading in serum containing medium

One of the first things we investigated was the effect of loading our cells with Fluo-4-AM in buffer with 10% FCS (Appendix A: 5.17) compared to medium (DMEM, 10% FCS). Fluorescence intensity measurements by Flexstation demonstrated a greater response to PE (10μM) in cells loaded with buffer compared with cells loaded in media (Figure 8.10:A). Moreover live calcium imaging of dye loading, visualised using confocal microscopy, also demonstrated that dye loading was better in buffer compared to medium where although the same number of cells were seeded in each case more cells showed successful loading in buffer compared to medium (Figure 8.10:B).



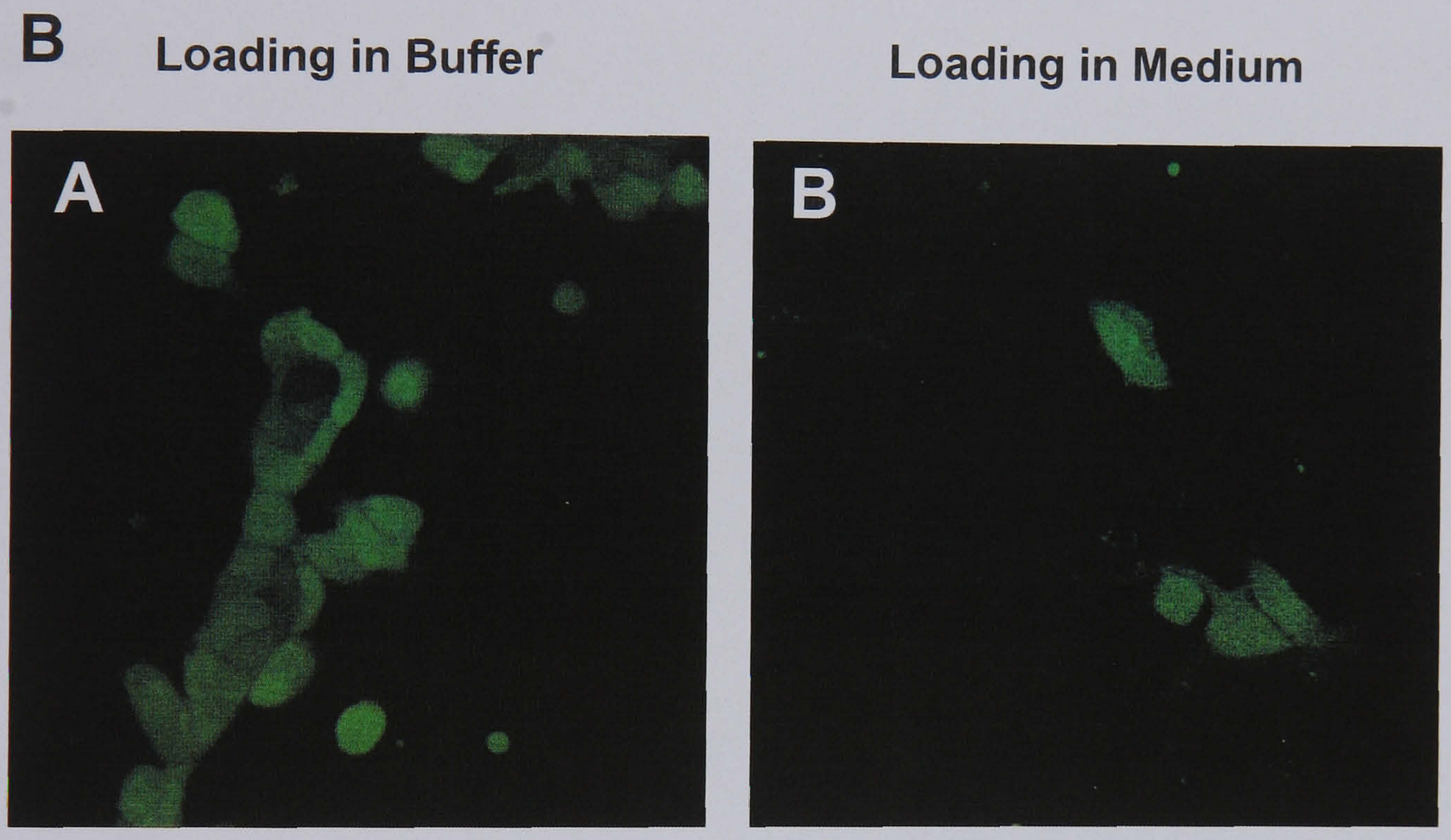


*Figure 8.10 Fluo-4-AM loading in buffer versus medium. A higher fluorescence intensity was measured in cells loaded with Fluo-4-AM in buffer compared to medium following addition of PE (▼10μM), Ionomycin (●10μM) and EGTA (▲10mM), using Flexstaion (**A**). Similarly, shown below performing live calcium imaging of HVTs-SM1 cells loaded with Fluo-4-AM in buffer (A) compared to medium (**B**). Both studies indicate that our cells Fluo-4-AM were loaded more successfully in buffer than in medium. HVTs-SM1 cells kept at 37℃ were used. Dye loading was monitored by live calcium imaging (Zeiss Axiovert 100M, x40 lens, software Carl Zeiss LSM 5).*

8.9.2 Improvements of loading with addition of Pluronic acid

Because acetoxymethyl (AM) esters have low aqueous solubility, dispersing agents, typically fetal calf serum, bovine serum albumin or Pluronic acid are often used to facilitate cell loading. We investigated the usefulness of using Pluronic F-127 (2.5mM, Molecular Probes P-3000MP, 20% solution in DMSO) which is a non-ionic and nondenaturing detergent, to help disperse Fluo-4-AM in the loading medium. As can be demonstrated in Figure 8.11 fluorescence measurements in response to PE (10μM) were considerably enhanced in the presence of Pluronic acid.

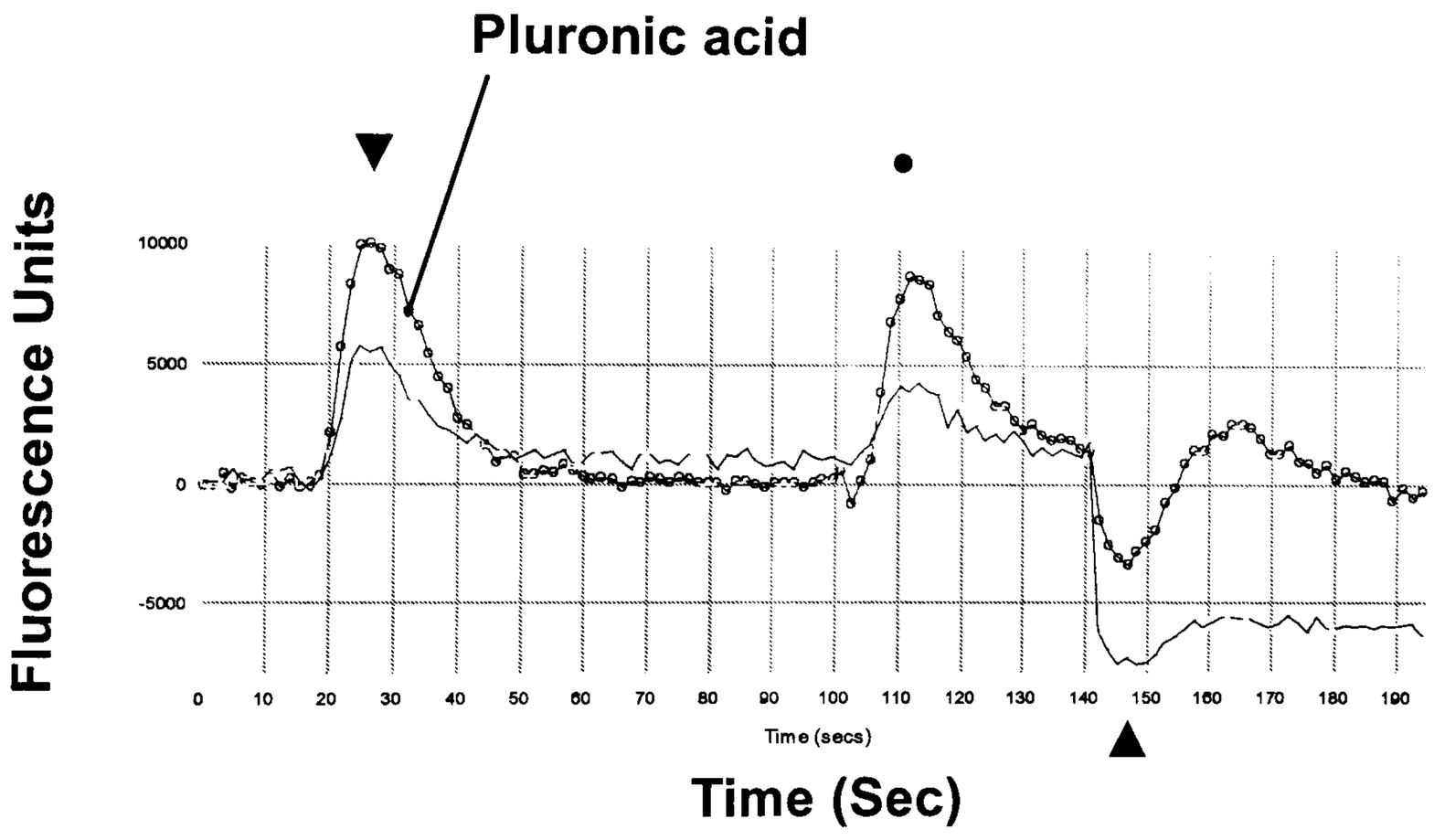


Figure 8.11. The beneficial role of presence of Pluronic acid (2.5mM) for improved intracellular calcium measurements using Fluo-4-AM. Changes in intracellular calcium were measured with Flexstation upon following addition of PE (▼10μM), Ionomycin (●10μM) and EGTA (▲10mM). Presence of Pluronic acid improved dye loading. HVTs-SM1 cells kept at 37℃ were studied.

8.9.3 Improvements of loading with addition of Probenecid

Leakage of the active indicator dye from loaded cells can also occur. Many cell types have organic ion transport systems, such as the P-glycoprotein multidrug-transporter, which are capable of actively eliminating the indicator dye from the cell. This leakage of dye by extrusion of anionic indicators from cells by organic ion transporters can be reduced by Probenecid. Addition of Probenecid may increase dye retention due to its action as anion exchange protein inhibitor. To investigate whether Probenecid had an effect on dye loading in the HVTs-SM1 cells fluorescence measurements in response to PE (10^{-5}M) were compared in cells with and without the addition of Probenecid (2.5mM, Sigma, P-8761) to the loading buffer. As can be seen in figure 8.11 the presence of Probenecid clearly enhanced fluorescence measurements in HVTs-SM1 cells.

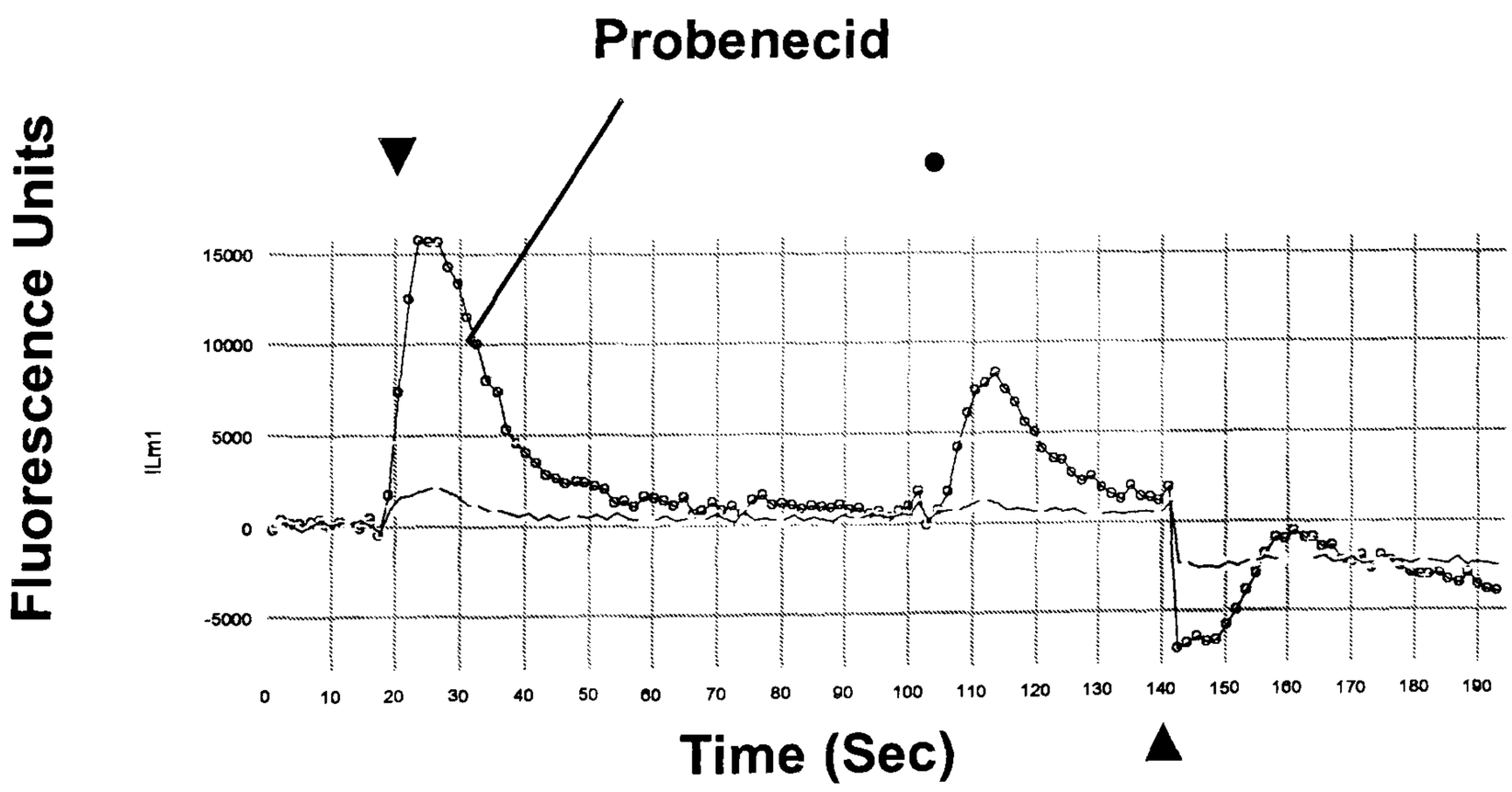


Figure 8.12. The beneficial role of presence of Probenecid for improved intracellular calcium measurements using Fluo-4-AM. Changes in intracellular calcium were measured with Flexstation following addition of PE (▼10μM), Ionomycin (●10μM) and EGTA (▲10mM). Presence of Probenecid shows a great beneficial role for dye retention in HVTs-SM1 cells (37℃).

8.9.4 Improvements of loading with Albumin

The presence of Albumin (1μg/ml) in the loading buffer could help preventing compounds from sticking to the plastic. To further optimise our loading condition we compared the effects of Albumin (1μg/ml) in the loading buffer. Fluorescence measurements in response to PE (10μM) indicated a slight increase in the presence of Albumin.

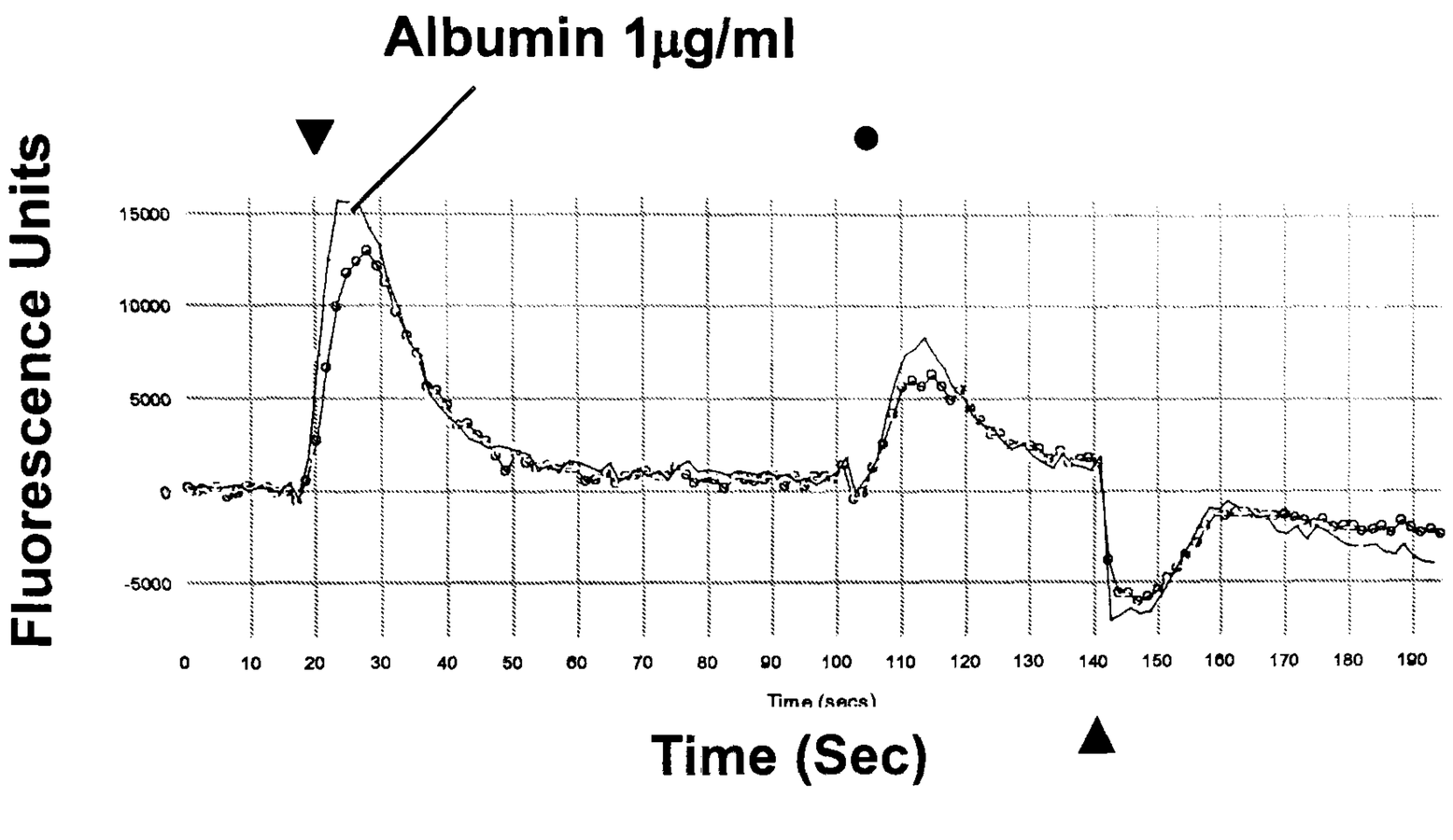
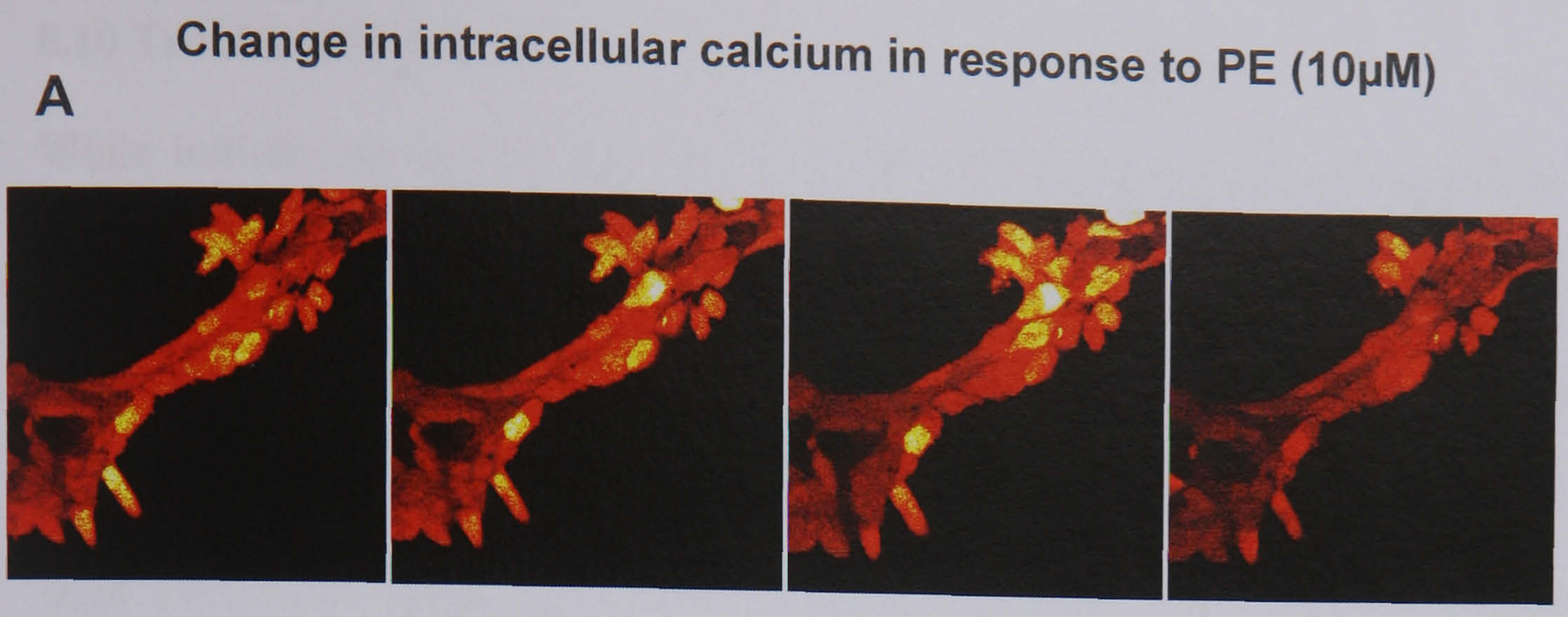


Figure 8.13. The effect of Albumin on Fluo-4-AM loading in HVSMCs (37℃). Changes in intracellular calcium were measured with Flexstation following addition of PE (▼10μM), Ionomycin (●10μM) and EGTA (▲10mM). A slight improvement in dye loading was achieved in presence of Albumin (1μg/ml).

8.9.5 Change in intracellular calcium in response to PE (10μM)

In continued studies cells Fluo-4-AM loading was performed in buffer (FCS 10%) in presence of Pluronic acid (2.5mM), Probenecid (2.5mM) and Albumin (1μg/ml). Figure 8.14 demonstrate measurements of intracellular calcium using the optimised condition for Fluo-4-AM loading in HVTs-SM1 using live calcium imaging (8.14.A) and Flexstation (8.14.B).



$[Ca^{2+}]_i = K_d^{(*)} \times (F-F_{min})/(F_{max}-F)) = 484nM$

Figure 8.14 Measurements of $[Ca^{2+}]_i$ of HVTs-SM1 cells. ***A****. Live calcium imaging of cells indicating successful loading without compartmentalisation. Addition of PE (▼, 10μM) increases the level of calcium, seen by the higher colour intensity upon increased calcium bound Fluo-4-AM. An even higher level of calcium bound Fluo-4 is seen upon addition of Ionomycin (●, 10μM). Following addition of EGTA (▲, 10mM), the level of $[Ca^{2+}]_i$ goes down to lower than basal level.* ***B****. The same experiment but perform on the Flex station where similar changes in level of calcium is measured thus level of changes of fluorescence of Fluo-4-AM is demonstrated as a time course instead of colour intensity. HVTs-SM1 cells kept at 37℃ were studied.*

8.10 Trouble shooting with detachment of HVTs-SM1 cells.

While initially we did not have any problems with detachment it soon became apparent that cell detachment occasionally was an issue with the HVTs-SM1-cells. As shown in figure 8.16 there is a visual difference in cell disruption before and after addition of agonist. Also, it should be borne in mind that the pressure from Flexstation dispensers results in a more powerful addition than manual addition of drug by pipetting.

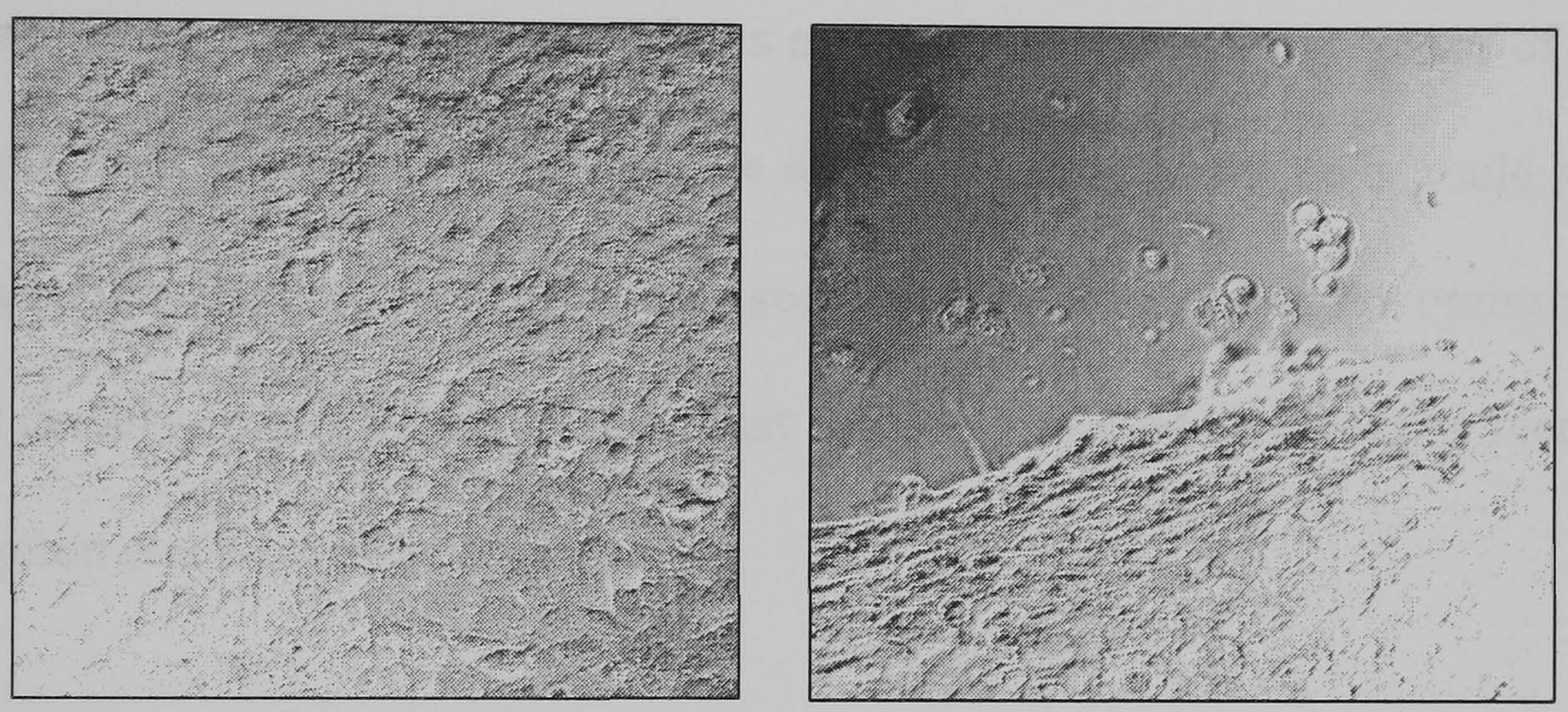


Figure 8.15 Detachment of cells. Phase contrast microscope of HVTs-SM1 cells (at 37℃) picture before (left) compared to after (right) addition of agonist.

There are a few factors involved in the actual addition step that should be considered. As after pipettor of the Flexstation picks up fluid from the compound plate, it draws a small bubble of air into the bottom of each pipette tip to ensure that fluid doesn't leak out the bubble will be the first thing out of the pipette tip when fluid is dispensed. Therefore best to start dispensing with tips above the fluid level in the wells. It is also preferable to have the pipettor tips submerged after the addition has been completed, to ensure complete sample dispensing. It's

preferable to dispense as fast as possible to enhance mixing of the compounds in the wells. Another factor that may have an impact is the speed of additions of the compound. A too rapid addition can dislodge some types of cells form the plate. We were using the addition speed recommended from manual when working with cells that are prone to fall off.

As a consequence of detachment of cells a drop in fluorescence occurred following addition of compound. Technical support advised to change the addition speed and utilise coated plates and explained that the presence of more than one layer of cells in the wells due to over seeding of the cells could be the reason behind the drop in fluorescence seen. Our study regarding the optimisation of cell density (figure 8.4) confirmed that cells only formed a monolayer therefore that option could be excluded.

8.10.1 Detachment of cells

Yet taking these considerations, we noticed that cells were falling off already at the first wash step out of the three which follows after dye loading to remove unbound dye. To study the impact on different washes we took phased microscope pictures after the three different washes. As seen in figure 8.17, there is a clear pattern of increased cell disruption with exposure to an increased number of washes. Most marked disruption occurred after the third wash where an obvious pattern of round circles without any cells were seen. This disruption of the cells is probably due to suction of old buffer or the slight pressure applied on the cells upon addition of fresh medium with the pipette.

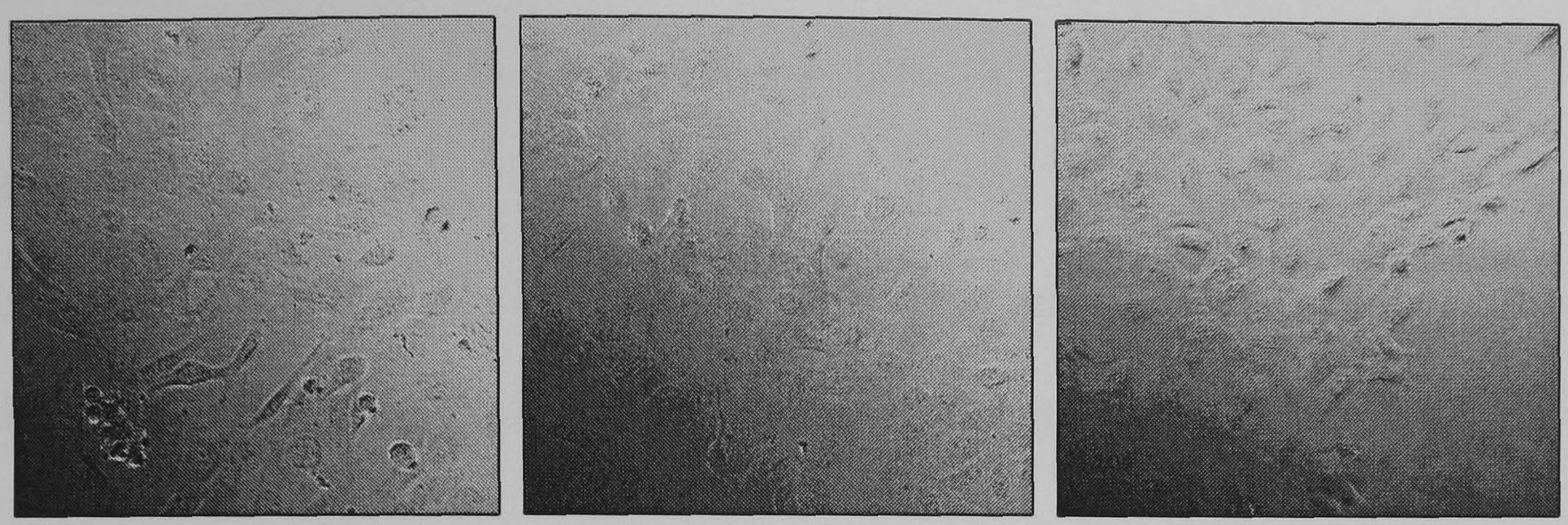


Figure 8.16 Disruption of cells due to increase in washes. Phase microscope picture of Sm-1 cells (kept at 37°C) wells from 96 well plate of cells seeded at 2.5 x 10^5 cells/well. Shown from left to right is the effect of cell disruption with exposure to increased number of washes. Following the third wash areas of round circles, absent of cells appeared. This disruption of the cells is probably due to suction of old buffer or the slight pressure applied on the cells upon addition of fresh medium with the pipette.

8.10.2 Improvement of attachment by lysine coating of wells

In attempt to improve attachment of the cells we tried coating the surface of the well with Poly-L-Lysine. Poly-L-Lysine is a highly positively charged amino acid chain commonly used as a coating agent to promote cell adhesion in culture. Poly L-lysine solution (0.01% in ddH_2O) and as well as Poly-D-lysine coating (50µg/ml) solution in water was tried out. The solution containing poly-L- or D-lysine was rocked gently to ensure even spreading of the well. The plate was then left to sit in room temperature for 30min followed by aspiration after which the plate was left to dry completely for 1-2h with lid off in hood. Unfortunately no

improvement in attachement was seen and again all cells fell off. Flow charts from Flexstation are not included as they are just blank.

8.10.3 Batch problem

In addition to the occasional problem with attachment we also noted a great difference in growth of the HVTs-SM1 cells, as seen in figure 8.17.

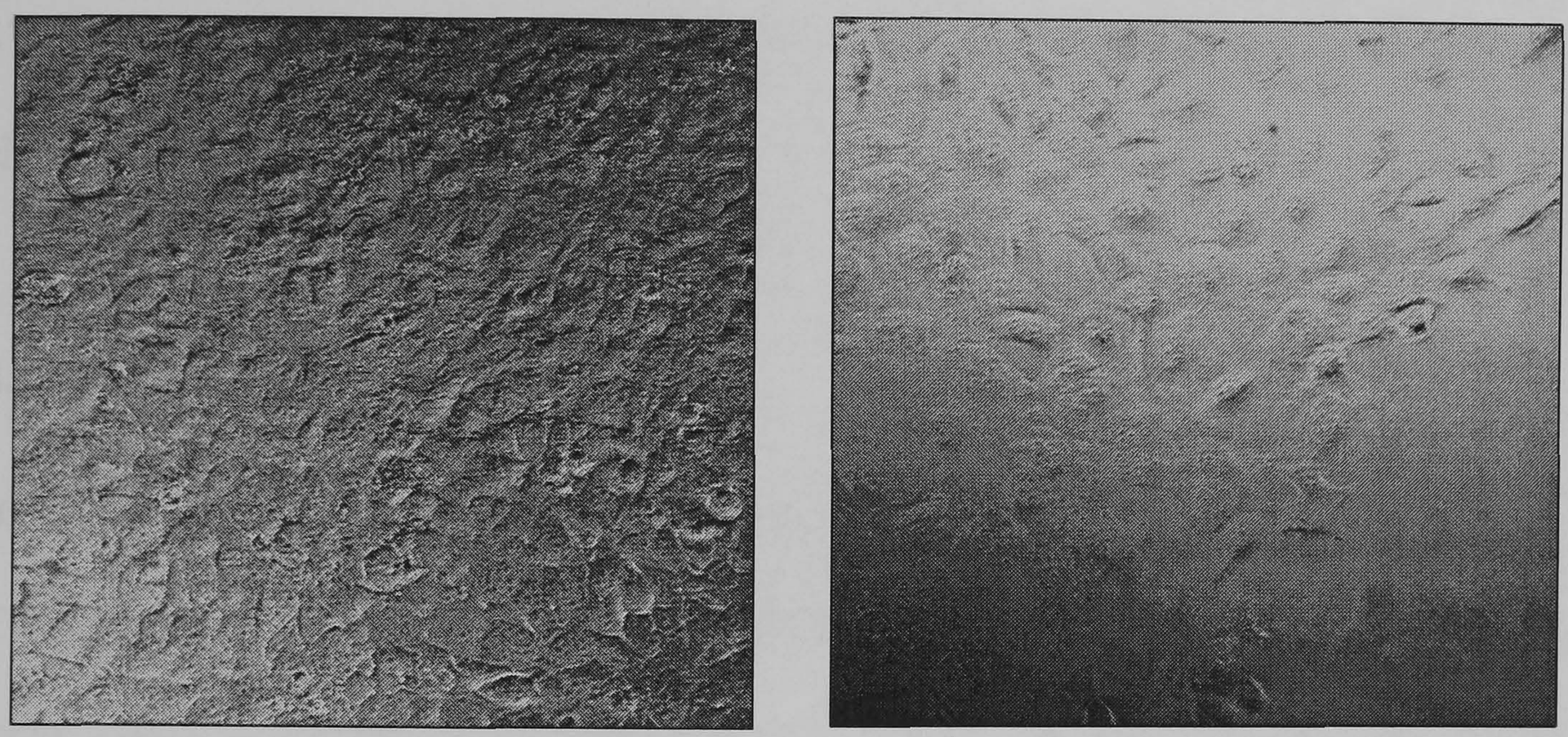


Figure 8.17. Difference in growth and detachment in between batches of HVTs-SM1 cells. Phase contrast microscopic pictures of two different batches of HVTs-SM1 cells kept at 37°C seeded at $2.5x10^5$ cells/well and washed 3 times.

In addition these cells were less responsive to agonists and the small and slower response to ionomyosin suggests the presence of dye leakage. These findings indicate a great variance between the different batches of HVTs-SM1 cells.

8.11 Measurements of changes in $[Ca^{2+}]_i$ following addition of agonists

Once having optimised conditions for the measurement of changes in intracellular calcium using Fluo-4-AM changes in fluorescence occurring inside the cells following agonist stimulation was measured using the Flexstation.

The response to four different agonists Phenylepherine, PDGF-BB, Histamine and Fibronectin was examined and compared in our HVTs-SM1 cells, kept at 37°C respectively 39°C, to investigate the effect on agonist responses following a change in phenotype.

8.11.1 Phenylepherine

In order to gain a better functional understanding of the complex formation of TG2-PLCδ_1 we wanted to examine the signal transduction pathway whereby TG2, acting as a GTPase, couples α_{1B}- and α_{1D}-adrenoreceptors (Feng, J.F., *et al.* 1998) to phospholipase Cδ_1 (PLCδ_1). We therefore utilised phenylepherine (PE), which specifically acts on α_1-adrenergic receptors.

The calcium signal in response to increasing concentrations of PE (10^{-10} -10^{-5}M) was examined in HVTs-SM1 cells at 37°C and at 39°C (figure 8.18).

Vascular α_1-adrenoceptors (ARs) mediate sympathetic regulation of smooth muscle cell (SMC) contraction for control of blood flow, pressure, and vascular wall compliance. These receptors may also regulate growth of vascular wall cells, although much less is known about this possibility.

All three α_1-ARs can couple to a variety of G-proteins and second-messenger systems and can signal through both pertussis toxin-sensitive G-proteins (Perez,

D.M., *et al.* 1993) and G-proteins of the G_q family (Wu, D., *et al.* 1992). Studies in both transiently and stably transfected cells have demonstrated that α_1-ARs activate phospholipases C and A_2 (Schwinn, D.A., *et al.* 1991; Perez, D.M., *et al.* 1993). In addition to mobilizing intracellular calcium (which would occur subsequent to activation of phospholipase C), the α_1-ARs have also been shown to activate calcium influx via voltage-dependent and -independent calcium channels (Sayet, I., *et al.* 1993; Lazou, A., *et al.* 1994; Minneman, K.P. and T.A. Esbenshade, 1994).

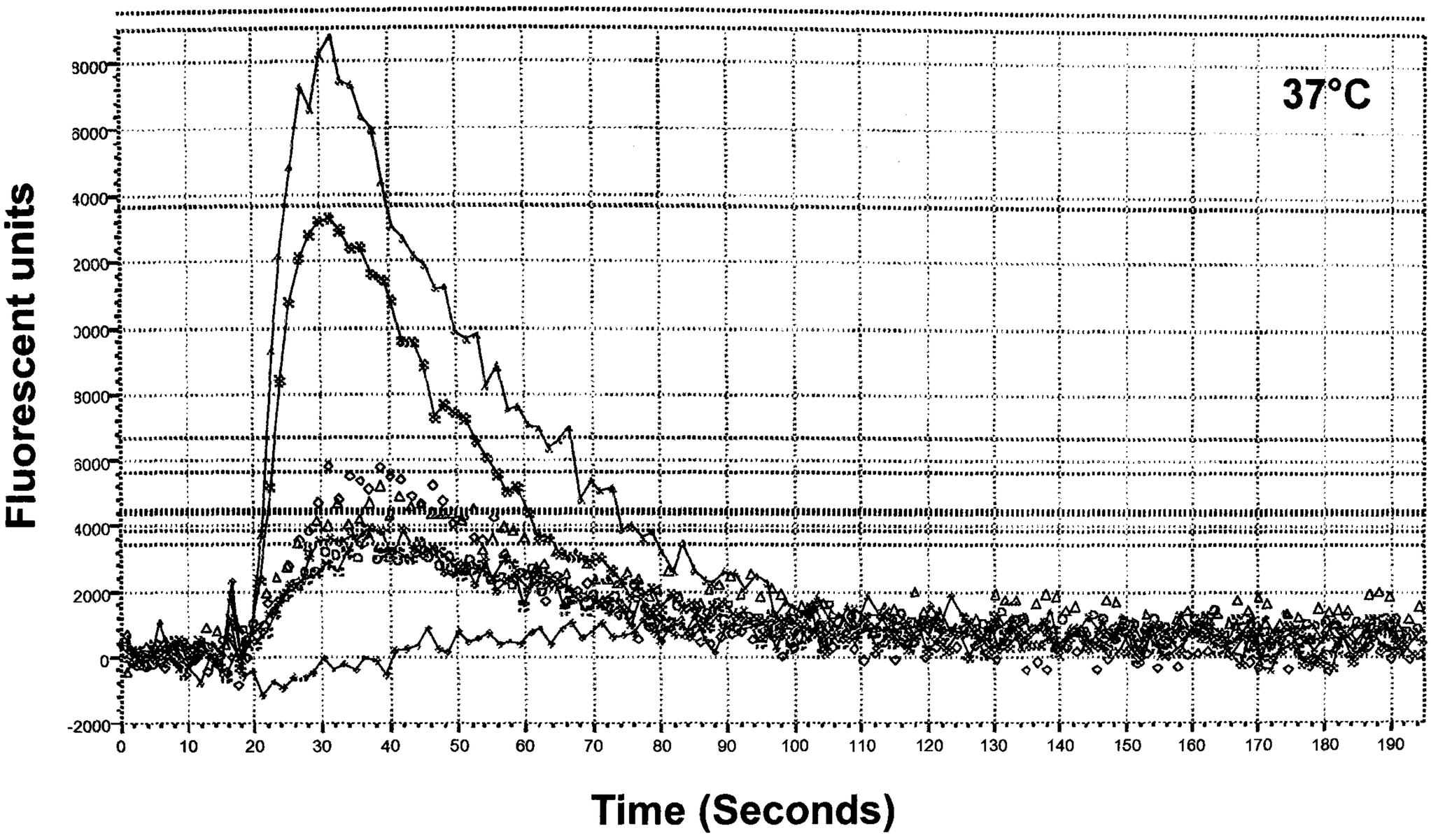
In most mammalian species, contraction of vascular smooth muscle is predominantly mediated via α_1 -adrenoceptors, although which α_1-adrenoceptor subtype(s) (α_{1A}, α_{1B}, and/or α_{1D} –AR) that is/are involved in specific vasoconstrictive responses is still unclear. Rudner *et al.* studied the subtypes of α_1-adrenergic receptors in human vascular bed and showed that apart from aorta, where α_{1D} –AR expression was dominant, α_{1A}–AR was expressed to a greater extent compared to α_{1B} - and α_{1D} - ARs (Rudner, X.L., *et al.* 1999). Functional results in rat revealed that the α_{1A}- and α_{1D} -adrenoceptor subtypes regulate the larger vessels, whereas the α_{1B} -adrenoceptors control the small resistance vessels (Leech, C.J. and J.E. Faber, 1996; Piascik, M.T., *et al.* 1997).

8.11.2 Dose-response to Phenylepherine, PE (10^{-10}-10^{-5}M)

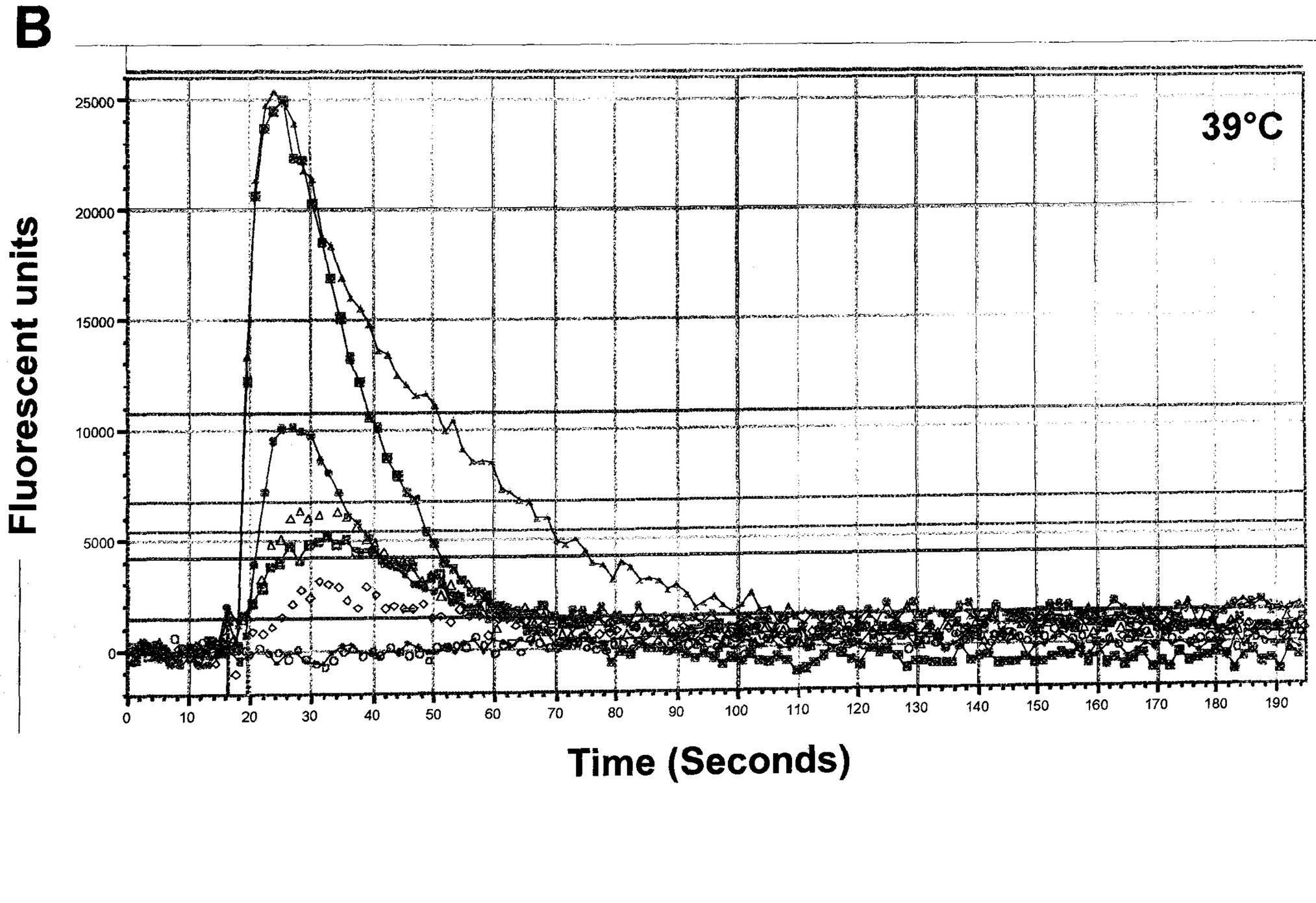
Similar responses were achieved in HVTs-SM1 cells kept at 37°C and 39°C. However, calcium signal was enhanced in HVTs-SM1 cells at 39°C at all concentrations. A significantly higher (38%) mean peak fluorescence was measured in HVTs-SM1 cells kept at 39°C (23967 ± 1814, n=3) compared to

37°C (14865 ± 1408, n=3) following exposure to PE (10^{-10}-10^{-5}M). Peak fluorescence occurred 5 seconds earlier in cells kept at 39°C compared to those in 37°C (t=20sec). Similar transient calcium responses could be seen in both conditions having dropped back to basal after about 70 seconds. Consequently when plotting dose-responses out they were both sigmoidal shape and dose-response of cells at 37°C was shifted to the right indicating the higher EC_{50} for cells at 37°C. This show that HVTs-SM1 cells cultured at 39°C are more sensitive to PE.

A


Dose-response to PE (10^{-10} to 10^{-5}M)
37°C
Fluorescent units
8000
6000
4000
2000
0
-2000
0 10 20 30 40 50 60 70 80 90 100 110 120 130 140 150 160 170 180 190
Time (Seconds)

B


39°C
Fluorescent units
25000
20000
15000
10000
5000
0
0 10 20 30 40 50 60 70 80 90 100 110 120 130 140 150 160 170 180 190
Time (Seconds)

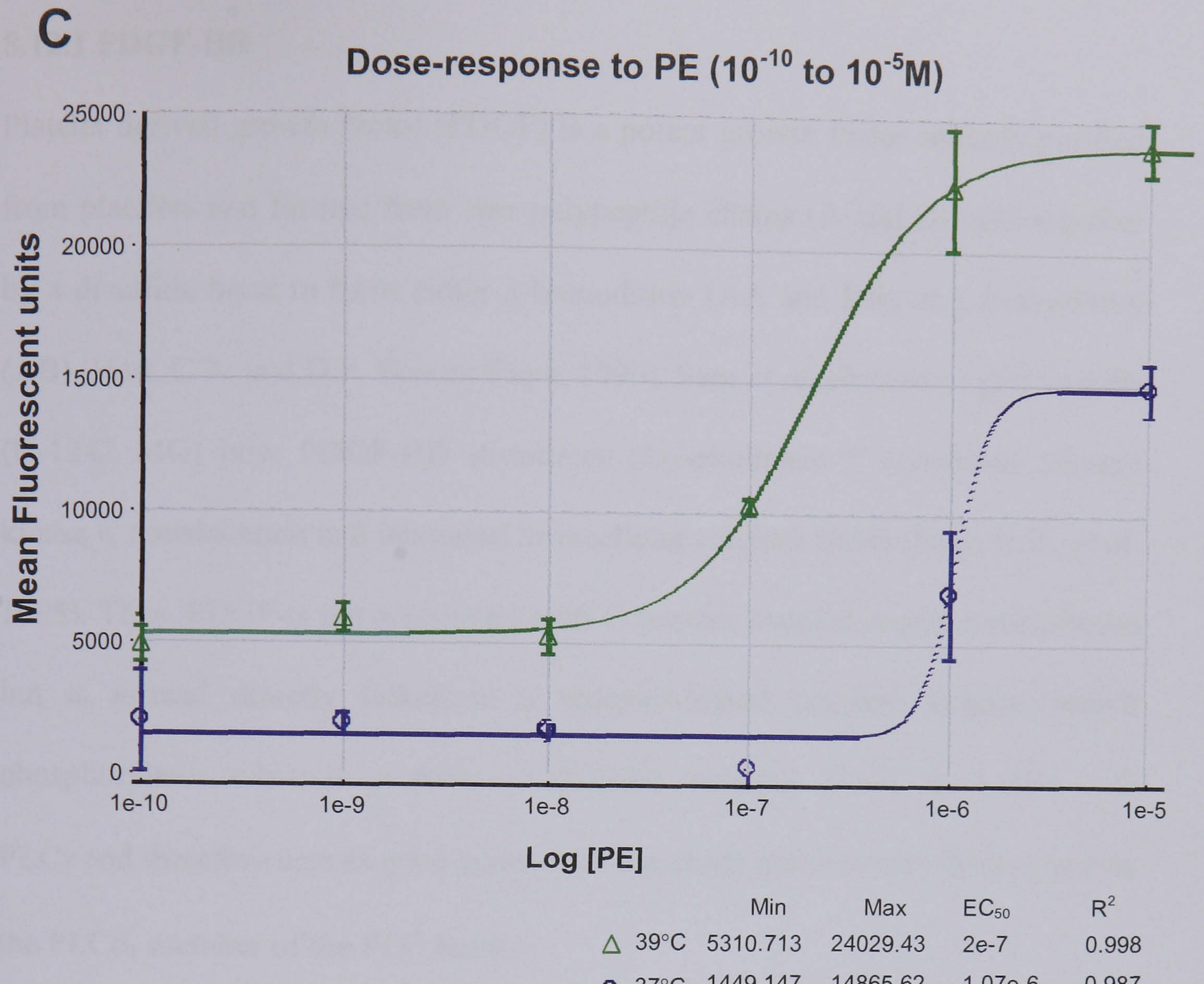


*Figure 8.18 PE-induced increases in intracellular calcium. Time course from Flex station using Fluo-4-AM loading. Changes in fluorescent units were measured over time in HVTs-SM1 cells at 37°C (**A**) compared to 39°C (**B**). Graph showing dose response curves (**C**) to PE in HVTs-SM1cells at 37°C (o) compared to 39°C (Δ). Changes in intra cellular calcium in response to PE were only transient and the level of calcium returned to baseline within 70sec after stimulation. Peak fluorescence was reach 5sec earlier in 39°C which also showed a significantly higher response to PE (23967) compared to 37°C (14865). Both conditions showed a well fitted sigmoid response curve with R^2 almost equal to 1. More differentiated state (39°C) showed a ten times lower EC_{50} (n=6).*

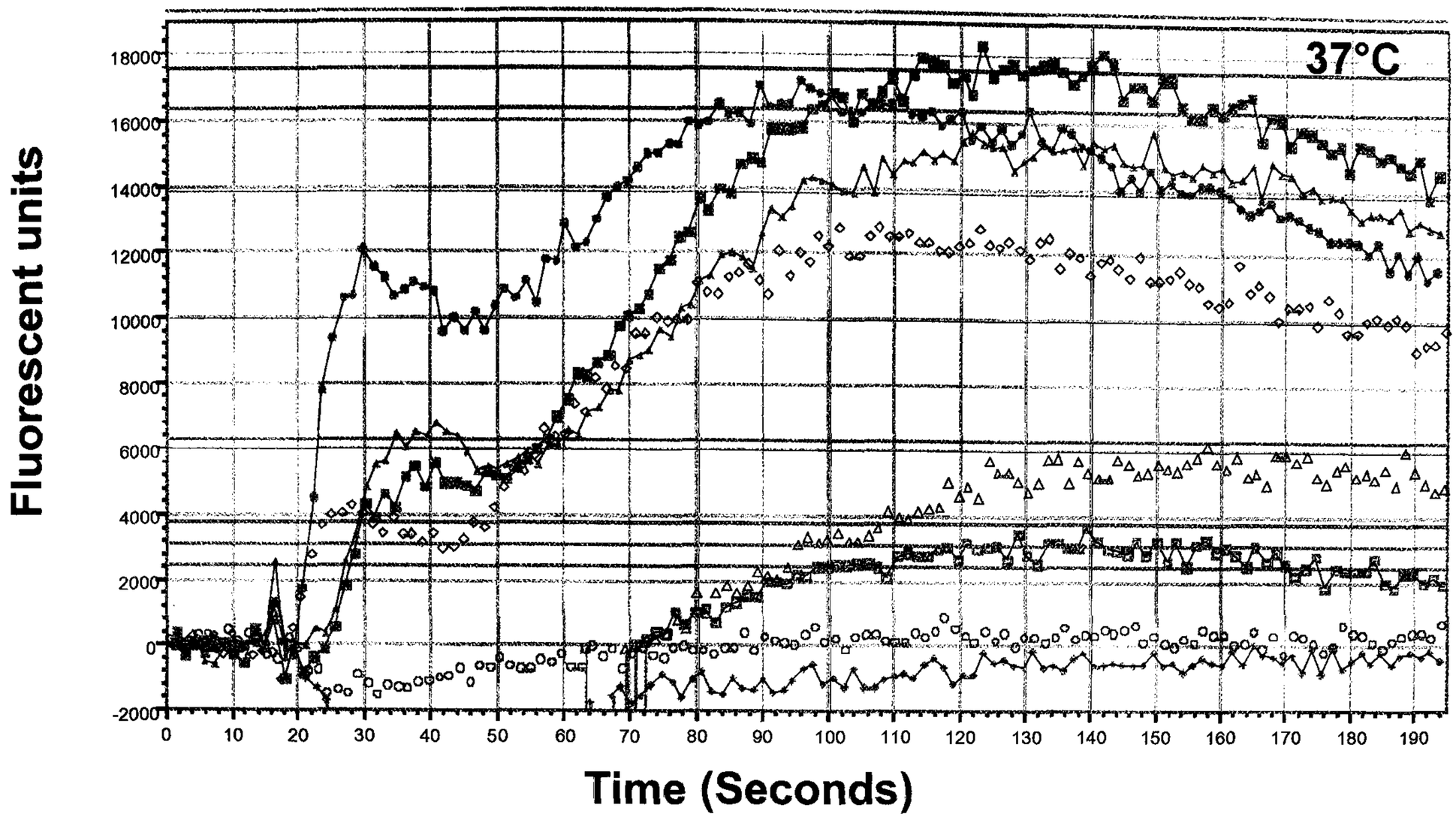
8.12.1 PDGF-BB

Platelet derived growth factor (PDGF) is a potent growth factor initially purified from platelets and formed from two polypeptide chains (A and B) held together by a disulfide bond to form either a homodimer (AA and BB) or a heterodimer (AB) (Hart, C.A. and D.F. Bowen-Pope, 1990). Saqr *et al.* showed in glioma cells (U-1242 MG) how PDGF-BB stimulates phospholipase C activation, protein kinase C translocation and increased intracellular calcium levels (Saqr, H.E., *et al.* 1995). Thus, PDGF is not associated with G-protein coupled receptor stimulation but is instead directly linked to a receptor-linked tyrosine kinsase, which phosphorylates substrate proteins on tyrosine residues. PDGF associates with PLCγ and therefore acts as good control for our study and interest which concerns the PLCδ_1 member of the PLC family.

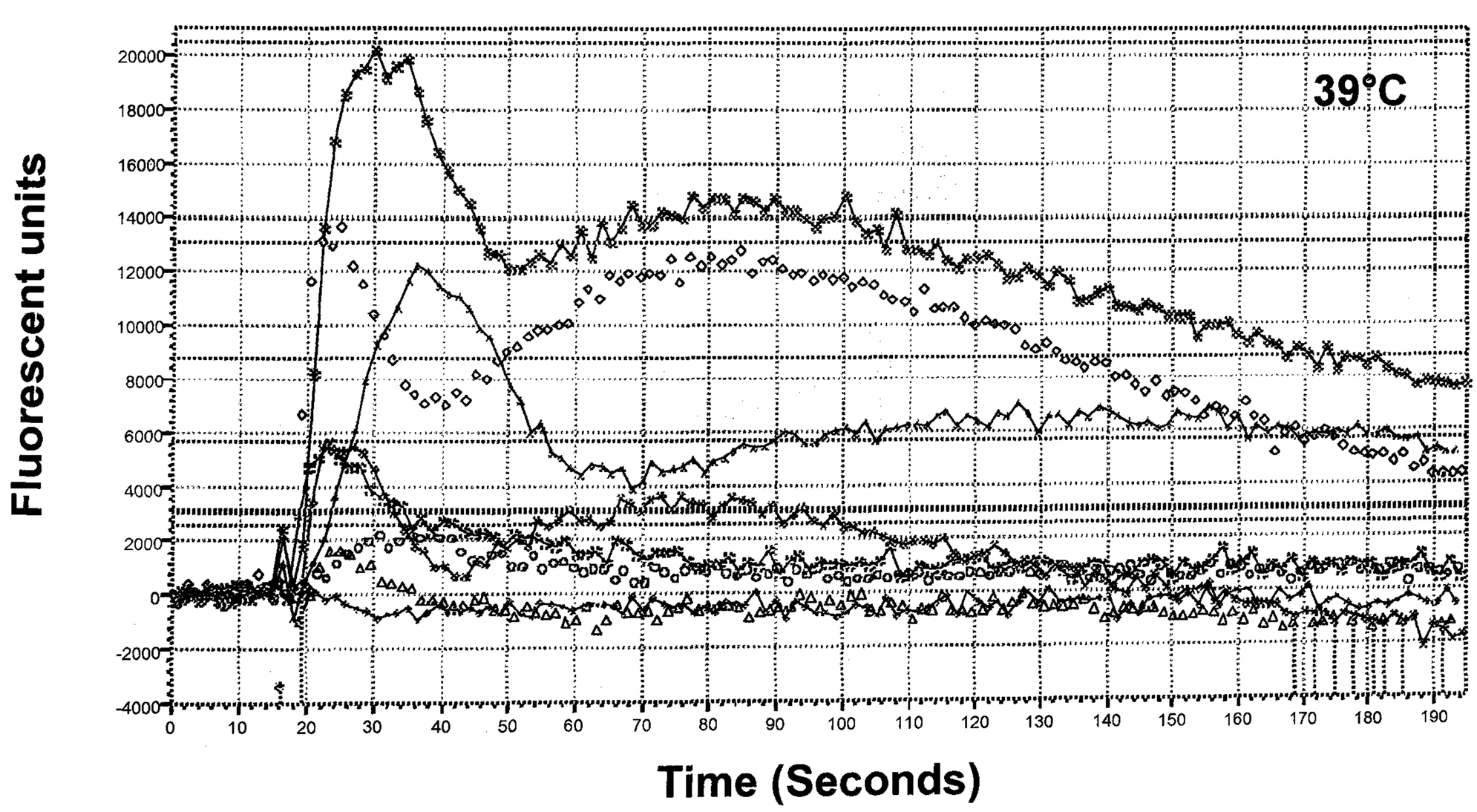
PDGF-BB isoform is most potent for stimulating intracellular Ca^{2+} mobilization. In addition, the PDGF-BB type receptor has been found to dominate in VSMCs (Diliberto, PA., *et al.* 1991) acting as a potent stimulant of both SMC proliferation and migration. (Liu, B., *et al.* 2004). Therefore, in this study we have used the PDGF-BB isoforms.

The calcium signal in response to increasing concentrations of PDGF-BB (1-50ng/ml) was examined in HVTs-SM1 cells at both 37°C and 39°C (figure 8.19).

A


Dose-response to PDGF-BB (1-50ng/ml)
37°C
Fluorescent units
Time (Seconds)
18000
16000
14000
12000
10000
8000
6000
4000
2000
0
-2000
0 10 20 30 40 50 60 70 80 90 100 110 120 130 140 150 160 170 180 190

B


39°C
Fluorescent units
Time (Seconds)
20000
18000
16000
14000
12000
10000
8000
6000
4000
2000
0
-2000
-4000
0 10 20 30 40 50 60 70 80 90 100 110 120 130 140 150 160 170 180 190

C

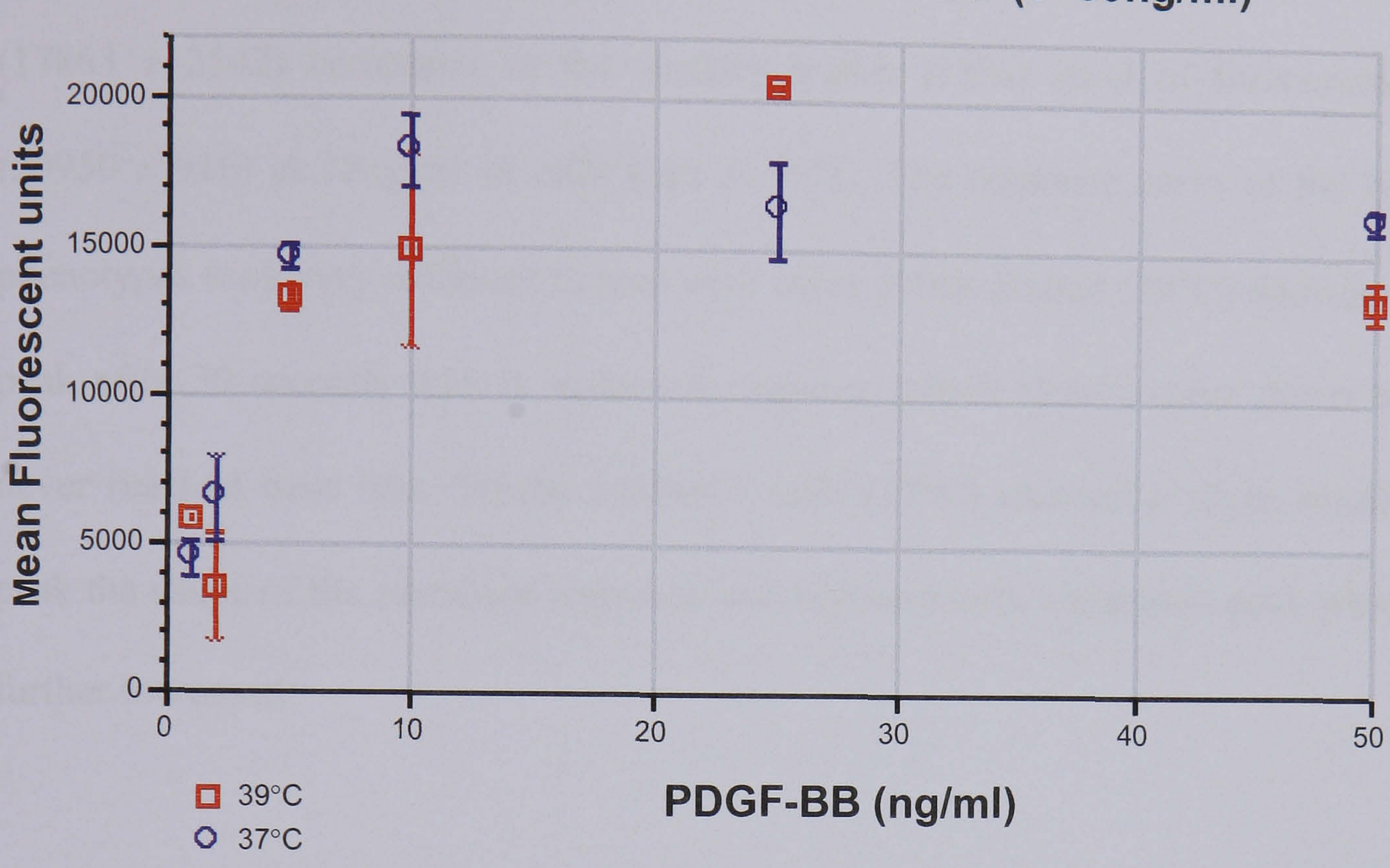


*Figure 8.19 PDGF-BB induced increase in intracellular calcium. Measurements of changes in intracellular calcium, measured by Flex station using Fluo-4-HVTs-SM1 cells, show a different response to PDGF-BB in 37°C (**A**, ○) compared to 39°C (**B**, □). Peak value in response to PDGF-BB is slightly higher at HVTs-SM1 cells at 39°C (20422) compared to 37°C (18230). However, most noticeable is the difference in shape of the dose response curves (**C**), with peak value occurring at 10sec at 37°C compared to after 25sec in HVTs-SM1 cells at 39°C (n=4).*

8.12.2 Dose-response to PDGF-BB (1-50ng/ml)

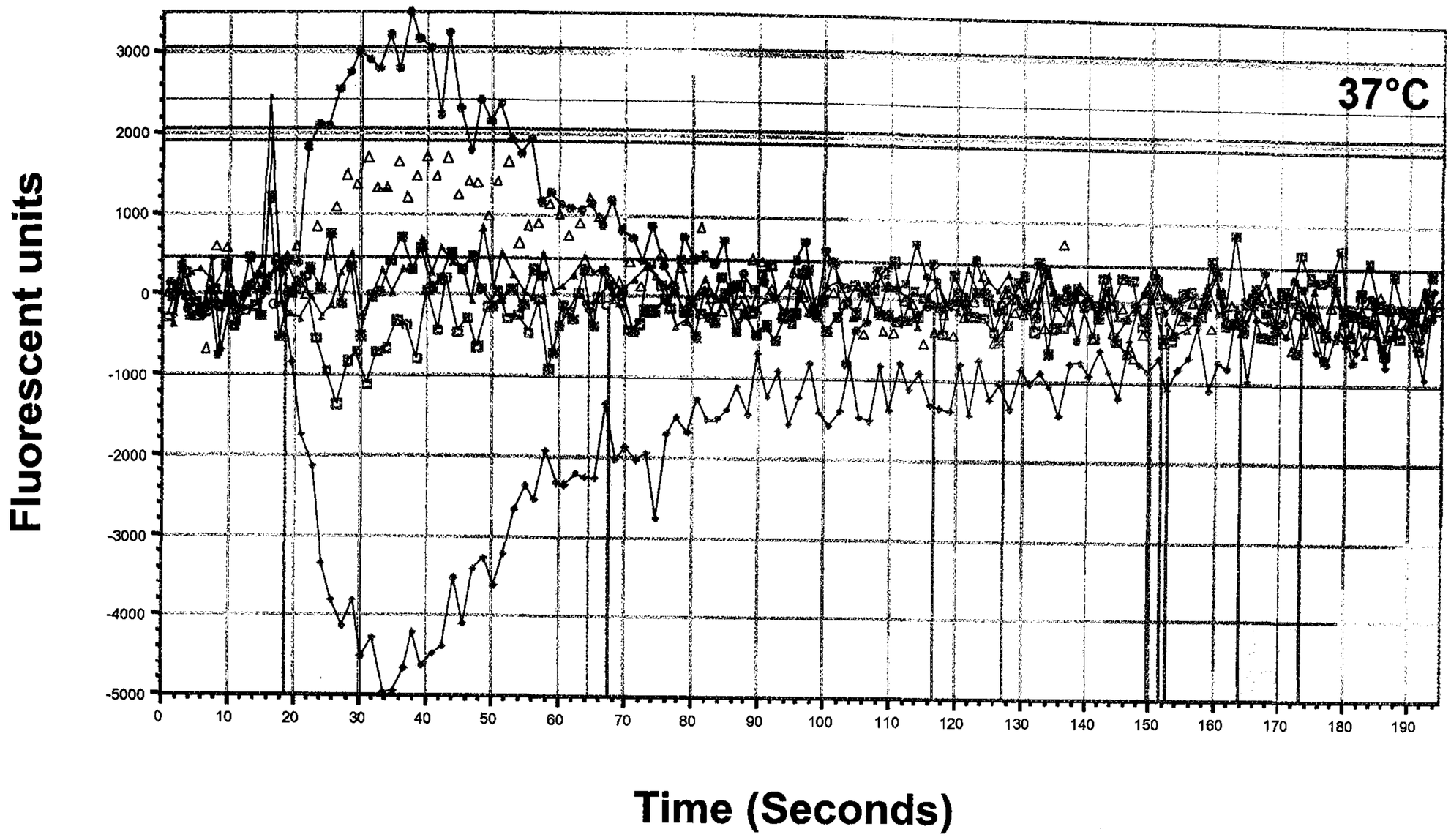
No significant change of peak fluorescence was measured following exposure to PDGF-BB. Thus, peak fluorescence in cells at 37°C was yielded at 10ng/ml (17863 ± 2542) compared to the slightly higher (15%) level of fluorescence (20950 ± 916) at 25ng/ml in cells kept at 39°C. The response curve of the two phenotypes took very different shapes with more differentiated (39°C) showing a peak after 30 seconds with a sustained response which slowly came down but never reached base line. Whilst synthetic cells (37°C) showed a slight smaller peak the shape of the sustained response was biphasic with a transient peak which further increased.

Although peak fluorescence measured of the two different conditions was not significantly different the mechanism by which fluorescence is obtained is of very different mechanisms.

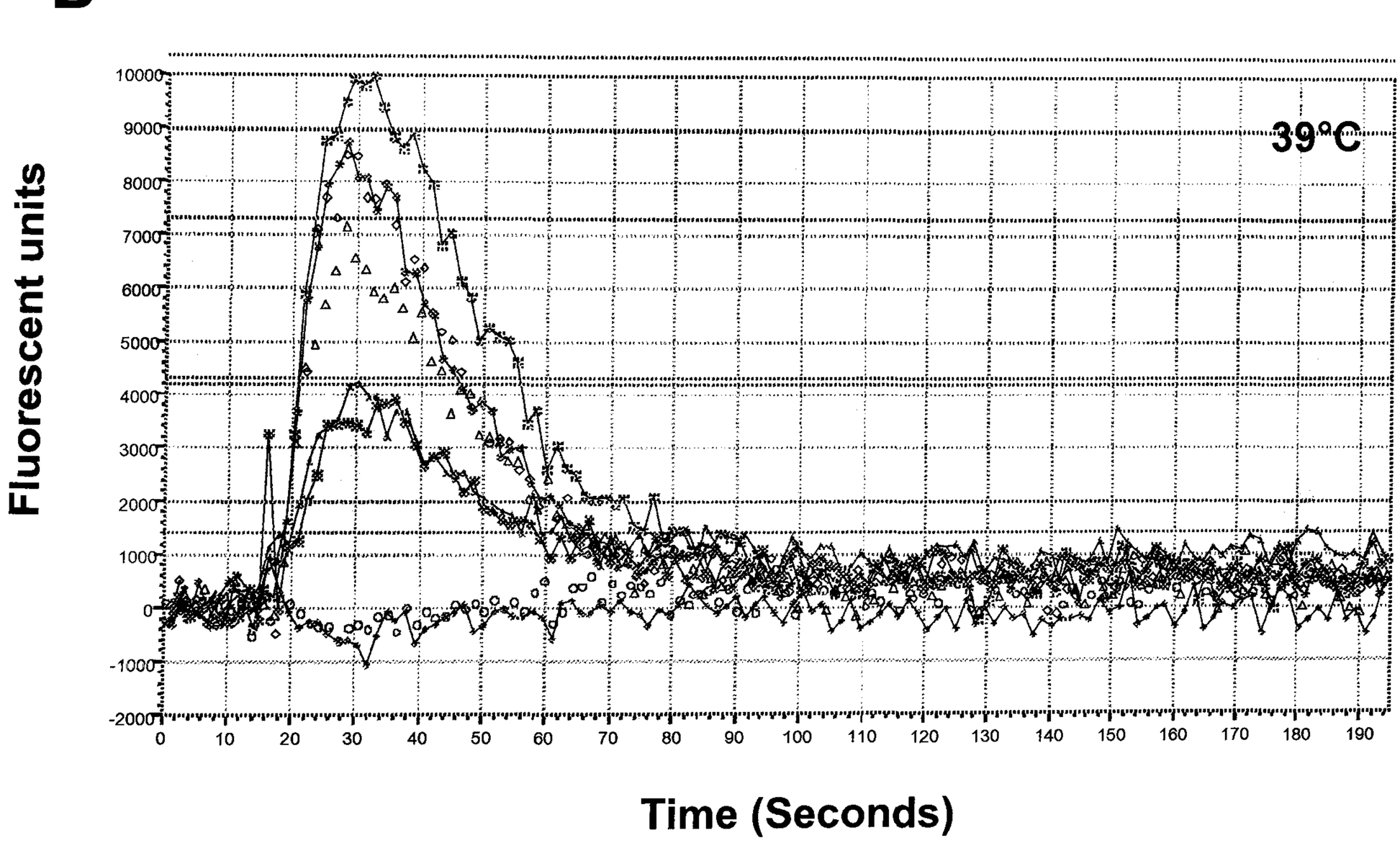
8.13.1 Histamine

Histamine acts on three specific histamine receptors, H1, H2 and H3 all of which are G-protein-coupled receptors. In human smooth muscle Histamine acts on the H1- receptor, which result in contraction of blood vessels (Jutel, M., *et al*. 2002). The primary signal from H1R is delivered through activation of phospholipase C with generation of IP_3 and DAG (1,2-diacylglycerol) and increased cytosolic Ca^{2+} (Hill, J.S., *et al*. 1991).

A **Dose response curve to Histamine (10^{-10}-10^{-5}M)**



B



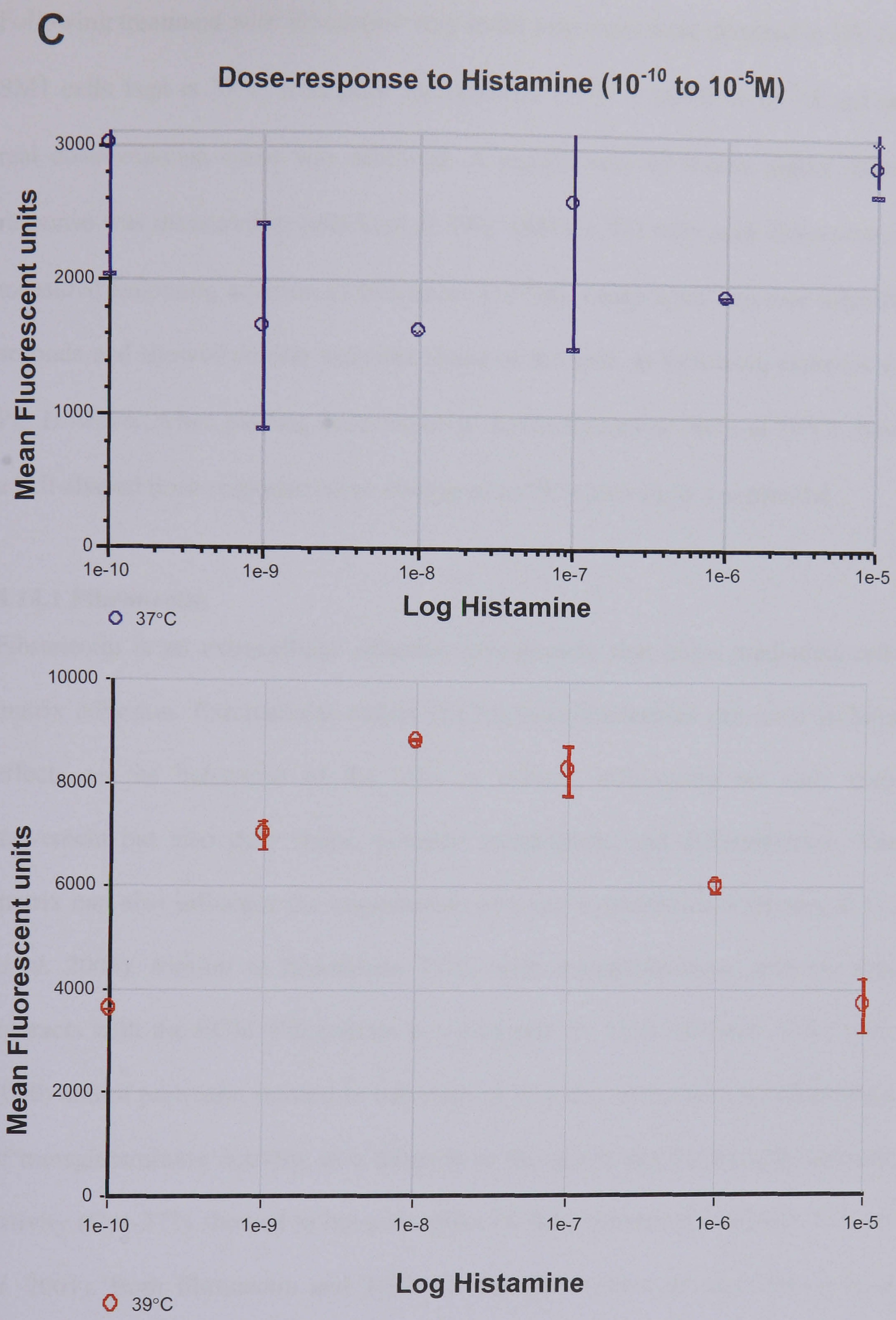


*Figure 8.20 Histamine induced increase in intracellular calcium measured by Flex station (**A** and **B**) using Fluo-4-AM. Dose response curves (**C**) to Histamine was observed in HVTs-SM1 cells at 37°C (○) compared to 39°C (○) (n=4).*

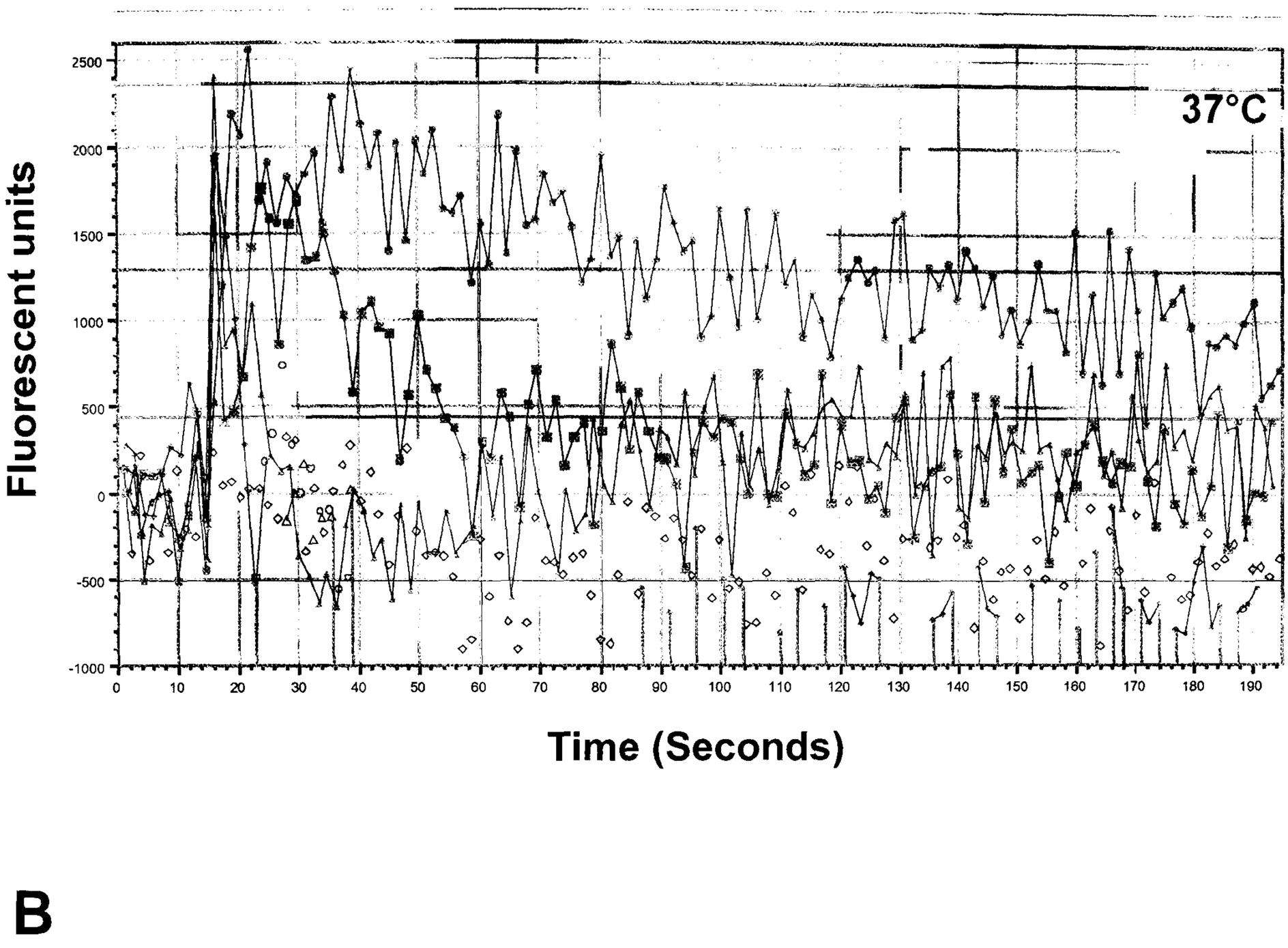
8.13.2 Dose-response to Histamine (10^{-10}-10^{-5}M)

Following treatment with Histamine very small responses were detected in HVTs-SM1 cells kept at 37°C with peak fluorescence (3592 ± 1008) at 10^{-7}M and no real dose-response curve was achieved. A significantly (p=0.009) higher (59%) response was measured in cells kept at 39°C (8819 ± 91) with peak fluorescence measured following addition of Histamine (10^{-8}M). Peaks were achieved after 20 seconds and showed similar transient shape of the peak as following exposure to PE. However, when plotting dose-response curves Histamine (cells at 39°C) show a bell-shaped dose-response curve compared to PE which show a sigmoidal.

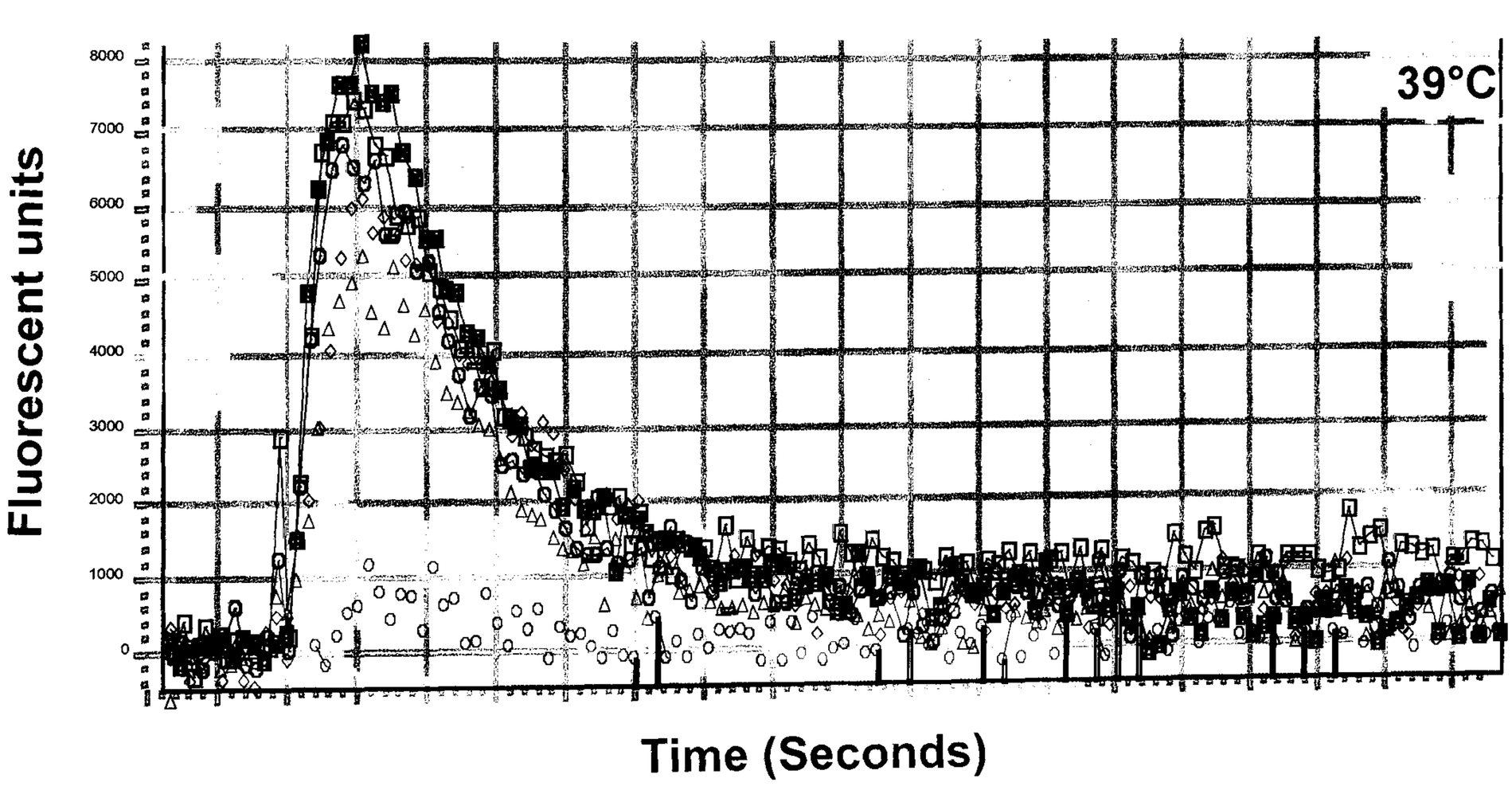
8.14.1 Fibronectin

Fibronectin is an extracellular adhesive glycoprotein that helps mediating cell-matrix adhesion. Extracellular matrix (ECM) macromolecules can have striking effects on the behaviour of the cells in culture, influencing not only their movement but also their shape, polarity, metabolism, and differentiation. The matrix can also influence the organisation of a cell's cytoskeleton (Hynes, R.O., *et al*. 2004). Similar to fibronectin TGII, with transglutaminase activity, also interacts with the ECM. Fibronectin is a substrate for TGII (Akimov, S.S., *et al*. 2000) and of particular interest to our study is how this interaction is independent of transglutaminase activity, as a deletion in the active site for transglutaminase activity (Cys-277) showed to have no effect on this interaction (Akimov, S.S., *et al*. 2001). Both fibronectin and TGII are thought to have an important role in vascular remodelling (Langville, B.L. and D. Dajnowiec, 2005; Rybarczyk, B.J., *et al*. 1999).

A


Dose response curve to Fibronectin (0.05-5mg/ml)
37°C
Fluorescent units
2500
2000
1500
1000
500
0
-500
-1000
0
10
20
30
40
50
60
70
80
90
100
110
120
130
140
150
160
170
180
190
Time (Seconds)

B


39°C
Fluorescent units
8000
7000
6000
5000
4000
3000
2000
1000
0
Time (Seconds)

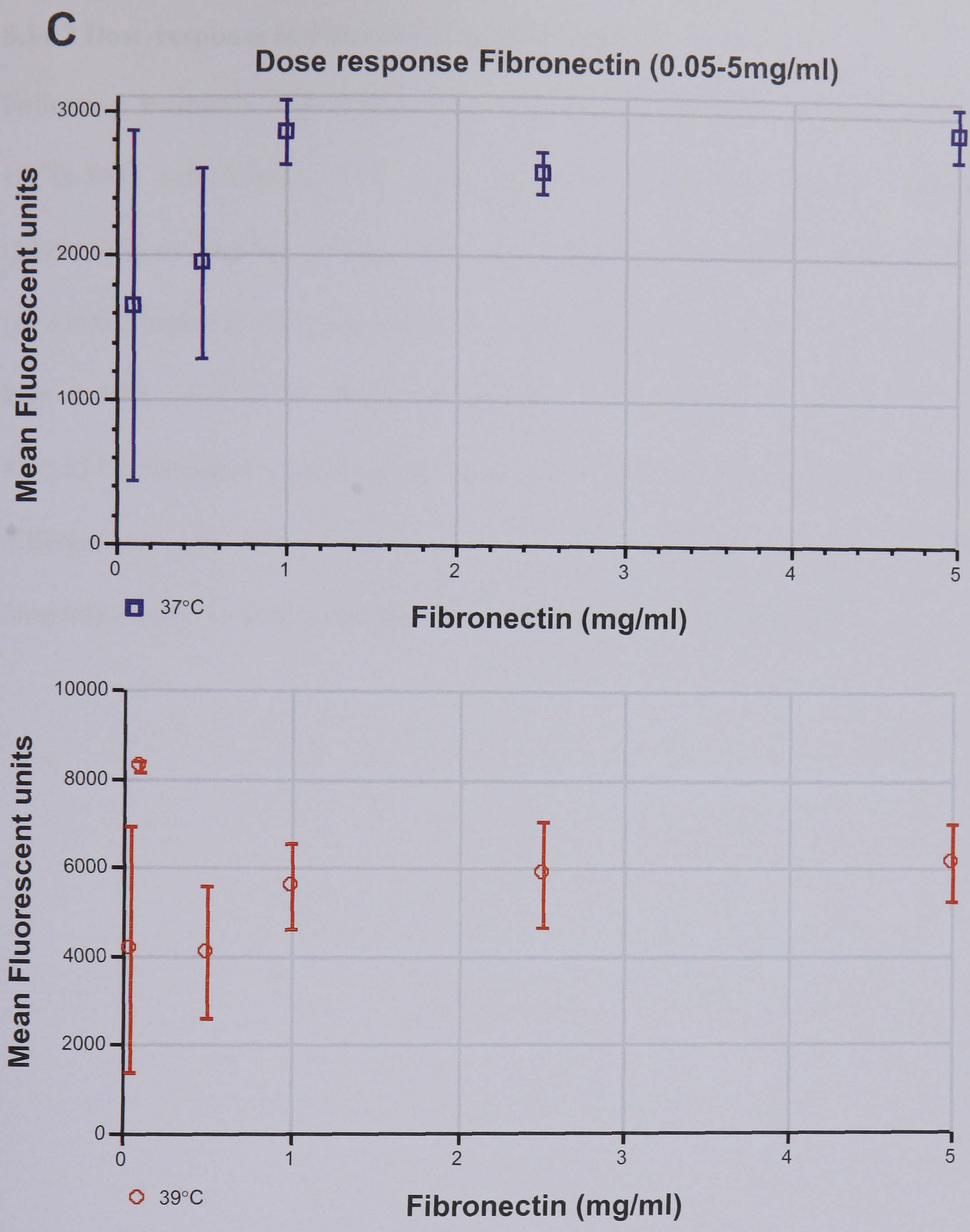


*Figure 8.21 Fibronectin induced increase in intracellular calcium measured by Flex station using Fluo-4-AM (**A** and **B**). Dose response curves (**C**) to Fibronectin was observed in HVTs-SM1 cells at 37°C (□) compared to 39°C (○), n=4.*

8.14.2 Dose-response to Fibronectin (0.05-5mg/ml)

Following treatment with Fibronectin very small responses were detected in HVTs-SM1 cells kept at 37°C with only a small transient peak fluorescent (2879±318) at highest concentration of Fibronectin (5mg/ml). A significant ($p=0.0001$) higher (53%) peak fluorescent was measured after 20 seconds in cells kept at 39°C (6137±173) following addition of Fibronectin (the highest value, 8271±173, measured at 0.05mg/ml was counted as an out layer). Although more differentiated cells (39°C) showed to be more responsive the dose curve (0.05-5mg/ml) showed in both conditions a sustained response to Fibronectin.

8.15. Summary of response to agonists

Table 8.1. Summary of Mean response to agonist (Florescence units)

Agonist	37°C	39°C	T-test	% change
PE	14865 ± 1408	23967 ± 1814	0.0048	38%
PDGF-BB	17863 ± 2542	20950 ± 916	0.059	15%
Histamine	3592 ± 1008	8819 ± 91	0.0091	59%
Fibronectin	2879 ± 318	6137 ± 153	0.0001	53%

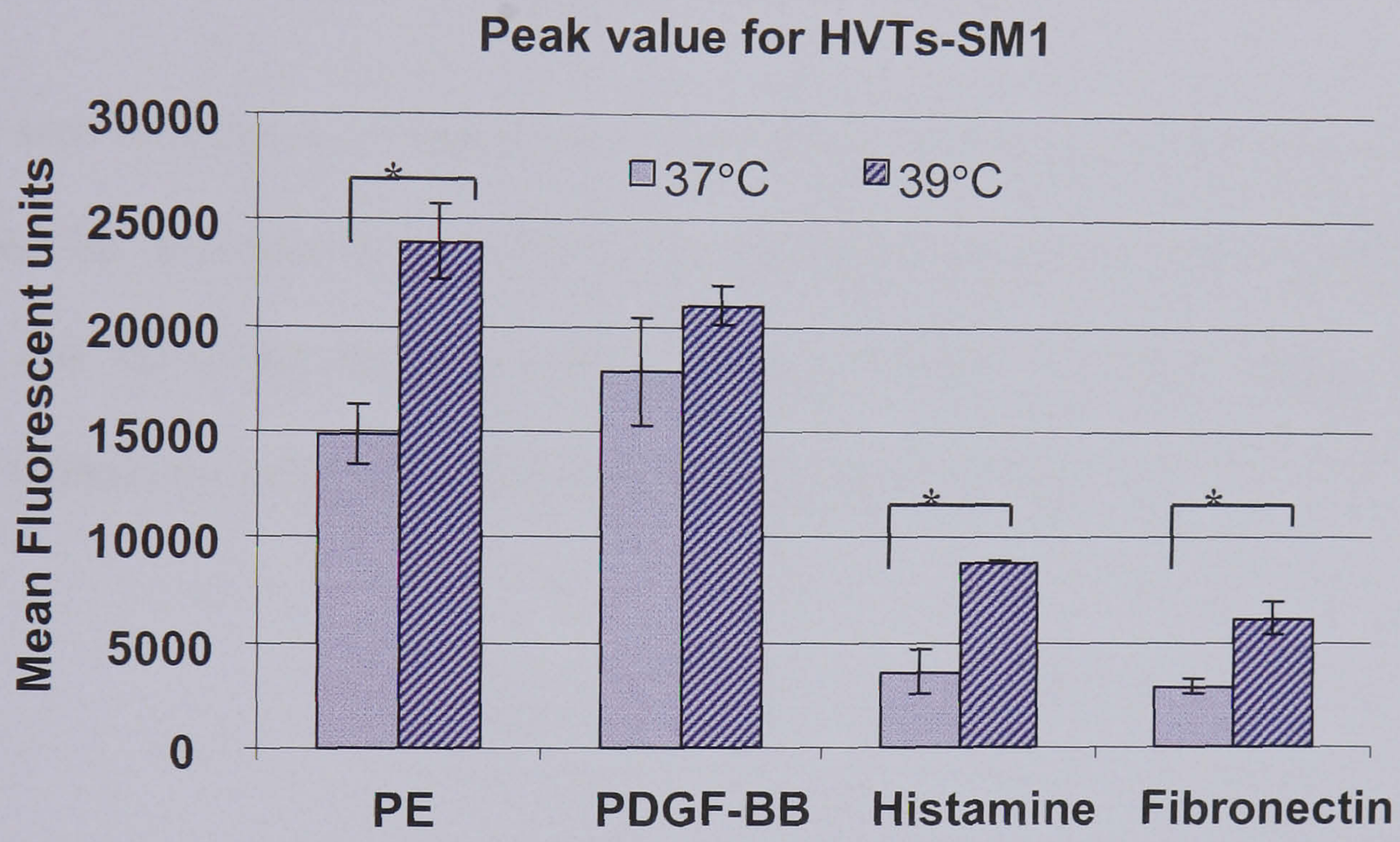


Figure 8.22 Mean peak fluorescence of HVTs-SM1 cells kept at 37℃ versus 39℃. Changes in intracellular calcium was measured in cells following exposure to PE (10^{-10}-10^{-5}M, n=6), PDGF-BB (1-50ng/ml, n=4), Histamine (10^{-10}-10^{-5}M n=4) and Fibronectin (0.05-5mg/ml, n=4). Rise in $[Ca^{2+}]_i$ was measured using Fluo-4-AM and fluorescence, emitted light from when dye binds to calcium, was monitored with Flexstation. Data shown are mean of peak fluorescence ± SEM.. A value of $p<0.05$ (*) was considered to indicate statistical significance.

8.16.1 Response to PE and PDGF-BB in presence of Genistein (50μM)

We used Genistein, a specific inhibitor for tyrosine kinases (Akiyama, T., *et al.* 1987) to evaluate the possible involvement of tyrosine kinases in mediating the action of PE- and PDGF-BB-induced changes in intracellular free calcium concentration, $[Ca^{2+}]_i$ in HVTs-SM1 cells. $[Ca^{2+}]_i$ was measured using Flexstation and Fluo-4-AM.

As seen in figure 8.23 treatment of Genistein (30min, 50μM) had no significant effect on responses (1352±102 versus Genistein treated 14020±480, $p>0.05$) to PE (10^{-5}M) whilst responses to PDGF-BB (25ng/ml) was significantly reduced ($p=0.0061$) by 38% (9320±720 versus treated 5810±1780).

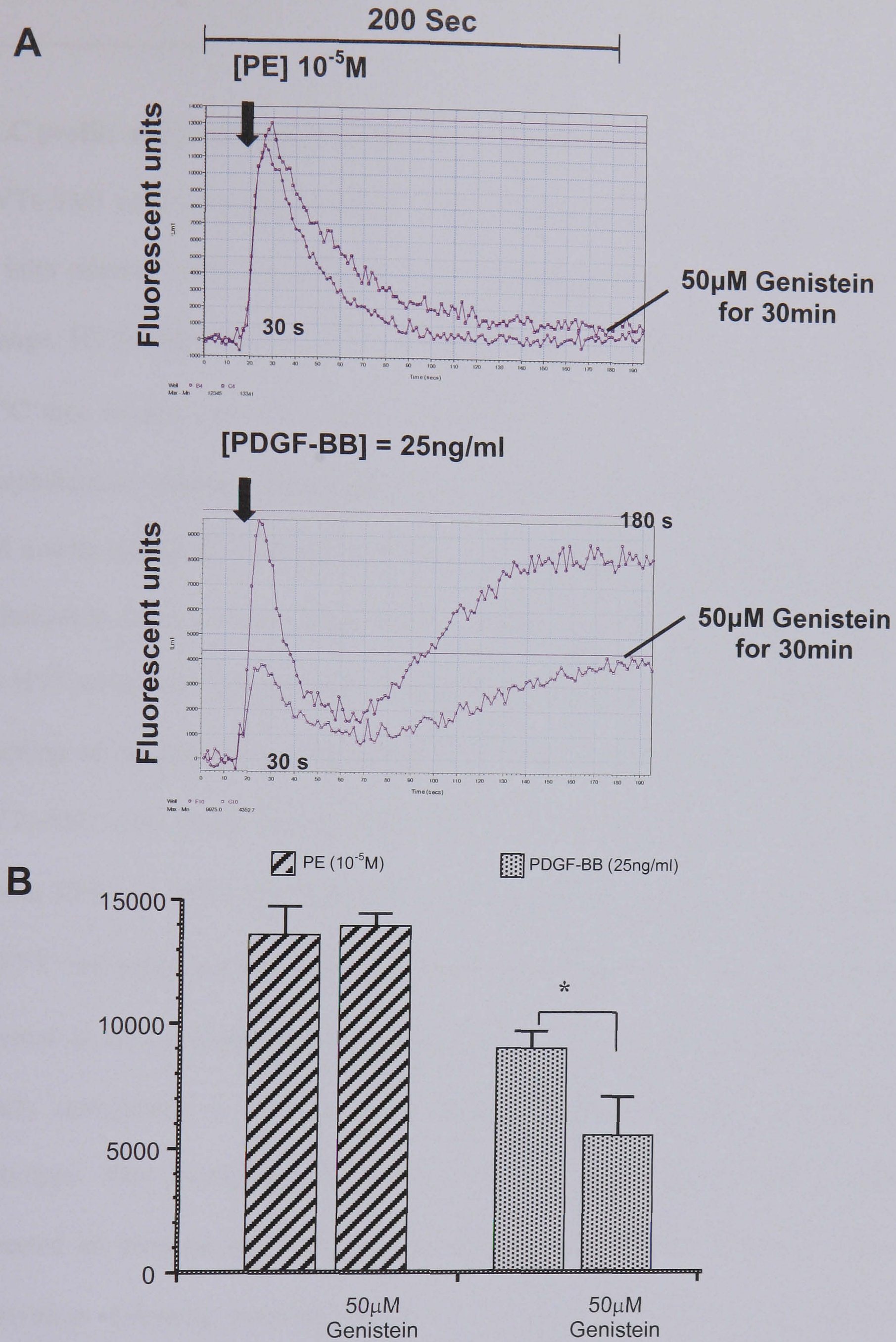


Figure 8.23 Effect of Genistein on responses to PE and PDFG-BB. ***A.*** *Fluorescent measurements using Flexstation and Fluo-4-AM showed that Genistein treatment (30min, 50µm) had no effect on responses to PE whilst Genistein significantly (p=0.0061) reduced responses to PDGF-BB by 38% (****B****).*

DISCUSSION CALCIUM MEASURMENTS

PLC profile and TGII expression in HVTs-SM1 cells

HVTs-SM1 cells were used in this study to facilitate comparisons of measurements of intra cellular levels of calcium, following agonist activation, during phenotypic change. HVTs-SM1 cells kept at 37°C are randomly cycling whilst when kept at 39°C they switch and take a more differentiated state, which is clearly seen by morphological changes. The profile of PLC isoforms expression and presence of SM α-actin and TGII in HVTs-SM1 cells was investigated using Western blotting technique to attain a clearer understanding of which PLC isoform(s) are present in the HVTs-SM1 cell line and may be potential candidate(s) for contributing to the coupling of receptor by agonist stimulation. In terms of PLC isoforms present in HVTs-SM1 cells $PLC\beta_1$, $PLC\beta_2$ and $PLC\beta_4$ were not detected in cells cultures at neither 37°C nor 39°C. $PLC\beta_3$ however was undoubtedly detected in cells cultured at 37°C but could not be detected in cells cultured at 39°C. $PLC\delta_1$ was clearly detected at cells cultured at both temperatures. Moreover $PLC\delta_1$ expression was clearly upregulated in cells at 39°C, which represent the more differentiated phenotype. This correlates well with our previous data of the HVSMCs which indicated an increase in $PLC\delta_1$ expression following redifferentiation by serum deprivation. Likewise previous studies in our group of saphenous vein-derived human VSMC, from which the HVTs-SM1 cells are derived, demonstrated that the PLC isoforms β_1, β_2, β_3, β_4, γ_1, γ_2, δ_1 and δ_2 were all detected in samples of rat brain but only $PLC\gamma_1$ and $PLC\delta_1$ were detected in saphenous vein-derived VSMC lysates.

This suggests that signalling HVTs-SM1 cells may occur through PLCδ_1. TGII was present in cells cultured at both 37°C and 39°C. Likewise SM α-actin was detected at both temperatures but unexpectedly to a less degree in HVTs-SM1 cells kept at 39°C.

Fluo-4-AM loading

Intracellular calcium was measured by a combination of Flexstation, which allows fluorescent measurements, and a dye that fluoresces upon binding to calcium. Our HVTs-SM1 cells were loaded with the indicator dye Fluo-4-AM in Ca^{2+}-buffer (10% FSC) in presence of both Probenecid and Pluronic acid. The addition of Albumin to the loading buffer showed slightly more advantageous loading. One of the additional benefits of using Fluo-4 as a dye, apart from yielding a higher fluorescence measurements compared to Fura-2, was that we could perform live calcium imaging. This technique allowed us to properly confirm dye loading in our cells and that no leakage occurred nor compartmentalisation during the time required for measurements. Compartmentalisation of Fluo-4-AM was not detected until one hour after measurements. With measurements never exceeding 15min we were assured that the possibility of compartmentalisation of Fluo-4 never had to be taken into account. Three loaded cells showed similar response to PE (10μM), indicating similar loading of our cells.

Change in intracellular calcium in cells at 37°C respectively 39°C

Very small responses to Histamine and Fibronectin were measured at 37°C whilst both evoke a response in cells kept at 39°C. Similarly, Li *et al.* showed an

elevation of cytoplasmic calcium upon activation of redifferentiated cells with Histamine (1μM), which was induced by serum deprivation (Li, S., *et al.* 1999). Dose responses to Histamine at 39°C showed a bell shaped curve similar to both conditions following treatment to PDGF-BB whilst PE was sigmoidal. As expected more differentiated cells (at 39°C) were more responsive to PE, α_1-AR agonist, showing a higher response and lower EC50 to PE. No significant difference was measured between peak fluorescence following addition of PDGF-BB thus the shape of the responses was very different with cells at 39°C showed a transient peak that slowly dropped off whilst cells at 39°C showed a bell shaped response with a peak followed by an additional rise resulting in a sustained response. Similar to our data other reports demonstrate that the PDGF-induced increase in $[Ca^{2+}]_i$ has two phases: one that is transient and a second that is sustained, presumably a consequence of Ca^{2+} entry from the extracellular space (Nishimura, J., *et al.*1982; Mogami, H., *et al.* 1993). Presence of Genistein significantly reduced responses to PDGF-BB as expected as it signals through Tyrosine kinases whilst no significant effect was measured on PE responses. Nishimura *et al* demonstrated similar results to ours thus completely blocked the first but not the second calcium elevation in primary rat aortic smooth muscle cells (Nishimura, J., et al. 1993). Interestingly, in addition to a significantly higher response to PE a clear rise in PLCδ_1 was detected in more differentiated HVT-SM1 cells suggesting its implication in receptor coupling.

Unfortunately we had problems with detachment of cells. As measurements using Flexstation require a confluency of 90-100% of the well further measurements could not be performed. Thus, before this problem occurred we

did manage to get some basic dose responses of PE, PDGF-BB, Histamine and Fibronectin. Several attempts were performed to improve attachment of cells by lysine coating of plates, optimised height of pipettor and addition speed of agonists, thus without success. Variations in batches of the HVTs-SM1 cells could explain the issues behind the sporadic dilemma with detachment of cells, slower growth and smaller or absence of response to agonists measured.

The literature suggests that receptors use multiple signalling pathways through which they can initiate signal in their target cells. The reason behind is still unclear and may be down to differences among cell types and species. Subtypes of receptors might exist in different tissue and thereby mediate different signals for different functions/due to different conditions. Two distinct oxytocin subtypes have been suggested in rat myometrium and deciduas (Chan, W.Y., *et al.* 1993) and kidney (Rpin-Bott, M.P, *et al.* 1997). Additionally, different G-proteins and PLC isoenzymes might be mediators of different activation pathways. For example Vezza *et al.* showed how both isoforms of Thrombin isoforms signal via Gq, but only the α-isoform signals via TGII to active PLCδ_1 (Vezza, R., *et al.* 1999). Pathological or other environmental conditions may also play a factor. Vincan *et al.* reported that in isolation and culture of neonatal cardiomyocytes resulted in a decreased expression of TGII without reducing content of Gq or Gi, thus TGII was without doubt detected in extracts from intact heart tissue from newborns and adults (Vincan, E., *et al.* 1995). Much work is still needed to get an understanding in the preference, choices and reason behind the different receptor isoforms and signal transduction pathways with its resulting effect.

FINAL SUMMARY & FUTURE WORK

With the aim to investigate the association between tissue transglutaminase II, TGII and PLCδ_1 in vascular smooth muscle and the effect of differentiation status on this association the data clearly show how both TGII and PLCδ_1 are affected by a phenotypic change. Redifferentiation, induced by seven days serum deprivation, significantly increased the expression of PLCδ_1 whilst TGII was significantly reduced. Our data indicated that this reduction of TGII occurs around day 4, which corresponds in timing with when growth arrest is achieved in these cells following serum withdrawal. This contrasts with the time course for up regulation of PLCδ_1 expression which takes longer and seems to correspond better with the appearance of markers of re-differentiation, actin and calponin. Serum withdrawal also resulted in a cellular re-localisation of both PLCδ_1 and TGII with a greater level of co-localisation of PLCδ_1 and TGII in serum-deprived cells. Serum withdrawal not only led to a decrease in TGII protein expression and colocalization with PLCδ_1 but also resulted in a relative reduction in secreted TGII.

Previous data from this laboratory has shown that RhoA acts as an inhibitory modulator for PLCδ_1 activity and suggested that the activity of this isoform may be dual regulated by GTP-binding proteins in vascular smooth muscle (Hodson, E., *et al*, 1998). The physical association between PLCδ_1 and TGII in redifferentiated HVSMC shown here coupled with literature data from other cell types (Das, T., *et al.* 1993; Feng, J.F-., *et al.* 1996) suggests that TGII may be acting as the positive modulator of PLCδ_1 activity although this needs to be further addressed.

Functional studies of PLCδ_1 and TGII and their association with the cytoskeleton revealed that disruption of actin filaments, by cytochalasin D treatment, resulted in a decrease in the expression of both proteins and was coupled with an alteration in their cellular localisation. This data correlates well with previous data from this laboratory which indicates that PLCδ_1 expression is associated with contractile ability in cultured vessels (Harrington, L.S., *et al.* 2002). Further examination of the association between PLCδ_1 and TGII with the cytoskeleton is however required. One of the key questions which still needs to be addressed is the possibility of a co-localisation between TGII and cytoskeletal proteins which has previously been suggested in both human aortic VSMCs and HUVECs (Chowdhury, Z.A., *et al.* 1997) and whether this is affected by differentiation status. The effect of the cytoskeletal regular protein RhoA would also be of particular interest to study. RhoA negatively regulates PLCδ_1 activity (Hodson, E., *et al.* 1998) and TGII, with transglutaminase activity, has been reported to be essential for expression of RhoA and some of its downstream signalling pathways. Investigating PLCδ_1 and TGII expression, activity, subcellular localisation in cells in which RhoA is knocked down by siRNA and/or transfection with dominant negative RhoA as well as in cells which express constitutively active RhoA would give a further insight into this question. It may turn out that RhoA plays a role in the regulation of the association of PLCδ_1 and TGII, acting perhaps as the 'finger on the switch'.

While recent data has given us a better insight there is still a great deal of work to be looked at to clarify the regulation and function of PLCδ_1. At present we know that RhoA and TGII are important players in the regulatory process and in addition that PLCδ_1 is not regulated by tyrosine-phosphorylation like PLCγ or by

heterotrimeric G-proteins like PLCβ. By performing overexpression as well as dominant-negative studies of both PLCδ_1 and TGII, followed by measurements of protein expression and activity of PLCδ_1 and TGII we would hopefully gain a better insight of their association and PLCδ_1 regulation. Also, looking at the effect on actin cytoskeleton following changes in PLCδ_1 and TGII expression would further complement our findings of a reduced PLCδ_1 and TGII expression and altered cellular localisation following actin disruption and could help define functional role of PLCδ_1.

While we have been unable to demonstrate the presence of any PLCβ isoforms in either our HVSMCs or the fresh saphenous vein from which they are derived [Harrington, L.S., PhD-thesis, 2003) there is still some considerable debate regarding the presence of these isoforms in vascular smooth muscle (Blayney, L.M., *et al.* 1996; Kato, H., *et al.* 1992; LaBelle, E.F and F., Polyak, 1996). Clarification of this issue would be particularly useful as PLCβ has been suggested to have a role as a potential regulator of PLCδ_1 (Guy, Y., *et al.* 2004). In respect to this question this laboratory is currently conducting RT-PCR to examine the presence of PLCβ isoform specific mRNA in randomly cycling and redifferentiated VSMCs.

While it has not proved possible to utilise column chromatography techniques to investigate the association between PLCδ_1 and TGII further use of the FlexStation to measure intracellular calcium levels in response to agonist stimulation could contribute significantly towards the knowledge regarding this association. Understanding why TGII and PLCδ_1 couple just to certain isoenzymes of receptors such as α_{1C}- and α_{1D}- but not α_{1A} – Adreno receptor and the α-

isoenzyme but not the β-Thromboxane A2 receptor could reveal more about its functional implications and attaining a better understanding if this is due to differential expression in tissue, variances in cellular localisation of receptor isoenzymes or the actual physiological need of multiple signal pathways. While it is documented that although TGII couple several isoenzyme of receptors to $PLC\delta_1$ it is not the major link and its contribution to agonist stimulation is relatively minor (Zhang, J., *et al.* 1999) we need to be careful regarding our interpretation of this data with respect to human vascular smooth muscle in health and disease. If we take oxytocin signalling as an example this agonist has been linked to PLCβ in a number of animal studies (Strakova, Z., et al, 1997; Mhaouty-Kodja, S., et al, 2001) and in human myometrial cells in culture (Phaneuf, S., et al, 1996; Dodge, K.L. & B.M., Sanborn, 1998. However the only study to investigate oxytocin signalling in fresh human myometrium clearly identified TGII and $PLC\delta_1$ as the effectors (Park, E-S., et al, 1997).

Literature suggests the implication of both proteins in several pathological conditions such as wound healing, repair and Alzheimer's disease. It may be of interest therefore to compare the association between $PLC\delta_1$ and TGII in normal conditions with that in pathological condition such as studies performed in Spontaneous Hypertensive rat (SHR), an animal model of hypertension or their implication in repair and wound healing by applying an *in vitro* scratch wound model. Using an in vitro wound healing model such as scratch wound would enable to gain more insight of the function and interaction of $PLC\delta_1$ and TGII using several interesting investigations such as measurements of intracellular calcium and by incorporation of fluorescent labelled putrescence would allow measurements of the contribution of transglutaminase versus GTP binding

activity of TGII. Investigating changes in the complex formation as well as PLCδ_1 and TGII expression during this pathological condition and in presence/absence of C3 (inhibitor of RhoA), cystamine (transglutaminase inhibitor), changes in [GTP] and $[Ca^{2+}]_i$ and U73122, PLC inhibitor would add to the knowledge for a better understanding or their function and regulation. A useful tool in terms of discerning the functional association between PLCδ_1 and TGII would be the use of TGII knock out mice (Nanda, N. *et al.* 2001) respectively PLCδ_1-deficient mice (Nakamura, Y., *et al*, 2001). It would be interesting to utilise this model to determine how the expression levels and cellular localisation of PLCδ_1 and TGII are affected.

Despite compelling evidence that phenotypic modulation of the SMC plays a key role in vascular injury repair and in the development and/or progression of diseases as hypertension and atherosclerosis, to date, little is known regarding the cellular and molecular processes that govern differentiation of VSMC and how these might be deregulated in vascular diseases. With a better understanding in the field of vascular biology will help to understand vascular disease and this is the driving force toward understanding SM biology. Insights gained from these studies, with new future innovation such as SMC progenitors as targets for novel therapeutic approaches against proliferative vascular diseases, may someday help us to design molecular strategies aimed at regenerating healthy VSMC in diseased vessels.

Abe, M., Takahashi, K., and Hiwada, K. Effect of calponin on actin-activated myosin ATPase activity. J Biochem (Tokyo), 108: 835-838, 1990.

Abouzaglou, J., Benistant, C., Gimona, M., Roustan, C., Kassab, R., and Fattoum, A. Tyrosine phosphorylation of calponins. Inhibition of the interaction with F-actin. Eur J Biochem, 271: 2615-2623, 2004.

Absher, M., Woodcock-Mitchell, J., Mitchell, J., Baldor, L., Low, R., and Warshaw, D. Characterization of vascular smooth muscle cell phenotype in long-term culture. In Vitro Cell Dev Biol, 25: 183-192, 1989.

Absher, M., Woodcock-Mitchell, J., Mitchell, J., Baldor, L., Low, R., and Warshaw, D. Characterization of vascular smooth muscle cell phenotype in long-term culture. In Vitro Cell Dev Biol, 25: 183-192, 1989.

Aeschlimann, D., Wetterwald, A., Fleisch, H., and Paulsson, M. Expression of tissue transglutaminase in skeletal tissues correlates with events of terminal differentiation of chondrocytes. J Cell Biol, 120: 1461-1470, 1993.

Aeschlimann, D., Koeller, M. K., len-Hoffmann, B. L., and Mosher, D. F. Isolation of a cDNA encoding a novel member of the transglutaminase gene family from human keratinocytes. Detection and identification of transglutaminase gene products based on reverse transcription-polymerase chain reaction with degenerate primers. J Biol Chem, 273: 3452-3460, 1998.

Aeschlimann, D. and Thomazy, V. Protein crosslinking in assembly and remodelling of extracellular matrices: the role of transglutaminases. Connect Tissue Res, 41: 1-27, 2000.

Ahmadian, M. R., Wittinghofer, A., and Schmidt, G. The actin filament architecture: tightly regulated by the cells, manipulated by pathogens. International Titisee Conference on the actin cytoskeleton: from signalling to bacterial pathogenesis. EMBO Rep, 3: 214-218, 2002.

Akimov, S. S., Krylov, D., Fleischman, L. F., and Belkin, A. M. Tissue transglutaminase is an integrin-binding adhesion coreceptor for fibronectin. J Cell Biol, 148: 825-838, 2000.

Akiyama, T., Ishida, J., Nakagawa, S., Ogawara, H., Watanabe, S., Itoh, N., Shibuya, M., and Fukami, Y. Genistein, a specific inhibitor of tyrosine-specific protein kinases. J Biol Chem, 262: 5592-5595, 1987.

Allen, V., Swigart, P., Cheung, R., Cockcroft, S., and Katan, M. Regulation of inositol lipid-specific phospholipase cdelta by changes in Ca2+ ion concentrations. Biochem J, 327 (Pt 2): 545-552, 1997.

Amendola, A., Gougeon, M. L., Poccia, F., Bondurand, A., Fesus, L., and Piacentini, M. Induction of "tissue" transglutaminase in HIV pathogenesis: evidence for high rate of apoptosis of CD4+ T lymphocytes and accessory cells in lymphoid tissues. Proc Natl Acad Sci U S A, 93: 11057-11062, 1996.

Amendola, A., Fesus, L., Piacentini, M., and Szondy, Z. "Tissue" transglutaminase in AIDS. J Immunol Methods, 265: 145-159, 2002.

Ananthanarayanan, B., Das, S., Rhee, S. G., Murray, D., and Cho, W. Membrane targeting of C2 domains of phospholipase C-delta isoforms. J Biol Chem, 277: 3568-3575, 2002.

Andringa, G., Lam, K. Y., Chegary, M., Wang, X., Chase, T. N., and Bennett, M. C. Tissue transglutaminase catalyzes the formation of alpha-synuclein crosslinks in Parkinson's disease. FASEB J, 18: 932-934, 2004.

Antonyak, M. A., Singh, U. S., Lee, D. A., Boehm, J. E., Combs, C., Zgola, M. M., Page, R. L., and Cerione, R. A. Effects of tissue transglutaminase on retinoic acid-induced cellular differentiation and protection against apoptosis. J Biol Chem, 276: 33582-33587, 2001.

Antonyak, M. A., Boehm, J. E., and Cerione, R. A. Phosphoinositide 3-kinase activity is required for retinoic acid-induced expression and activation of the tissue transglutaminase. J Biol Chem, 277: 14712-14716, 2002.

Axel, D. I., Frigge, A., Dittmann, J., Runge, H., Spyridopoulos, I., Riessen, R., Viebahn, R., and Karsch, K. R. All-trans retinoic acid regulates proliferation, migration, differentiation, and extracellular matrix turnover of human arterial smooth muscle cells. Cardiovasc Res, 49: 851-862, 2001.

Baek, K. J., Kwon, N. S., Lee, H. S., Kim, M. S., Muralidhar, P., and Im, M. J. Oxytocin receptor couples to the 80 kDa Gh alpha family protein in human myometrium. Biochem J, 315 (Pt 3): 739-744, 1996.

Baek, K. J., Kang, S., Damron, D., and Im, M. Phospholipase Cdelta1 is a guanine nucleotide exchanging factor for transglutaminase II (Galpha h) and promotes alpha 1B-adrenoreceptor-mediated GTP binding and intracellular calcium release. J Biol Chem, 276: 5591-5597, 2001.

Bailey, C. D. and Johnson, G. V. Developmental regulation of tissue transglutaminase in the mouse forebrain. J Neurochem, 91 : 1369-1379, 2004.

Bakker, E. N., Buus, C. L., Spaan, J. A., Perree, J., Ganga, A., Rolf, T. M., Sorop, O., Bramsen, L. H., Mulvany, M. J., and Vanbavel, E. Small artery remodeling depends on tissue-type transglutaminase. Circ Res, 96: 119-126, 2005.

Balklava, Z., Verderio, E., Collighan, R., Gross, S., Adams, J., and Griffin, M. Analysis of tissue transglutaminase function in the migration of Swiss 3T3 fibroblasts: the active-state conformation of the enzyme does not affect cell motility but is important for its secretion. J Biol Chem, 277: 16567-16575, 2002.

Banno, Y., Nakashima, T., Kumada, T., Ebisawa, K., Nonomura, Y., and Nozawa, Y. Effects of gelsolin on human platelet cytosolic phosphoinositide-phospholipase C isozymes. J Biol Chem, 267: 6488-6494, 1992.

Bernassola, F., Boumis, G., Corazzari, M., Bertini, G., Citro, G., Knight, R. A., Amiconi, G., and Melino, G. Osmotic resistance of high-density erythrocytes in

transglutaminase 2-deficient mice. Biochem Biophys Res Commun, 291: 1123-1127, 2002.

Berridge, M. J. Inositol trisphosphate and diacylglycerol: two interacting second messengers. Annu Rev Biochem, 56: 159-193, 1987.

Berridge, M. J., Bootman, M. D., and Roderick, H. L. Calcium signalling: dynamics, homeostasis and remodelling. Nat Rev Mol Cell Biol, 4: 517-529, 2003.

Blanchette-Mackie, E. J., Dwyer, N. K., Barber, T., Coxey, R. A., Takeda, T., Rondinone, C. M., Theodorakis, J. L., Greenberg, A. S., and Londos, C. Perilipin is located on the surface layer of intracellular lipid droplets in adipocytes. J Lipid Res, 36: 1211-1226, 1995.

Bolton, T. B., Gordienko, D. V., Pucovsky, V., Parsons, S., and Povstyan, O. Calcium release events in excitation-contraction coupling in smooth muscle. Novartis Found Symp, 246: 154-168, 2002.

Bou-Gharios, G., Ponticos, M., Rajkumar, V., and Abraham, D. Extra-cellular matrix in vascular networks. Cell Prolif, 37: 207-220, 2004.

Campbell, G. R. and Chamley, J. H. Thick filaments in vertebrate smooth muscle. Cell Tissue Res, 156: 201-216, 1975.

Caprini, M., Gomis, A., Cabedo, H., Planells-Cases, R., Belmonte, C., Viana, F., and Ferrer-Montiel, A. GAP43 stimulates inositol trisphosphate-mediated calcium release in response to hypotonicity. EMBO J, 22: 3004-3014, 2003.

Carmichael, J. D., Winder, S. J., Walsh, M. P., and Kargacin, G. J. Calponin and smooth muscle regulation. Can J Physiol Pharmacol, 72: 1415-1419, 1994.

Chadwick, C. C., Saito, A., and Fleischer, S. Isolation and characterization of the inositol trisphosphate receptor from smooth muscle. Proc Natl Acad Sci U S A, 87: 2132-2136, 1990.

Chamley-Campbell, J., Campbell, G. R., and Ross, R. The smooth muscle cell in culture. Physiol Rev, 59: 1-61, 1979.

Chamley-Campbell, J. H. and Campbell, G. R. What controls smooth muscle phenotype? Atherosclerosis, 40: 347-357, 1981.

Chan, P., Munro, E., Patel, M., Betteridge, L., Schachter, M., Sever, P., and Wolfe, J. Cellular biology of human intimal hyperplastic stenosis. Eur J Vasc Surg, 7: 129-135, 1993.

Chan, W. Y., Chen, D. L., and Manning, M. Oxytocin receptor subtypes in the pregnant rat myometrium and decidua: pharmacological differentiations. Endocrinology, 132: 1381-1386, 1993.

Chang, L. and Goldman, R. D. Intermediate filaments mediate cytoskeletal crosstalk. Nat Rev Mol Cell Biol, 5: 601-613, 2004.

Chen, S., Lin, F., Iismaa, S., Lee, K. N., Birckbichler, P. J., and Graham, R. M. Alpha1-adrenergic receptor signaling via Gh is subtype specific and independent of its transglutaminase activity. J Biol Chem, 271: 32385-32391, 1996.

Chiocca, E. A., Davies, P. J., and Stein, J. P. The molecular basis of retinoic acid action. Transcriptional regulation of tissue transglutaminase gene expression in macrophages. J Biol Chem, 263: 11584-11589, 1988.

Chong, L. D., Traynor-Kaplan, A., Bokoch, G. M., and Schwartz, M. A. The small GTP-binding protein Rho regulates a phosphatidylinositol 4- phosphate 5-kinase in mammalian cells. Cell, 79: 507-513, 1994.

Chowdhury, Z. A., Barsigian, C., Chalupowicz, G. D., Bach, T. L., Garcia-Manero, G., and Martinez, J. Colocalization of tissue transglutaminase and stress fibers in human vascular smooth muscle cells and human umbilical vein endothelial cells. Exp Cell Res, 231: 38-49, 1997.

Chrzanowska-Wodnicka, M. and Burridge, K. Rho-stimulated contractility drives the formation of stress fibers and focal adhesions. J Cell Biol, 133: 1403-1415, 1996.

Citron, B. A., SantaCruz, K. S., Davies, P. J., and Festoff, B. W. Intron-exon swapping of transglutaminase mRNA and neuronal Tau aggregation in Alzheimer's disease. J Biol Chem, 276: 3295-3301, 2001.

Clapham, D. E. Calcium signaling. Cell, 80: 259-268, 1995.

Cockcroft, S. and Thomas, G. M. Inositol-lipid-specific phospholipase C isoenzymes and their differential regulation by receptors. Biochem J, 288 (Pt 1): 1-14, 1992.

Collin, P., Kaukinen, K., Vogelsang, H., Korponay-Szabo, I., Sommer, R., Schreier, E., Volta, U., Granito, A., Veronesi, L., Mascart, F., Ocmant, A., Ivarsson, A., Lagerqvist,

C., Burgin-Wolff, A., Hadziselimovic, F., Furlano, R. I., Sidler, M. A., Mulder, C. J., Goerres, M. S., Mearin, M. L., Ninaber, M. K., Gudmand-Hoyer, E., Fabiani, E., Catassi, C., Tidlund, H., Alainentalo, L., and Maki, M. Antiendomysial and antihuman recombinant tissue transglutaminase antibodies in the diagnosis of coeliac disease: a biopsy-proven European multicentre study. Eur J Gastroenterol Hepatol, 17: 85-91, 2005.

D'Argenio, G., Sorrentini, I., Ciacci, C., Spagnuolo, S., Ventriglia, R., de, C. A., and Mazzacca, G. Human serum transglutaminase and coeliac disease: correlation between serum and mucosal activity in an experimental model of rat small bowel enteropathy. Gut, 30: 950-954, 1989.

Das, T., Baek, K. J., Gray, C., and Im, M. J. Evidence that the Gh protein is a signal mediator from alpha 1-adrenoceptor to a phospholipase C. II. Purification and characterization of a Gh-coupled 69-kDa phospholipase C and reconstitution of alpha 1-adrenoceptor, Gh family, and phospholipase C. J Biol Chem, 268: 27398-27405, 1993.

De, L., V and Melino, G. Gene disruption of tissue transglutaminase. Mol Cell Biol, 21: 148-155, 2001.

Desai, A. and Mitchison, T. J. Microtubule polymerization dynamics. Annu Rev Cell Dev Biol, 13: 83-117, 1997.

Desmouliere, A., Rubbia-Brandt, L., Abdiu, A., Walz, T., ieira-Coelho, A., and Gabbiani, G. Alpha-smooth muscle actin is expressed in a subpopulation of cultured

and cloned fibroblasts and is modulated by gamma-interferon. Exp Cell Res, 201: 64-73, 1992.

DiDonato, D. and Brasaemle, D. L. Fixation methods for the study of lipid droplets by immunofluorescence microscopy. J Histochem Cytochem, 51: 773-780, 2003.

Diliberto, P. A., Gordon, G., and Herman, B. Regional and mechanistic differences in platelet-derived growth factor-isoform-induced alterations in cytosolic free calcium in porcine vascular smooth muscle cells. J Biol Chem, 266: 12612-12617, 1991.

Doevendans, P. A. and van Eys, G. Smooth muscle cells on the move: the battle for actin. Cardiovasc Res, 54: 499-502, 2002.

Drayer, A. L., Van der, K. J., Mayr, G. W., and Van Haastert, P. J. Role of phospholipase C in Dictyostelium: formation of inositol 1,4,5-trisphosphate and normal development in cells lacking phospholipase C activity. EMBO J, 13: 1601-1609, 1994.

Drobak, B. K., Watkins, P. A., Bunney, T. D., Dove, S. K., Shaw, P. J., White, I. R., and Millner, P. A. Association of multiple GTP-binding proteins with the plant cytoskeleton and nuclear matrix. Biochem Biophys Res Commun, 210: 7-13, 1995.

Dupuis, M., Levy, A., and Mhaouty-Kodja, S. Functional coupling of rat myometrial alpha 1-adrenergic receptors to Gh alpha/tissue transglutaminase 2 during pregnancy. J Biol Chem, 279: 19257-19263, 2004.

Esposito, C. and Caputo, I. Mammalian transglutaminases. FEBS J, 272: 615-631, 2005.

Essen, L. O., Perisic, O., Cheung, R., Katan, M., and Williams, R. L. Crystal structure of a mammalian phosphoinositide-specific phospholipase C delta. Nature, 380: 595-602, 1996.

Fatigati, V. and Murphy, R. A. Actin and tropomyosin variants in smooth muscles. Dependence on tissue type. J Biol Chem, 259 : 14383-14388, 1984.

Fattoum, A., Roustan, C., Smyczynski, C., Der, T. E., and Kassab, R. Mapping the microtubule binding regions of calponin. Biochemistry, 42: 1274-1282, 2003.

Faxon, D. P., Creager, M. A., Smith, S. C., Jr., Pasternak, R. C., Olin, J. W., Bettmann, M. A., Criqui, M. H., Milani, R. V., Loscalzo, J., Kaufman, J. A., Jones, D. W., and Pearce, W. H. Atherosclerotic Vascular Disease Conference: Executive summary: Atherosclerotic Vascular Disease Conference proceeding for healthcare professionals from a special writing group of the American Heart Association. Circulation, 109: 2595-2604, 2004.

Feng, J. F., Rhee, S. G., and Im, M. J. Evidence that phospholipase delta1 is the effector in the Gh (transglutaminase II)-mediated signaling. J Biol Chem, 271: 16451-16454, 1996.

Feng, J. F., Gray, C. D., and Im, M. J. Alpha 1B-adrenoceptor interacts with multiple sites of transglutaminase II: characteristics of the interaction in binding and activation. Biochemistry, 38: 2224-2232, 1999.

Ferguson, K. M., Lemmon, M. A., Schlessinger, J., and Sigler, P. B. Structure of the high affinity complex of inositol trisphosphate with a phospholipase C pleckstrin homology domain. Cell, 83: 1037-1046, 1995.

Festoff, B. W., SantaCruz, K., Arnold, P. M., Sebastian, C. T., Davies, P. J., and Citron, B. A. Injury-induced "switch" from GTP-regulated to novel GTP-independent isoform of tissue transglutaminase in the rat spinal cord. J Neurochem, 81: 708-718, 2002.

Fesus, L. and Piacentini, M. Transglutaminase 2: an enigmatic enzyme with diverse functions. Trends Biochem Sci, 27: 534-539, 2002.

Flavahan, N. A., Bailey, S. R., Flavahan, W. A., Mitra, S., and Flavahan, S. IMAGING REMODELING OF THE ACTIN CYTOSKELETON IN VASCULAR SMOOTH MUSCLE CELLS FOLLOWING MECHANOSENSITIVE ARTERIOLAR CONSTRICTION. Am J Physiol Heart Circ Physiol, 2004.

Flick, J. S. and Thorner, J. Genetic and biochemical characterization of a phosphatidylinositol-specific phospholipase C in Saccharomyces cerevisiae. Mol Cell Biol, 13: 5861-5876, 1993.

Folk, J. E., Mullooly, J. P., and Cole, P. W. Mechanism of action of guinea pig liver transglutaminase. II. The role of metal in enzyme activation. J Biol Chem, 242: 1838-1844, 1967.

Fritz, K. E., Jarmolych, J., and Daoud, A. S. Association of DNA synthesis and apparent dedifferentiation of aortic smooth muscle cells in vitro. Exp Mol Pathol, 12: 354-362, 1970.

Gabbiani, G., Schmid, E., Winter, S., Chaponnier, C., de, C. C., Vandekerckhove, J., Weber, K., and Franke, W. W. Vascular smooth muscle cells differ from other smooth muscle cells: predominance of vimentin filaments and a specific alpha-type actin. Proc Natl Acad Sci U S A, 78: 298-302, 1981.

Garcia, P., Gupta, R., Shah, S., Morris, A. J., Rudge, S. A., Scarlata, S., Petrova, V., McLaughlin, S., and Rebecchi, M. J. The pleckstrin homology domain of phospholipase C-delta 1 binds with high affinity to phosphatidylinositol 4,5-bisphosphate in bilayer membranes. Biochemistry, 34: 16228-16234, 1995.

Gaudry, C. A., Verderio, E., Aeschlimann, D., Cox, A., Smith, C., and Griffin, M. Cell surface localization of tissue transglutaminase is dependent on a fibronectin-binding site in its N-terminal beta-sandwich domain. J Biol Chem, 274: 30707-30714, 1999.

Gaudry, C. A., Verderio, E., Jones, R. A., Smith, C., and Griffin, M. Tissue transglutaminase is an important player at the surface of human endothelial cells: evidence for its externalization and its colocalization with the beta(1) integrin. Exp Cell Res, 252: 104-113, 1999.

Gaudry, C. A., Verderio, E., Aeschlimann, D., Cox, A., Smith, C., and Griffin, M. Cell surface localization of tissue transglutaminase is dependent on a fibronectin-binding site in its N-terminal beta-sandwich domain. J Biol Chem, 274: 30707-30714, 1999.

Gendek-Kubiak, H. and Gendek, E. G. Expression of tissue transglutaminase in blood and lymphatic vessel endothelia and in mesothelium. Rocz Akad Med Bialymst, 49 Suppl 1: 195-197, 2004.

Gentile, V., Thomazy, V., Piacentini, M., Fesus, L., and Davies, P. J. Expression of tissue transglutaminase in Balb-C 3T3 fibroblasts: effects on cellular morphology and adhesion. J Cell Biol, 119: 463-474, 1992.

Gerecht-Nir, S., Ziskind, A., Cohen, S., and Itskovitz-Eldor, J. Human embryonic stem cells as an in vitro model for human vascular development and the induction of vascular differentiation. Lab Invest, 83: 1811-1820, 2003.

Gimona, M., Herzog, M., Vandekerckhove, J., and Small, J. V. Smooth muscle specific expression of calponin. FEBS Lett, 274: 159-162, 1990.

Gollasch, M., Haase, H., Ried, C., Lindschau, C., Morano, I., Luft, F. C., and Haller, H. L-type calcium channel expression depends on the differentiated state of vascular smooth muscle cells. FASEB J, 12 : 593-601, 1998.

Gonzalez, M. C., Arribas, S. M., Molero, F., and Fernandez-Alfonso, M. S. Effect of removal of adventitia on vascular smooth muscle contraction and relaxation. Am J Physiol Heart Circ Physiol, 280: H2876-H2881, 2001.

Gray-Bablin, J., Rao, S., and Keyomarsi, K. Lovastatin induction of cyclin-dependent kinase inhibitors in human breast cells occurs in a cell cycle-independent fashion. Cancer Res, 57: 604-609, 1997.

Greenberg, C. S., Achyuthan, K. E., Borowitz, M. J., and Shuman, M. A. The transglutaminase in vascular cells and tissues could provide an alternate pathway for fibrin stabilization. Blood, 70: 702-709, 1987.

Greenberg, C. S., Birckbichler, P. J., and Rice, R. H. Transglutaminases: multifunctional cross-linking enzymes that stabilize tissues. FASEB J, 5: 3071-3077, 1991.

Grenard, P., Bresson-Hadni, S., El, A. S., Chevallier, M., Vuitton, D. A., and Ricard-Blum, S. Transglutaminase-mediated cross-linking is involved in the stabilization of extracellular matrix in human liver fibrosis. J Hepatol, 35: 367-375, 2001.

Grobler, J. A. and Hurley, J. H. Catalysis by phospholipase C delta1 requires that Ca2+ bind to the catalytic domain, but not the C2 domain. Biochemistry, 37: 5020-5028, 1998.

Gross, S. R., Balklava, Z., and Griffin, M. Importance of tissue transglutaminase in repair of extracellular matrices and cell death of dermal fibroblasts after exposure to a solarium ultraviolet A source. J Invest Dermatol, 121: 412-423, 2003.

Grynkiewicz, G., Poenie, M., and Tsien, R. Y. A new generation of Ca2+ indicators with greatly improved fluorescence properties. J Biol Chem, 260: 3440-3450, 1985.

Guo, Y., Rebecchi, M., and Scarlata, S. Phospholipase C{beta}2 Binds to and Inhibits Phospholipase C{delta}1. J Biol Chem, 280: 1438-1447, 2005.

Hall, A. Signal transduction pathways regulated by the Rho family of small GTPases. Br J Cancer, 80 Suppl 1: 25-27, 1999.

Hall, A. and Nobes, C. D. Rho GTPases: molecular switches that control the organization and dynamics of the actin cytoskeleton. Philos Trans R Soc Lond B Biol Sci, 355: 965-970, 2000.

Haroon, Z. A., Hettasch, J. M., Lai, T. S., Dewhirst, M. W., and Greenberg, C. S. Tissue transglutaminase is expressed, active, and directly involved in rat dermal wound healing and angiogenesis. FASEB J, 13: 1787-1795, 1999.

Haroon, Z. A., Wannenburg, T., Gupta, M., Greenberg, C. S., Wallin, R., and Sane, D. C. Localization of tissue transglutaminase in human carotid and coronary artery atherosclerosis: implications for plaque stability and progression. Lab Invest, 81: 83-93, 2001.

Hart, C. E. and Bowen-Pope, D. F. Platelet-derived growth factor receptor: current views of the two-subunit model. J Invest Dermatol, 94: 53S-57S, 1990.

Hedin, U., Sjolund, M., Hultgardh-Nilsson, A., and Thyberg, J. Changes in expression and organization of smooth-muscle-specific alpha-actin during fibronectin-mediated modulation of arterial smooth muscle cell phenotype. Differentiation, 44: 222-231, 1990.

Hill, S. J. Histamine receptors and interactions between second messenger transduction systems. Agents Actions Suppl, 33: 145-159, 1991.

Hodgkinson, J. L. Actin and the smooth muscle regulatory proteins: a structural perspective. J Muscle Res Cell Motil, 21: 115-130, 2000.

Hodson, E. A., Ashley, C. C., Hughes, A. D., and Lymn, J. S. Regulation of phospholipase C delta 1 activity by GTP-binding proteins: rhoA as an inhibitory modulator. Biochem Soc Trans, 26: S128, 1998.

Hodson, E. A., Ashley, C. C., and Lymn, J. S. Association of heterotrimeric G-proteins with bovine aortic phospholipase C gamma. Biochem Biophys Res Commun, 258: 425-430, 1999.

Homma, Y., Sakamoto, H., Tsunoda, M., Aoki, M., Takenawa, T., and Ooyama, T. Evidence for involvement of phospholipase C-gamma 2 in signal transduction of platelet-derived growth factor in vascular smooth- muscle cells. Biochem J, 290 (Pt 3): 649-653, 1993.

Homma, Y. and Emori, Y. A dual functional signal mediator showing RhoGAP and phospholipase C-delta stimulating activities. EMBO J, 14: 286-291, 1995.

Hopwood, D. Fixatives and fixation: a review. Histochem J, 1: 323-360, 1969.

Hsieh, J. K., Kletsas, D., Clunn, G., Hughes, A. D., Schachter, M., and Demoliou-Mason, C. p53, p21(WAF1/CIP1), and MDM2 involvement in proliferation and apoptosis in an in vitro model of conditionally immortalized human vascular smooth muscle cells. Arterioscler Thromb Vasc Biol, 20 : 636-644, 2000.

Hungerford, J. E. and Little, C. D. Developmental biology of the vascular smooth muscle cell: building a multilayered vessel wall. J Vasc Res, 36: 2-27, 1999.

Hwang, K. C., Gray, C. D., Sivasubramanian, N., and Im, M. J. Interaction site of GTP binding Gh (transglutaminase II) with phospholipase C. J Biol Chem, 270: 27058-27062, 1995.

Hwang, K. C., Gray, C. D., Sivasubramanian, N., and Im, M. J. Interaction site of GTP binding Gh (transglutaminase II) with phospholipase C. J Biol Chem, 270: 27058-27062, 1995.

Hwang, K. C., Gray, C. D., Sweet, W. E., Moravec, C. S., and Im, M. J. Alpha 1-adrenergic receptor coupling with Gh in the failing human heart. Circulation, 94: 718-726, 1996.

Hwang, K. C., Lim, S., Kwon, H. M., Bae, Y. S., Kang, S. M., Chung, K. H., Graham, R. M., Rhee, S. G., and Jang, Y. Phospholipase C-delta1 rescues intracellular Ca2+ overload in ischemic heart and hypoxic neonatal cardiomyocytes. J Steroid Biochem Mol Biol, 91: 131-138, 2004.

Hynes, R. O. The emergence of integrins: a personal and historical perspective. Matrix Biol, 23: 333-340, 2004.

Iismaa, S. E., Chung, L., Wu, M. J., Teller, D. C., Yee, V. C., and Graham, R. M. The core domain of the tissue transglutaminase Gh hydrolyzes GTP and ATP. Biochemistry, 36: 11655-11664, 1997.

Iismaa, S. E., Wu, M. J., Nanda, N., Church, W. B., and Graham, R. M. GTP binding and signaling by Gh/transglutaminase II involves distinct residues in a unique GTP-binding pocket. J Biol Chem, 275: 18259-18265, 2000.

Intengan, H. D. and Schiffrin, E. L. Vascular remodeling in hypertension: roles of apoptosis, inflammation, and fibrosis. Hypertension, 38: 581-587, 2001.

Irino, Y., Cho, H., Nakamura, Y., Nakahara, M., Furutani, M., Suh, P. G., Takenawa, T., and Fukami, K. Phospholipase C delta-type consists of three isozymes: bovine PLCdelta2 is a homologue of human/mouse PLCdelta4. Biochem Biophys Res Commun, 320: 537-543, 2004.

Irvine, R. Phospholipid signalling. Taking stock of PI-PLC. Nature, 380: 581-583, 1996.

Isogai, S., Horiguchi, M., and Weinstein, B. M. The vascular anatomy of the developing zebrafish: an atlas of embryonic and early larval development. Dev Biol, 230: 278-301, 2001.

Janmey, P. A. and Stossel, T. P. Gelsolin-polyphosphoinositide interaction. Full expression of gelsolin-inhibiting function by polyphosphoinositides in vesicular form and inactivation by dilution, aggregation, or masking of the inositol head group. J Biol Chem, 264: 4825-4831, 1989.

Janmey, P. A. The cytoskeleton and cell signaling: component localization and mechanical coupling. Physiol Rev, 78: 763-781, 1998.

Johnson, T. S., El-Koraie, A. F., Skill, N. J., Baddour, N. M., El Nahas, A. M., Njloma, M., Adam, A. G., and Griffin, M. Tissue transglutaminase and the progression of human renal scarring. J Am Soc Nephrol, 14: 2052-2062, 2003.

Jones, R. A., Nicholas, B., Mian, S., Davies, P. J., and Griffin, M. Reduced expression of tissue transglutaminase in a human endothelial cell line leads to changes in cell spreading, cell adhesion and reduced polymerisation of fibronectin. J Cell Sci, 110 (Pt 19): 2461-2472, 1997.

Kaibuchi, K., Kuroda, S., and Amano, M. Regulation of the cytoskeleton and cell adhesion by the Rho family GTPases in mammalian cells. Annu Rev Biochem, 68: 459-486, 1999.

Kang, S. K., Yi, K. S., Kwon, N. S., Park, K. H., Kim, U. H., Baek, K. J., and Im, M. J. Alpha1B-adrenoceptor signaling and cell motility: GTPase function of Gh/transglutaminase 2 inhibits cell migration through interaction with cytoplasmic tail of integrin alpha subunits. J Biol Chem, 279: 36593-36600, 2004.

Kato, H., Fukami, K., Shibasaki, F., Homma, Y., and Takenawa, T. Enhancement of phospholipase C delta 1 activity in the aortas of spontaneously hypertensive rats. J Biol Chem, 267: 6483-6487, 1992.

Kawai, K., Yamaga, M., Iwamae, Y., Kiyota, M., Kamata, H., Hirata, H., Homma, Y., and Yagisawa, H. A PLCdelta1-binding protein, p122RhoGAP, is localized in focal adhesions. Biochem Soc Trans, 32: 1107-1109, 2004.

Kelley, G. G., Reks, S. E., Ondrako, J. M., and Smrcka, A. V. Phospholipase C(epsilon): a novel Ras effector. EMBO J, 20: 743-754, 2001.

Kenworthy, A. K. Imaging protein-protein interactions using fluorescence resonance energy transfer microscopy. Methods, 24: 289-296, 2001.

Kim, S. Y. New target against inflammatory diseases: transglutaminase 2. Arch Immunol Ther Exp (Warsz), 52: 332-337, 2004.

Kim, Y. H., Park, T. J., Lee, Y. H., Baek, K. J., Suh, P. G., Ryu, S. H., and Kim, K. T. Phospholipase C-delta1 is activated by capacitative calcium entry that follows phospholipase C-beta activation upon bradykinin stimulation. J Biol Chem, 274: 26127-26134, 1999.

Kohda, D., Hatanaka, H., Odaka, M., Mandiyan, V., Ullrich, A., Schlessinger, J., and Inagaki, F. Solution structure of the SH3 domain of phospholipase C-gamma. Cell, 72: 953-960, 1993.

Kolakowski, J., Makuch, R., Stepkowski, D., and Dabrowska, R. Interaction of calponin with actin and its functional implications. Biochem J, 306 (Pt 1): 199-204, 1995.

Korponay-Szabo, I. R., Halttunen, T., Szalai, Z., Laurila, K., Kiraly, R., Kovacs, J. B., Fesus, L., and Maki, M. In vivo targeting of intestinal and extraintestinal transglutaminase 2 by coeliac autoantibodies. Gut, 53: 641-648, 2004.

Kosaka, C., Sasaguri, T., Komiyama, Y., and Takahashi, H. All-trans retinoic acid inhibits vascular smooth muscle cell proliferation targeting multiple genes for cyclins and cyclin-dependent kinases. Hypertens Res, 24: 579-588, 2001.

Kumar, M. S. and Owens, G. K. Combinatorial control of smooth muscle-specific gene expression. Arterioscler Thromb Vasc Biol, 23: 737-747, 2003.

Kweon, S. M., Lee, Z. W., Yi, S. J., Kim, Y. M., Han, J. A., Paik, S. G., and Ha, S. S. Protective role of tissue transglutaminase in the cell death induced by TNF-alpha in SH-SY5Y neuroblastoma cells. J Biochem Mol Biol, 37: 185-191, 2004.

LaBelle, E. F. and Polyak, F. Phospholipase C beta 2 in vascular smooth muscle. J Cell Physiol, 169: 358-363, 1996.

LaBelle, E. F., Wilson, K., and Polyak, E. Subcellular localization of phospholipase C isoforms in vascular smooth muscle. Biochim Biophys Acta, 1583: 273-278, 2002.

Lai, T. S., Bielawska, A., Peoples, K. A., Hannun, Y. A., and Greenberg, C. S. Sphingosylphosphocholine reduces the calcium ion requirement for activating tissue transglutaminase. J Biol Chem, 272: 16295-16300, 1997.

Lai, T. S., Slaughter, T. F., Peoples, K. A., Hettasch, J. M., and Greenberg, C. S. Regulation of human tissue transglutaminase function by magnesium-nucleotide complexes. Identification of distinct binding sites for Mg-GTP and Mg-ATP. J Biol Chem, 273: 1776-1781, 1998.

Lai, T. S., Hausladen, A., Slaughter, T. F., Eu, J. P., Stamler, J. S., and Greenberg, C. S. Calcium regulates S-nitrosylation, denitrosylation, and activity of tissue transglutaminase. Biochemistry, 40: 4904-4910, 2001.

Langille, B. L. and Dajnowiec, D. Cross-linking vasomotor tone and vascular remodeling: a novel function for tissue transglutaminase? Circ Res, 96: 9-11, 2005.

Lazou, A., Fuller, S. J., Bogoyevitch, M. A., Orfali, K. A., and Sugden, P. H. Characterization of stimulation of phosphoinositide hydrolysis by alpha 1-adrenergic agonists in adult rat hearts. Am J Physiol, 267: H970-H978, 1994.

Lee, K. H., Lee, N., Lim, S., Jung, H., Ko, Y. G., Park, H. Y., Jang, Y., Lee, H., and Hwang, K. C. Calreticulin inhibits the MEK1,2-ERK1,2 pathway in alpha 1-adrenergic receptor/Gh-stimulated hypertrophy of neonatal rat cardiomyocytes. J Steroid Biochem Mol Biol, 84: 101-107, 2003.

Lee, K. N., Arnold, S. A., Birckbichler, P. J., Patterson, M. K., Jr., Fraij, B. M., Takeuchi, Y., and Carter, H. A. Site-directed mutagenesis of human tissue transglutaminase: Cys-277 is essential for transglutaminase activity but not for GTPase activity. Biochim Biophys Acta, 1202: 1-6, 1993.

Lee, M. Y., Chung, S., Bang, H. W., Baek, K. J., and Uhm, D. Modulation of large conductance Ca2+-activated K+ channel by Galphah (transglutaminase II) in the vascular smooth muscle cell. Pflugers Arch, 433: 671-673, 1997.

Lee, Z. W., Kwon, S. M., Kim, S. W., Yi, S. J., Kim, Y. M., and Ha, K. S. Activation of in situ tissue transglutaminase by intracellular reactive oxygen species. Biochem Biophys Res Commun, 305: 633-640, 2003.

Leech, C. J. and Faber, J. E. Different alpha-adrenoceptor subtypes mediate constriction of arterioles and venules. Am J Physiol, 270: H710-H722, 1996.

Lenhardt, A., Plebani, A., Marchetti, F., Gerarduzzi, T., Not, T., Meini, A., Villanacci, V., Martelossi, S., and Ventura, A. Role of human-tissue transglutaminase IgG and

anti-gliadin IgG antibodies in the diagnosis of coeliac disease in patients with selective immunoglobulin A deficiency. Dig Liver Dis, 36: 730-734, 2004.

Lesort, M., Attanavanich, K., Zhang, J., and Johnson, G. V. Distinct nuclear localization and activity of tissue transglutaminase. J Biol Chem, 273: 11991-11994, 1998.

Li, S., Sims, S., Jiao, Y., Chow, L. H., and Pickering, J. G. Evidence from a novel human cell clone that adult vascular smooth muscle cells can convert reversibly between noncontractile and contractile phenotypes. Circ Res, 85: 338-348, 1999.

Li, X., Tsai, P., Wieder, E. D., Kribben, A., Van, P., V, Schrier, R. W., and Nemenoff, R. A. Vascular smooth muscle cells grown on Matrigel. A model of the contractile phenotype with decreased activation of mitogen-activated protein kinase. J Biol Chem, 269: 19653-19658, 1994.

Lindqvist, A., Nilsson, B. O., Ekblad, E., and Hellstrand, P. Platelet-derived growth factor receptors expressed in response to injury of differentiated vascular smooth muscle in vitro: effects on Ca2+ and growth signals. Acta Physiol Scand, 173: 175-184, 2001.

Lipp, P. and Niggli, E. A hierarchical concept of cellular and subcellular Ca(2+)-signalling. Prog Biophys Mol Biol, 65: 265-296, 1996.

Liu, B., Itoh, H., Louie, O., Kubota, K., and Kent, K. C. The role of phospholipase C and phosphatidylinositol 3-kinase in vascular smooth muscle cell migration and proliferation. J Surg Res, 120: 256-265, 2004.

Liu, S., Cerione, R. A., and Clardy, J. Structural basis for the guanine nucleotide-binding activity of tissue transglutaminase and its regulation of transamidation activity. Proc Natl Acad Sci U S A, 99: 2743-2747, 2002.

Lomasney, J. W., Cheng, H. F., Wang, L. P., Kuan, Y., Liu, S., Fesik, S. W., and King, K. Phosphatidylinositol 4,5-bisphosphate binding to the pleckstrin homology domain of phospholipase C-delta1 enhances enzyme activity. J Biol Chem, 271: 25316-25326, 1996.

Lu, J., Landerholm, T. E., Wei, J. S., Dong, X. R., Wu, S. P., Liu, X., Nagata, K., Inagaki, M., and Majesky, M. W. Coronary smooth muscle differentiation from proepicardial cells requires rhoA-mediated actin reorganization and p160 rho-kinase activity. Dev Biol, 240: 404-418, 2001.

Machesky, L. M. and Hall, A. Role of actin polymerization and adhesion to extracellular matrix in Rac- and Rho-induced cytoskeletal reorganization. J Cell Biol, 138: 913-926, 1997.

Manabe, I. and Nagai, R. Regulation of smooth muscle phenotype. Curr Atheroscler Rep, 5: 214-222, 2003.

Martinez, J., Chalupowicz, D. G., Roush, R. K., Sheth, A., and Barsigian, C. Transglutaminase-mediated processing of fibronectin by endothelial cell monolayers. Biochemistry, 33: 2538-2545, 1994.

Mastroberardino, P. G., Iannicola, C., Nardacci, R., Bernassola, F., De, L., V, Melino, G., Moreno, S., Pavone, F., Oliverio, S., Fesus, L., and Piacentini, M. 'Tissue'

transglutaminase ablation reduces neuronal death and prolongs survival in a mouse model of Huntington's disease. Cell Death Differ, 9: 873-880, 2002.

Matthew, J. D., Khromov, A. S., McDuffie, M. J., Somlyo, A. V., Somlyo, A. P., Taniguchi, S., and Takahashi, K. Contractile properties and proteins of smooth muscles of a calponin knockout mouse. J Physiol, 529 Pt 3: 811-824, 2000.

McDonough, P. M. and Button, D. C. Measurement of cytoplasmic calcium concentration in cell suspensions: correction for extracellular Fura-2 through use of Mn2+ and probenecid. Cell Calcium, 10: 171-180, 1989.

McGough, A. F-actin-binding proteins. Curr Opin Struct Biol, 8: 166-176, 1998.

Mehta, K., Fok, J., Miller, F. R., Koul, D., and Sahin, A. A. Prognostic significance of tissue transglutaminase in drug resistant and metastatic breast cancer. Clin Cancer Res, 10: 8068-8076, 2004.

Meiri, K. F. Membrane/cytoskeleton communication. Subcell Biochem, 37: 247-282, 2004.

Mhaouty-Kodja, S. Ghalpha/tissue transglutaminase 2: an emerging G protein in signal transduction. Biol Cell, 96: 363-367, 2004.

Miano, J. M. Mammalian smooth muscle differentiation: origins, markers and transcriptional control. Results Probl Cell Differ, 38: 39-59, 2002.

Michell, R. H. Inositol phospholipids and cell surface receptor function. Biochim Biophys Acta, 415: 81-47, 1975.

Milakovic, T., Tucholski, J., McCoy, E., and Johnson, G. V. Intracellular localization and activity state of tissue transglutaminase differentially impacts cell death. J Biol Chem, 279: 8715-8722, 2004.

Min, D. S., Kim, D. M., Lee, Y. H., Seo, J., Suh, P. G., and Ryu, S. H. Purification of a novel phospholipase C isozyme from bovine cerebellum. J Biol Chem, 268: 12207-12212, 1993.

Minneman, K. P. and Esbenshade, T. A. Alpha 1-adrenergic receptor subtypes. Annu Rev Pharmacol Toxicol, 34: 117-133, 1994.

Mogami, H. and Kojima, I. Stimulation of calcium entry is prerequisite for DNA synthesis induced by platelet-derived growth factor in vascular smooth muscle cells. Biochem Biophys Res Commun, 196: 650-658, 1993.

Mohan, K., Pinto, D., and Issekutz, T. B. Identification of tissue transglutaminase as a novel molecule involved in human CD8+ T cell transendothelial migration. J Immunol, 171: 3179-3186, 2003.

Monsonego, A., Shani, Y., Friedmann, I., Paas, Y., Eizenberg, O., and Schwartz, M. Expression of GTP-dependent and GTP-independent tissue-type transglutaminase in cytokine-treated rat brain astrocytes. J Biol Chem, 272: 3724-3732, 1997.

Monsonego, A., Friedmann, I., Shani, Y., Eisenstein, M., and Schwartz, M. GTP-dependent conformational changes associated with the functional switch between Galpha and cross-linking activities in brain-derived tissue transglutaminase. J Mol Biol, 282: 713-720, 1998.

Morishige, K., Shimokawa, H., Eto, Y., Hoshijima, M., Kaibuchi, K., and Takeshita, A. In vivo gene transfer of dominant-negative rho-kinase induces regression of coronary arteriosclerosis in pigs. Ann N Y Acad Sci, 947: 407-411, 2001.

Murtaugh, M. P., Mehta, K., Johnson, J., Myers, M., Juliano, R. L., and Davies, P. J. Induction of tissue transglutaminase in mouse peritoneal macrophages. J Biol Chem, 258: 11074-11081, 1983.

Murthy, S. N., Lomasney, J. W., Mak, E. C., and Lorand, L. Interactions of G(h)/transglutaminase with phospholipase Cdelta1 and with GTP. Proc Natl Acad Sci U S A, 96: 11815-11819, 1999.

MYCEK, M. J., CLARKE, D. D., NEIDLE, A., and WAELSCH, H. Amine incorporation into insulin as catalyzed by transglutaminase. Arch Biochem Biophys, 84: 528-540, 1959.

Nagy, L., Saydak, M., Shipley, N., Lu, S., Basilion, J. P., Yan, Z. H., Syka, P., Chandraratna, R. A., Stein, J. P., Heyman, R. A., and Davies, P. J. Identification and characterization of a versatile retinoid response element (retinoic acid receptor response element-retinoid X receptor response element) in the mouse tissue transglutaminase gene promoter. J Biol Chem, 271: 4355-4365, 1996.

Nagy, L., Thomazy, V. A., Saydak, M. M., Stein, J. P., and Davies, P. J. The promoter of the mouse tissue transglutaminase gene directs tissue-specific, retinoid-regulated and apoptosis-linked expression. Cell Death Differ, 4: 534-547, 1997.

Nagy, L., Thomazy, V. A., Heyman, R. A., and Davies, P. J. Retinoid-induced apoptosis in normal and neoplastic tissues. Cell Death Differ, 5: 11-19, 1998.

Nair, S., Mayotte, J., Lokshin, A., and Levitt, M. Induction of squamous differentiation by interferon beta in a human non-small-cell lung cancer cell line. J Natl Cancer Inst, 86: 378-383, 1994.

Nakamura, M., Sunagawa, M., Kosugi, T., and Sperelakis, N. Actin filament disruption inhibits L-type Ca(2+) channel current in cultured vascular smooth muscle cells. Am J Physiol Cell Physiol, 279: C480-C487, 2000.

Nakamura, Y., Fukami, K., Yu, H., Takenaka, K., Kataoka, Y., Shirakata, Y., Nishikawa, S., Hashimoto, K., Yoshida, N., and Takenawa, T. Phospholipase Cdelta1 is required for skin stem cell lineage commitment. EMBO J, 22: 2981-2991, 2003.

Nakaoka, H., Perez, D. M., Baek, K. J., Das, T., Husain, A., Misono, K., Im, M. J., and Graham, R. M. Gh: a GTP-binding protein with transglutaminase activity and receptor signaling function. Science, 264 : 1593-1596, 1994.

Nanda, N., Iismaa, S. E., Owens, W. A., Husain, A., Mackay, F., and Graham, R. M. Targeted inactivation of Gh/tissue transglutaminase II. J Biol Chem, 276: 20673-20678, 2001.

Nara, K., Nakanishi, K., Hagiwara, H., Wakita, K., Kojima, S., and Hirose, S. Retinol-induced morphological changes of cultured bovine endothelial cells are accompanied by a marked increase in transglutaminase. J Biol Chem, 264: 19308-19312, 1989.

Narumiya, S., Ishizaki, T., and Watanabe, N. Rho effectors and reorganization of actin cytoskeleton. FEBS Lett, 410: 68-72, 1997.

Nicholas, B., Smethurst, P., Verderio, E., Jones, R., and Griffin, M. Cross-linking of cellular proteins by tissue transglutaminase during necrotic cell death: a mechanism for maintaining tissue integrity. Biochem J, 371: 413-422, 2003.

Nishimura, J., Huang, J. S., and Deuel, T. F. Platelet-derived growth factor stimulates tyrosine-specific protein kinase activity in Swiss mouse 3T3 cell membranes. Proc Natl Acad Sci U S A, 79: 4303-4307, 1982.

Nishizuka, Y. Studies and perspectives of protein kinase C. Science, 233: 305-312, 1986.

Noda, S., Ito, M., Watanabe, S., Takahashi, K., and Maruyama, K. Conformational changes of actin induced by calponin. Biochem Biophys Res Commun, 185: 481-487, 1992.

Nogales, E. Structural insights into microtubule function. Annu Rev Biochem, 69: 277-302, 2000.

Oliverio, S., Amendola, A., Di, S. F., Farrace, M. G., Fesus, L., Nemes, Z., Piredda, L., Spinedi, A., and Piacentini, M. Tissue transglutaminase-dependent posttranslational modification of the retinoblastoma gene product in promonocytic cells undergoing apoptosis. Mol Cell Biol, 17: 6040-6048, 1997.

Osborn, M. and Weber, K. The display of microtubules in transformed cells. Cell, 12: 561-571, 1977.

Ou, H., Haendeler, J., Aebly, M. R., Kelly, L. A., Cholewa, B. C., Koike, G., Kwitek-Black, A., Jacob, H. J., Berk, B. C., and Miano, J. M. Retinoic acid-induced tissue transglutaminase and apoptosis in vascular smooth muscle cells. Circ Res, 87: 881-887, 2000.

Owens, G. K. Regulation of differentiation of vascular smooth muscle cells. Physiol Rev, 75: 487-517, 1995.

Pandey, S. C., Pandey, G. N., and Smith, T. L. Chronic ethanol effects on the expression of phospholipase C isozymes and Gq/11-protein in primary cultures of astrocytes. Alcohol, 13: 487-492, 1996.

Park, E. S., Won, J. H., Han, K. J., Suh, P. G., Ryu, S. H., Lee, H. S., Yun, H. Y., Kwon, N. S., and Baek, K. J. Phospholipase C-delta1 and oxytocin receptor signalling: evidence of its role as an effector. Biochem J, 331 (Pt 1): 283-289, 1998.

Park, H., Park, E. S., Lee, H. S., Yun, H. Y., Kwon, N. S., and Baek, K. J. Distinct characteristic of Galpha(h) (transglutaminase II) by compartment: GTPase and transglutaminase activities. Biochem Biophys Res Commun, 284: 496-500, 2001.

Park, K. C., Chung, K. C., Kim, Y. S., Lee, J., Joh, T. H., and Kim, S. Y. Transglutaminase 2 induces nitric oxide synthesis in BV-2 microglia. Biochem Biophys Res Commun, 323: 1055-1062, 2004.

Pascal, S. M., Singer, A. U., Gish, G., Yamazaki, T., Shoelson, S. E., Pawson, T., Kay, L. E., and Forman-Kay, J. D. Nuclear magnetic resonance structure of an SH2 domain of phospholipase C-gamma 1 complexed with a high affinity binding peptide. Cell, 77: 461-472, 1994.

Pasquali, D., Rossi, V., Prezioso, D., Gentile, V., Colantuoni, V., Lotti, T., Bellastella, A., and Sinisi, A. A. Changes in tissue transglutaminase activity and expression during retinoic acid-induced growth arrest and apoptosis in primary cultures of human epithelial prostate cells. J Clin Endocrinol Metab, 84: 1463-1469, 1999.

Paterson, H. F., Savopoulos, J. W., Perisic, O., Cheung, R., Ellis, M. V., Williams, R. L., and Katan, M. Phospholipase C delta 1 requires a pleckstrin homology domain for interaction with the plasma membrane. Biochem J, 312 (Pt 3): 661-666, 1995.

Pawelczyk, T. and Matecki, A. Localization of phospholipase C delta3 in the cell and regulation of its activity by phospholipids and calcium. Eur J Biochem, 257: 169-177, 1998.

Pawelczyk, T. Isozymes delta of phosphoinositide-specific phospholipase C. Acta Biochim Pol, 46: 91-98, 1999.

Perez, D. M., DeYoung, M. B., and Graham, R. M. Coupling of expressed alpha 1B- and alpha 1D-adrenergic receptor to multiple signaling pathways is both G protein and cell type specific. Mol Pharmacol, 44: 784-795, 1993.

Piacentini, M., Annicchiarico-Petruzzelli, M., Oliverio, S., Piredda, L., Biedler, J. L., and Melino, E. Phenotype-specific "tissue" transglutaminase regulation in human

neuroblastoma cells in response to retinoic acid: correlation with cell death by apoptosis. Int J Cancer, 52: 271-278, 1992.

Piacentini, M. Tissue transglutaminase: a candidate effector element of physiological cell death. Curr Top Microbiol Immunol, 200: 163-175, 1995.

Piascik, M. T., Hrometz, S. L., Edelmann, S. E., Guarino, R. D., Hadley, R. W., and Brown, R. D. Immunocytochemical localization of the alpha-1B adrenergic receptor and the contribution of this and the other subtypes to vascular smooth muscle contraction: analysis with selective ligands and antisense oligonucleotides. J Pharmacol Exp Ther, 283: 854-868, 1997.

Puato, M., Faggin, E., Favaretto, E., Bertipaglia, B., Rattazzi, M., Rizzoni, D., Gamba, G. P., Sartore, S., Rosei, E. A., Pessina, A. C., and Pauletto, P. Prevalence of fetal-type smooth muscle cells in the media of microvessels from hypertensive patients. Hypertension, 44: 191-194, 2004.

Rebecchi, M. J. and Pentyala, S. N. Structure, function, and control of phosphoinositide-specific phospholipase C. Physiol Rev, 80: 1291-1335, 2000.

Rescan, C., Coutant, A., Talarmin, H., Theret, N., Glaise, D., Guguen-Guillouzo, C., and Baffet, G. Mechanism in the sequential control of cell morphology and S phase entry by epidermal growth factor involves distinct MEK/ERK activations. Mol Biol Cell, 12: 725-738, 2001.

Rhee, S. G. and Bae, Y. S. Regulation of phosphoinositide-specific phospholipase C isozymes. J Biol Chem, 272: 15045-15048, 1997.

Rhee, S. G. Regulation of phosphoinositide-specific phospholipase C. Annu Rev Biochem, 70: 281-312, 2001.

Ridley, A. J. and Hall, A. Distinct patterns of actin organization regulated by the small GTP-binding proteins Rac and Rho. Cold Spring Harb Symp Quant Biol, 57: 661-671, 1992.

Ritter, S. J. and Davies, P. J. Identification of a transforming growth factor-beta1/bone morphogenetic protein 4 (TGF-beta1/BMP4) response element within the mouse tissue transglutaminase gene promoter. J Biol Chem, 273: 12798-12806, 1998.

Ross, R. The pathogenesis of atherosclerosis: a perspective for the 1990s. Nature, 362: 801-809, 1993.

Rovner, A. S., Murphy, R. A., and Owens, G. K. Expression of smooth muscle and nonmuscle myosin heavy chains in cultured vascular smooth muscle cells. J Biol Chem, 261: 14740-14745, 1986.

rpin-Bott, M. P., Waltisperger, E., Freund-Mercier, M. J., and Stoeckel, M. E. Two oxytocin-binding site subtypes in rat kidney: pharmacological characterization, ontogeny and localization by in vitro and in vivo autoradiography. J Endocrinol, 153: 49-59, 1997.

Rudner, X. L., Berkowitz, D. E., Booth, J. V., Funk, B. L., Cozart, K. L., D'Amico, E. B., El-Moalem, H., Page, S. O., Richardson, C. D., Winters, B., Marucci, L., and Schwinn, D. A. Subtype specific regulation of human vascular alpha(1)-adrenergic receptors by vessel bed and age. Circulation, 100: 2336-2343, 1999.

Rybarczyk, B. J., Lawrence, S. O., and Simpson-Haidaris, P. J. Matrix-fibrinogen enhances wound closure by increasing both cell proliferation and migration. Blood, 102: 4035-4043, 2003.

Saqr, H. E., Walters, J. D., Guan, Z., Stokes, B. T., and Yates, A. J. Gangliosides inhibit PDGF-induced signal transduction events in U-1242 MG human glioma cells. Neurochem Res, 20: 1389-1395, 1995.

Sato, M., Ozawa, T., Inukai, K., Asano, T., and Umezawa, Y. Fluorescent indicators for imaging protein phosphorylation in single living cells. Nat Biotechnol, 20: 287-294, 2002.

Sayet, I., Neuilly, G., Rakotoarisoa, L., Mironneau, C., and Mironneau, J. Relation between alpha 1-adrenoceptor subtypes and noradrenaline-induced contraction in rat portal vein smooth muscle. Br J Pharmacol, 110: 207-212, 1993.

Schildmeyer, L. A., Braun, R., Taffet, G., Debiasi, M., Burns, A. E., Bradley, A., and Schwartz, R. J. Impaired vascular contractility and blood pressure homeostasis in the smooth muscle alpha-actin null mouse. FASEB J, 14: 2213-2220, 2000.

Schnabel, C., Sawitza, I., Tag, C. G., Lahme, B., Gressner, A. M., and Breitkopf, K. Expression of cytosolic and membrane associated tissue transglutaminase in rat hepatic stellate cells and its upregulation during transdifferentiation to myofibroblasts in culture. Hepatol Res, 28: 140-145, 2004.

Schwartz, S. M., Heimark, R. L., and Majesky, M. W. Developmental mechanisms underlying pathology of arteries. Physiol Rev, 70: 1177-1209, 1990.

Schwinn, D. A., Correa-Sales, C., Page, S. O., and Maze, M. Functional effects of activation of alpha-1 adrenoceptors by dexmedetomidine: in vivo and in vitro studies. J Pharmacol Exp Ther, 259: 1147-1152, 1991.

Shanahan, C. M., Weissberg, P. L., and Metcalfe, J. C. Isolation of gene markers of differentiated and proliferating vascular smooth muscle cells. Circ Res, 73: 193-204, 1993.

Shimohama, S., Sasaki, Y., Fujimoto, S., Kamiya, S., Taniguchi, T., Takenawa, T., and Kimura, J. Phospholipase C isozymes in the human brain and their changes in Alzheimer's disease. Neuroscience, 82: 999-1007, 1998.

Singh, U. S., Kunar, M. T., Kao, Y. L., and Baker, K. M. Role of transglutaminase II in retinoic acid-induced activation of RhoA-associated kinase-2. EMBO J, 20: 2413-2423, 2001.

Singh, U. S., Pan, J., Kao, Y. L., Joshi, S., Young, K. L., and Baker, K. M. Tissue transglutaminase mediates activation of RhoA and MAP kinase pathways during retinoic acid-induced neuronal differentiation of SH-SY5Y cells. J Biol Chem, 278: 391-399, 2003.

SLOANE-STANLEY, G. H. Anaerobic reactions of phospholipins in brain suspensions. Biochem J, 53: 613-619, 1953.

Small, J. V. Organization of actin in the leading edge of cultured cells: influence of osmium tetroxide and dehydration on the ultrastructure of actin meshworks. J Cell Biol, 91: 695-705, 1981.

Small, J. V., Rottner, K., and Kaverina, I. Functional design in the actin cytoskeleton. Curr Opin Cell Biol, 11: 54-60, 1999.

Smethurst, P. A. and Griffin, M. Measurement of tissue transglutaminase activity in a permeabilized cell system: its regulation by Ca2+ and nucleotides. Biochem J, 313 (Pt 3): 803-808, 1996.

Smith, P. K., Krohn, R. I., Hermanson, G. T., Mallia, A. K., Gartner, F. H., Provenzano, M. D., Fujimoto, E. K., Goeke, N. M., Olson, B. J., and Klenk, D. C. Measurement of protein using bicinchoninic acid. Anal Biochem, 150: 76-85, 1985.

Sohn, R. H., Chen, J., Koblan, K. S., Bray, P. F., and Goldschmidt-Clermont, P. J. Localization of a binding site for phosphatidylinositol 4,5- bisphosphate on human profilin. J Biol Chem, 270: 21114-21120, 1995.

Solway, J., Forsythe, S. M., Halayko, A. J., Vieira, J. E., Hershenson, M. B., and Camoretti-Mercado, B. Transcriptional regulation of smooth muscle contractile apparatus expression. Am J Respir Crit Care Med, 158: S100-S108, 1998.

Somlyo, A. V. and Somlyo, A. P. Intracellular signaling in vascular smooth muscle. Adv Exp Med Biol, 346: 31-38, 1993.

Sotiropoulos, A., Gineitis, D., Copeland, J., and Treisman, R. Signal-regulated activation of serum response factor is mediated by changes in actin dynamics. Cell, 98: 159-169, 1999.

Stauffer, T. P., Ahn, S., and Meyer, T. Receptor-induced transient reduction in plasma membrane PtdIns(4,5)P2 concentration monitored in living cells. Curr Biol, 8: 343-346, 1998.

Stephens, P., Grenard, P., Aeschlimann, P., Langley, M., Blain, E., Errington, R., Kipling, D., Thomas, D., and Aeschlimann, D. Crosslinking and G-protein functions of transglutaminase 2 contribute differentially to fibroblast wound healing responses. J Cell Sci, 117: 3389-3403, 2004.

Stewart, A. J., Mukherjee, J., Roberts, S. J., Lester, D., and Farquharson, C. Identification of a novel class of mammalian phosphoinositol-specific phospholipase C enzymes. Int J Mol Med, 15: 117-121, 2005.

Streb, H., Irvine, R. F., Berridge, M. J., and Schulz, I. Release of Ca2+ from a nonmitochondrial intracellular store in pancreatic acinar cells by inositol-1,4,5-trisphosphate. Nature, 306: 67-69, 1983.

Suto, N., Ikura, K., and Sasaki, R. Expression induced by interleukin-6 of tissue-type transglutaminase in human hepatoblastoma HepG2 cells. J Biol Chem, 268: 7469-7473, 1993.

Szondy, Z., Sarang, Z., Molnar, P., Nemeth, T., Piacentini, M., Mastroberardino, P. G., Falasca, L., Aeschlimann, D., Kovacs, J., Kiss, I., Szegezdi, E., Lakos, G., Rajnavolgyi, E., Birckbichler, P. J., Melino, G., and Fesus, L. Transglutaminase 2-/- mice reveal a phagocytosis-associated crosstalk between macrophages and apoptotic cells. Proc Natl Acad Sci U S A, 100: 7812-7817, 2003.

Taylor, S. J., Chae, H. Z., Rhee, S. G., and Exton, J. H. Activation of the beta 1 isozyme of phospholipase C by alpha subunits of the Gq class of G proteins. Nature, 350: 516-518, 1991.

Thomazy, V. and Fesus, L. Differential expression of tissue transglutaminase in human cells. An immunohistochemical study. Cell Tissue Res, 255: 215-224, 1989.

Thyberg, J., Palmberg, L., Nilsson, J., Ksiazek, T., and Sjolund, M. Phenotype modulation in primary cultures of arterial smooth muscle cells. On the role of platelet-derived growth factor. Differentiation, 25: 156-167, 1983.

Tucholski, J. and Johnson, G. V. Tissue transglutaminase directly regulates adenylyl cyclase resulting in enhanced cAMP-response element-binding protein (CREB) activation. J Biol Chem, 278: 26838-26843, 2003.

Tuzi, S., Uekama, N., Okada, M., Yamaguchi, S., Saito, H., and Yagisawa, H. Structure and dynamics of the phospholipase C-delta1 pleckstrin homology domain located at the lipid bilayer surface. J Biol Chem, 278: 28019-28025, 2003.

Uehata, M., Ishizaki, T., Satoh, H., Ono, T., Kawahara, T., Morishita, T., Tamakawa, H., Yamagami, K., Inui, J., Maekawa, M., and Narumiya, S. Calcium sensitization of smooth muscle mediated by a Rho-associated protein kinase in hypertension. Nature, 389: 990-994, 1997.

Upchurch, H. F., Conway, E., Patterson, M. K., Jr., and Maxwell, M. D. Localization of cellular transglutaminase on the extracellular matrix after wounding: characteristics of the matrix bound enzyme. J Cell Physiol, 149: 375-382, 1991.

Vega, Q. C., Cochet, C., Filhol, O., Chang, C. P., Rhee, S. G., and Gill, G. N. A site of tyrosine phosphorylation in the C terminus of the epidermal growth factor receptor is required to activate phospholipase C. Mol Cell Biol, 12: 128-135, 1992.

Verderio, E., Nicholas, B., Gross, S., and Griffin, M. Regulated expression of tissue transglutaminase in Swiss 3T3 fibroblasts: effects on the processing of fibronectin, cell attachment, and cell death. Exp Cell Res, 239: 119-138, 1998.

Vezza, R., Habib, A., and FitzGerald, G. A. Differential signaling by the thromboxane receptor isoforms via the novel GTP-binding protein, Gh. J Biol Chem, 274: 12774-12779, 1999.

Vincan, E., Neylon, C. B., Jacobsen, A. N., and Woodcock, E. A. Reduction in Gh protein expression is associated with cytodifferentiation of vascular smooth muscle cells. Mol Cell Biochem, 157: 107-110, 1996.

Walter, G. Production and use of antibodies against synthetic peptides. J Immunol Methods, 88: 149-161, 1986.

Wang, C. Y., Zhong, W. B., Chang, T. C., Lai, S. M., and Tsai, Y. F. Lovastatin, a 3-hydroxy-3-methylglutaryl coenzyme A reductase inhibitor, induces apoptosis and differentiation in human anaplastic thyroid carcinoma cells. J Clin Endocrinol Metab, 88: 3021-3026, 2003.

Weissberg, P. L., Cary, N. R., and Shanahan, C. M. Gene expression and vascular smooth muscle cell phenotype. Blood Press Suppl, 2: 68-73, 1995.

Winder, S. J. and Walsh, M. P. Calponin: thin filament-linked regulation of smooth muscle contraction. Cell Signal, 5: 677-686, 1993.

Wissler, R. W. The arterial medial cell, smooth muscle, or multifunctional mesenchyme? Circulation, 36: 1-4, 1967.

Worth, N. F., Rolfe, B. E., Song, J., and Campbell, G. R. Vascular smooth muscle cell phenotypic modulation in culture is associated with reorganisation of contractile and cytoskeletal proteins. Cell Motil Cytoskeleton, 49: 130-145, 2001.

Worth, N. F., Campbell, G. R., Campbell, J. H., and Rolfe, B. E. Rho expression and activation in vascular smooth muscle cells. Cell Motil Cytoskeleton, 59: 189-200, 2004.

Wu, D., Katz, A., Lee, C. H., and Simon, M. I. Activation of phospholipase C by alpha 1-adrenergic receptors is mediated by the alpha subunits of Gq family. J Biol Chem, 267: 25798-25802, 1992.

Yagisawa, H., Tanase, H., and Nojima, H. Phospholipase C-delta gene of the spontaneously hypertensive rat harbors point mutations causing amino acid substitutions in a catalytic domain. J Hypertens, 9: 997-1004, 1991.

Yagisawa, H., Sakuma, K., Paterson, H. F., Cheung, R., Allen, V., Hirata, H., Watanabe, Y., Hirata, M., Williams, R. L., and Katan, M. Replacements of single basic amino acids in the pleckstrin homology domain of phospholipase C-delta1 alter the ligand binding, phospholipase activity, and interaction with the plasma membrane. J Biol Chem, 273: 417-424, 1998.

Yamaga, M., Fujii, M., Kamata, H., Hirata, H., and Yagisawa, H. Phospholipase C-delta1 contains a functional nuclear export signal sequence. J Biol Chem, 274: 28537-28541, 1999.

Yamaga, M., Sekimata, M., Fujii, M., Kawai, K., Kamata, H., Hirata, H., Homma, Y., and Yagisawa, H. A PLCdelta1-binding protein, p122/RhoGAP, is localized in caveolin-enriched membrane domains and regulates caveolin internalization. Genes Cells, 9: 25-37, 2004.

Yin, H. L. and Janmey, P. A. Phosphoinositide regulation of the actin cytoskeleton. Annu Rev Physiol, 65: 761-789, 2003.

Zhang, J., Tucholski, J., Lesort, M., Jope, R. S., and Johnson, G. V. Novel bimodal effects of the G-protein tissue transglutaminase on adrenoreceptor signalling. Biochem J, 343 Pt 3: 541-549, 1999.

Zhang, Z., Vezza, R., Plappert, T., McNamara, P., Lawson, J. A., Austin, S., Pratico, D., Sutton, M. S., and FitzGerald, G. A. COX-2-dependent cardiac failure in Gh/tTG transgenic mice. Circ Res, 92: 1153-1161, 2003.